Interaction between viruses and prokaryotes in the sea

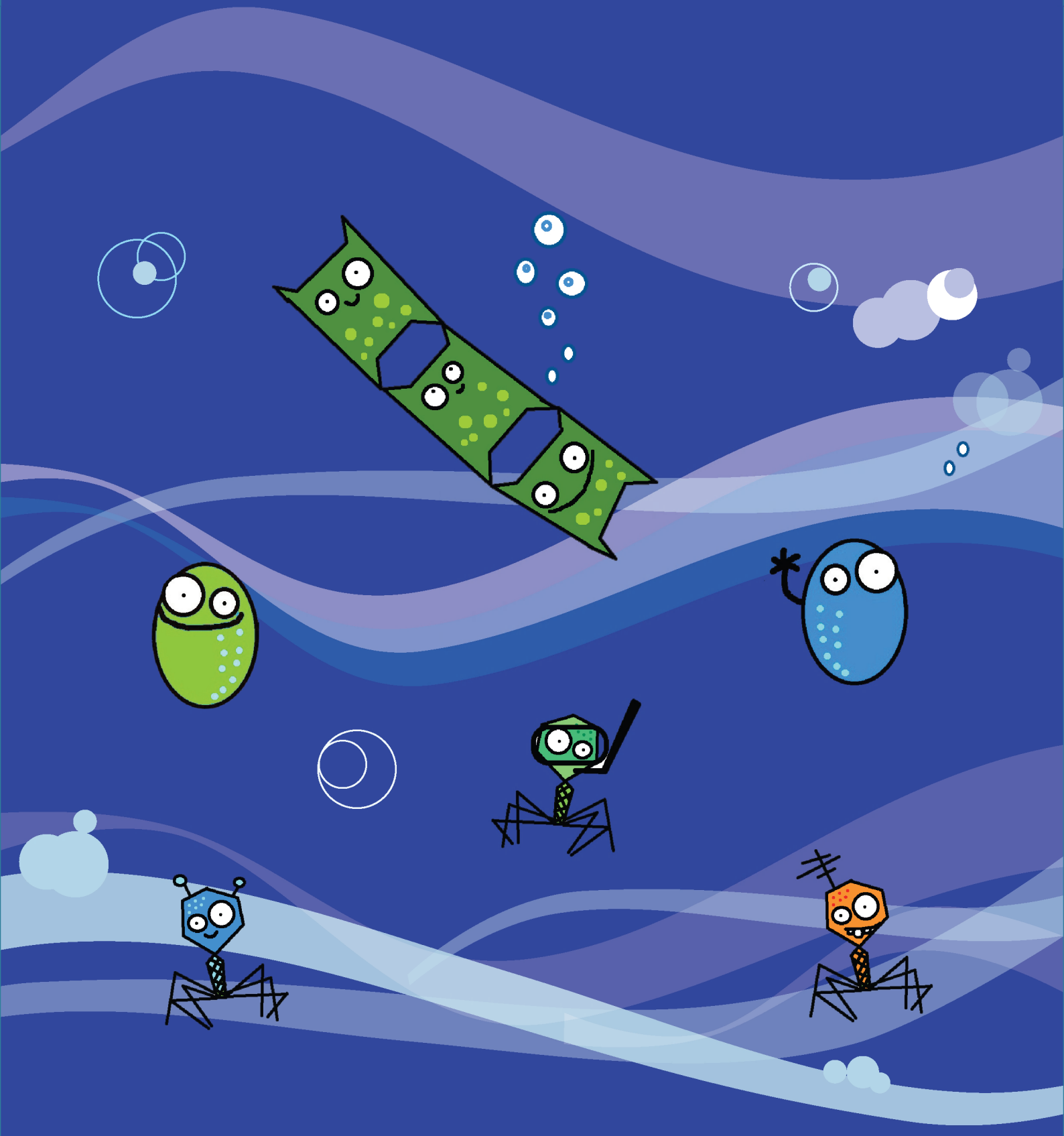

Daniele De Corte

Interaction between viruses and prokaryotes in the sea

Cover Illustration by : Maite Fuertes Arrizabalaga
Clara Ruíz-González

RIJKSUNIVERSITEIT GRONINGEN

Interaction between viruses and prokaryotes in the sea

Proefschrift

ter verkrijging van het doctoraat in de
Wiskunde en Natuurwetenschappen
aan de Rijksuniversiteit Groningen
op gezag van de
Rector Magnificus, dr. E. Sterken,
in het openbaar te verdedigen op
maandag 23 april 2012
om 11:00 uur

door

Daniele De Corte

geboren op 16 juni 1978
te Rome, Italië

Promotor: Prof. dr. H.J.W. de Baar

Prof. dr. G.J. Herndl

Beoordelingscommissie: Prof. dr. J.D. van Elsas

Prof. dr. H.J. Laanbroek

Prof. dr. M. Middelboe

ISBN: 978-90-367-5507-8

Paranimfen: Eva Sintes
Harry Witte

"Virtute enim ipsa non tam multi praediti esse quam videri volunt"
Marcus Tullius Cicero (106-43 BC)

The work presented in this thesis was carried out at the Royal Netherlands Institute for Sea Research (NIOZ), Department of Biological Oceanography. Financial support was provided by NWO-ALW.

To my parents and to my friends for their uncoditional support.

Contents

Introduction

The marine environment is the largest ecosystem on Earth with a volume of approximately 1.33 x 10^9 km^3 and accounting for more than 70% of the Earth's surface. Marine microbes are the most abundant and diverse organisms in the oceans, and thus constituting the major fraction of the living biomass and diversity on Earth. Consequently, the marine microorganisms are the major force behind the oceanic biogeochemical cycles with viruses playing a key role in controlling the microorganisms' mortality and indirectly, their activity.

Marine Prokaryotes

The microbial loop hypothesis provided the conceptual framework for the position of prokaryotes in marine food webs and ecosystems (Azam et al., 1983). In aquatic environments, microbes constitute the base of the food web. Autotrophic prokaryotes dominate the biomass of vast areas of the euphotic layer of the oceans (Scanlan and West, 2002). Additionally, heterotrophic prokaryotes efficiently convert DOC (dissolved organic carbon) not accessible to other organisms, into POC (particulate organic carbon), which then becomes accessible to the higher trophic levels.

Molecular analyses of bacterioplankton at the 16S rRNA level reveal a few dominant and a large number of low abundant species, that account for a long tail in the rank – frequency distribution of prokaryotes (Fuhrman and Hagström, 2008, Pedros-Alio, 2006). This distribution may result from a strong competition for common resources and/or high turnover rate of the low abundant species (Wilson and Lundberg, 2004). Laboratory and mesocosm experiments conducted with different nutrient additions on cultures and environmental samples clearly show that the marine prokaryotes compete for specific limiting elements (Carlson et al., 2002, Kirchman et al., 2003, Weaver et al., 2003), indicating that even surface water prokaryotic community composition can be bottom-up controlled. Other factors that can influence the structure of the prokaryotic community are predation and interspecies interaction.

The top-down control (i.e., predation) can affect the prokaryotic community structure through selective grazing on specific taxa that due to their size and/or shape might be more vulnerable to predation than others (Simek et al., 1999). Also viruses can affect the composition of the prokaryotic community (Bouvier and del Giorgio, 2007, Hewson and Fuhrman, 2006, Jardillier et al., 2005, Winter et al., 2004) due to their reported species specificity (Ackermann and DuBow, 1987). Prokaryotic communities may also be affected by interspecies interactions: there are reports on antagonistic interactions among marine prokaryotes which compete for common resources (Long and Azam, 2001) but also on synergistic interactions between bacteria, metabolizing organic matter in a concerted action involving both bacterial taxa.

What is a virus?

Viruses are obligate intracellular parasites that cannot replicate independently of a host cell. They are able to exist outside the host through an extracellular form that facilitates the infection, but they are unable to move thus, they depend on passive diffusion to find the host cells. Their genetic information is organized in DNA or RNA genomes engulfed by a protein shell, the capsid (Weinbauer, 2004).

Viruses are the most abundant and diverse entities in the marine ecosystems (Rohwer, 2003) and they are pathogens of macro- and microorganisms. Most marine viruses are phages that infect heterotrophic and autotrophic microbes (Bacteria, Archaea and eukaryotic phytoplankton). The viral infection is, besides direct grazing by eukaryotes, the major source of mortality for these microbes (Fuhrman and Noble, 1995). As viruses are species- and even strain-selective in their infection, viruses are capable of influencing the phylogenetic composition of marine microbial communities and consequently play a major role in the biogeochemical cycles (Suttle, 2007). The viral succession is not only dependent on the parasite multiplication rate but also on the survival rate depending on the capability to found a suitable host (De Paepe and Taddei, 2006). However, up to now the range of specificity of viruses remains unclear in natural systems.

There are two main viral reproduction strategies: the lytic and the lysogenic cycles. In the lytic cyle, viruses replicate themselves after successful infection, inducing the host's metabolic system to produce the components needed to generate new virions. The infection leads to cell lysis and to the consequent release of the viruses' progeny (Weinbauer, 2004). The lysogenic cycle is characterized by the integration of the bacteriophage nucleic acid into the host's genome. The newly integrated genetic material, coined prophage, can be transmitted to daughter cells with each subsequent cell division, and it can be released at a later moment, causing the proliferation of new phages via the lytic cycle (Weinbauer, 2004). Different environmental conditions, might favor either one of the two viral life strategies. Lysogeny is considered to be an adaptation to low host abundance and activity, whereas the lytic cycle dominates at high host abundance and activity (Weinbauer, 2003).

Abundance, diversity and production of marine viruses

Viruses are ubiquitously distributed in aquatic environments and they are present at high abundance. Generally, their abundance is one or two orders of magnitude higher than that of the prokaryotes (Weinbauer, 2004). Although viruses are the most abundant entities in the marine ecosystems, accounting for more than 94% of the total microbial abundance, they account for only 5% of the total biomass due to their small size (Suttle, 2007). In contrast, prokaryotes account for only 10% of abundance but 90% of biomass in the marine environment (Suttle, 2007). Virioplankton are a dynamic component of marine systems thus, viral abundances vary along trophic gradients (Bongiorni et al., 2005, Weinbauer et al., 1993), depth (Hara et al., 1996, Parada et al., 2007), and, similarly to prokaryotes and eukaryotic phytoplankton, they are influenced by

seasonal physical and chemical fluctuations in the environment (Winget et al., 2011). Overall, viral abundance and production in aquatic ecosystems vary along with prokaryotic abundance and activity (De Corte et al., 2010). Metagenomic analysis used to study the (DNA) viral community structure showed a high global viral diversity with consistent differences among different latitudes (Angly et al., 2006).

Viral implication in the microbial food web

Viruses efficiently convert particulate organic matter (POM) into dissolved organic matter (DOM) through the lysis of the host cells, which can subsequently be utilized by prokaryotes (Middelboe et al., 2003). Viral infection caused similar mortality rates as by protists (Fuhrman and Noble, 1995). Viral lysis, however, has different effects on the biogeochemical cycles than protistan grazing. Grazing of prokaryotes by protists facilitates the transfer of particulate organic carbon (POC) and nutrients to higher trophic levels, while viral lysis converts particulate organic carbon into dissolved organic carbon (DOC), which remains available for heterotrophic prokaryotes (a process that is called 'viral shunt' (Suttle, 2007)). The release of DOM by viral lysis can lead to an increase of prokaryotic production (by ~30%) whereas the heterotrophic nanoplankton production decreases (by ~20%) (Fuhrman and Suttle, 1993). The effect of the viral lysis on the prokaryotic community has relevant implications on the global carbon cycle by affecting the biological pump. The biological pump is the sum of the biological processes transporting organic carbon from the euphotic layer to the deep ocean (Ducklow et al., 2001) .

Thesis Outline

The aim of the thesis was to advance our knowledge on the dynamics of prokaryotic and viral abundance, production and diversity in marine ecosystems, knowing that the variability of the viral communities is highly dependent on the host's (prokaryotes) metabolic activity, abundance, and diversity.

Chapter 1

The Arctic coastal areas experience large fluctuations in environmental conditions (UV exposure time, temperature, input of fresh water and terrestrial particles) during the spring to summer transition period. Under these changing conditions, we investigated the changes in the relations between prokaryotic and viral communities along a transect located in the Kongsfjorden (Ny-Ålesund, Spitsbergen, Norway) during June-July 2008.

Chapter 2

The aim of this study was to determine the distribution of prokaryotic and viral abundance, production and community composition throughout the water column in the (sub)tropical Atlantic

Ocean from the epi- to the abyssopelagic realm to assess the potential variations in the relation between viruses and prokaryotes in the various zones of the oceanic water column. Random Amplification of Polymorphic DNA- PCR (RAPD-PCR) method was used to investigate the viral diversity, and the results obtained were compared with the bacterial and archaeal community composition revealed by automated ribosomal intergenic spacer analysis (ARISA) and terminal-restriction fragment length polymorphism (T-RFLP), respectively.

Chapter 3

The main focus of this study was to investigate the factors that control the viral abundance and production, and the distribution of different viral sub-populations along a latitudinal transect from about 60°N to 10°S in the Atlantic covering the entire water column. The distance-based multivariate analysis for a linear model using forward selection (DISTLM forward) was used to identify the best set of environmental parameters that account for the variations in these viral parameters. The results were also used to assess the changes in the relation between the bacterial and viral communities under contrasting environmental conditions.

Chapter 4

Ammonia oxidation is a key process in the global nitrogen cycle that was thought to be mediated exclusively by a few bacterial groups. Recent studies have shown that also mesophilic marine Crenarchaeota Group I (MCGI) are capable to perform the initial nitrification step. During the Poseidon-2 cruise in the Eastern Mediterranean Sea, we investigated the abundance of ammonia-oxidizing Bacteria and Archaea using the ammonia monooxygenase-alpha subunit (*amo*A) gene as functional marker combined with quantitative PCR. The abundance of bacterial and archaeal *amo*A was related to the abundance of Bacteria and Archaea (assessed by fluorescence in situ hybridization), respectively, throughout the whole water column.

Chapter 5

Over the last decades several studies investigated the complexity of the prokaryotic communities using the 16S rDNA. However, the total DNA pool of the prokaryotic community consists of DNA originated from living, dormant or even dead cells. In this study, we investigated the composition of the active *versus* total bacterial community in the coastal Arctic (Ny Ålesund, Spitsbergen, Norway) during the spring to summer transition period (2008), combining 16S rDNA and 16S rRNA cloning and sequencing and MICRO-CARD-FISH (microautoradiography combined with catalyzed reporter deposition fluorescence in situ hybridization) approaches.

References

Ackermann HW, DuBow MS. (1987). Viruses of prokaryotes. *General properties of bacteriophages*. CRC.

Angly FE, Felts B, Breitbart M, Salamon P, Edwards RA, Carlson C, Chan AM, Haynes M, Kelley S, Liu H, Mahaffy JM, Mueller JE, Nulton J, Olson R, Parsons R, Rayhawk S, Suttle CA, Rohwer F. (2006). The marine viromes of four oceanic regions. *PLoS Biology* **4**:2121-2131

Azam F, Fenchel T, Field JG, Gray JS, Meyerreil LA, Thingstad F. (1983). The ecological role of water-column microbes in the sea. *Mar Ecol-Prog Ser* **10:** 257-263.

Bongiorni L, Magagnini M, Armeni M, Noble R, Danovaro R. (2005). Viral production, decay rates, and life strategies along a trophic gradient in the north Adriatic sea. *Appl Environ Microbiol* **71:** 6644-6650.

Bouvier T, del Giorgio PA. (2007). Key role of selective viral-induced mortality in determining marine bacterial community composition. *Environ Microbiol* **9:** 287-297.

Carlson CA, Giovannoni SJ, Hansell DA, Goldberg SJ, Parsons R, Otero MP, Vergin K, Wheeler BR. (2002). Effect of nutrient amendments on bacterioplankton production, community structure, and DOC utilization in the northwestern Sargasso Sea. *Aquat Microb Ecol* **30:** 19-36.

De Corte D, Sintes E, Winter C, Yokokawa T, Reinthaler T, Herndl GJ. (2010). Links between viral and prokaryotic communities throughout the water column in the (sub)tropical Atlantic Ocean. *ISME J* **4:**1431-1442.

De Paepe M, Taddei F. (2006). Viruses' life history: Towards a Mechanistic Basis of a Trade-off between survival and reproduction among phages. *PLoS Biol* **4**:1248-1256

Ducklow HW, Steinberg DK, Buesseler KO. (2001). Upper ocean carbon export and the biological pump. *Oceanography* **14:** 50-58.

Fuhrman JA, Suttle CA. (1993). Viruses in marine planktonic systems. *Oceanography* **6:** 51-63.

Fuhrman JA, Noble RT. (1995). Viruses and protists cause similar bacterial mortality in coastal seawater. *Limnol Oceanogr* **40:** 1236-1242.

Fuhrman JA, Hagström Å. (2008). Bacterial and archaeal community ctructure and its patterns. In: Kirchman DL (ed). *Microbial Ecology of the Oceans*, 2nd edn. John Wiley & Sons: New York, p 45-90.

Hara S, Koike I, Terauchi K, Kamiya H, Tanoue E. (1996). Abundance of viruses in deep oceanic waters. *Mar Ecol-Prog Ser* **145:** 269-277.

Hewson I, Fuhrman JA. (2006). Viral impacts upon marine bacterioplankton assemblage structure. *J Mar Biol Assoc UK* **86:** 577-589.

Jardillier L, Bettarel Y, Richardot M, Bardot C, Amblard C, Sime-Ngando T, Debroas D. (2005). Effects of viruses and predators on prokaryotic community composition. *Microb Ecol* **50:** 557-569.

Kirchman DL, Hoffman KA, Weaver R, Hutchins DA. (2003). Regulation of growth and energetics of a marine bacterium by nitrogen source and iron availability. *Mar Ecol-Prog Ser* **250:** 291-296.

Long RA, Azam F. (2001). Antagonistic interactions among marine pelagic bacteria. *Appl Environ Microbiol* **67:** 4975-4983.

Middelboe M, Riemann L, Steward GF, Hansen V, Nybroe O. (2003). Virus-induced transfer of organic carbon between marine bacteria in a model community. *Aquat Microb Ecol* **33:** 1-10.

Parada V, Sintes E, van Aken HM, Weinbauer MG, Herndl GJ. (2007). Viral abundance, decay, and diversity in the meso- and bathypelagic waters of the North Atlantic. *Appl Environ Microbiol* **73:** 4429-4438.

Pedros-Alio C. (2006). Marine microbial diversity: can it be determined? *Trends Microbiol* **14:** 257-263.

Rohwer F. (2003). Global phage diversity. *Cell* **113:** 141-141.

Scanlan DJ, West NJ. (2002). Molecular ecology of the marine cyanobacterial genera Prochlorococcus and Synechococcus. *FEMS Microbiol Ecol* **40:** 1-12.

Simek K, Kojecka P, Nedoma J, Hartman P, Vrba J, Dolan JR. (1999). Shifts in bacterial community composition associated with different microzooplankton size fractions in a eutrophic

reservoir. *Limnol Oceanogr* **44:** 1634-1644.

Suttle CA. (2007). Marine viruses - major players in the global ecosystem. *Nat Rev Microbiol* **5:** 801-812.

Weaver RS, Kirchman DL, Hutchins DA. (2003). Utilization of iron/organic ligand complexes by marine bacterioplankton. *Aquat Microb Ecol* **31:** 227-239.

Weinbauer MG, Fuks D, Peduzzi P. (1993). Distribution of viruses and dissolved DNA along a coastal trophic gradient in the northern Adriatic sea. *Appl Environ Microbiol* **59:** 4074-4082.

Weinbauer MG. (2004). Ecology of prokaryotic viruses. *FEMS Microbiol Rev* **28:** 127-181.

Wilson WG, Lundberg P. (2004). Biodiversity and the Lotka-Volterra theory of species interactions: open systems and the distribution of logarithmic densities. *P Roy Soc Lond B Bio* **271:** 1977-1984.

Winget DM, Helton RR, Williamson KE, Bench SR, Williamson SJ, Wommack KE. (2011). Repeating patterns of virioplankton production within an estuarine ecosystem. *P Natl Acad Sci USA* **108**:11506-11511

Winter C, Smit A, Herndl GJ, Weinbauer MG. (2004). Impact of virioplankton on archaeal and bacterial community richness as assessed in seawater batch cultures. *Appl Environ Microbiol* **70:** 804-813.

Chapter 1

Changes in viral and bacterial communities during the ice-melting season in the coastal Arctic (Kongsfjorden, Ny-Ålesund)

Daniele De Corte, Eva Sintes, Taichi Yokokawa and Gerhard J. Herndl

Published in Environmental Microbiology (2011) 13: 1827-1841

Abstract

Microbial communities in Arctic coastal waters experience dramatic changes in environmental conditions during the spring– summer transition period.

Physico-chemical and biological parameters were determined during the ice-melting season in the coastal Arctic (Kongsfjorden, Ny-Ålesund) to assess the variation in the relationships between viral and prokaryotic communities.

The bacterial and viral abundance increased during the spring to summer transition period, probably associated to the increase in temperature and the development of a phytoplankton bloom. The increase in viral abundance was less pronounced than the increase in prokaryotic abundance; consequently, the viral to prokaryotic abundance ratio decreased. The bacterial and viral communities were stratified as determined by Automated Ribosomal Intergenic Spacer Analysis and Randomly Amplified Polymorphic DNA–PCR (RAPD-PCR), respectively. Both, the bacterial and viral communities were characterized by a relatively low number of operational taxonomic units (OTUs). Despite the apparent low complexity of the bacterial and viral communities, the link between these two communities was weak over the melting season, as suggested by the different trends of prokaryotic and viral abundance during the sampling period. This weak relationship between the two communities might be explained by UV radiation and suspended particles differently affecting the virus-like particles (VLP) and the prokaryotes in the coastal Arctic during the studied period. Based on our results, we conclude that the viral and bacterial communities in the Arctic were strongly affected by the variability of the environmental conditions during the transition period between spring and summer.

Introduction

The Arctic Ocean experiences large seasonal fluctuations in light availability, freshwater input and phytoplankton productivity and to a lesser extent in seawater temperature. Temperature is one of the major factors influencing prokaryotic and indirectly, viral activity (Winter et al., 2005a, De Paepe & Taddei, 2006, Wells & Deming, 2006b, Winter et al., 2008). Particularly at low temperatures, small changes in temperature might provoke substantial changes in prokaryotic growth rates (Kirchman et al., 2009) which in turn, affect viral activity.

The near-surface plankton communities are exposed to high ultraviolet (UV) radiation levels potentially causing DNA damage to a variety of marine microorganisms including prokaryotes and viruses (Kaiser & Herndl, 1997, Weinbauer et al., 1997, Arrieta et al., 2000, Winter et al., 2001, Jacquet & Bratbak, 2003). Although prokaryotes and viruses exhibit efficient photoreactivation repair (Kaiser & Herndl, 1997, Weinbauer et al., 1997), UV radiation might modify the composition of each of the two communities as interspecific variability has been reported in bacteria towards UV stress and in the recovery efficiency (Arrieta et al., 2000).

Viruses have been shown to be highly abundant, diverse and dynamic in temperate (Maranger & Bird, 1995, Sano et al., 2004, Angly et al., 2006) as well as in Arctic ecosystems (Middelboe et al., 2002, Hodges et al., 2005, Angly et al., 2006, Wells & Deming, 2006a, b). Several studies in polar regions and the dark ocean have shown that viruses maintain their infectivity at low temperatures (Middelboe et al., 2002, Gowing et al., 2003, Weinbauer et al., 2003) and that viral lysis can be as important as protistan grazing in controlling prokaryotic abundance (Guixa-Boixereu et al., 2002, Wells & Deming, 2006c). Viral lysis of prokaryotes might also influence the composition of the prokaryotic community (Weinbauer & Rassoulzadegan, 2004) and provoke the release of intracellular material upon lysis which, in turn, stimulates dissolved organic matter cycling by heterotrophic prokaryotes (Fuhrman, 2000, Middelboe & Jorgensen, 2006, Middelboe & Lyck, 2002, Middelboe et al., 2003). In near-shore Arctic waters, however, the commonly tight coupling between prokaryotic and viral abundance and activity (Choi et al., 2003, Hewson et al., 2006) might be substantially distorted by the high particle load entering the costal Arctic waters via run-off from the adjacent land. The high load of terrestrial-derived suspended solids (silt and clay) may substantially reduce the ability of viruses to infect prokaryotes as viruses are efficiently adsorbed by silt and clay (Murray & Jackson, 1992).

Hence, we hypothesized a loose coupling between prokaryotes and viruses during periods of high particle load in the coastal Arctic Ocean originating from terrestrial run-off, in contrast in regions with low particle load, a close coupling between prokaryotes and viruses was expected, albeit at a lower heterotrophic prokaryotic activity. We tested this hypothesis during the ice-melting season (June-July) in the coastal Arctic sea (Kongsfjorden, Ny-Ålesund, Spitsbergen, Norway).

Materials and Methods

Study area and sampling. Seven stations located in Kongsfjorden (Ny-Ålesund, Spitsbergen, Norway) were sampled following a transect from the mouth of a glacier towards open waters (Fig. 1). Water samples were obtained from the surface (~1.5 m) to a maximum depth of ~300 m over a four weeks period from June to July 2008. Sampling was performed from a boat with a CTD rosette sampling system holding three 10-L Niskin bottles and sensors for conductivity, temperature, fluorescence and depth.

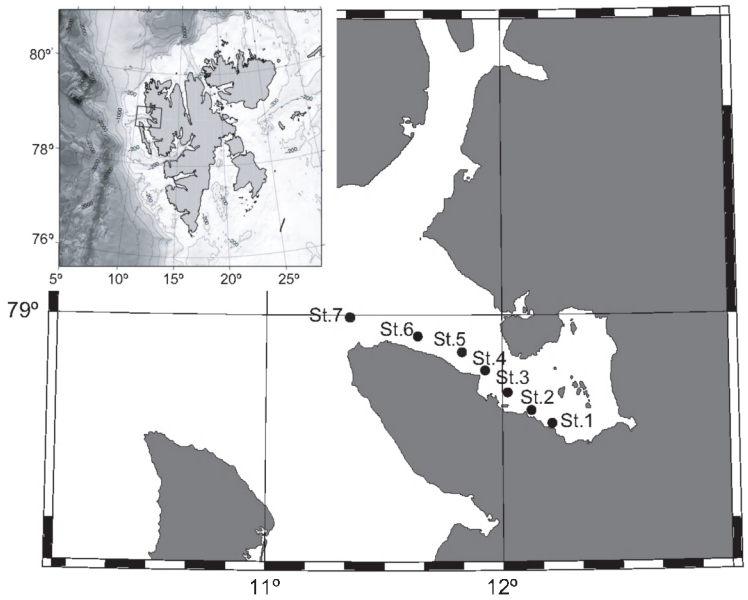

Figure 1. Location of the sampling area. The full circles indicate the distribution of the stations along the Kongsfjorden (Ny-Ålesund).

Prokaryotic and viral abundance. Samples for prokaryotic and viral abundance were collected at St.1 at 1.5, 50 and 20 m depth, St.2 at 1.5, 50 and 100 m depth, St.3 at 1.5, 50 and 200 m depth, St.4 at 1.5, 50 and 300 m depth, St.5 1.5, 50 and 280, St.6 1.5, 50, 270 m, St.7 1.5, 50, 290. These parameters were collected once per week during the four weeks of investigation period (11/06/08-02/07/08). Prokaryotic and viral abundance were determined by flow cytometry (Del Giorgio et al., 1996, Brussaard, 2004). Two mL water samples were fixed with 0.5 % glutaraldehyde, shock-frozen in liquid N_2 and kept at -80°C until analysis. The prokaryotes were enumerated on a FACScalibur flow cytometer (Becton Dickinson) by their signature in a plot of green fluorescence *versus* side scatter. Viral abundance was measured by flow cytometry after SYBR Green I staining. The virus-like particles (VLP) were enumerated on a FACScalibur flow cytometer (Becton Dickinson) by their signature in a plot of green fluorescence *versus* side scatter.

Depending on their respective signature in the cytogram of green fluorescence *vs*. side scatter, two different prokaryotic populations (high and low nucleic acid content prokaryotes) and three different viral populations (high, medium and low fluorescence viruses) were discriminated.

Viral production. The viral production was measured at selected stations, depths and date (Table 4). The lytic and lysogenic viral production were measured at four stations and three different depths. For viral production, the dilution approach was used (Wilhelm et al., 2002a). Briefly, 50 mL of the prokaryotic concentrate obtained by 0.2 μm tangential-flow filtration (Vivascience) was added to 450 mL of virus-free filtrate produced from the same water sample using a 30 kDa molecular weight cut-off tangential-flow filtration (Vivascience). This approach resulted in a prokaryotic abundance similar to *in situ* prokaryotic abundance and viral abundance reduced 1.5 to 3 times as compared to the in situ concentration.

Subsamples were taken to enumerate prokaryotes and viruses at 4 h intervals over a time span of 48 h. The experiments were performed in duplicate at *in situ* temperature in the dark with and without the addition of mitomycin C (final concentration 5 μg mL^{-1}; SIGMA) (Ortmann et al., 2002). Mitomycin C was added to induce the lytic cycle of lysogenic viruses. Viral production (VP) was calculated as the slope of a first order regression line of viral abundance *vs.* incubation time for the samples that showed a single peak (Wilhelm et al., 2002a). For the samples showing two peaks, viral production was calculated according to the formula: $[(V_{max1}-V_{min1}) + (V_{max2}-V_{min2})]/(t_{max2}-t_{min1})$ where V=viral abundance, t=time and subscripts 1 and 2 denote the increase in viral abundance leading to the first and the second peak in viral abundance (Winter et al., 2004).

The lytic viral production was determined as the VP in the incubations without mitomycin C added, and the lysogenic VP as the difference between the VP obtained in the mitomycin C-treated samples and the samples without mitomycin C.

Viral decay. The viral decay was measured in the same samples as used for viral production measurements (Table 4). Samples for viral decay were filtered twice through 0.2 μm (tangential-flow filtration, Vivascience). One liter of the obtained prokaryote-free seawater was incubated in duplicate at *in situ* temperature in the dark. Subsamples for viral abundance were taken every 4-7 h for up to 56 h. The viral decay was calculated from the decrease in viral abundance over time, fitting a linear regression to the log of the viral abundance *vs.* time.

Prokaryotic leucine incorporation. The leucine incorporation rate was colleted at the same stations, depths and dates as the prokaryotic and viral abundance. Two 5 mL samples and one formaldehyde-killed control were inoculated with ^{3}H-leucine (20 nM final concentration, specific activity 160 Ci $mmol^{-1}$, Amersham, GE Healthcare) and incubated in the dark at *in situ* temperature for 2 h. Subsequently, the samples were fixed with formaldehyde (2% final concentration), filtered onto 0.2 μm polycarbonate GTTP filters (Millipore) supported by Millipore HAWP filters, and rinsed three times with 10 mL of 5% ice-cold trichloroacetic acid. Thereafter, the filters were transferred into scintillation vials and air-dried. Then, 8 mL of scintillation cocktail (Packard Filter Count, PerkinElmer) was added to each vial and the disintegrations per minute (DPM) determined in a LKB liquid scintillation counter after 18 h. The obtained DPM were converted to leucine

incorporation rates.

Viral community composition. The viral community composition was measured in all the station at selected dates (Figure 3a). For the analysis of the viral community composition, seven stations were sampled at three different depths. Per sample, 15 L of water was collected and pre-filtered through a 0.2 μm polycarbonate filter (Whatman Nuclepore). The filtrate was subsequently concentrated to a final volume of ~50 mL by tangential-flow filtration with a 30 kDa molecular weight cut-off filter (Vivascience) and stored at -80°C until DNA extraction. The viral concentrate was further concentrated to a final volume of 200 μL by centrifugation (5000x *g* for 20 min) with an Amicon Ultra 30 kDa molecular weight cut-off spin filter (Millipore). DNA extraction was performed with QIAmp MinElute Virus Spin Kit (QIAGEN) using the protocol of the manufacturer and the extract was directly used as PCR template. For RAPD-PCR, the primer CRA-22 (5'-CCGCAGCCAA-3') was used to amplify virioplankton DNA (Wommack et al., 1999b, Winget & Wommack, 2008) in 50 μL of PCR mixture. Samples were amplified by an initial denaturation step at 94°C for 10 min, followed by 30 cycles of annealing at 35°C for 3 min, extension at 72°C for 1 min and denaturation at 94°C for 30 s. The cycle was completed by a final extension at 72°C for 10 min, and then the product was kept at 4°C. The quality of the RAPD-PCR products was checked on 2% agarose gel. The products were purified with the Quick PCR purification kit (Genscript) and quantified with a Nanodrop spectrophotometer. Subsequently, the purified RAPD-PCR products were separated by electrophoresis with an Experion automated electrophoresis system (Bio-Rad), and the obtained images were analyzed with Fingerprinting II software (Bio-Rad).

Bacterial community composition. Samples for bacterial community composition were taken at the same depths, stations and dates as those for viral community composition (Figure 2a). Five hundred mL of seawater was filtered onto a 0.2 μm polycarbonate filter (47 mm diameter, Whatman Nuclepore) and the filters were stored at -80°C until further processing. DNA extraction was performed with a Soil Kit extraction (MoBIO laboratories) using the manufacturer's protocol.

To determine bacterial community composition, ARISA-PCR was used as described elsewhere (Borneman & Triplett, 1997) with modifications. One μL of the DNA extract was used as template in a 40 μL PCR mixture. The primers used were ITSf, 5'GTCGTAACAAGGTAGCCGTA-3' and ITSr eub, 5'-GCCAAGGCATCCACC-3' (Cardinale et al., 2004). The primer ITSf was end-labeled with phosphoramidite fluorochrome 5- carboxy-fluorescein dye 5-FAM. Samples were amplified by an initial denaturation step at 94°C for 2 min, followed by 32 cycles of amplification at 94°C for 15 s, 55°C for 30 s, and 72°C for 3 min and a final extension of 72°C for 9 min. Five μL of PCR products were run on 2.0% agarose gels to check the quality of the products. The PCR products were purified with Quick Clean PCR product purification kit (Genscript) and quantified using a Nanodrop spectrophotometer. Fluorescently labeled fragments (8 ng μL^{-1} of sample) were separated and detected with an ABI Prism 310 capillary sequencer (Applied Biosystems) run under GeneScan mode. The size of the fluorescently labeled fragments was determined by comparison

with X-Rhodamine MapMarker 1000 (BIO Ventures, Inc.) as the size standard. Injection was performed electrokinetically at 10 kV for 5 s (adjustable) and the run was conducted at 10 kV and 60°C within 60 min.

The output from the ABI Genescan software was transferred to the Fingerprinting II program (Bio-Rad) to determine the area of the peaks and for standardizing the peaks using the size marker. The obtained matrix was analyzed with the Primer software (Primer-E) to determine the similarity of ARISA patterns of different samples.

Statistical analysis. Spearman rank correlation was performed to analyze the relationship between the different parameters. Analysis of variance (ANOVA on rank) was performed to test possible differences among depth layers and time. If significant differences were observed, the post-hoc Dunn's test was also performed. Analysis of covariance (ANCOVA on rank) was performed to test whether the bacterial and viral OTUs covaried significantly. The distance-based multivariate analysis for a linear model using forward selection (DISTLM forward) was performed to test the relationships between the bacterial and viral communities and the biotic (bacterial, viral abundance and production) and abiotic (temperature, salinity, density) variables (Anderson et al., 2004). Correlation and linear regression analyses and ANOVA test were performed with SigmaPlot 10.00 (Systat Software, Inc.) while ANCOVA test was performed with PAST 1.94a (Hammer et al. , 2001). The Principal Component Analysis (PCA) was used to determine the factors contributing most to the variance between the samples. The PCA was implemented in Primer-E software.

Results

Physico-chemical parameters.

Over the investigation period, the temperature in Kongsfjorden (Fig. 1) increased in the surface layer and in the 20-100 m layer from 3.4±0.4 to 5.4±0.8°C and from 2.1±0.7 to 2.7±0.4°C, respectively (ANOVA on ranks $p < 0.001$) (Table 1 and S1, Fig. S1). In the 200-300 m depth layer, however, temperature did not change over the four weeks (Table 1 and S1, Fig. S1). Generally, temperature significantly decreased with depth from the surface to the bottom layers (ANOVA on ranks $p < 0.001$, post-hoc Dunn's test $p < 0.05$) (Table 2, Fig. S1).

In the surface layer, salinity decreased from 34.6±0.1 at the beginning to 34.0±0.4 at the end of the investigation period (ANOVA on ranks $p < 0.001$) (Table 1). In the layers below 20 m, however, salinity did not change significantly over the study period (Table 1 and S1). Salinity increased with depth from the surface to the bottom at all the stations (ANOVA on ranks $p < 0.001$, post-hoc Dunn's test $p < 0.05$) (Table 2). The density followed similar trends as salinity decreasing in the surface layer over the four-week period (ANOVA on ranks $p < 0.001$) while no changes over time were detected below 20 m depth.

Table 1. Results of the Spearman rank correlation coefficient test performed to determine the variation of the prokaryotic and viral parameters *vs.* time.

Time	Surface			20-100 m			200-300 m		
	rs	p	n	rs	p	n	rs	p	n
Temperature	0.664	<0.0001	29	0.523	<0.0001	37	0.302	0.181	21
Salinity	-0.778	<0.0001	29	0.153	0.362	37	0.045	0.841	21
Oxygen	0.273	0.150	29	0.121	0.474	37	0.323	0.152	21
Density	-0.798	<0.0001	29	-0.428	0.008	37	-0.050	0.824	21
Fluorescence	-0.441	0.017	29	0.014	0.930	37	-0.856	<0.0001	21
PA	0.855	<0.0001	29	0.911	<0.0001	37	0.878	<0.0001	21
VA	0.678	<0.0001	29	0.697	<0.0001	37	0.586	0.005	21
VPR	-0.656	<0.0001	29	-0.858	<0.0001	37	0.009	0.966	21
PHP	0.578	<0.0001	29	0.759	<0.0001	37	0.536	0.012	21
POC	-0.287	0.130	29	-0.0498	0.768	37	-0.068	0.767	21
%HNA	0.720	<0.0001	29	0.858	<0.0001	37	0.307	0.171	21
% High VLP	-0.316	0.094	29	0.299	0.072	37	-0.089	0.694	21
% Medium VLP	-0.126	0.509	29	-0.049	0.769	37	0.191	0.402	21
% Low VLP	0.261	0.169	29	-0.409	0.012	37	-0.181	0.428	21

Relevant (-0.5 > rs > 0.5), statistically significant P<0.05.

Abbreviation: PA, prokaryotic abundance; VLP, virus-like particles; VPR, ratio of viral to prokaryotic abundance; PHP, bulk leucine incorporation rate; POC, particulate organic carbon; %HNA, percentage of high nucleic acid prokaryotes; %High VLP, percentage of high fluorescence viruses; %Medium VLP, percentage of Medium fluorescence viruses; %Low VLP, percentage of Low fluorescence viruses; n, number of samples.

Inorganic nutrients.

PO_4^{3+} ranged between 0.09±0.02 and 0.69±0.07 μmol/L during the investigation period, in surface and deep waters, respectively. Inorganic phosphorus significantly increased with depth (Anova on rank p<0.001, post-hoc Dunn's test $p < 0.05$) (Table S1), but no significant changes with time were detected over the four weeks study. Ammonium significantly increased with time in the surface layer and in the 200-300 m layer from 0.17±0.03 to 0.44±0.1 μmol/L and from 2.1±0.5 to 3.2±0.3 μmol/L (ANOVA on rank $p < 0.001$) (Table S1), respectively, while in the 20-100 m layer NH_4^+ did not significantly changed. NO_2^- ranged between 0.03±0.01 and 0.16±0.05 μmol/L whereas NO_3^- ranged between 0.11±0.05 and 7.0±1.6 μmol/L (Table S1). NH_4^+, NO_2^- and NO_3^- significantly decreased from the surface to the deeper layers (Anova on rank $p < 0.001$, post-hoc Dunn's test $p < 0.05$).

Prokaryotic and viral abundance and activity.

In the top 20 m layer, prokaryotic abundance increased with time over the four-week investigation period from an average of 3.8±0.7 x 10^5 cells mL^{-1} in the first week to 15.6±1.0 x 10^5 cells mL^{-1} in the final week (Table 3). In the 20-100 m depth layer, prokaryotic abundance increased from 2.8±1.8 x 10^5 cells mL^{-1} to 12.9±4.1 x 10^5 cells mL^{-1} during this period (Table 3). Hence in both, the top 20 m and the 20-100 m layer prokaryotic abundance increased by a factor of 4. In the deep layer (200-300 m depth), however, prokaryotic abundance increased only 1.5 times, from 3.5±0.4 x 10^5 cells mL^{-1} to 5.3±0.5 x 10^5 cells mL^{-1} (ANOVA on ranks, $p < 0.001$) (Table 1, 3, Figure S1).

Table 2. Results of the Spearman rank correlation coefficient test performed to determine the variation of the prokaryotic and viral parameters *vs.* depth (Abbreviation as in Table 1).

Depth (m)	rs	p	n
Temperature	-0.943	<0.0001	87
Salinity	0.918	<0.0001	87
Oxygen	-0.822	<0.0001	87
Density	0.957	<0.0001	87
Fluorescence	0.555	<0.0001	87
PA	-0.497	<0.0001	87
VA	-0.463	<0.0001	87
VPR	0.216	0.044	87
PHP	-0.792	<0.0001	87
POC	-0.790	<0.0001	87
%HNA	-0.023	0.832	87
% High VLP	0.615	<0.0001	87
% Medium VLP	0.387	<0.0001	87
% Low VLP	-0.503	<0.0001	87
Lytic VP	-0.693	0.021	10

Relevant ($-0.5 > r_s > 0.5$), statistically significant $P<0.05$.

Similar to prokaryotic abundance, viral abundance significantly increased during the sampling period (Table 3). Viral abundance increased in the surface waters from 2.1±0.4 x 10^6 viruses mL^{-1} to 5.5±0.8 x 10^6 viruses mL^{-1}, in the 20-100 m depth layer from 1.7±0.7 x 10^6 viruses mL^{-1} to 3.9±0.6 x 10^6 viruses mL^{-1}, and in the deep layer from 1.3±0.3 x 10^6 viruses mL^{-1} to 2.4±0.2 x10^6 viruses mL^{-1} (ANOVA on ranks $p < 0.001$) (Table 1, 3, Figure S1).

The virus to prokaryote ratio (VPR) significantly decreased from 5.5±0.8 to 3.6±0.6 in the surface layer (ANOVA on ranks $p < 0.001$) and from 7.2±1.9 to 3.1±0.6 in the 20-100 m depth layer (ANOVA on ranks $p < 0.001$) during the investigation period. The VPR in the deep layer, however, did not significantly change over time (Table 1, 3, Fig. S2).

Similar to prokaryotic abundance, leucine incorporation rates (as a measure of heterotrophic prokaryotic biomass production) significantly increased over this four-week period from 76.5±37.8 pmol leu L^{-1} h^{-1} to 240.2±64.8 pmol leu L^{-1} h^{-1} (ANOVA on ranks, $p < 0.001$) in the surface layer, from 28.6±30 to 116.1±52 pmol leu L^{-1} h^{-1} at the 20 to 100 m depth layer (ANOVA on ranks, $p < 0.001$), and from 11.1±1.8 to 30.4±7.1 in the deep waters (ANOVA on ranks, $p = 0.001$) (Table 1, 3, Fig. S1). The leucine incorporation rates significantly decreased from the surface to the bottom layers (ANOVA on ranks $p < 0.001$, post-hoc Dunn's test, $p < 0.05$) (Table 2, 3, Fig. S2). Hence, leucine incorporation increased in all three depth layers by a factor of 3 to 4, including in the deep waters where the increase in prokaryotic abundance was only 1.5 over the investigation period.

The percentage of high nucleic acid content (HNA) prokaryotes also significantly increased over the study period from 41.3% to 69.8% in the surface layer (ANOVA on ranks, $p < 0.001$) and from 38.8% to 66.8% at the 20 to 100 m depth layer (ANOVA on ranks, $p < 0.001$) (Table 1, 3). In the deep waters, the % HNA cells did not change with time (Table 1, 3). Also, the % HNA cells did not significantly vary with depth (Table 2, 3, Fig. S2), however, correlated with prokaryotic

abundance and production in the surface ($r=0.83$, $p<0.001$ and $r=0.85$ $p<0.001$, respectively) and intermediate layers ($r=0.89$ $p<0.001$ and $r=0.76$, $p<0.001$, respectively).

In contrast to the prokaryotic community, the three viral populations distinguished by flow cytometry (high, medium and low fluorescence) did not significantly change with time (Table 1, 3). However, the high fluorescence viral population significantly increased from the surface to the deep waters (ANOVA on ranks, $p < 0.001$, post-hoc Dunn's test, $p < 0.05$), while the low fluorescence viral population decreased with depth (ANOVA on ranks, $p < 0.001$, post-hoc Dunn's test $p < 0.05$) (Table 2).

Viral production and decay.

The lytic viral production ranged from 0.38×10^5 viruses mL^{-1} h^{-1} at St. 5 at 280 m depth to 3.55×10^5 viruses mL^{-1} h^{-1} at St. 7 at 1.5 m depth (Table 4). Lytic viral production significantly decreased with depth (Table 2), while no clear trend was apparent for the lysogenic viral production (Table 2, 4). Lysogenic production was only detectable in 4 out of 12 samples (Table 4).

Viral decay rates ranged between 1.4×10^{-3} viruses mL^{-1} h^{-1} at St. 1 at 20 m depth and 5.2×10^{-3} viruses mL^{-1} h^{-1} at St. 4 at 290 m depth with no clear spatial trend (Table 4) and hence, were 1-2 orders of magnitude lower than lytic viral production.

Bacterial and viral community composition.

The fingerprinting pattern of the bacterial community obtained with ARISA revealed a total of 56 operational taxonomic units (OTUs) ranging from 109 bp to 1007 bp (Fig. 2a). The lowest number of OTUs (5) was found at St. 3 at 200 m depth, the highest number of OTUs (25) was detected at St. 7 at 290 m depth. One OTU (571 bp) was ubiquitously present while 16 OTUs were found only once. The average number of OTUs ranged between 11 at the surface and 14 at the deeper layers (Fig. 2a). The number of OTUs did not show a clear trend neither with distance from the coast or with the depth. The Jaccard similarity cluster analysis of the ARISA fingerprints revealed a clear stratification of the community with depth and three main bacterial clusters: a surface cluster with bacterial communities from 1.5 m to 50 m depth, a cluster dominated by bacterial communities from 50 m depth, and a deep water cluster composed of bacterial communities from 200 m to 300 m depth (Fig. 2b).

The viral community assessed by the RAPD-PCR revealed in total 20 different OTUs ranging between 163 to 1065 bp (Fig. 3a). Only one OTU was found at St. 5 at 270 m depth and 2 viral OTUs were detected for St. 3 at 1.5 m and St. 4 at 300 m depth (Fig. 3a). The highest number of OTUs (8) was found at St. 2 at 100 m depth. The 554 bp viral OTU was the most abundant viral OTU, present in 60% of the samples. The number of OTUs was not related to the location of the station or to depth. As for the bacterial community, the Jaccard similarity analysis of the RAPD-PCR fingerprints of the viral community revealed a stratification with depth albeit not as surface cluster comprising the majority of the viral communities from 1.5 m depth, an pronounced as

Table 3. Prokaryotic, viral parameters and particulate organic carbon in samples collected at the three depth layers (Surface, 20-100 m and 200-300 m) in the Kongsfjorden (Ny-Alesund) over a four-week investigation period (Abbreviation as in Table 1).

	Surface					20-100 m					200-300 m				
	Avg	SD	min	max	n	Avg	SD	min	max	n	Avg	SD	min	max	n
Week 1															
PA(x10^5 mL^{-1})	3.8	0.7	2.6	4.4	6	2.8	1.8	1.3	5.1	8	3.5	0.4	3.0	3.8	4
VA(x10^6 mL^{-1})	2.1	0.4	1.7	2.8	6	1.7	0.7	1.0	2.9	8	1.3	0.3	1.0	1.7	4
VPR	5.5	0.8	4.6	6.4	6	7.2	1.9	3.8	9.2	8	3.9	0.7	3.0	4.4	4
PHP(pmol leu L^{-1} h^{-1})	76.5	37.8	35.5	133.3	6	28.6	30.0	1.8	96.6	8	11.1	1.8	9.1	13.2	4
POC (mgC/L)	0.24	0.05	0.21	0.34	6	0.15	0.03	0.12	0.21	8	0.10	0.01	0.09	0.11	4
%HNA	41.3	7.8	27.7	51.1	6	38.8	10.8	25.1	55.3	8	57.3	12.0	39.7	65.5	4
%High VLP	8.6	1.1	7.0	9.6	6	13.4	3.0	7.6	16.5	8	16.5	2.2	14.3	19.4	4
%MediumVLP	29.9	4.6	24.6	38.1	6	32.3	5.1	25.6	41.9	8	38.7	9.4	30.8	51.2	4
% Low VLP	62.5	5.1	53.6	69.0	6	55.3	6.8	47.3	67.4	8	45.8	11.6	29.7	54.8	4
Week 2															
PA(x10^5 mL^{-1})	10.0	2.9	5.2	12.8	8	4.9	1.4	2.5	7.2	10	4.2	0.6	3.7	5.2	6
VA(x10^6 mL^{-1})	4.0	1.8	1.6	6.2	8	3.0	0.6	2.0	3.7	10	2.5	0.6	2.0	3.2	6
VPR	3.8	0.9	2.4	4.8	8	6.4	1.3	4.6	8.5	10	5.8	0.7	5.2	7.0	6
PHP(pmol leu L^{-1} h^{-1})	154.8	50.2	95.2	265.2	8	35.6	9.9	19.2	52.2	10	18.8	6.6	12.6	29.6	6
POC mgC/L	0.27	0.06	0.19	0.37	8	0.12	0.03	0.08	0.20	10	0.11	0.01	0.10	0.12	6
%HNA	66.2	5.6	54.6	71.5	8	56.5	7.0	42.2	67.5	10	61.9	5.9	52.2	67.8	6
%High VLP	7.9	4.2	4.5	15.2	8	9.1	2.1	5.5	11.2	10	10.8	0.7	9.8	11.7	6
%MediumVLP	29.2	4.7	24.6	36.8	8	31.5	3.5	25.7	37.5	10	30.8	2.5	27.6	34.0	6
% Low VLP	63.9	8.7	49.1	71.8	8	60.4	5.1	54.5	69.3	10	58.7	3.4	54.4	63.7	6
Week 3															
FA(x10^5 mL^{-1})	10.8	2.0	8.6	13.9	8	8.0	1.4	5.7	10.8	10	4.7	0.4	4.3	5.1	6
VA(x10^6 mL^{-1})	5.5	1.9	3.4	8.4	8	3.3	0.7	2.5	4.4	10	2.6	0.5	2.0	3.4	6
VPR	5.0	1.2	3.4	6.5	8	4.1	0.5	3.4	4.9	10	5.6	1.1	4.3	7.2	6
PHP(pmol leu L^{-1} h^{-1})	103.0	30.1	69.2	143.1	8	63.6	28.5	30.7	128.2	10	13.2	7.7	0.4	20.1	6
POC (mgC/L)	0.18	0.03	0.14	0.22	8	0.13	0.05	0.09	0.22	10	0.11	0.03	0.07	0.16	6
%HNA	59.3	3.1	55.3	63.5	8	62.0	1.5	59.7	64.3	10	61.4	5.6	52.5	67.4	6
%High VLP	6.0	1.9	3.8	10.1	8	8.1	1.2	6.1	10.6	10	10.4	2.5	6.9	13.5	6
%MediumVLP	25.1	5.2	18.7	36.1	8	28.2	2.4	22.7	32.0	10	30.6	5.2	23.7	35.6	6
% Low VLP	69.8	6.7	55.9	78.4	8	64.6	3.1	60.2	70.6	10	59.3	8.3	50.1	69.9	6
Week 4															
PA(x10^5 mL^{-1})	15.6	1.0	14.1	17.0	7	12.9	4.1	7.7	19.2	9	5.3	0.5	4.5	5.7	5
VA(x10^6 mL^{-1})	5.5	0.8	3.7	6.1	7	3.9	0.6	3.0	4.9	9	2.4	0.2	2.1	2.6	5
VPR	3.6	0.6	2.4	4.3	7	3.1	0.6	2.2	3.9	9	4.5	0.2	4.3	4.7	5
PHP(pmol leu L^{-1} h^{-1})	240.2	64.8	136.0	326.2	7	116.1	52.4	46.0	212.3	9	30.4	7.1	24.6	39.4	5
POC (mgC/L)	0.24	0.05	0.18	0.34	7	0.16	0.04	0.11	0.22	9	0.12	0.04	0.08	0.19	5
%HNA	69.8	3.8	66.1	75.8	7	66.8	4.7	58.4	74.0	9	66.0	4.6	58.7	71.4	5
% High VLP	7.2	1.2	5.9	9.0	7	9.1	1.2	7.2	10.5	9	13.0	0.5	12.4	13.7	5
% Medium VLP	29.7	3.2	25.2	34.7	7	31.6	1.6	28.0	33.8	9	37.8	3.1	34.0	40.7	5
% Low VLP	64.0	4.7	56.9	70.0	7	60.4	2.5	57.2	65.7	9	49.5	4.2	44.7	54.9	5

Average, Standard Deviation (SD) and range (Min-Max value) are indicated for all the parameters.

Table 4. Lytic and lysogenic viral production and viral decay rate sampled at different stations and depths in the Kongsfjorden (Ny-Ålesund).

Station	Date	Depth (m)	Lytic VP ($x10^5$ $mL^{-1}h^{-1}$)	Lysogenic VP ($x10^5$ $mL^{-1}h^{-1}$)	Viral Decay ($x10^3$ $mL^{-1}h^{-1}$)	r^2
St.1	24/6/08	1.5	1	n.d.	3.7	0.6
St.1	24/6/08	20	0.8	n.d.	1.4	0.6
St.1	24/6/08	50	0.9	n.d.	3.2	0.8
St.4	11/6/08	3	0.6	0.3	n.d.	n.d.
St.4	11/6/08	250	0.6	2.9	n.d.	n.d.
St.4	11/6/08	300	1.5	0.06	5.2	0.8
St.5	16/6/08	1.5	2.9	n.d.	2.2	0.7
St.5	16/6/08	50	n.d.	n.d.	3.4	0.6
St.5	16/6/08	280	0.4	0.2	n.d.	n.d.
St.7	1/7/08	1.5	3.5	n.d.	3.2	0.8
St.7	1/7/08	50	n.d	n.d.	n.d.	n.d.
St.7	1/7/08	290	0.5	n.d.	3.4	0.5

nd, not detectable
r^2= coefficient of determination of the viral decay rate

for bacteria (Fig. 3b). At least three viral community clusters were distinguishable: intermediate water cluster consisting of the viral communities from 20 and 50 m depth, and a deep water cluster consisting mainly of the viral communities from 270 m and 290 m depth (Fig. 3b). The bacterial and viral communities were not significant related to biotic and or abiotic parameters (DISTLM forward test $p>0.1$)

Biotic and abiotic parameters determining water column variability as revealed by PCA.

The PC1 and the PC2 explained 79.5% of the variation; the main contribution to the PC1 was depth and temperature (Eigenvector=0.452 and -0.439, respectively) while the main contribution to PC2 was time (Eigenvector=0.637) (Fig. 4). A clear distribution of the samples over depth, temperature and time was found. The samples corresponding to the different sampling dates were distributed along the PC2 axis which, as mentioned above, was associated to time, while the samples corresponding to different depths and temperature were mostly distributed along the PC1 axis (Fig. 4).

Discussion

Environmental variability in the coastal Arctic during the spring to summer transition.

The decrease in salinity and density in the surface layers (Fig. S1b, Table 1, S1) during the spring to summer transition period (June-July 2008) indicates enhanced freshwater input originating from melting ice and snow into the fjord. The surface layers and the stations located close to the coast were more subjected to increasing temperature and decreasing salinity than the deep waters. The

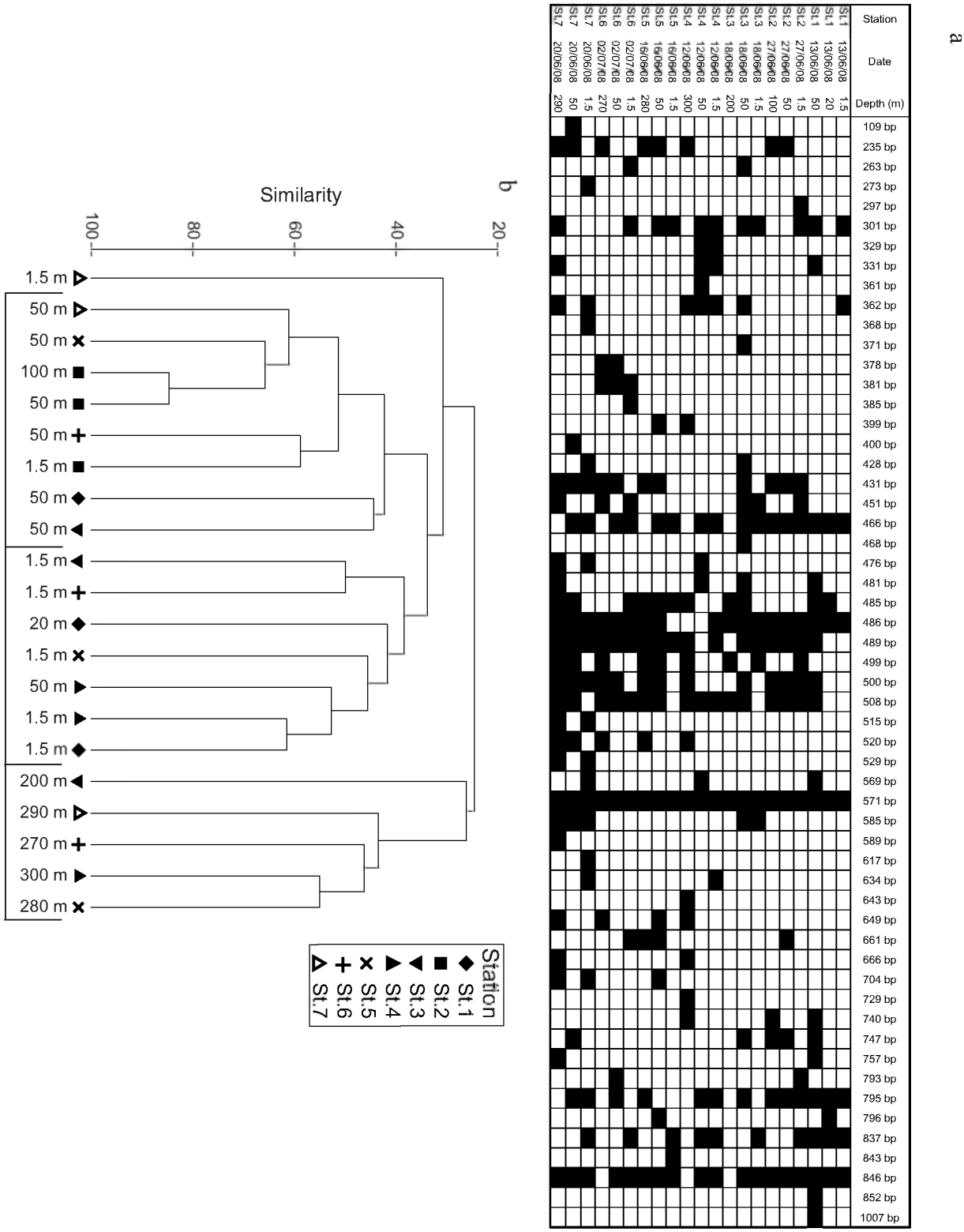

Figure 2. Bacterial community composition as revealed by ARISA (Automated Ribosomal Intergenic Spacer Analysis). Distribution of the presence/absence of OTUs at the stations and depths sampled. Jaccard cluster analyses of the bacterial OTUs based on the ARISA fingerprints.

concentration of particulate organic carbon (POC) was negatively correlated with salinity and depth (Table 2), suggesting that the majority of particles in the surface waters are of terrestrial origin in the coastal Arctic during the melting period of the snow and ice.

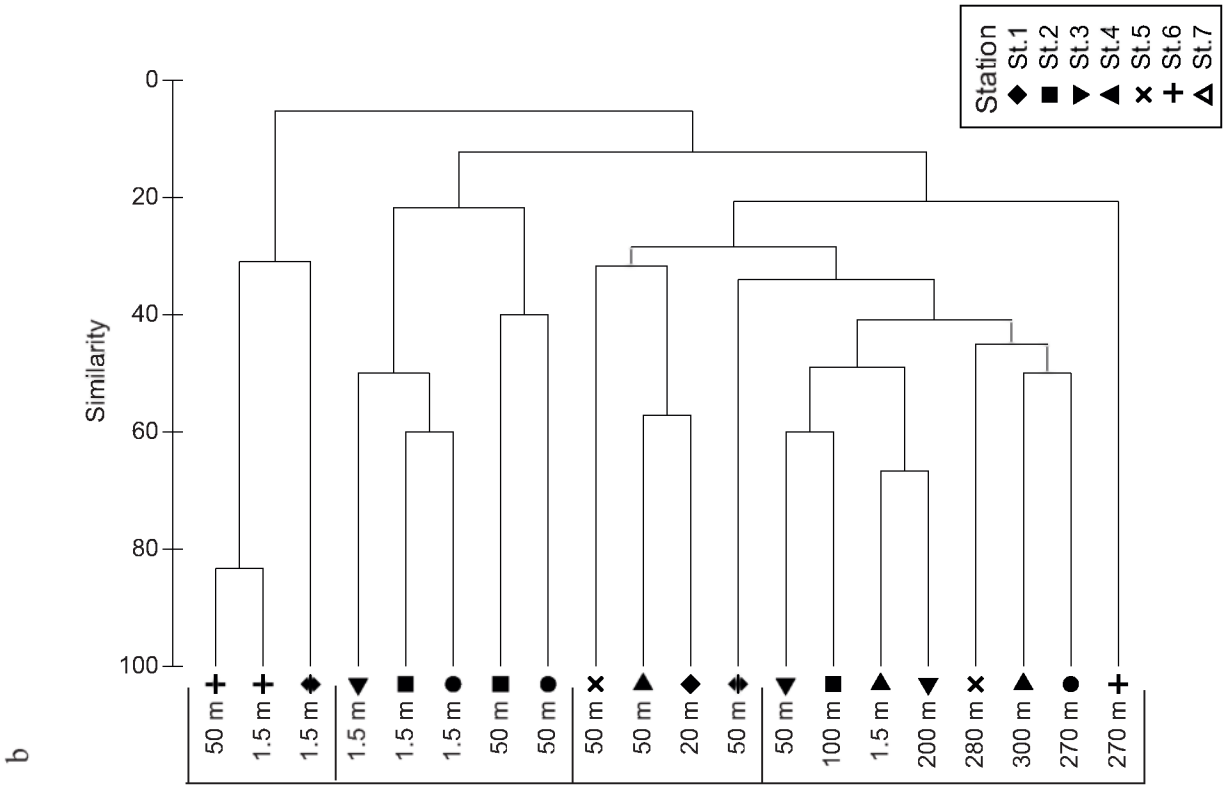

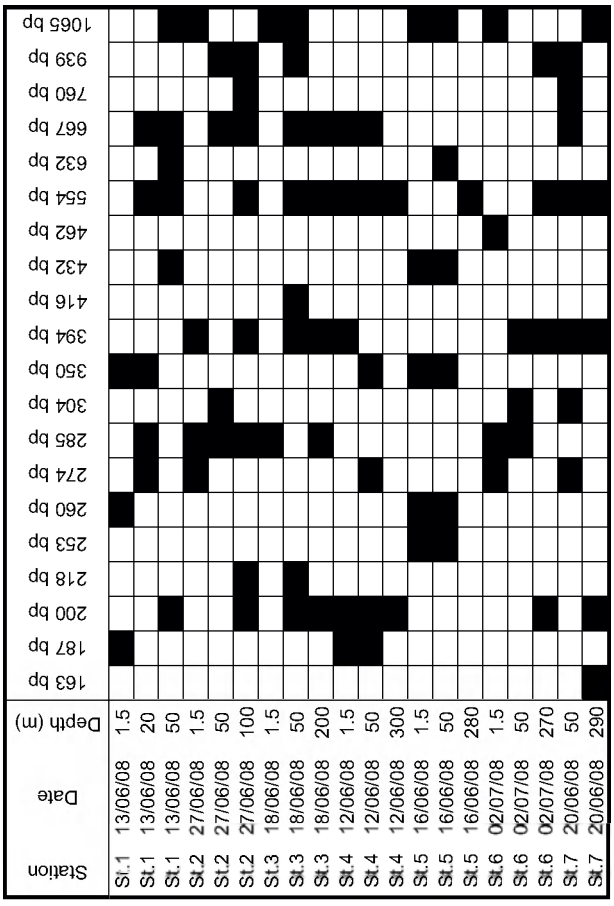

Figure 3. Viral community composition as revealed by RAPD-PCR (Randomly Amplified Polymorphic DNA–PCR). Distribution of the viral OTUs at the stations and depths sampled. Jaccard cluster analyses of the viral OTUs based on the RAPD-PCR fingerprints.

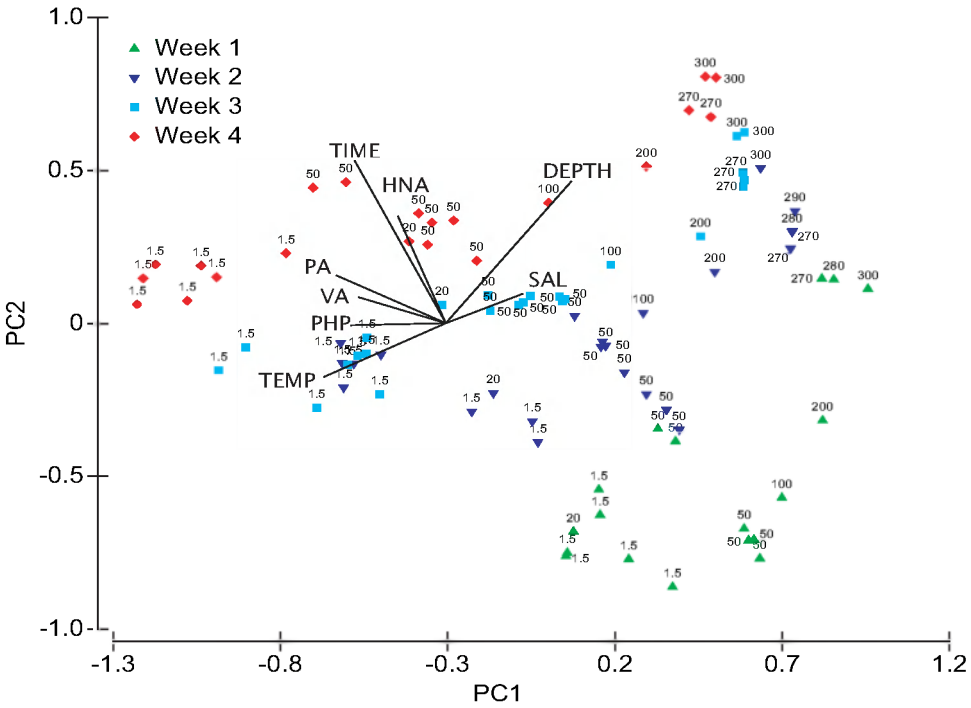

Figure 4. Principal Component Analyses (PCA) of the variability of the biotic and abiotic parameters over time at different depths. The PC1 and PC2 explained 53% and 26%, respectively. Abbreviation as Table 2.

Variability of prokaryotic and viral parameters over time.

The prokaryotic and viral variables were mainly related to time and depth (Table 1, 2, 3, Fig. S2). The prokaryotic and viral parameters changed during the spring to summer transition period throughout the water column, although changes in these parameters were less pronounced in the deeper layers than in the surface waters.

The prokaryotic and viral abundance generally increased over time during the spring to summer transition, probably associated to the increase in temperature and the proliferation of the phytoplankton and the associated release of freshly produced DOM by the blooming phytoplankton. The prokaryotic abundance we report here is comparable to the abundance reported for other coastal Arctic areas (Bano & Hollibaugh, 2002, Kirchman et al., 2007). The viral abundance, however, is one order of magnitude lower than reported for temperate coastal systems (Winter et al., 2004, Parada et al. 2008, Winget & Wommack, 2009) and Antarctic waters (Guixa-Boixereu et al., 2002) resulting also in low viral to prokaryotic ratio (VPR) (Magagnini et al. 2007, De Corte et al., 2010). The low abundance of viruses might be due to the scavenging of viruses by suspended inorganic particles introduced into the coastal Arctic via the run-off from the adjacent land and by organic detrital particles derived from phytoplankton blooms (Schoemann et al., 2005). The low viral abundance generally observed in the presence of high suspended particle load might be caused not only by adsorption to suspended particles but also by a high dissolved aminopeptidase

activity released by particle-associated bacteria, capable of cleaving the proteins of the viral capsid (Simon et al., 2002).

The viral abundance increased over time coinciding with the increase in prokaryotic abundance (Table 3). The increase of the viral abundance, however, was not as pronounced as the increase of prokaryotic abundance. Consequently, the viral to prokaryote abundance ratio (VPR) decreased during the spring-summer transition period in the surface and intermediate water layers (Table 3).

The heterotrophic prokaryotic production rates obtained in this study are similar to those determined in a previous study in coastal Artic waters during summer (Vallières et al., 2008) and exhibited pronounced seasonal variability and vertical stratification. Similar to the differences in the increase in abundance between prokaryotes and viruses at the onset of the summer season, the increase in heterotrophic prokaryotic production was higher than the concomitant increase in viral production, suggesting a weak link between these two microbial components in the coastal Artic, at least during this period of the year.

The positive correlation between the % HNA prokaryotes and prokaryotic production and abundance in the surface and intermediate layers suggests that the high nucleic acid prokaryotes mostly consist of active cells, in agreement with previous studies (Gasol et al., 1999, Yanada et al., 2000, Lebaron et al., 2001), but in contrast to others showing that LNA cells might have equal or even higher growth rates than the HNA cells (Zubkov et al., 2001, Longnecker et al., 2006, Mary et al., 2006). Bouvier et al., (2007) put forward a different hypothesis to explain the nature of the HNA and LNA prokaryotes, in which parts of the populations are dynamically exchanging between the two fractions.

In contrast to prokaryotes, viral populations distinguished by FCM were less variable over time, moreover the high and low fluorescence significantly changed with depth. The low fluorescence population dominated the viral community in terms of abundance over the entire investigation period in the coastal Arctic waters as reported previously for coastal and temperate waters as well (Table 1, 2, 3) (Marie et al., 1999, Brussaard, 2004, Pan et al., 2007).

Viral production and decay.

Viral production and decay rates were only assessed at selected stations and depths. As described above, viral production exhibited a similar vertical stratification as prokaryotic heterotrophic production and abundance, and was significantly correlated with viral abundance ($r=0.60$, $p=0.059$) (Table 3, 4). The lytic viral production was one order of magnitude lower than reported for temperate coastal waters (Wilhelm et al., 2002a) but similar to a previous study in the North Sea during the spring season (Winter et al., 2005b). Lysogeny was not detected in 8 out of 12 incubations (Table 4). If detectable, however, it was of similar magnitude as lytic production.

The viral decay rates were similar to a previous study conducted at comparable temperature range to our viral decay experiments in the meso- and bathypelagic layers of the North Atlantic (Parada et al., 2007). This similarity and the discrepancy to decay rates determined in the surface waters of coastal and open temperate regions (Parada et al., 2007) suggest that one of the main factors

affecting viral decay is temperature (De Paepe & Taddei, 2006). It appears that low temperature favors the persistence of viruses.

Another factor, which might influence viral production and decay rates in the surface waters is the prolonged exposure time to solar radiation during the Arctic summer. This solar radiation might change interactions between viruses and their host drastically. Our study was carried out during continuous light conditions with a daily dose of total ultraviolet radiation ranging between 1.0 and 1.6 $x10^3$ J m^{-2} during the sampling period (Fig. S3) and increasing stratification, with warm water at the surface and low density water coming from the glaciar in the top layers (Fig. S1a, b). The relatively lower increase in the viral abundance as compared to the prokaryotic abundance might be related to the increase in the total radiation dose during the study period. In surface layers, radiation affects viruses relatively more than prokaryotes (Suttle & Feng, 1992, Weinbauer et al., 1999, Wilhelm et al., 2002b, Wilhelm et al., 2003), the latter having efficient repair mechanisms to repair DNA damage (Kaiser & Herndl, 1997, Arrieta et al., 2000). The mechanism of photoreactivation in marine viral communities (Weinbauer et al., 1997) might not compensate the UV damage of viral DNA in the surface waters of the Arctic Ocean.

Bacterial and viral community composition.

In our study, the bacterial community is characterized by a relatively low number of OTUs (56) compared to the North Atlantic (Hewson et al., 2006) and the Eastern Mediterranean Sea (Yokokawa et al., 2010). Low diversity was also found in clone libraries collected during the sampling period (data not shown) The number of OTUs did not significantly differ, neither between stations or depths, albeit the community composition was clearly stratified (Fig. 2b). Moreover, only one OTU was ubiquitously present, indicating a drastic change of the bacterial community along different stations and depths (Fig. 2). The unique OTUs were randomly distributed between stations and depths amounting to 14% of the total number of OTUs (Fig. 2a, 3a).

The number of viral OTUs obtained by the RAPD-PCR was lower than in the subtropical Atlantic Ocean (De Corte et al., 2010) and in Chesapeake Bay surface waters using Pulsed Field Gel Electrophoresis (Wommack et al., 1999a). The viral and bacterial OTUs significantly co-varied throughout the depth profiles (ANCOVA on rank $p=0.21$, the slopes are not significantly different). This could be interpreted as a tight coupling between viruses and bacteria, albeit the low resolution of ARISA and RAPD-PCR prevents any firm conclusions. Similar tight coupling between viruses and their host was also suggested in nutrient manipulated mesocosm experiments in the Catalan coast (Sandaa et al., 2009).

In summary, the coastal Arctic waters exhibit major changes in the prokaryotic and viral parameters during the transition period from spring to summer. The physico-chemical characteristics drastically changed during the investigation period, especially in the surface layers, and the biological parameters changed accordingly. Apparently, the viral and bacterial communities are strongly affected by the changes in the environmental conditions. Two main factors appear to

drive these changes in the environmental characteristics, time and depth, both resulting mainly in temperature changes (Fig. 4). The two communities were highly stratified and tightly coupled, as suggested by the low OTU numbers and by the co-variation of the viral and bacterial OTU numbers through the water column, although the prokaryotic and viral abundance and production rates indicate a weak link between the two communities. These apparently contrasting results might be explained by the differential effect of the UV radiation on the prokaryotic and viral production, and/or the high particle load. The high particle load associated with the melting of ice and snow from the surrounding glaciers and the high radiation conditions during the spring and summer might play a key role in the structuring of the microbial food web in the coastal Arctic regions.

Supplementary Information

Materials and Methods

Inorganic nutrient analyses. The concentrations of inorganic nutrients (PO_4^{3-} NH_4^+, NO_3^-, NO_2^-) were determined immediately after collection of the samples and gentle filtration through 0.2 µm filters (Acrodisc, Gelman Science) in a TRAACS autoanalyzer system. Inorganic PO_4^{3-} was determined via the molybdenum blue complex at 880 nm according to Murphy and Riley, (1962). NH_4^+ was detected with the indo-phenol-blue-method (pH 10.5) at 630 nm (Helder and de Vries, 1979). NO_2^- was detected after diazotation with sulphanilamide and *N*-(1-naphtyl)-ethylene diammonium-dichloride as the reddish-purple dye complex at 540 nm (Parsons et al., 1984). NO_3^- was reduced in a copper cadmium coil to nitrite (with imidazole as a buffer) and then measured as nitrite.

Particulate organic carbon. Particulate organic carbon (POC) was collected on precombusted (24 h, 450°C) glass 193 fiber filters (Whatman GF/F, 25mm). Filters were dried and stored. The POC was quantified using a model CHN 2400 analyzer (Perkin Elmer 2400, Waltham, MA) following Pregl, (1924) and Sharp, (1974).

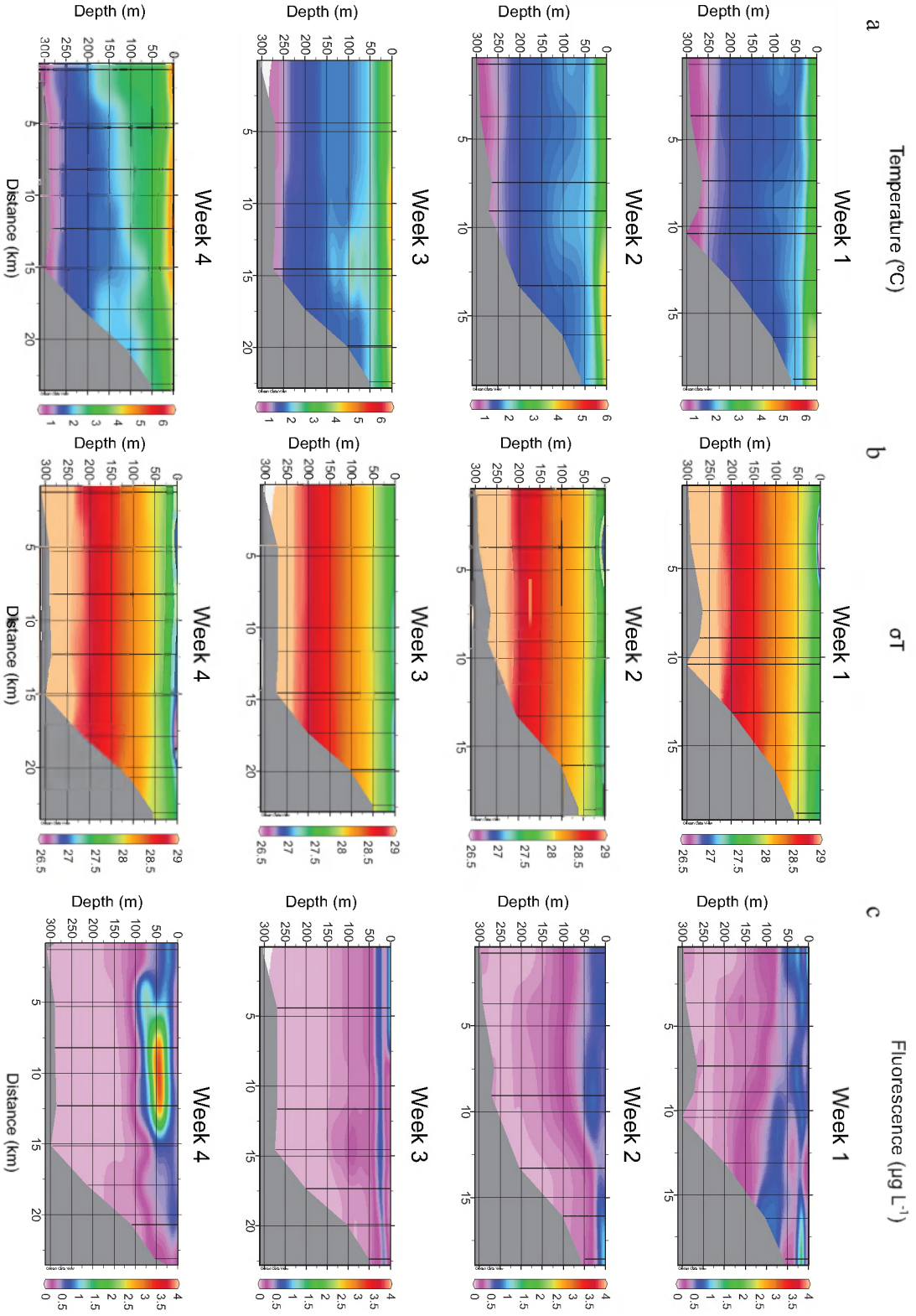

Figure S1. Physico-chemical parameters measured along the fjord at different depths during the four weeks of sampling; (a) Temperature, (b) density, (c) fluorescence.

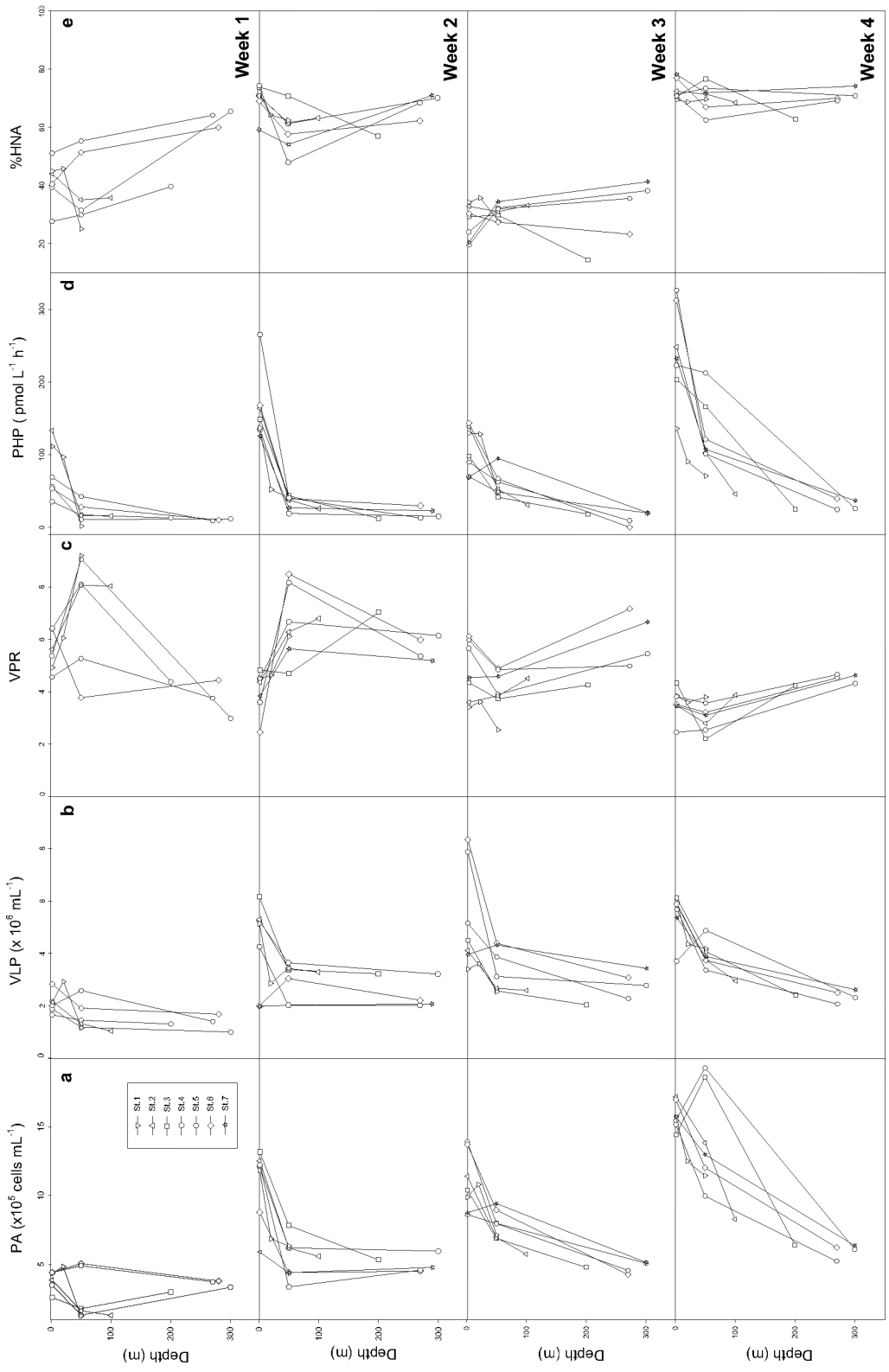

Figure S2. Biotic parameters measured along the fjord at different depths during the four weeks period. (a) Prokaryotic abundance (PA), (b) Virus-like particles (VLP), (c) Virus to Prokaryote Ratio (VPR), (d) Prokaryotic heterotrophic production (PHP), (e) Percentage of high nucleic acid content prokaryotes (%HNA).

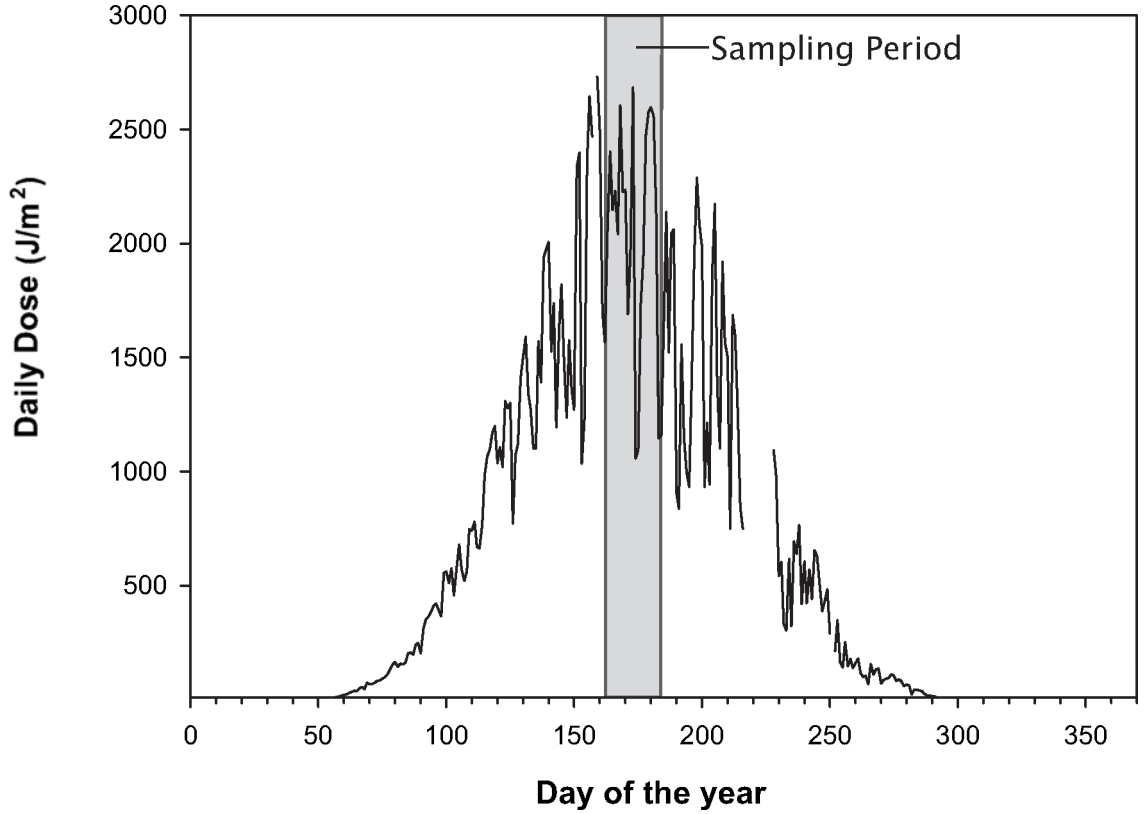

Figure S3. Total ultraviolet radiation measured during 2008 (data obtained from Norwegian Institute for Air Research and Norwegian Radiation Protection Authority).

Table S1. Physico-chemical parameters sampled at the three depth layers (Surface, 20-100 m and 200-300 m) in the Kongsfjorden (Ny-Ålesund) over the four-week investigation period

		Surface					20-100 m					200-300 m				
		Avg	SD	min	max	n	Avg	SD	min	max	n	Avg	SD	min	max	n
Week 1	Temp. (°C)	3.4	0.5	2.9	4.1	6	2.1	0.7	1.6	3.8	8	1.0	0.3	0.8	1.4	4
	Salinity	34.6	0.1	34.5	34.7	6	34.7	0.1	34.5	34.8	8	34.9	0.0	34.8	34.9	4
	sT	27.5	0.1	27.4	27.6	6	28.0	0.2	27.5	28.3	8	29.2	0.3	28.8	29.4	4
	Fluor. (µg L^{-1})	0.31	0.12	0.14	0.48	6	0.61	0.42	0.22	1.41	8	0.05	0.02	0.04	0.08	4
	PO_4^+ (µM)	0.09	0.02	0.08	0.12	6	0.20	0.10	0.08	0.38	8	0.64	0.11	0.48	0.70	4
	NH_4^+ (µM)	0.17	0.03	0.13	0.19	6	1.07	0.57	0.19	1.96	8	2.16	0.55	1.70	2.95	4
	NO_2^- (µM)	0.03	0.01	0.02	0.04	6	0.03	0.02	0.02	0.08	8	0.12	0.03	0.07	0.15	4
	NO_3^- (µM)	0.11	0.05	0.05	0.17	6	0.89	1.26	0.06	3.66	8	6.87	2.09	3.76	8.28	4
Week 2	Temp. (°C)	3.8	0.4	3.3	4.2	8	1.9	0.7	1.4	3.9	10	0.9	0.2	0.8	1.4	6
	Salinity	34.4	0.2	34.2	34.6	8	34.7	0.1	34.4	34.8	10	34.9	0.0	34.8	34.9	6
	sT	27.4	0.2	27.2	27.6	8	28.0	0.2	27.4	28.3	10	29.2	0.2	28.8	29.4	6
	Fluor. (µg L^{-1})	0.33	0.15	0.18	0.60	8	0.23	0.30	0.03	1.05	10	0.03	0.01	0.02	0.04	6
	PO_4^+ (µM)	0.11	0.07	0.06	0.24	8	0.35	0.10	0.21	0.49	10	0.66	0.07	0.54	0.75	6
	NH_4^+ (µM)	0.36	0.24	0.15	0.76	8	2.30	0.50	1.33	3.18	10	2.46	0.50	2.07	3.45	6
	NO_2^- (µM)	0.06	0.04	0.02	0.15	8	0.05	0.02	0.03	0.08	10	0.13	0.04	0.07	0.19	6
	NO_3^- (µM)	0.52	0.65	0.02	1.73	8	2.07	1.23	0.76	3.98	10	6.99	1.48	4.23	8.16	6
Week 3	Temp. (°C)	5.2	0.9	3.7	6.3	8	2.4	0.4	1.8	3.1	10	1.1	0.3	0.8	1.5	6
	Salinity	34.2	0.2	33.9	34.5	8	34.8	0.1	34.6	34.9	10	34.9	0.0	34.8	34.9	6
	sT	27.0	0.2	26.6	27.3	8	28.0	0.1	27.8	28.3	10	29.2	0.2	28.8	29.4	6
	Fluor. (µg L^{-1})	1.01	2.43	0.04	7.02	8	0.90	1.67	0.07	5.48	10	0.02	0.00	0.02	0.02	6
	PO_4^+ (µM)	0.11	0.03	0.09	0.19	8	0.24	0.08	0.11	0.42	10	0.65	0.07	0.52	0.71	6
	NH_4^+ (µM)	0.43	0.27	0.25	1.09	8	1.66	0.63	0.45	2.98	10	2.74	0.49	2.46	3.74	6
	NO_2^- (µM)	0.08	0.05	0.02	0.17	8	0.04	0.01	0.01	0.06	10	0.14	0.04	0.08	0.21	6
	NO_3^- (µM)	0.36	0.38	0.04	1.28	8	1.04	0.65	0.09	2.43	10	6.89	1.69	3.53	8.09	6
Week 4	Temp. (°C)	5.4	0.8	3.9	6.3	7	2.7	0.4	1.9	3.1	8	1.1	0.3	0.9	1.6	5
	Salinity	34.0	0.4	33.3	34.4	7	34.8	0.0	34.7	34.9	8	34.9	0.0	34.8	34.9	5
	sT	26.8	0.3	26.3	27.3	7	28.0	0.1	27.9	28.3	8	29.2	0.2	28.8	29.4	5
	Fluor. (µg L^{-1})	0.18	0.10	0.08	0.32	7	1.41	1.75	0.05	5.48	8	0.02	0.00	0.01	0.02	5
	PO_4^+ (µM)	0.11	0.03	0.08	0.14	7	0.27	0.11	0.12	0.42	8	0.69	0.07	0.56	0.74	5
	NH_4^+ (µM)	0.44	0.17	0.30	0.77	7	1.64	0.65	0.45	2.77	8	3.23	0.35	2.81	3.62	5
	NO_2^- (µM)	0.03	0.02	0.01	0.07	7	0.06	0.04	0.02	0.13	8	0.16	0.05	0.08	0.22	5
	NO_3^- (µM)	0.35	0.24	0.05	0.66	7	1.53	1.40	0.15	3.72	8	7.04	1.66	4.09	4.09	5

Acknowledgments

We thank A. K. Olstad, captain of the Teisten, and the lab manager E. Austerheim from Kings Bay AS, for their support and splendid atmosphere on board. T.Y. was supported by the Japanese Society for the Promotion of Science (JSPS) Postdoctoral Fellowship for research abroad, E.S. was supported by the Earth and Life Science Division of the Dutch Science Foundation (ALW-NWO). D.D.C. received a fellowship of the Univ. of Groningen. Lab work was supported by the project 'Pelagic Archaea in the Changing Coastal Arctic (PACCA)', financed by an ALW-IPY project (NWO). Data of the total solar radiation were obtained from the Norwegian Institute for Air Research (NILU, www.nilu.no) and the Norwegian Radiation Protection Authority (NRPA, www.nrpa.no).

References

Anderson M, Ford R, Feary D, Honeywill C. (2004). Quantitative measures of sedimentation in an estuarine system and its relationship with intertidal soft-sediment infauna. *Mar Ecol-Prog Ser* **272**:33-48.

Angly FE, Felts B, Breitbart M, Salamon P, Edwards RA, Carlson C, Chan AM, Haynes M, Kelley S, Liu H, Mahaffy JM, Mueller JE, Nulton J, Olson R, Parsons R, Rayhawk S, Suttle CA, Rohwer F. (2006). The marine viromes of four oceanic regions. *PLoS Biology* **4**:2121-2131.

Arrieta JM, Weinbauer MG, Herndl GJ. (2000). Interspecific variability in sensitivity to UV radiation and subsequent recovery in selected isolates of marine bacteria. *Appl Environ Microbiol* **66**:1468-1473.

Bano N, Hollibaugh JT. (2002). Phylogenetic composition of bacterioplankton assemblages from the Arctic Ocean. *Appl Environ Microbiol* **68**:505-518.

Borneman J, Triplett EW. (1997). Molecular microbial diversity in soils from eastern Amazonia: Evidence for unusual microorganisms and microbial population shifts associated with deforestation. *Appl Environ Microbiol* **63**:2647-2653.

Brussaard CPD. (2004). Optimization of procedures for counting viruses by flow cytometry. *Appl Environ Microbiol* **70**:1506-1513.

Cardinale M, Brusetti L, Quatrini P, Borin S, Puglia A, Rizzi A, Zanardini E, Sorlini C, Corselli C, Daffonchio D. (2004). Comparison of different primer sets for use in automated ribosomal

intergenic spacer analysis of complex bacterial communities. *Appl Environ Microbiol* **70**:6147-6156.

Choi DH, Hwang CY, Cho BC. (2003). Comparison of virus- and bacterivory-induced bacterial mortality in the eutrophic Masan Bay, Korea. *Aquat Microb Ecol* **30**: 117-125.

De Corte D, Sintes E, Winter C, Yokokawa T, Reinthaler T, Herndl GJ. (2010). Links between viral and prokaryotic communities throughout the water column in the (sub)tropical Atlantic Ocean. *ISME J* **4**:1431-1442.

De Paepe M, Taddei F. (2006). Viruses' life history: Towards a Mechanistic Basis of a Trade-off between survival and reproduction among phages. *PLoS Biol* **4**:1248-1256

Del Giorgio PA, Bird DF, Prairie YT, Planas D. (1996). Flow cytometric determination of bacterial abundance in lake plankton with the green nucleic acid stain SYTO 13. *Limnol Oceanogr* **41**:1169-1179.

Fuhrman JA. (2000). Impact of viruses on bacterial processes. In: Kirchmam DL (ed) *Microbial Ecology of the Oceans*. John Wiley & Sons: New York, p 327-350.

Gasol JM, Zweifel UL, Peters F, Fuhrman JA, Hagstrom A. (1999). Significance of size and nucleic acid content heterogeneity as measured by flow cytometry in natural planktonic bacteria. *Appl Environ Microbiol* **65**:4475-4483.

Gowing MM, Riggs BE, Garrison DL, Gibson AH, Jeffries MO. (2003). Large viruses in Ross Sea late autumn pack ice habitats (vol 241, pg 1, 2002). *Mar Ecol-Prog Ser* **254**:313-313.

Guixa-Boixereu N, Vaque D, Gasol JM, Sanchez-Camara J, Pedros-Alio C. (2002). Viral distribution and activity in Antarctic waters. *Deep Sea Res Pt II* **49**:827-845.

Hammer Ø, Harper DAT, Ryan PD. (2001). PAST: Paleontological statistics software package for education and data analysis. *Palaeontologia Electronica* **4**:9.

Helder W, Vries R de, (1979). An automatic phenol-hypochlorite method for the detection of ammonia in sea- and brackish waters. *Neth J Sea Res* **13**:154-160.

Hewson I, Wingett DM, Williamson KE, Fuhrman JA, Wommack KE. (2006). Viral and bacterial assemblage covariance in oligotrophic waters of the West Florida Shelf (Gulf of Mexico). *J Mar Biol Ass UK* **86**: 591-603.

Hewson I, Steele JA, Capone DG, Fuhrman JA. (2006). Remarkable heterogeneity in meso- and bathypelagic bacterioplankton assemblage composition. *Limnol Oceanogr* **51**:1274-1283.

Hodges LR, Bano N, Hollibaugh JT, Yager PL. (2005). Illustrating the importance of particulate organic matter to pelagic microbial abundance and community structure - an Arctic case study. *Aquat Microb Ecol* **40**:217-227.

Jacquet S, Bratbak G. (2003). Effects of ultraviolet radiation on marine virus-phytoplankton interactions. *FEMS Microbiol Ecol* **44**:279-289.

Kaiser E, Herndl GJ. (1997). Rapid recovery of marine bacterioplankton activity after inhibition by UV radiation in coastal waters. *Appl Environ Microbiol* **63**:4026-4031.

Kirchman DL, Elifantz H, Dittel AI, Malmstrom RR, Cottrell MT. (2007). Standing stocks and activity of Archaea and Bacteria in the western Arctic Ocean. *Limnol Oceanogr* **52**:495-507.

Kirchman DL, Moran XAG, Ducklow H. (2009). Microbial growth in the polar oceans - role of temperature and potential impact of climate change. *Nat Rev Microbiol* **7**:451-459.

Lebaron P, Servais P, Agogue H, Courties C, Joux F. (2001). Does the high nucleic acid content of individual bacterial cells allow us to discriminate between active cells and inactive cells in aquatic systems? *Appl Environ Microbiol* **67**:1775-1782.

Longnecker K, Sherr BF, Sherr EB. (2006). Variation in cell-specific rates of leucine and thymidine incorporation by marine bacteria with high and with low nucleic acid content off the Oregon coast. *Aquat Microb Ecol* **43**:113-125.

Magagnini M, Corinaldesi C, Monticelli LS, De Domenico E, Danovaro R. (2007). Viral abundance and distribution in mesopelagic and bathypelagic waters of the Mediterranean Sea. *Deep Sea Res Pt I* **54**:1209-1220.

Maranger R, Bird DF. (1995). Viral abundance in aquatic systems - a comparison between marine and fresh-waters. *Mar Ecol-Prog Ser* **121**:217-226.

Marie D, Brussaard CPD, Thyrhaug R, Bratbak G, Vaulot D. (1999). Enumeration of marine viruses in culture and natural samples by flow cytometry. *Appl Environ Microbiol* **65**:45-52.

Mary I, Heywood JL, Fuchs BM, Amann R, Tarran GA, Burkill PH, Zubkov MV. (2006). SAR11

dominance among metabolically active low nucleic acid bacterioplankton in surface waters along an Atlantic meridional transect. *Aquat Microb Ecol* **45**:107–113

Middelboe M, and Jorgensen NOG. (2006). Viral lysis of bacteria: an important source of dissolved amino acids and cell wall compounds. *J Mar Biol Assoc Uk* **86**: 605-612.

Middelboe M, and Lyck PG. (2002). Regeneration of dissolved organic matter by viral lysis in marine microbial communities. *Aquat Microb Ecol* **27**: 187-194.

Middelboe M, Riemann L, Steward GF, HansenvV, Nybroe O. (2003). Virus-induced transfer of organic carbon between marine bacteria in a model community. *Aquat Microb Ecol* **33**: 1-10.

Middelboe M, Nielsen TG, Bjornsen PK. (2002). Viral and bacterial production in the North Water: in situ measurements, batch-culture experiments and characterization and distribution of a virus-host system. *Deep Sea Res Pt II* **49**:5063-5079.

Murphy J, Riley JP. (1962). A modified single solution method for the determination of phosphate in natural waters. *Anal Chim Acta* **27**: 31-36.

Murray AG, Jackson GA. (1992). Viral dynamics: a model of the effect of size, shape, motion and abundance of single-celled planktonic organisms and other particles. *Mar Ecol-Prog Ser* **89**:103-116.

Ortmann AC, Lawrence JE, Suttle CA. (2002). Lysogeny and lytic viral production during a bloom of the cyanobacterium Synechococcus spp. *Microbial Ecol* **43**:225-231.

Pan LA, Zhang J, Zhang LH. (2007). Picophytoplankton, nanophytoplankton, heterotrohpic bacteria and viruses in the Changjiang Estuary and adjacent coastal waters. *J Plankton Res* **29**:187-197.

Parada V, Baudoux AC, Sintes E, Weinbauer MG, Herndl GJ. (2008). Dynamics and diversity of newly produced virioplankton in the North Sea. *ISME J* **2**:924-936.

Parada V, Sintes E, van Aken HM, Weinbauer MG, Herndl GJ. (2007). Viral abundance, decay, and diversity in the meso- and bathypelagic waters of the North Atlantic. *Appl Environ Microbiol* **73**:4429-4438.

Parsons T, Maita, Y, Lalli C, 1984. A Manual of chemical and biological methods for seawater analysis. Pergamon Press, Oxford, UK, 173 p.

Pregl, F (1924) Quantitative organic microanalysis. Translation from Fyleman E., edited by: Churchill, J. and A., London, 69 p.

Sandaa RA, Gomez-Consarnau L, Pinhassi J, Riemann L, Malits A, Weinbauer MG, Gasol JM, Thingstad TF (2009) Viral control of bacterial biodiversity - evidence from a nutrient-enriched marine mesocosm experiment. *Environ Microbiol* **11**: 2585-2597.

Sano E, Carlson S, Wegley L, Rohwer F. (2004). Movement of viruses between biomes. *Appl Environ Microbiol* **70**:5842-5846.

Schoemann V, Becquevort S, Stefels J, Rousseau W, Lancelot C. (2005). Phaeocystis blooms in the global ocean and their controlling mechanisms: a review. *J Sea Res* **53**:43-66

Sharp JH. (1974). Improved analysis for particulate organic carbon and nitrogen from seawater, *Limnol Oceanogr* **19**:984-989.

Simon M, Grossart HP, Schweitzer B, Ploug H. (2002). Microbial ecology of organic aggregates in aquatic ecosystems. *Aquat Microb Ecol* **28**:175-211.

Suttle CA, Feng C. (1992). Mechanisms and rates of decay of marine viruses in seawater. *Appl Environ Microb* **58**:3721-3729.

Vallières C, Retamal L, Ramlal P, Osburn CL, Vincent WF. (2008). Bacterial production and microbial food web structure in a large arctic river and the coastal Arctic Ocean. *J Mar Syst* **74**:756–773.

Weinbauer MG, Brettar I, Hofle MG. (2003). Lysogeny and virus-induced mortality of bacterioplankton in surface, deep, and anoxic marine waters. *Limnol Oceanogr* **48**:1457-1465

Weinbauer MG, Rassoulzadegan F. (2004). Are viruses driving microbial diversification and diversity? *Environ Microbiol* **6**:1-11.

Weinbauer MG, Wilhelm SW, Suttle CA, Garza DR. (1997). Photoreactivation compensates for UV damage and restores infectivity to natural marine virus communities. *Appl Environ Microbiol* **63**:2200-2205.

Weinbauer MG, Wilhelm SW, Suttle CA, Pledger RJ, Mitchell DL. (1999). Sunlight-induced DNA damage and resistance in natural viral communities. *Aquat Microb Ecol* **17**:111-120.

Wells LE, Deming JW. (2006a). Characterization of a cold-active bacteriophage on two psychrophilic marine hosts. *Aquat Microb Ecol* **45**:15-29.

Wells LE, Deming JW. (2006b). Effects of temperature, salinity and clay particles on inactivation and decay of cold-active marine Bacteriophage 9A. *Aquat Microb Ecol* **45**:31-39.

Wells LE, Deming JW. (2006c). Significance of bacterivory and viral lysis in bottom waters of Franklin Bay, Canadian Arctic, during winter. *Aquat Microb Ecol* **43**:209-221.

Wilhelm SW, Brigden SM, Suttle CA. (2002a). A dilution technique for the direct measurement of viral production: A comparison in stratified and tidally mixed coastal waters. *Microbial Ecol* **43**:168-173.

Wilhelm SW, Jeffrey WH, Dean AL, Meador J, Pakulski JD, Mitchell DL. (2003). UV radiation induced DNA damage in marine viruses along a latitudinal gradient in the southeastern Pacific Ocean. *Aquat Microb Ecol* **31**:1-8.

Wilhelm SW, Jeffrey WH, Suttle CA, Mitchell DL. (2002b). Estimation of biologically damaging UV levels in marine surface waters with DNA and viral dosimeters. *Photochem Photobiol* **76**:268-273.

Winget DM, Wommack KE. (2008). Randomly amplified polymorphic DNA PCR as a tool for assessment of marine viral richness. *Appl Environ Microbiol* **74**:2612-2618.

Winget DM, Wommack KE. (2009). Diel and daily fluctuations in virioplankton production in coastal ecosystems. *Environ Microbiol* **11**:2904-2914.

Winter C, Herndl GJ, Weinbauer MG. (2004). Diel cycles in viral infection of bacterioplankton in the North Sea. *Aquat Microb Ecol* **35**:207-216.

Winter C, Moeseneder MM, Herndl GJ (2001) Impact of UV radiation on bacterioplankton community composition. *Appl Environ Microbiol* **67**:665-672.

Winter C, Moeseneder MM, Herndl GJ, Weinbauer MG. (2008). Relationship of geographic distance, depth, temperature, and viruses with prokaryotic communities in the eastern tropical Atlantic Ocean. *Microbial Ecol* **56**:383-389.

Winter C, Smit A, Herndl GJ, Weinbauer MG. (2005a). Linking bacterial richness with viral

abundance and prokaryotic activity. *Limnol Oceanogr* **50**:968-977.

Winter C, Smit A, Szoeke-Denes T, Herndl GJ, Weinbauer MG. (2005b). Modelling viral impact on bacterioplankton in the North Sea using artificial neural networks. *Environ Microbiol* **7**:881-893.

Wommack KE, Ravel J, Hill RT, Chun JS, Colwell RR. (1999a). Population dynamics of Chesapeake bay virioplankton: Total-community analysis by pulsed-field gel electrophoresis. *Appl Environ Microbiol* **65**:231-240.

Wommack KE, Ravel J, Hill RT, Colwell RR. (1999b). Hybridization analysis of Chesapeake Bay virioplankton. *Appl Environ Microbiol* **65**:241-250.

Yanada M, Yokokawa T, Lee CW, Tanaka H, Kudo I, Maita Y. (2000). Seasonal variation of two different heterotrophic bacterial assemblages in subarctic coastal seawater. *Mar Ecol-Prog Ser* **204**:289-292.

Yokokawa T, De Corte D, Sintes E, Herndl GJ. (2010). Spatial patterns of bacterial abundance, activity and community composition in relation to water masses in the Eastern Mediterranean Sea. *Aquat Microb Ecol* **59**:185-195.

Zubkov MV, Fuchs BM, Burkill PH, Amann R. (2001). Comparison of cellular and biomass specific activities of dominant bacterioplankton groups in stratified waters of the Celtic Sea. *Appl Environ Microbiol* **67**:5210-5218.

Chapter 2

Links between viral and prokaryotic communities throughout the water column in the (sub)tropical Atlantic Ocean

Daniele De Corte, Eva Sintes, Christian Winter, Taichi Yokokawa, Thomas Reinthaler, Gerhard J. Herndl

Published in ISME Journal (2010) 4:1501-1529

Abstract

Viral and prokaryotic abundance, production and diversity were determined throughout the water column of the subtropical Atlantic Ocean to assess potential variations in the relation between viruses and prokaryotes. Prokaryotic abundance and heterotrophic activity decreased by one and three orders of magnitude, respectively, from the epi- to the abyssopelagic layer. While the lytic viral production decreased with depth, lysogenic viral production was variable throughout the water column and did not show any trend with depth. The bacterial, archaeal and viral community composition were depth-stratified as determined by the Automated Ribosomal Intergenic Spacer Analysis (ARISA), Terminal-Restriction Fragment Length Polymorphism (T-RFLP) and Randomly Amplified Polymorphic DNA–PCR (RAPD-PCR), respectively. Generally, the number of operational taxonomic units (OTUs) did not reveal consistent trends throughout the water column. The viral and prokaryotic abundance were strongly related with heterotrophic prokaryotic production, suggesting similar linkage strength between viral and prokaryotic communities from the lower epi- to the abyssopelagic layers in the Atlantic Ocean. Strikingly, the prokaryotic and viral parameters exhibited a similar variability throughout the water column down to the abyssopelagic layers suggesting that the dark ocean is an as dynamic system as the lower epipelagic layer. It also indicates that viruses are apparently playing a similar role for prokaryotic mortality in the dark oceanic realm as in surface waters. The more than twofold increase in bacterial OTUs from 2750m depth to >5000m depth and the concurrent decrease in viral OTUs, however, suggests that viruses might exhibit a wider host range in deep waters than in surface waters.

Introduction

Viruses play a key role in the biogeochemical processes of the ocean (Fuhrman, 1999; Suttle, 1999; Wilhelm & Suttle, 1999). Marine viruses may also control prokaryotic abundance and diversity (Thingstad & Lignell, 1997; Weinbauer & Rassoulzadegan 2004; Breitbart et al., 2008) and are agents of transfer of genetic material between microorganisms (transduction and transformation; Fuhrman, 2000).

There are two main viral life strategies: lysogeny and lysis (Ackermann & DuBow, 1987). These different strategies may have a different impact on the structure of the prokaryotic community. Lysogeny is considered to be an adaptation to low host abundance and/or activity since lysogeny has been reported to increase with depth, while the lytic cycle dominates at high host abundance and/or activity (Weinbauer et al., 2003a). Viruses are assumed to be host-specific (Ackermann & DuBow, 1987), however, some marine phages have been shown to exhibit a broad host range (Holmfeldt et al., 2007; Sano et al., 2004; Sullivan et al., 2003). The viral infection rate, among other parameters, depends on the host abundance (Murray & Jackson, 1992). Thus, viruses are assumed to preferentially infect the winners in the competition for nutrients, which may or may not be the most abundant members of the community but likely, the most active ones (Thingstad & Lignell, 1997; Thingstad, 2000; Bouvier & del Giorgio, 2007).

Prokaryotic community composition can be determined using fingerprinting techniques such as T-RFLP and DGGE targeting the 16S rRNA gene or ARISA targeting the intergenic spacer region in the rRNA operon. The composition of viral communities, representing the largest reservoir of genetic diversity in the ocean (Rohwer, 2003), is more difficult to determine due to the lack of universally conserved marker genes. Until recently, pulsed-field gel electrophoresis (PFGE) based on size fractionation of viral dsDNA was the main tool to investigate viral community composition (Klieve & Bauchop, 1988; Wommack et al., 1999b). The recently introduced randomly amplified polymorphic DNA (RAPD)-PCR approach allows resolving the viral community structure at a higher resolution than PFGE (Winget & Wommack, 2008).

The aim of this study was to determine the distribution of prokaryotic and viral abundance, production and community composition throughout the water column in the (sub)tropical Atlantic Ocean from the epi- to the abyssopelagic realm (from 100-7000m depth). Thus far, most of the studies on the interaction and relation of viral to prokaryotic abundance, production and community composition have been performed in surface waters. The recently reported increase in the ratio of viral to prokaryotic abundance from surface waters to bathypelagic layers in the Atlantic (Parada et al., 2007) in combination with the low growth rates of the bulk bathy- and abyssopelagic prokaryotic communities indicates, however, that the interactions between viruses and prokaryotes in the dark realm of the ocean might be fundamentally different from those in surface waters (Herndl et al., 2008). Thus, we specifically focused on indications of potential changes in the interaction between viruses and prokaryotes from the base of the epipelagic zone to the abyssopelagic layers.

Material and Methods

Study area and sampling. Water samples were obtained at 37 stations from the epi- (~ 100 m depth) to the abyssopelagic layer (to 7000 m depth) (Fig. 1) during the ARCHIMEDES-III cruise in the (sub)tropical Atlantic Ocean aboard the R/V *Pelagia* (December 2007/January 2008). Sampling was performed with a CTD (conductivity-temperature-depth) rosette sampler equipped with 12-L Niskin bottles. The Niskin bottles were flushed with bleach and rinsed with ambient seawater prior to collecting the samples by deploying them to 1000 m depth.

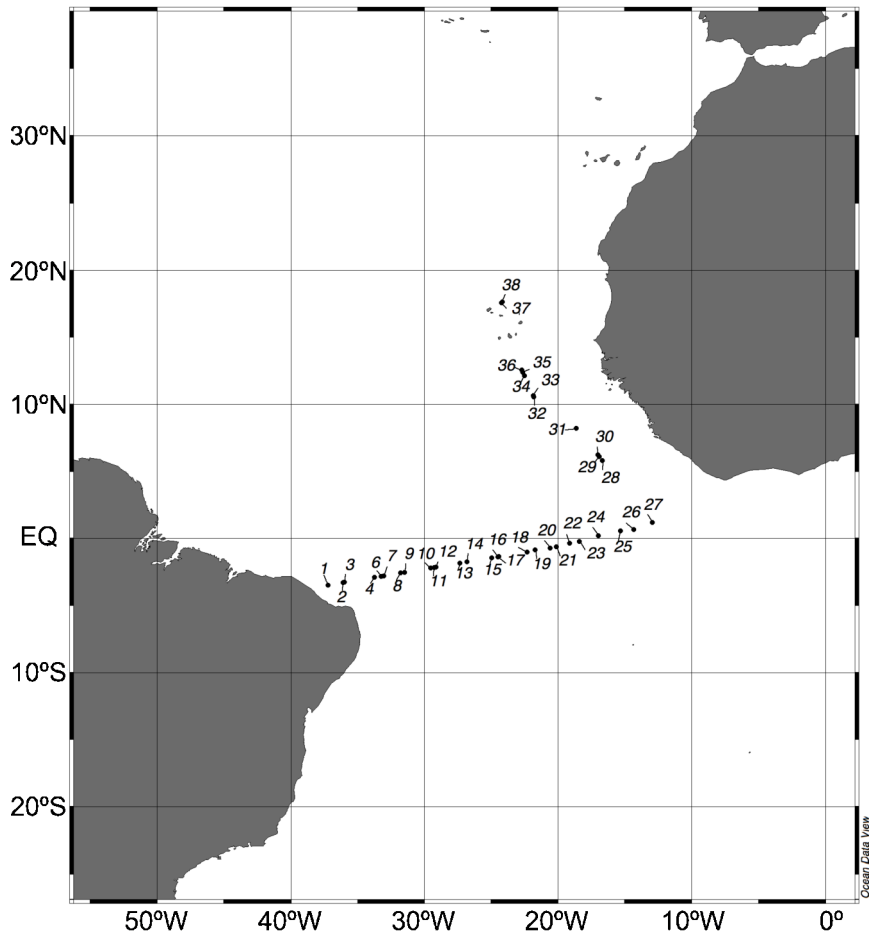

Figure 1. Sampling sites indicated by full circles during the ARCHIMEDES III cruise in the (sub)tropical Atlantic Ocean (water samples were not collected at St. 5).

Prokaryotic and viral abundance. Prokaryotic and viral abundance were determined by flow cytometry (Del Giorgio et al., 1996a; Brussaard, 2004). For enumerating prokaryotes, two mL samples were fixed with glutaraldehyde (0.5% final concentration), shock-frozen in liquid N_2 and kept at -80°C until analysis. Prior to flow cytometric analysis, samples were thawed to

room temperature and 0.5 mL subsamples stained with SYBR Green I in the dark for 10 min and subsequently, 1 x 10^5 mL^{-1} of 1 µm fluorescent latex beads (Molecular Probes, Invitrogen, Carlsbad, CA, USA) were added to each sample as internal standard. The prokaryotes were enumerated on a FACScalibur flow cytometer (Becton Dickinson, Fraklin Lakes, NJ, USA) by their signature in a plot of green fluorescence versus side scatter.

Viral abundance was measured by flow cytometry after SYBR Green I staining (Brussaard, 2004). Briefly, 2 mL samples were fixed with glutaraldehyde (0.5% final concentration), held at 4°C for 10-30 min, frozen in liquid N_2 and subsequently, stored at -80ºC until analysis. Prior to analysis, samples were thawed and 0.5 mL subsamples stained in the dark with SYBR Green I (Molecular Probes) at a final concentration of 0.5x of the manufacturer's stock solution at 80ºC for 10 min. Subsequently, 1 µm fluorescent latex beads (Molecular Probes) (10^5 mL^{-1}) were added to the samples as internal standard. The virus-like particles (VLP) were enumerated on a FACScalibur flow cytometer (Becton Dickinson) by their signature in a plot of green fluorescence *versus* side scatter.

Heterotrophic prokaryotic activity. Prokaryotic leucine incorporation was measured on triplicate 10-40 mL samples (depending on the expected activity) and on triplicate formaldehyde-killed blanks (Simon & Azam, 1989). The samples and the blanks were inoculated with 5 nM ^{3}H-leucine (final concentration, specific activity 160 Ci $mmol^{-1}$, Amersham, GE Healthcare, Buckinghamshire, UK) and incubated in the dark at *in situ* temperature for 4-24 h depending on the expected activity. Subsequently, the samples were fixed with formaldehyde (2% final concentration), filtered onto 0.2 µm polycarbonate GTTP filters (Millipore, Billerica, MA, USA) supported by Millipore HAWP filters, and rinsed three times with 10 mL of 5% ice-cold trichloroacetic acid. Thereafter, the filters were transferred into scintillation vials and dried at room temperature. Then, 8 mL of scintillation cocktail (Packard Filter Count, PerkinElmer, Waltham, MA, USA) was added to each vial and counted in a LKB liquid scintillation counter after 18 h. The obtained disintegrations per minute (DPM) were converted to leucine incorporation rates and prokaryotic carbon production was calculated from leucine incorporation rates using the conversion factor of 1.55 kg C mol leu^{-1} incorporated (Simon & Azam, 1989). Prokaryotic cell abundance was converted into prokaryotic carbon biomass assuming a carbon content of 20 fg C $cell^{-1}$ (Lee & Fuhrman, 1987). The turnover time of the heterotrophic prokaryotic community was calculated by dividing bulk prokaryotic biomass by prokaryotic carbon production.

Viral production. Viral production was measured by the dilution approach (Wilhelm et al., 2002). Briefly, 50 mL of the prokaryotic concentrate obtained by 0.2 µm tangential-flow filtration (Vivascience, Sartorius Stedim Biotech, Aubagne Cedex, France) was added to 450 mL of virus-free filtrate produced from the same water sample using a 30 kDa molecular weight cut-off tangential-flow filtration (Vivascience). This approach resulted in a prokaryotic abundance similar to *in situ* abundance. Subsamples were taken to enumerate prokaryotes and viruses at 7 h intervals

over a time span of 72 h. The experiments were performed in duplicate at *in situ* temperature in the dark with and without the addition of mitomycin C (final concentration 5 μg mL^{-1}; SIGMA, St. Louis, MO, USA; Ortmann et al., 2002). Mitomycin C was added to induce the lytic cycle of lysogenic viruses. Viral production (VP) was calculated as the slope of a first order regression line of viral abundance *versus* incubation time for the samples showing a single peak in viral abundance (Wilhelm et al., 2002). For samples with two peaks in viral abundance, the viral production was calculate using the formula:

$$VP = [(V_{max1}-V_{min1}) + (V_{max2}-V_{min2})]/(t_{max2}-t_{min1})$$

where V=viral abundance and t=time and subscript 1 and 2 refer to peaks 1 and 2 in viral abundance (Winter et al., 2004).

The lytic viral production was obtained from incubations without mitomycin C added. Lysogenic VP is the difference between the VP obtained in the mitomycin C-treated samples and the samples without mitomycin C.

Viral community composition. For the analysis of the viral community composition, one sample from each of the 9 stations sampled in total for this parameter was collected. For bathy- and abyssopelagic layers 150 L, and for the epi- and mesopelagic layers 70 L of water was collected and pre-filtered through a 0.22 μm polycarbonate filter (293 mm diameter, Whatman Nuclepore, Kent, UK). This 0.22 μm filtrate was subsequently concentrated to a final volume of ~50 mL by tangential-flow filtration with a 30 kDa molecular weight cut-off (Vivascience) and stored at -80°C until DNA extraction. The viral concentrate was further concentrated to a final volume of 200 μL by centrifugation (5000x *g* for 20 min) with Amicon Ultra 30 kDa molecular weight cut-off spin filters (Millipore). DNA extraction was performed with QIAmp MinElute Virus Spin Kit (QIAGEN, Hilden, German) using the protocol of the manufacturer. The extract was directly used as PCR template. For RAPD-PCR, the primer CRA-22 (5'-CCGCAGCCAA-3') was used to amplify virioplankton DNA (Winget & Wommack, 2008; Wommack et al., 1999b) in 50 μL of PCR mixture. Only one primer was used in each reaction, acting as forward and reverse primer. Samples were amplified by an initial denaturation step at 94°C for 10 min, followed by 30 cycles of annealing at 35°C for 3 min, extension at 72°C for 1 min and a denaturation at 94°C for 30 s. The cycle was completed by a final extension at 72°C for 10 min, and then kept at 4°C. The quality of the RAPD-PCR products was checked on 2% agarose gel. The products were purified with the Quick PCR purification kit (Genscript, Piscataway, NJ, USA) and quantified with a Nanodrop spectrophotometer. Subsequently, the purified RAPD-PCR products were separated by electrophoresis with an Experion automated electrophoresis system (Bio-Rad, Hercules, CA, USA). The obtained image was analyzed with Fingerprinting II software (Bio-Rad).

Prokaryotic community composition. Samples for prokaryotic community composition were taken at the same depths and stations as those for viral community composition. Ten L of seawater was filtered through a 0.22 μm Sterivex filter. Subsequently, 1.8 mL of lysis buffer (40 mM EDTA,

50 mM Tris-HCL, 0.75M sucrose) was added and the filters stored at -80°C until further processing. DNA extraction was performed with a Mega Kit extraction (MoBIO laboratories, Carlsbad, CA, USA) using the manufacturer's protocol. DNA extracts were concentrated (approx. 10 times) with a Centricon device (Millipore).

For archaeal community analysis, PCR and T-RFLP were used. PCR conditions and chemicals were applied as described by Moeseneder et al., (2001a). One mL of the DNA extract was used as a template in a 50 mL PCR mixture. The primers for PCR were the Archaea-specific primer pair 21F-FAM end-labelled with phosphoramidite fluorochrome 5- carboxy-fluorescein and 958R-JOE with 6-carboxy-4',5'-dichloro-2',7'-dimethoxyfluorescein (DeLong, 1992). Samples were amplified by an initial denaturation step at 94°C for 3 min, followed by 35 cycles of denaturation at 94°C for 1 min, annealing at 55°C for 1 min, and an extension at 72°C for 1 min. Cycling was completed by a final extension at 72°C for 7 min. The PCR products were run on 1.0% agarose gels. The gel was stained with a working solution of SYBR Gold®, the obtained bands excised, purified by Quick gel extraction kit (Genscript) and quantified using a Nanodrop spectrophotometer. Fluorescently labelled PCR products were digested at 37°C overnight. Each reaction contained 30 ng of cleaned PCR product, 5 U of the tetrameric restriction enzyme *Hha*I, and the respective buffer (Fermentas Life Science, Canada) filled up to a final volume of 50 μL with ultra-pure water (Sigma). The restriction enzyme was heat-inactivated and precipitated by adding 4.5 μL linear polyacrylamide (LPA, prepared with acrylamide, TEMED and APS in Tris-EDTA buffer) solution to 100 μL of 100% isopropanol. The samples were stored at room temperature for 15 min and subsequently centrifuged at 15000x *g* for 15 min. After removing the supernatant, the pellets were rinsed with 100 μL of 70% isopropanol and precipitated again by centrifugation (15000x *g* for 5 min). After removal of the supernatant, the samples were dried in the cycler at 94°C for 1 min and stored at -20°C.

The pellet was re-suspended in 2 μL of ultra-clean water (Sigma), and denatured after the addition of 7.8 μL of Hi-Di formamide (highly deionized formamide for capillary electrophoresis) (Applied Biosystems, Foster City, CA, USA) at 94°C for 3 min. Each sample contained 0.2 μL GeneTrace 1000 (X-Rhodamine labelled) marker (Applied Biosystems). Fluorescently labelled fragments were separated and detected with an ABI Prism 310 capillary sequencer (Applied Biosystems) run under GeneScan mode (Moeseneder et al., 2001a). The size of the fluorescently labelled fragments was determined by comparison with the internal size standard. Injection was performed electrokinetically at 15 kV for 15 s (adjustable), and the runs were conducted at 15 kV and 60°C within 38 min.

The output from the ABI Genescan software was transferred to the Fingerprinting II software (Bio-Rad) to calculate the area of the peaks and for standardizing them by the size marker. The obtained matrix was analyzed using Primer software (Primer-E, Ivybridge, UK) to determine the similarity between T-RFLP patterns obtained from different samples.

To assess bacterial community composition, ARISA-PCR was used following the method of Borneman & Triplett, (1997) with modifications. One μL of the DNA extract was used as a template

in a 40 μL PCR mixture. The primers used were ITSf, 5'GTCGTAACAAGGTAGCCGTA-3' and ITSr eub, 5'-GCCAAGGCATCCACC-3', (Cardinale et al., 2004); the primer ITSf was end-labelled with phosphoramidite fluorochrome 5- carboxy-fluorescein dye 5-FAM. Samples were amplified by an initial denaturation step at 94°C for 2 min, followed by 32 cycles of amplification at 94°C for 15 s, 55°C for 30 s, and 72°C for 3 min and a final extension of 72°C for 9 min. Five μL of PCR products were run on 2.0% agarose gels to check the quality of the products. The PCR products were purified with Quick Clean PCR product purification kit (Genscript) and quantified using a Nanodrop spectrophotometer. Fluorescently labelled fragments (8 ng μL^{-1} of sample) were separated and detected with an ABI Prism 310 capillary sequencer (Applied Biosystems) run under GeneScan mode (Kent et al., 2004). The size of the fluorescently labelled fragments was determined by comparison with X-Rhodamine MapMarker 1000 (BIO Ventures, Inc., Murfreesboro, TN, USA) and the size standard. Injection was performed electrokinetically at 10 kV for 5 s (adjustable) and the run was conducted at 10 kV and 60°C within 60 min. Subsequent data processing as done as described above for archaeal community analysis.

Statistical analysis. Spearman rank correlation was performed to analyze the relations between several measured parameters. The Distance-based multivariate analysis for a linear model using forward selection (DISTLM forward) was performed to test the relationships between the bacterial, archaeal, viral community and the biotic and abiotic environmental variability (Anderson et al., 2004).

Linear regression analysis was used to predict the relationship between the viral and bacterial abundance and the heterotrophic prokaryotic production. Analysis of variance (ANOVA on rank) was performed to test possible differences among depth layers and, when significant differences were observed, the post-hoc Dunn's test was also performed.

The Mantel test was used to test whether the differences of the biotic and abiotic parameters were due to the geographic distance. Correlation and linear regression analyses were performed with SigmaPlot 10.00 (Systat Software, Inc., Chicago, IL, USA), the Mantel test was done with Past 1.94a (Hammer et al., 2001).

Results

Physico-chemical variables.

The temperature decreased from the surface to the abyssopelagic waters (Table 1). The salinity varied from an average of 35.65±0.35 in the epipelagic to 34.79±0.05 in the abyssopelagic layers (Table 1). The salinity significantly decreased between the epipelagic layer and the meso-, bathy-, and abyssopelagic layers (ANOVA on ranks $p < 0.001$, post-hoc Dunn's tests $p < 0.05$). A pronounced oxygen minimum zone was detectable in the mesopelagic layers with O_2 concentrations as low as 42.45 μmol kg^{-1} (Table 1). No significant changes in the physico-chemical parameters were

Table 1. Physico-chemical characteristics, prokaryotic and viral parameters sampled in the epipelagic (<150m depth), mesopelagic (150-1000m depth), bathypelagic (1000-4000m depth) and abyssopelagic (>4000m depth) during the ARCHIMEDES III cruise in the subtropical Atlantic.

Parameter	Aver				SD				Min				Max				N			
	epi	meso	bathy	abysso	epi	meso	bathy	abysso	epi	meso	bathy	abysso	epi	meso	bathy	abysso	epi	meso	bathy	abysso
Temperature (°C)	15.63	8.21	3.01	1.47	2.20	3.26	0.64	0.45	13.31	4.28	2.10	1.00	23.68	13.74	3.99	2.30	18	46	57	29
Salinity	35.65	34.83	34.93	34.79	0.35	0.32	0.03	0.05	35.35	34.44	34.87	34.75	36.96	35.38	34.99	34.88	18	46	57	29
Oxygen (µmol kg^{-1})	134.61	119.54	241.67	229.75	34.83	35.34	8.55	6.41	78.07	42.45	216.75	222.42	199.14	176.37	255.53	243.88	18	46	57	29
PA (x 10^5 mL^{-1})	2.33	1.02	0.22	0.17	0.35	0.54	0.05	0.02	1.61	0.31	0.16	0.14	3.01	2.36	0.32	0.26	18	46	57	29
VLP (x10^6 mL^{-1})	2.54	0.96	0.44	0.43	1.09	0.44	0.07	0.08	1.59	0.37	0.26	0.23	5.58	1.92	0.72	0.70	18	46	57	29
VPR	9.51	9.82	20.56	25.18	2.63	2.00	3.97	4.48	6.30	5.58	10.94	12.26	15.86	15.87	29.64	33.53	18	46	57	29
PHP (10^{-2} pmol leu L^{-1} h^{-1})	397.00	68.07	0.79	0.54	189.66	110.79	0.40	0.30	156.87	1.28	0.11	0.15	749.99	520.49	2.06	1.25	18	46	57	29
Spec Leu (x10^{-4} fmol cell^{-1} d^{-1})	4.04	1.07	0.08	0.07	1.65	1.43	0.03	0.04	1.63	0.07	0.02	0.02	7.57	7.22	0.15	0.20	18	46	57	29
%HNA	45.79	54.44	56.67	61.08	4.98	3.60	4.08	5.90	35.65	45.97	47.29	50.72	55.94	63.34	67.17	78.65	18	46	57	29
VLP %High	15.71	11.94	10.60	12.87	3.59	1.99	1.13	1.67	11.34	8.31	6.76	7.19	24.37	16.04	13.39	14.59	18	46	57	29
VLP %Medium	78.58	78.91	80.41	77.12	3.98	3.97	3.32	6.18	71.06	63.18	66.93	47.71	83.94	83.84	85.69	83.58	18	46	57	29
VLP %Low	6.49	9.80	9.61	10.73	2.95	4.23	3.69	7.24	3.52	4.32	4.19	4.20	16.66	29.29	25.81	46.12	18	46	57	29

Abbreviation: PA, prokaryotic abundance; VLP, virus-like particles; VPR, ratio of viral to prokaryotic abundance; PHP, bulk leucine incorporation rate; Spec Leu, cell-specific leucine incorporation rate; %HNA, percentage of high nucleic acid prokaryotes; VLP% H, percentage of high fluorescence viral population; VLP% M, percentage of medium fluorescence viral population; VLP% L, percentage of low fluorescence viral population; N, number of samples. Average, Standard Deviation (SD) and range (Min-Max value) are indicated for all the parameters.

Table 2. Lytic and lysogenic viral production (VP) rates, percentage of lysogenic viral production *vs* total viral production and viral turnover time measured at different depths and at different stations during ARCHIMEDES III in the subtropical Atlantic Ocean.

Depth (m)	St.	Lytic VP (x10^5 mL^{-1} h^{-1})	Lysogenic VP(x10^5 mL^{-1} h^{-1})	% Lysogenic VP	Turnover time (h)
250	St.19	6.871	0.183	3	1.9
450	St.38	0.417	0.248	37	13.3
700	St.34	0.946	0.023	2	7.9
1750	St.22	0.283	n.d.	n.d.	25.6
2750	St.27	0.085	0.003	3	47.8
2750	St.31	0.04	0.062	61	39.6
2750	St.37	0.398	0.093	19	9.4
4500	St.13	0.04	0.002	6	78
4500	St.18	0.185	0.02	10	21.4
7000	St.23	0.188	0.138	42	13.4

nd, not detectable

noticeable along a horizontal scale.

Prokaryotic and viral abundance, heterotrophic production and turnover time.

Prokaryotic abundance decreased exponentially from an average of 2.3 x 10^5 cells mL^{-1} in the epipelagic layer to 0.2 x 10^5 cells mL^{-1} in the bathy- and abyssopelagic realm (ANOVA on ranks $p < 0.001$, post-hoc Dunn's tests $p < 0.05$) (Table 1 and 3, Fig. S1a). Leucine incorporation decreased from 7.49 pmol Leu L^{-1} h^{-1} in the epipelagic layer to 0.0011 pmol Leu L^{-1} h^{-1} in the abyssopelagic waters, hence by 3 orders of magnitude (ANOVA on ranks $p < 0.001$, post-hoc Dunn's tests $p < 0.05$) (Table 1 and 3, Fig. S1b). Cell-specific leucine incorporation rates decreased from an average of 4.04 x 10^{-4} ± 1.65 x10^{-4} fmol $cell^{-1}$ d^{-1} in the epipelagic layer to 7.6 x 10^{-6} ± 3.4 x 10^{-6} fmol $cell^{-1}$ d^{-1} in the abyssopelagic realm (Table 1, Fig. S1c). Thus, while leucine incorporation decreased by 3 orders of magnitude, cell-specific leu incorporation decreased only by 2 orders of magnitude. Heterotrophic prokaryotic turnover time significantly increased with depth ($R^2 = 0.84$, $p < 0.001$) ranging between 38 and 2278 d.

Viral abundance decreased from 5.58 x 10^6 VLP mL^{-1} in the epipelagic layer to 0.23 x 10^6 VLP mL^{-1} at 1000 m depth. The average viral abundance in the bathypelagic layer was not significantly different (ANOVA on ranks $p=0.461$) from that of the abyssopelagic, albeit exhibiting similar variability in these layers as in the epipelagic waters (Table 1 and 3, Fig. S2a). Over the entire water column, viral abundance was significantly related to prokaryotic abundance ($R^2 = 0.78$, $p < 0.0001$) and heterotrophic production ($R^2 = 0.65$, $p < 0.0001$).

The virus-to-prokaryote abundance ratio increased linearly from a mean of 9.51 ± 2.63 in epipelagic layer to 25.18 ± 4.48 in the abyssopelagic realm (ANOVA on ranks $p < 0.001$, post-hoc Dunn's tests $p < 0.05$) (Table 1 and 3, Fig. S2b).

Based on their signature of SYBR Green fluorescence and side scatter in flow cytometry, a high and a low nucleic acid content prokaryotic population were distinguishable (Fig. S3a). The fraction of the prokaryotic community with a high nucleic acid content generally increased with depth

Table 3. Results of the Spearman rank correlation coefficient test performed to determine the variation of the prokaryotic and viral parameters *vs.* depth.

	Depth		
	r_s	p	n
PA	-0.948	<0.0001	150
PHP	-0.910	<0.0001	150
Spec Leu	-0.820	<0.0001	150
VLP	-0.788	<0.0001	150
VPR	0.876	<0.0001	150
%HNA	0.598	<0.0001	150
VLP% H	-0.174	0.003	150
VLP% M	-0.030	0.716	150
VLP% L	0.254	0.001	150
LyticVP	-0.683	0.036	10
LysogenicVP	-0.400	0.264	9

Abbreviation: LyticVP, Total Lytic Viral Production; LysogenicVP, Total Lysogenic Viral Production; other abbreviations as in Table 1. Relevant ($-0.5 > r_s > 0.5$), statistically significant $p < 0.05$.

from the epipelagic to the abyssopelagic layers (ANOVA on ranks $p < 0.001$), reaching 79 % at the deepest station (Table 1 and 3, Fig. S3b). Three different viral populations were distinguished based on their fluorescence signal (Table 1, Fig. S4a). The high fluorescence fraction of the viral community ranged from 6 to 24% of total abundance with generally higher values in the epipelagic and abyssopelagic waters. It significantly decreased from the pelagic layers to the meso- and bathypelagic layers (ANOVA on ranks $p < 0.001$, post-hoc Dunn's tests $p < 0.05$) (Table 1 and 3, Fig. S4b). The medium fluorescence fraction comprised on average 79 ± 4% with no significant trend with depth (Table 1 and 3, Fig. S4c). The low fluorescence population ranged from 3 to 29%, again without a specific depth-related trend (Table 1 and 3, Fig. S4d).

Viral production was determined 10 times in total, at 9 stations and 8 depths (Table 2). Lytic viral production decreased linearly from about 6.8 x 10^5 VLP mL^{-1} h^{-1} in the epipelagic layer to 0.18 x 10^5 VLP mL^{-1} h^{-1} in the abyssopelagic realm (Table 2 and 3). The lysogenic viral production showed no clear trend with depth (Table 2). The total viral turnover time was calculated as the ratio between viral abundance and total (lytic plus lysogenic) viral production. Total viral turnover time ranged between 2 h and 3 d without any clear depth-related trend (Table 2).

No significant differences over geographic distance at specific depths were found for the prokaryotic and viral abundance and the heterotrophic prokaryotic production.

Viral and prokaryotic community composition.

The RAPD-PCR pattern of the viral community revealed in total 24 OTUs ranging from 182 to 1157 bp (Fig. 2a). The lowest number of OTUs (4) was found at St. 37 at 470 m depth, the highest (17 OTUs) at St. 7 at 2750 m depth. The OTUs 1037 and 686 bp were detected in all the

a

Stations	Depth (m)	182 bp	210 bp	255 bp	278 bp	283 bp	320 bp	333 bp	347 bp	363 bp	381 bp	400 bp	433 bp	456 bp	482 bp	538 bp	553 bp	577 bp	595 bp	645 bp	686 bp	746 bp	881 bp	1037 bp	1157 bp
St.35	100		1	1		1	1	1			1			1		1		1	1		1	1		1	1
St.17	250			1										1	1	1					1	1		1	
St.37	470														1						1	1		1	
St.29	750			1				1	1	1	1				1				1		1	1	1	1	
St.22	1750	1		1								1		1	1	1		1	1	1	1			1	1
St.7	2750	1		1	1	1	1			1	1	1	1	1	1	1	1		1		1	1		1	
St.24	3750	1		1		1	1		1	1				1	1				1		1	1		1	
St.18	4700	1		1		1	1			1				1	1	1			1		1			1	
St.27	5200	1					1		1					1	1				1		1			1	

b

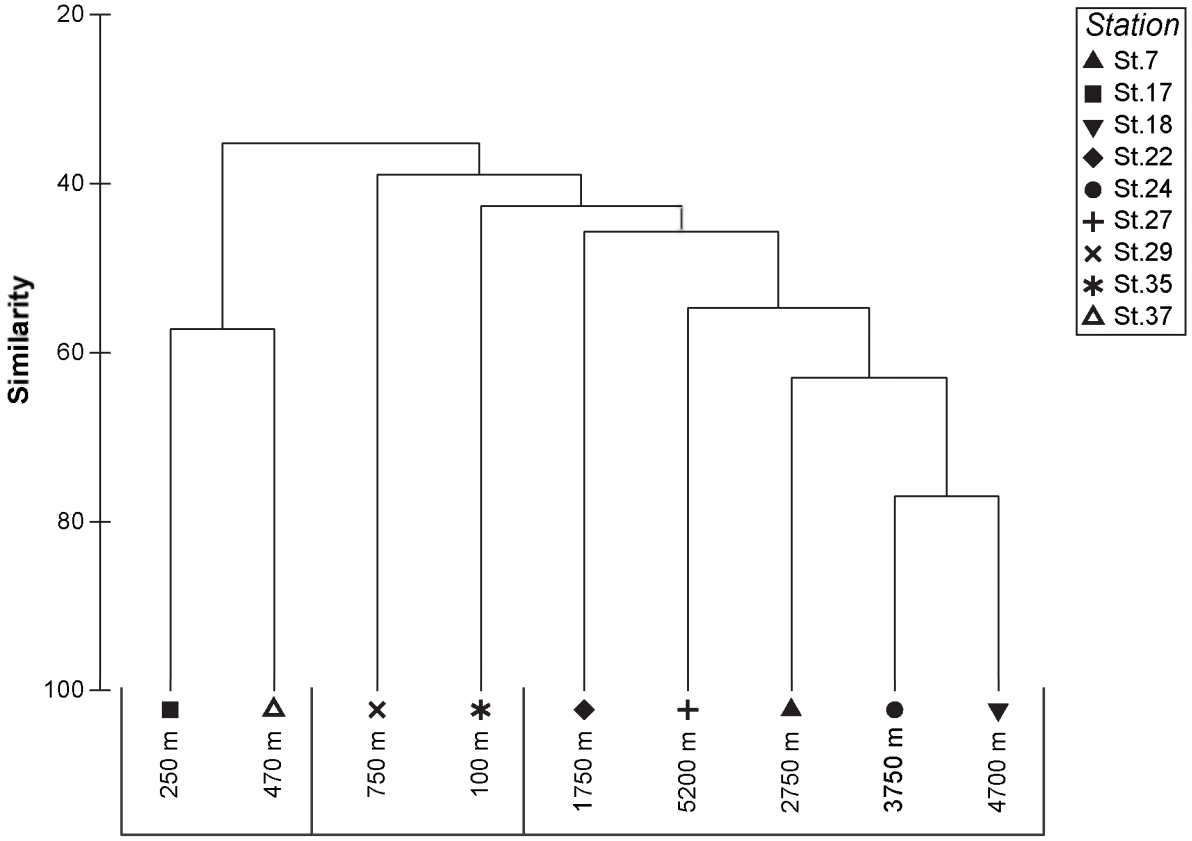

Figure 2. Viral community composition as revealed by RAPD-PCR. Presence/absence (filled/open squares, respectively) of viral OTUs at different stations and depths (a). Clustering of samples from different depths based on the Jaccard similarity matrix obtained from the presence/absence pattern of the viral OTUs (b).

samples, while six OTUs were detected only once (Fig. 2a). Jaccard similarity analysis of the viral community revealed a bathy-abyssopelagic cluster (1750m –5200 m depth), while the mesopelagic viral communities were characterized by generally low similarity (Fig. 2b).

The ARISA pattern of the bacterial community revealed in total 142 OTUs on the ITS level, ranging from 86 to 761 bp fragments (Fig. 3a). The lowest number of OTUs (23) was detected at St. 35 at 100 m depth, the highest (88) at St. 27 at 5200 m depth (Fig. 3a). Only one fragment was

detectable in all the samples (369 bp).

The T-RFLP pattern of the archaeal community revealed in total 10 OTUs on the 16s rDNA level, ranging from 72 to 919 bp fragments (Fig. 4a). The lowest number of OTUs (2) was detected at St. 27 at 5200 m depth and the highest (8) at St. 35 at 100 m depth (Fig. 4a). Two archaeal OTUs were present throughout the water column.

For the bacterial communities, the Jaccard similarity cluster analysis of the ARISA fingerprints revealed two distinct clusters: an epi-, mesopelagic cluster and a bathy-, abyssopelagic cluster (Fig. 3b). For the archaeal communities, Jaccard cluster analysis of the T-RFLP pattern indicated a meso- and upper bathypelagic cluster and a bathy-, abyssopelagic cluster (Fig. 4b). The archaeal community at 100 m and 5200 m depth were distinctly different from all the other samples (Fig. 4b). Overall, the viral, bacterial and archaeal community composition were not significantly related with any of the environmental variables measured (DISTLM test, $p>0.1$).

The rank-frequency distribution of OTUs obtained for the viral community indicated that half of the OTUs appeared in less than 45% of the samples, while 10 OTUs were present in more than 50% of the samples (Fig. 5). In contrast to viral community, rare OTUs were more frequently encountered in the bacterial community (Fig. 5). A high contribution (30% of the total number of OTUs) of unique bacterial OTUs was found in the oxygen minimum zone and at the deeper layer (20% of the total OTUs), while in the other depth layers the contribution of unique OTUs was limited to 1-4% of the total number of OTUs. Half of the bacterial OTUs were present in less than 22% of the samples and only 17% of the OTUs were present in more than 50% of the samples (Fig. 5). The rank-frequency distribution of the archaeal community revealed that half of the OTUs appeared in about 10% of the samples and only 3 OTUs (30%) were present in more than 50% of the samples (Fig. 5).

The number of OTUs of Archaea and viruses co-varied with depth, decreasing from the subsurface waters to the upper mesopelagic and remaining fairly constant until 3000-4000 m depth and decreasing towards greater depths (Fig. 6). The number of bacterial OTUs, however, increased from 3000 to 5200 m depth (Fig. 6). The number of archaeal OTUs were positively correlated with the number of viral OTUs ($r_s = 0.683$, $p = 0.036$) and negatively correlated with the number of bacterial OTUs ($r_s = -0.799$, $p = 0.006$), while the number of viral and bacterial OTUs were not significantly correlated ($r_s = -0.620$, $p = 0.067$). The number of bacterial OTUs was negatively correlated with the archaeal OTUs even when the unique bacterial OTUs were excluded from the analysis. The 25 most abundant bacterial OTUs were evenly distributed over depth as well as the total bacterial OTUs excluding the unique OTUs , with the exception of the oxygen minimum zone.

Discussion

Prokaryotic and viral abundance.

The average viral abundance in the deep (sub)tropical Atlantic reported in this study was one order of magnitude lower than in the meso- and bathypelagic waters further north in the Atlantic

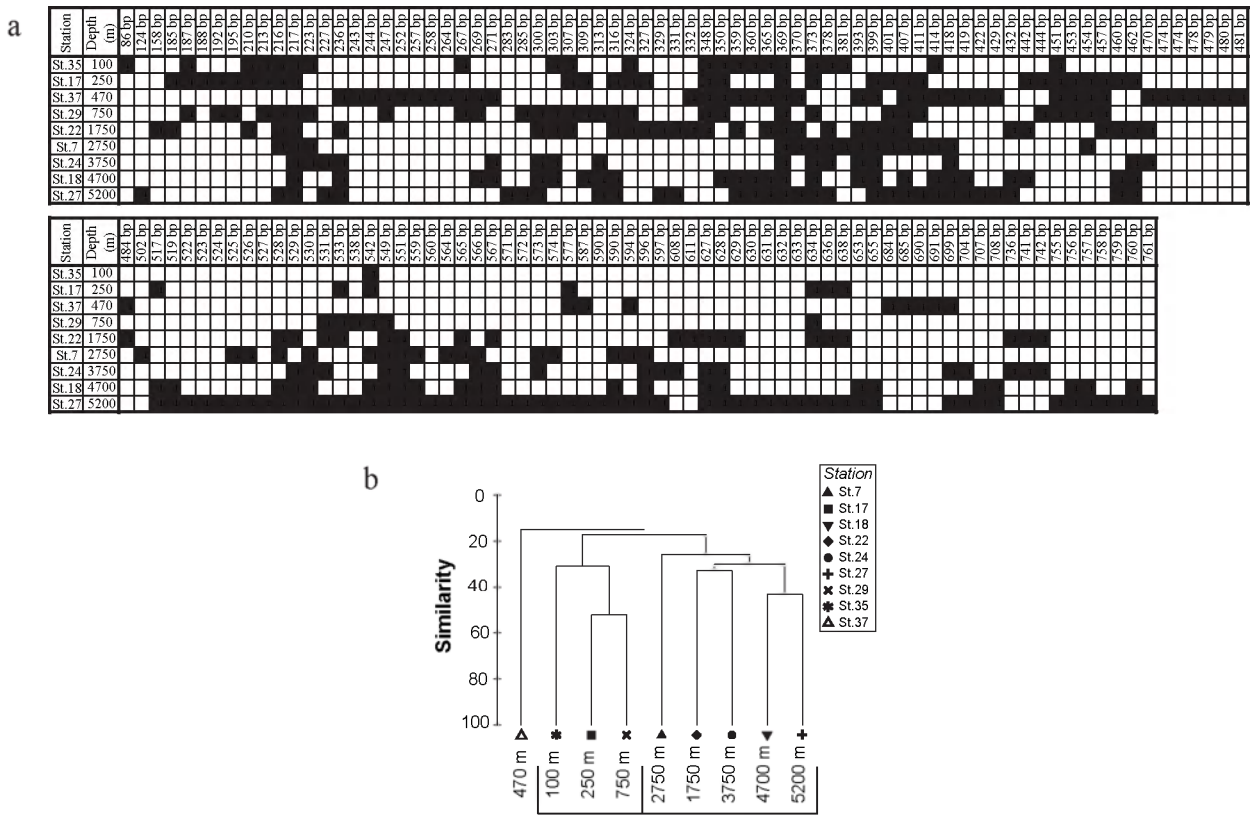

Figure 3. Bacterial community composition obtained by ARISA. Distribution (presence/absence) of bacterial OTUs at several stations and depths (a). Jaccard similarity matrices were used for cluster analysis based on ARISA fingerprints (b).

(Parada et al., 2007) but similar to the abundance reported for the deep subtropical Pacific (Hara et al., 1996). Although viral and prokaryotic abundance were related to each other, in agreement with previous studies from the eastern tropical Atlantic (Winter et al., 2008), the virus to prokaryote ratio (VPR) increased from 100 m to 7000 m depth from ~ 10 to ~30 (Table 1, Fig. S2b). The abundance of the three different viral populations distinguished by their fluorescence signal decreased with the depth. In terms of percentage, however, the medium and low fluorescence did not significantly change with depth (Table 1, Fig. S4). Unexpectedly, the most abundant viral population was the medium fluorescence population, in contrast to studies on coastal waters, which showed a clear dominance of the low fluorescence population (Kimmance et al., 2007; Larsen et al., 2001; Marie et al., 1999; Pan et al., 2007). This suggests a higher contribution of medium-high nucleic acid-content viruses in open and deep waters than in coastal areas. The percentage of the high fluorescence viruses decreased from the epipelagic to the meso- and bathypelagic layers and increased again in the abyssopelagic layers (Fig. S4).

Increasing VPRs with depth have been reported previously (Hara et al., 1996; Fuhrman, 2000; Weinbauer, 2004; Magagnini et al., 2007; Parada et al., 2007). The turnover time of viruses and their decay time, assuming that viral abundance is in steady state, was estimated to range from 11 d to 39 d in the bathypelagic North Atlantic (Parada et al., 2007) compared to 1-2 d in near-surface waters (Noble & Fuhrman, 1998; Winter et al., 2004). The substantially longer decay time in deep

waters might be one reason for the less pronounced decrease in the abundance of viruses than prokaryotes with depth (Table 1, Figs. S1a and S2a).

Increasing genome size of prokaryotes with depth as found in the present study (Table 1, Fig. S3b) appears to be a general feature and has been reported previously (Allen & Bartlett, 2002, DeLong et al., 2006; Reinthaler et al., 2006). Lauro & Bartlett, (2008) showed that bathypelagic prokaryotes have generally a high copy number of rRNA operons per genome and a larger intergenic region. Additionally, a large number of genes involved in the synthesis of the polyunsaturated fatty acids is found in deep ocean bacteria (Allen et al., 1999; Allen & Bartlett, 2002). Taken together, the notion emerges that deep-water prokaryotes are predominantly opportunists, presumably well adapted to a particle-attached life mode (Lauro & Bartlett, 2008; Aristegui et al., 2009), which might explain the need for a larger genome size. Hence, the larger genome of prokaryotes in the deep waters corresponds to the higher fraction of high fluorescence viruses found in the abyssopelagic as compared to the bathypelagic waters (Fig. S3b, Fig. S4b).

a

Station	Depth (m)	72 bp	135 bp	211 bp	248 bp	323 bp	325 bp	330 bp	333 bp	592 bp	919 bp
St.35	100	1		1	1	1		1	1	1	1
St.17	250					1			1	1	
St.37	470					1			1	1	
St.29	750					1			1	1	
St.22	1750					1			1	1	
St.7	2750		1			1			1	1	
St.24	3750		1			1	1		1	1	
St.18	4700		1			1			1	1	
St.27	5200					1				1	

b

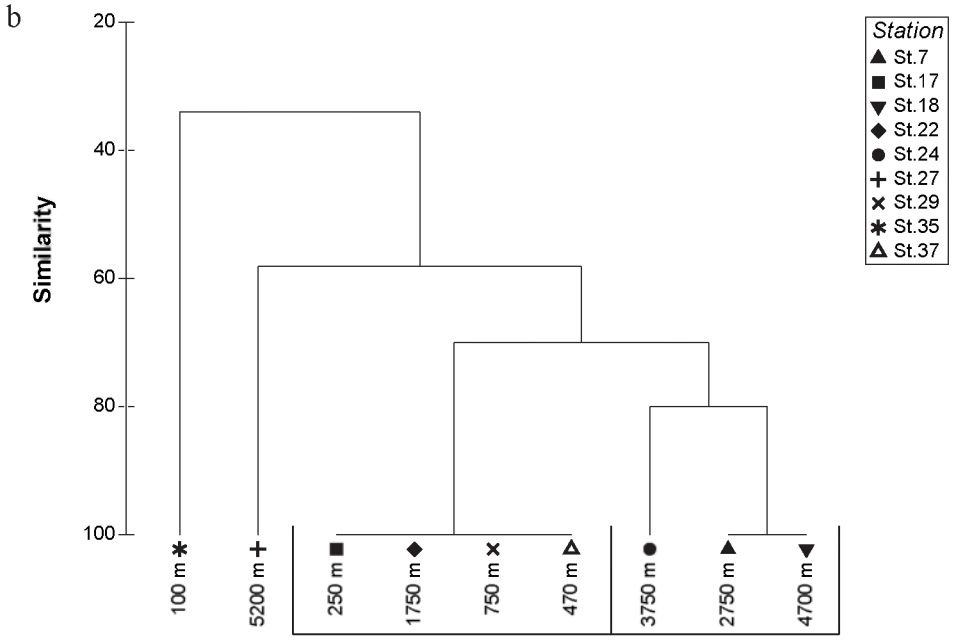

Figure 4. Archaeal community composition as revealed by T-RFLP. Distribution (presence/absence) of archaeal OTUs at several stations and depths (a). Jaccard similarity matrices were used for cluster analysis based on T-RFLP fingerprints (b).

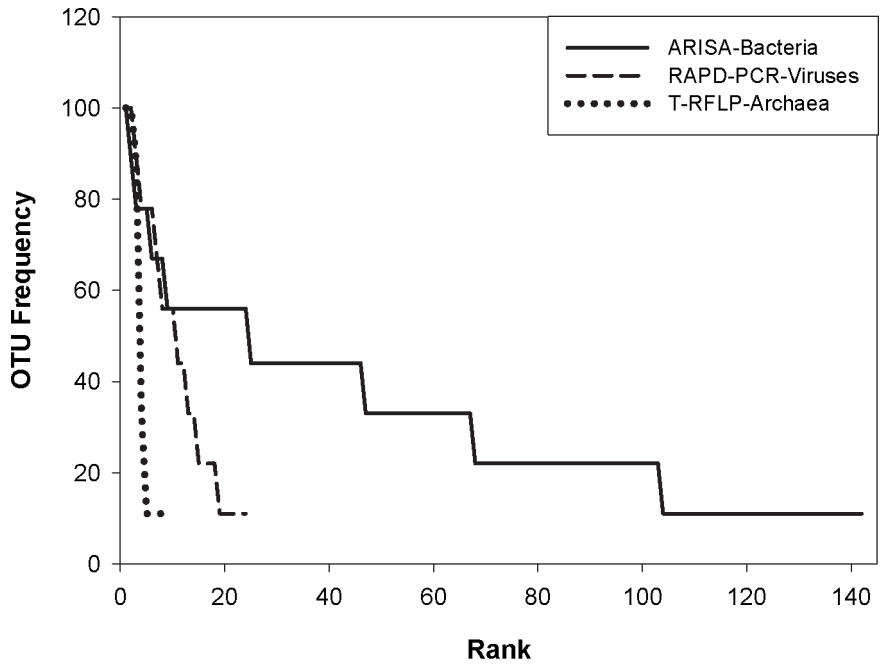

Figure 5. Rank-frequency distribution of archaeal, bacterial and viral OTUs obtained from samples collected throughout the water column of the (sub)tropical Atlantic.

Viral and heterotrophic prokaryotic production.

The total viral turnover time in the meso- to abyssopelagic waters ranged between 2 h and 3 d without any clear depth-related trend (Table 2). Our calculated viral turnover time based on total viral production is lower than the measured viral decay times (ranging between 11 and 39 d) for the North Atlantic Ocean (Parada et al., 2007). These viral decay times reported in Parada et al., (2007) were derived from the decrease in viral abundance in 0.2 µm filtered seawater over time. It is very likely, however, that viruses are loosing their infectivity prior to being undetectable by flow cytometry (Suttle, 2005). Hence, it is reasonable to assume that the viral turnover time based on viral production is lower than the estimated viral decay time.

Viral production depends on the abundance of their hosts, ultimately determining the contact rate (Murray and Jackson, 1992). Weinbauer et al., (2003a) proposed that the lysogenic cycle could be an adaptation to low host abundance and activity, thus indicating a shift in the viral life strategy from lysis to lysogeny with the increasing depth. The high percentage of lysogenic viral production at some specific stations in the bathy- and abyssopelagic zone of the Atlantic corroborate these findings with values of lysogeny up to 61% of the total viral production (Table 2). However, the lack of a specific trend with depth in lysogenic viral production along with its considerable variability points to substantial patchiness in the interaction between viruses and prokaryotes in the bathy- and abyssopelagic realm.

Recently, Aristegui et al., (2009) reviewed deep-water prokaryotic abundance and activity and viral abundance and concluded that the variability in these parameters is as high in the deep ocean as in surface waters despite their decrease in average abundance by orders of magnitude over this depth range. In our study, heterotrophic prokaryotic activity decreased by three orders of

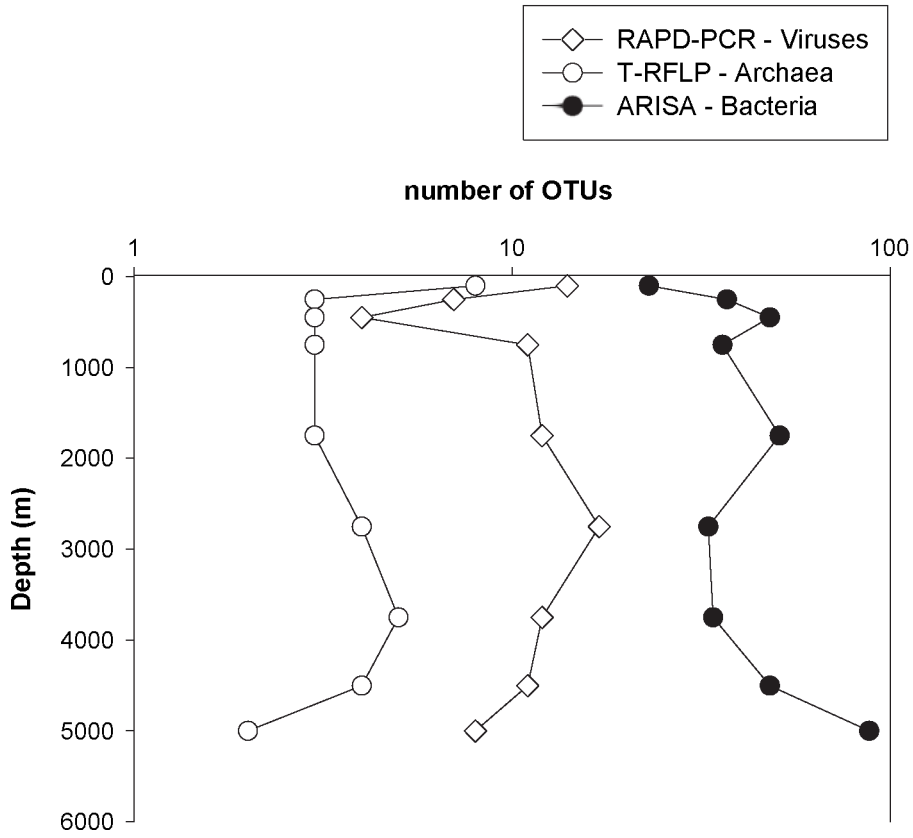

Figure 6. Distribution of the number of OTUs of Bacteria, Archaea and viruses throughout the water column of the (sub)tropical Atlantic.

magnitude from the epi- to the abyssopelagic layer and was generally similar that reported for the deep waters of the southern region of the North Atlantic (Reinthaler et al., 2006). As mentioned above, heterotrophic prokaryotic activity was strongly related to viral abundance. This tight relation is therefore not restricted to coastal and neritic seas such as the North Sea (Winter et al., 2005) and to surface waters but appears to hold also for the dark ocean down to abyssopelagic layers. This close relation indicates that also deep-water viruses are predominantly prokaryophages.

The prokaryotic turnover time increased with depth from the epi- to the abyssopelagic layer, as shown in a recent review (Aristegui et al., 2009). The prokaryotic turnover time is based on the abundance of prokaryotes, enumerated by flow cytometry and might include inactive, non-growing as well as dividing cells, while the viral turnover time is directly linked to the number of growing cells. This might, at least partly, explain the substantially higher (up to three orders of magnitude) viral than prokaryotic turnover time found in these deep waters.

Links between viral and prokaryotic community composition.

Three different methods were used to determine bacterial, archaeal and viral community composition targeting the intergenic spacers (ITS) region, 16S rRNA and viral dsDNA, respectively. ARISA and T-RFLP have been proven to be robust methods to determine the bacterial and archaeal community composition (Avaniss-Aghajani et al., 1994; Fisher & Triplett, 1999). RAPD-PCR has

only been recently introduced to assess viral community composition (Winget & Wommack, 2008) and represents a substantial improvement over pulsed field gel electrophoresis (PFGE) due to its higher resolution.

The number of viral OTUs obtained in this study by RAPD-PCR is substantially higher than that obtained with PFGE in the deep Atlantic waters (Parada et al., 2007), however, within the range reported for the Chesapeake Bay surface waters using PFGE (Wommack et al., 1999a). The Jaccard cluster analysis of the RAPD-PCR pattern showed a clear stratification of the viral community with depth (Fig. 2b) similar to that obtained for bacteria (Fig. 3b).

Relatively low numbers of archaeal OTUs per sample (ranging from 2 to 8) were detected by T-RFLP (Fig. 4a). The number of archaeal OTUs obtained in this study was lower than in previous studies on the deep tropical East-Atlantic (Winter et al., 2008) and in the deep Eastern Mediterranean Sea (Moeseneder et al., 2001a, 2001b, De Corte et al., 2009).

The Jaccard cluster analysis of the archaeal communities revealed two main clusters and generally, a much higher similarity between samples than for bacteria (Fig. 4b). In contrast to the archaeal community, relatively high numbers of bacterial OTUs were detected by ARISA. The large number of unique bacterial OTUs obtained on the ITS level is indicated by the long tail of the rank-frequency distribution of OTUs (Fig. 5). The higher contribution of unique bacterial OTUs was found in the oxygen minimum zone and in the deepest layer sampled than in the other water layers suggesting that these two layers might offer ecological niches different from the rest of the water column. The long tail in the rank-frequency distribution of bacterial OTUs was not found in the archaeal and viral community (Fig. 5). The Jaccard cluster analysis of the bacterial community also indicates a clustering with depth (Fig. 3b). The bacterial community richness, i.e., the number of OTUs, was negatively related to prokaryotic abundance due to the high number of OTUs detected in the bathy- and abyssopelagic zone where prokaryotic abundance is low.

The viral and bacterial richness exhibited a contrasting pattern with depth (Fig. 6). While the richness of the bacterial community increased from about 3000 m to 5000 m depth, the richness of the viral community decreased over this depth range (Fig. 6). It is well documented that different fingerprinting techniques differ in their resolution resulting in different numbers of OTUs as shown for ARISA and T-RFLP (Danovaro et al., 2006). Our observed trend in bacterial and viral communities with depth, however, is likely independent of the different resolution of the methods used assuming similar extraction and amplification efficiencies over the depth range of the water column sampled. Thus, the contrasting richness patterns between the bacterial and viral community together with the lack of a decrease in viral abundance from the bathy- to abyssopelagic waters might indicate a wider host range of viruses in these deep waters than in the near-surface layers.

In summary, our data show a high variability of prokaryotic and viral abundance and production in the bathy- and abyssopelagic zones suggesting that the dark ocean is more heterogeneous than commonly assumed. Despite the heterogeneity in prokaryotic and viral abundance and production in the deep Atlantic, archaeal, bacterial and viral community composition are stratified. Although viral turnover time does not exhibit a trend with depth in the deep ocean, bulk prokaryotic turnover

time increases linearly with depth. Together with the increase in the virus-to-prokaryote ratio with depth, it might indicate that viruses likely have a wider host range in the bathy- and abyssopelagic than in near surface waters allowing them to infect the deep-water prokaryotic community characterized by low abundance but relatively high richness.

Supplementary Information

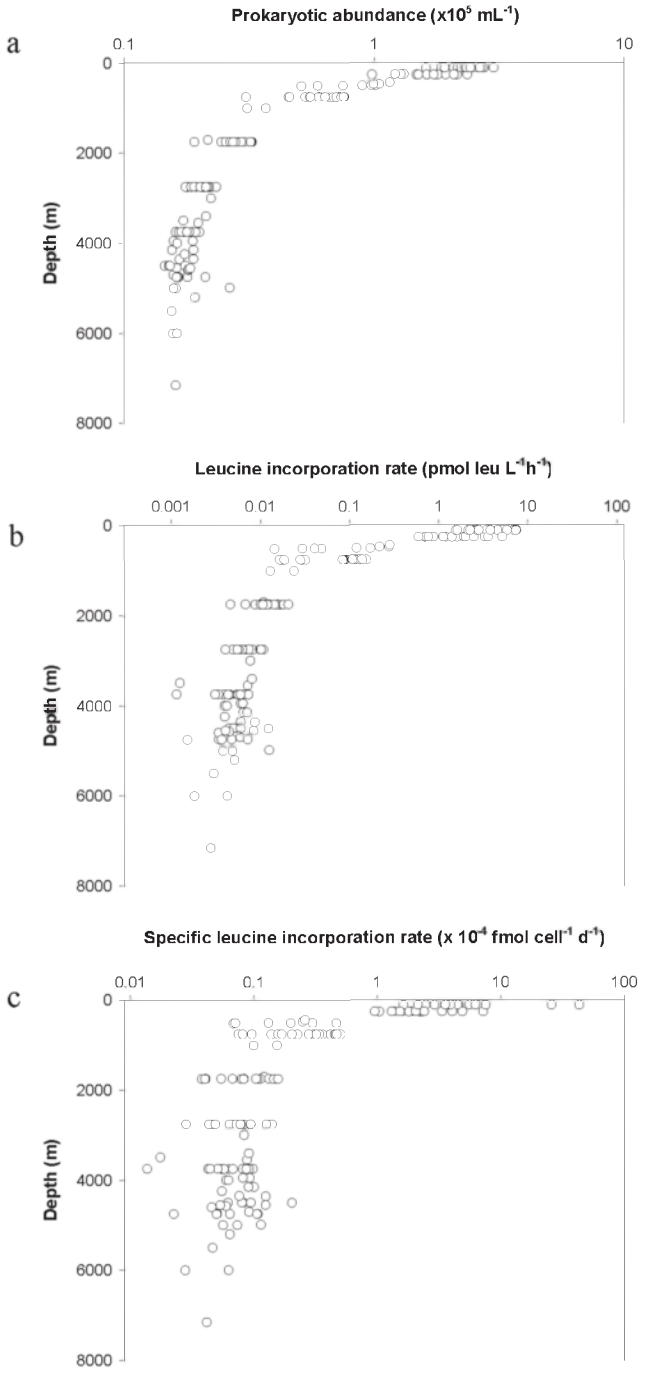

Figure S1. Distribution of prokaryotic abundance (a), bulk leucine incorporation (b), and cell-specific leucine incorporation rate throughout the water column of the (sub)tropical Atlantic at the different stations (c).

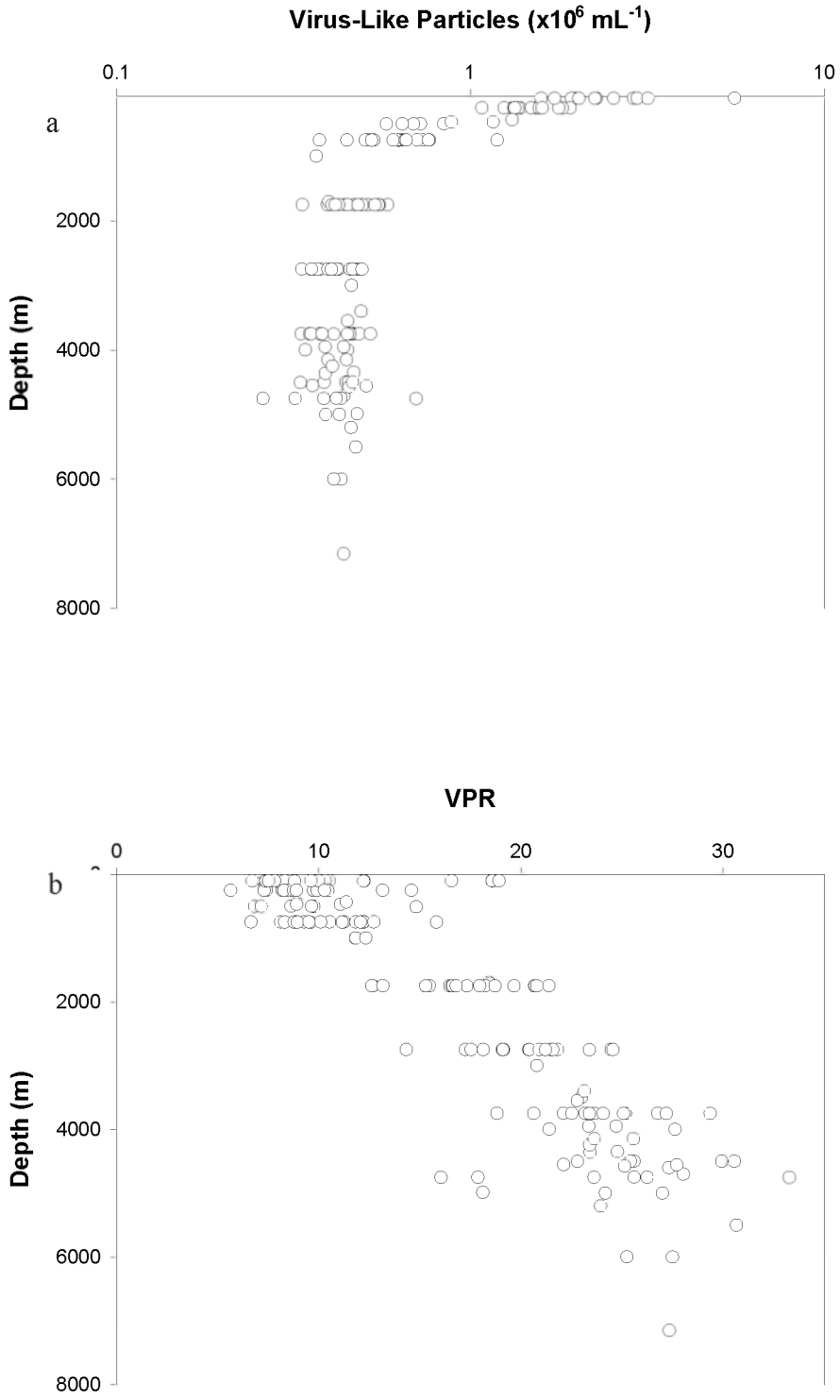

Figure S2. Vertical distribution of virus-like particles (VLP) (a), and the ratio of viral to prokaryotic abundance (VPR) (b) at the different stations.

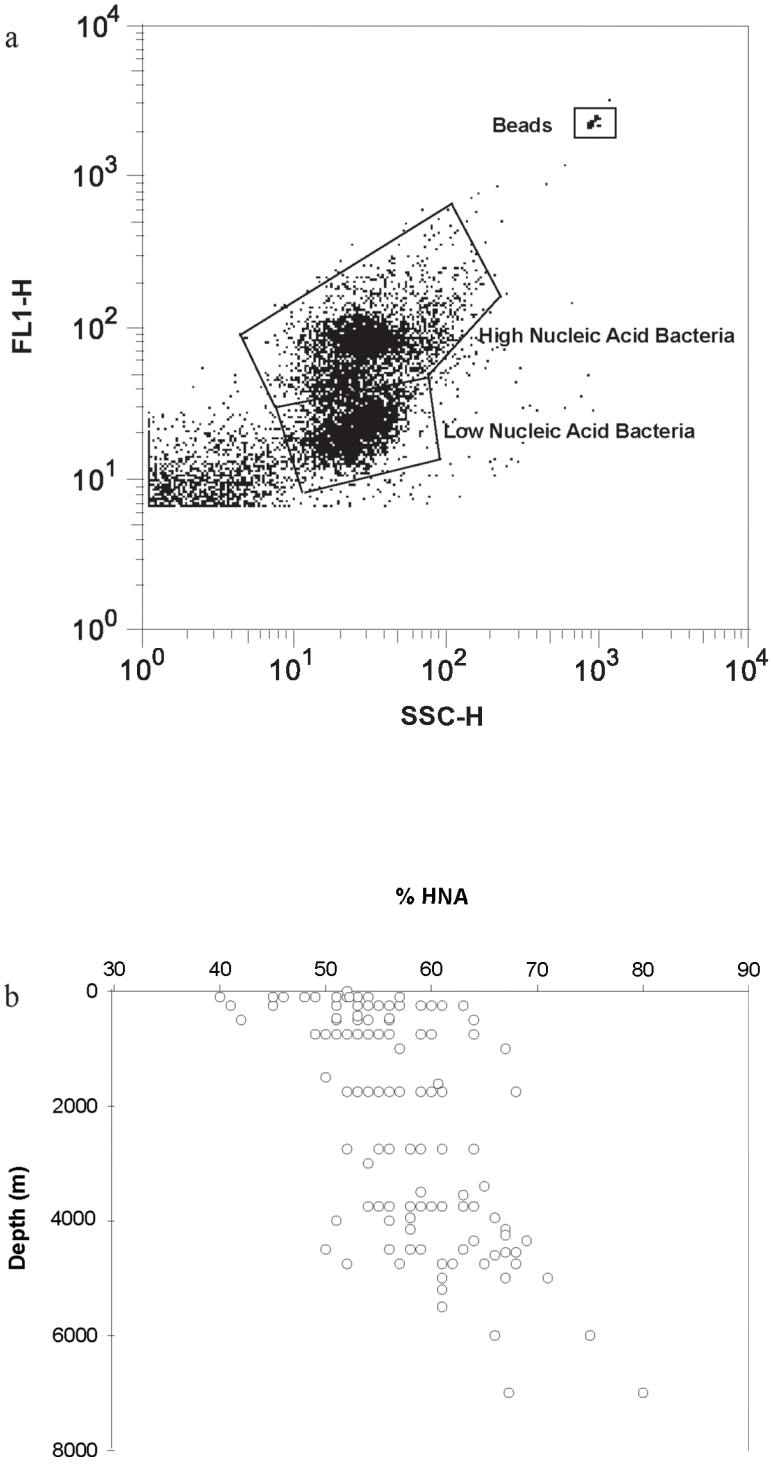

Figure S3. Cytogram of green fluorescence (FL1-H) versus side scatter (SSC-H) of the two different bacterial populations (a). Percentage of high nucleic acid prokaryotes (%HNA) versus depth (b).

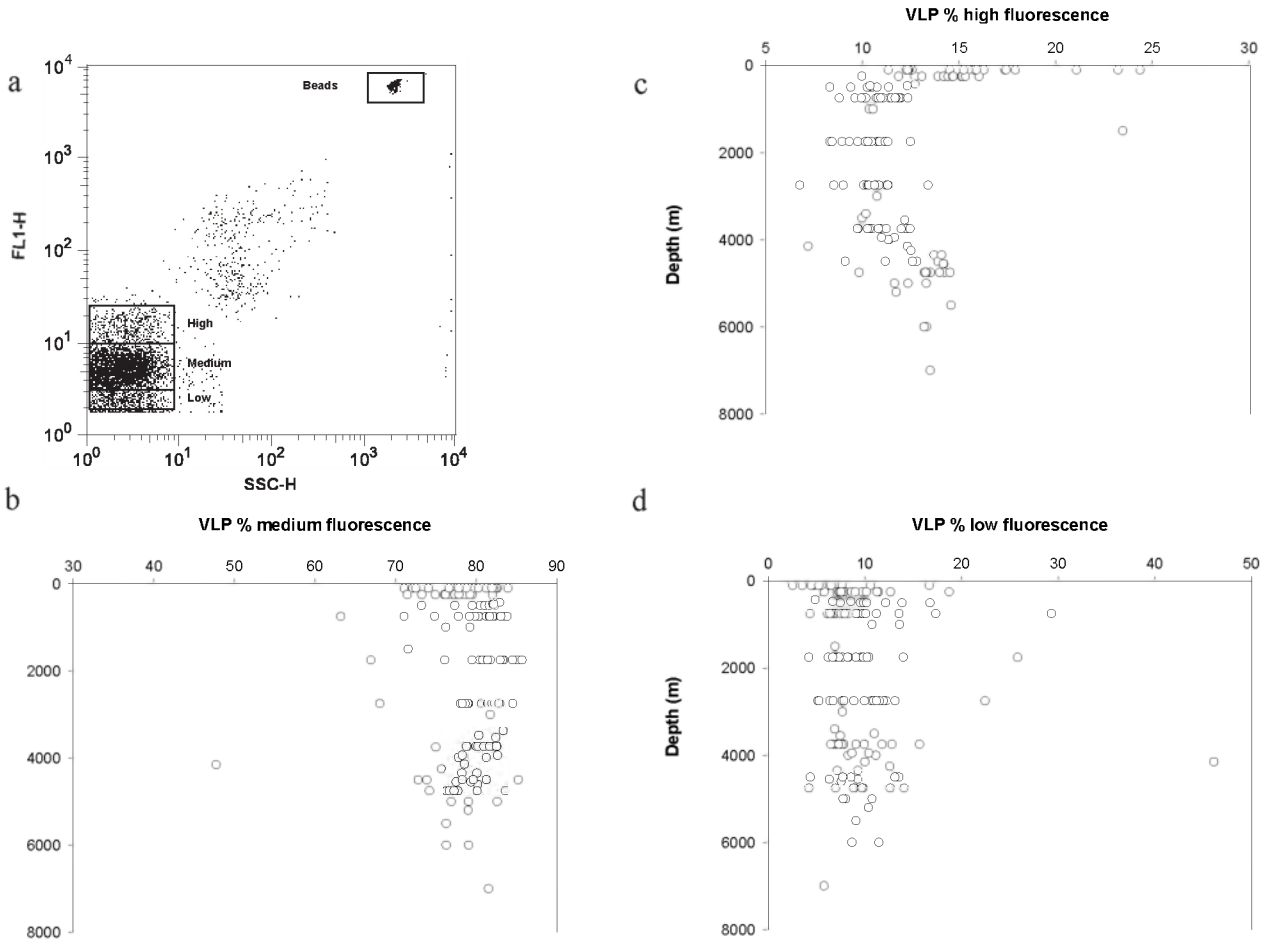

Figure S4. Cytogram of green fluorescence (FL1-H) versus side scatter (SSC-H) of the three different viral populations (a). Percentage of high (b), medium (c) and low fluorescence (d) viral populations throughout the water column of the (sub)tropical Atlantic.

Acknowledgements

We thank the captain and crew of R/V Pelagia, for their support and splendid atmosphere on board. E.S. was supported by the Dutch Science Foundation, T.Y. was supported by the Japanese Society for the Promotion of Science (JSPS) Postdoctoral Fellowship for research abroad, D.D.C. received a fellowship of the Univ. of Groningen. Lab work and molecular analyses were supported by a grant of the Earth and Life Science Division of the Dutch Science Foundation (ARCHIMEDES project, 835.20.023) to G.J.H. The work was carried out within the frame of the 'Networks of Excellence' MarBef and EurOceans of the 6th Framework Program of the European Union. This work is in partial fulfillment of the requirements for a Ph.D. degree from the University of Groningen by D.D.C.

References

Ackermann HW, DuBow MS. (1987). Viruses of prokaryotes. In: *General properties of bacteriophages*, Vol 1. CRC.

Allen EE, Bartlett DH. (2002). Structure and regulation of the omega-3 polyunsaturated fatty acid synthase genes from the deep-sea bacterium Photobacterium profundum strain SS9. *Microbiology* **148**:1903-1913.

Allen EE, Facciotti D, Bartlett DH. (1999). Monounsaturated but Not Polyunsaturated Fatty Acids Are Required for Growth of the Deep-Sea Bacterium Photobacterium profundum SS9 at High Pressure and Low Temperature. *Appl Environ Microbiol* **65**:1710-1720.

Anderson MJ, Ford RB, Feary DA, Honeywill C. (2004). Quantitative measures of sedimentation in an estuarine system and its relationship with intertidal soft-sediment infauna. *Mar Ecol-Prog Ser* **272**:33-48.

Aristegui J, Gasol JM, Duarte CM, Herndl GJ. (2009). Microbial oceanography of the dark ocean's pelagic realm *Limnol Oceanog* **54**: 1501-1529 .

Avaniss-Aghajani E, Jones K, Chapman D, Brunk C. (1994). A molecular technique for identification of bacteria using small subunit risomal RNA sequences. *BioTechniques* **17**:144-149.

Borneman J, Triplett EW. (1997). Molecular microbial diversity in soils from eastern Amazonia: Evidence for unusual microorganisms and microbial population shifts associated with deforestation. *Appl Environ Microbiol* **63**:2647-2653.

Bouvier T, del Giorgio PA. (2007). Key role of selective viral-induced mortality in determining marine bacterial community composition. *Environ Microbiol* **9**:287-297.

Breitbart M, Middelboe M, Rohwer F. (2008). Marine viruses: community dynamics, diversity and impact on microbial processes. In: Kirchmam DL (ed) *Microbial Ecology of the Oceans*. 2nd edn. John Wiley & Sons: New York, p 443-479.

Brussaard CPD. (2004). Optimization of procedures for counting viruses by flow cytometry. *Appl Environ Microbiol* **70:**1506-1513.

Cardinale M, Brusetti L, Quatrini P, Borin S, Puglia AM, Rizzi A, Zanardini E, Sorlini C, Corselli C, and Daffonchio D. (2004). Comparison of different primer sets for use in automated

ribosomal intergenic spacer analysis of complex bacterial communities. *Appl Environ Microbiol* **70**:6147-6156.

Danovaro R, Luna GM, Dell'Anno A, Pietrangeli B. (2006). Comparison of two fingerprinting techniques, terminal restriction fragment length polymorphism and automated ribosomal intergenic spacer analysis, for determination of bacterial diversity in aquatic environments. *Appl Environ Microbiol* **72**:5982-5989

De Corte D, Yokokawa T, Varela MM, Agogue H, Herndl GJ. (2009). Spatial distribution of Bacteria and Archaea and amoA gene copy numbers throughout the water column of the Eaastern Mediterranean Sea. *ISME J* **3**:147-158.

De Paepe M, Taddei F. (2006). Viruses' life history: towards a mechanistic basis of a trade-off between survival and reproduction among phages. *PLoS Biol* **4**:1248-1256.

Del Giorgio PA, Bird DF, Prairie YT, Planas D. (1996a). Flow cytometric determination of bacterial abundance in lake plankton with the green nucleic acid stain SYTO 13. *Limnol Oceanogr* **41**:783-789.

Del Giorgio PA, Gasol JM, Vaqué D, Mura P, Agustì S, Duarte CM. (1996b). Bacterioplankton community structure: Protists control net production and the proportion of active bacteria in a coastal marine community. *Limnol Oceanogr* **41**:1169-1179.

DeLong EF. (1992). Archaea in coastal marine environments. *Proc Natl Acad Sci USA* **89**: 5685–5689.

DeLong EF, Preston CM, Mincer T, Rich V, Hallam SJ, Frigaard N-U, Martinez A, Sullivan MB, Edwards R, Brito BR, Chisholm SW, Karl DM. (2006). Community genomics among stratified microbial assemblages in the ocean's interior. *Science* **311**:496-503.

Fisher MM, Triplett EW. (1999). Automated approach for ribosomal intergenic spacer analysis of microbial diversity and its application to freshwater bacterial communities. *Appl Environ Microbiol* **65**:4630-4636.

Fuhrman JA. (1999). Marine viruses and their biogeochemical and ecological effects. *Nature* **399**:541-548.

Fuhrman JA. (2000). Impact of viruses on bacterial processes. In: Kirchmam DL (ed) *Microbial Ecology of the Oceans*. John Wiley & Sons: New York, p 327-350.

Hammer Ø, Harper DAT, Ryan PD. (2001). PAST: Paleontological statistics software package for education and data analysis. *Palaeontol Electron* **4**:9.

Hara S, Koike I, Terauchi K, Kamiya H, Tanoue E. (1996). Abundance of viruses in deep oceanic waters. *Mar Ecol-Prog Ser* **145**:269-277.

Herndl GJ, Agogue H, Baltar F, Reinthaler T, Sintes E, Varela MM. (2008). Regulation of aquatic microbial processes: the A 'microbial loop' of the sunlit surface waters and the dark ocean dissected. *Aquat Microb Ecol* **53**:59-68.

Holmfeldt K, Middelboe M, Nybroe O, Riemann L. (2007). Large variabilities in host strain susceptibility and phage host range govern interactions between lytic marine phages and their Flavobacterium hosts. *Appl Environ Microbiol* **73**:6730-6739.

Kent AD, Jones SE, Yannarell AC, Graham JM, Lauster GH, Kratz TK, Triplett EW. (2004). Annual patterns in bacterioplankton community variability in a humic lake. *Microb Ecol* **48**:550-560.

Kimmance SA, Wilson WH, Archer SD. (2007). Modified dilution technique to estimate viral versus grazing mortality of phytoplankton: limitations associated with method sensitivity in natural waters. *Aquat Microb Ecol* **49**:207-222.

Klieve AV, Bauchop T. (1988). Morphological diversity of ruminal bacteriophages from sheep and cattle. *Appl Environ Microbiol* **54**:1637-1641.

Larsen A, Castberg T, Sandaa RA, Brussaard CPD, Egge J, Heldal M, Paulino A, Thyrhaug R, van Hannen EJ, Bratbak G. (2001). Population dynamics and diversity of phytoplankton, bacteria and viruses in a seawater enclosure. *Mar Ecol-Prog Ser* **221**:47-57.

Lauro FM, Bartlett DH. (2008). Prokaryotic lifestyles in deep sea habitats. *Extremophiles* **12**:15-25.

Lee S, Fuhrman JA. (1987). Relationships between biovolume and biomass of naturally-derived marine bacterioplankton. *Appl Environ Microbiol* **53**: 1298-l 303.

Magagnini M, Corinaldesi C, Monticelli LS, De Domenico E, Danovaro R. (2007). Viral abundance and distribution in mesopelagic and bathypelagic waters of the Mediterranean Sea. *Deep-Sea Res Part I* **54**:1209-1220.

Makino SI, Okada Y, Maruyama T, Kaneko S, Sasakawa C. (1994). PCR-based random amplified polymorphic DNA-fingerprinting of Yersinia-Pseudotuberculosis and its practical applications. *J Clin Microbiol* **32**:65-69

Marie D, Brussaard CPD, Thyrhaug R, Bratbak G, Vaulot D. (1999). Enumeration of marine viruses in culture and natural samples by flow cytometry. *Appl Environ Microbiol* **65**:45-52.

Moeseneder MM, Winter C, Arrieta JM, Herndl GJ. (2001a). Terminal-restriction fragment length polymorphism (T-RFLP) screening of a marine archaeal clone library to determine the different phylotypes. *J Microbiol Meth* **44**:159-172.

Moeseneder MM, Winter C, Herndl GJ. (2001b). Horizontal and vertical complexity of attached and free-living bacteria of the eastern Mediterranean Sea, determined by 16S rDNA and 16S rRNA fingerprints. *Limnol Oceanogr* **46**:95-107.

Murray AG, Jackson GA. (1992). Viral dynamics: A model of the effects size, shape, motion and abundance of single-celled planktonic organisms and other particles. *Mar Ecol-Prog Ser* **89**: 103-116.

Noble RT, Fuhrman JA. (1998). Use of SYBR Green I for rapid epifluorescence counts of marine viruses and bacteria. *Aquat Microb Ecol* **14**:113-118.

Nocker A, Burr M, Camper AK. (2007). Genotypic microbial community profiling: A critical technical review. *Microb Ecol* **54**:276-289.

Ortmann AC, Lawrence JE, Suttle CA. (2002). Lysogeny and lytic viral production during a bloom of the Cyanobacterium Synechococcus spp. *Microb Ecol* **43**:225-231.

Pan LA, Zhang J, Zhang LH. (2007). Picophytoplankton, nanophytoplankton, heterotrohpic bacteria and viruses in the Changjiang Estuary and adjacent coastal waters. *J Plankton Res* **29**:187-197.

Parada V, Herndl GJ, Weinbauer MG. (2006). Viral burst size of heterotrophic prokaryotes in aquatic systems. *J Mar Biol Assoc UK* **86**:613-621.

Parada V, Sintes E, van Aken HM, Weinbauer MG, Herndl GJ. (2007). Viral abundance, decay, and diversity in the meso- and bathypelagic waters of the North Atlantic. *Appl Environ Microbiol* **73**:4429-4438.

Reinthaler T, van Aken H, Veth C, Aristegui J, Robinson C, Williams PJLR, Lebaron P, Herndl GJ. (2006). Prokaryotic respiration and production in the meso- and bathypelagic realm of the eastern and western North Atlantic basin. *Limnol Oceanogr* **51**:1262-1273.

Rohwer F. (2003). Global phage diversity. *Cell* **113**:141-141.

Sano, E., Carlson, S., Wegley, L., and Rohwer, F. (2004). Movement of viruses between biomes. *Appl Environ Microbiol* **70**: 5842–5846.

Simon M, Azam F. (1989). Protein content and protein synthesis rates of planktonic marine bacteria, *Mar Ecol-Prog Ser* **51**:201–213.

Sullivan MB, Waterbury JB, Chisholm SW. (2003). Cyanophages infecting the oceanic cyanobacterium Prochlorococcus. *Nature* **424**:1047-1051.

Suttle CA. (1999). Do viruses control the oceans? *Natural History* **108**:48-51.

Suttle CA. (2005). Viruses in the sea. *Nature* **437**:356-361.

Suzuki MT, Giovannoni SJ. (1996). Bias caused by template annealing in the amplification of mixtures of 16S rRNA genes by PCR. *Appl Environ Microbiol* **62**:625-630.

Thingstad TF, Lignell R. (1997). Theoretical models for the control of bacterial growth rate, abundance, diversity and carbon demand. *Aquat Microb Ecol* **13**:19-27.

Thingstad, TF. (2000). Elements of a theory for the mechanisms controlling abundance, diversity, and biogeochemical role of lytic bacterial viruses in aquatic systems. *Limnol Oceanogr* **45**: 1320-1328.

Weinbauer MG. (2004). Ecology of prokaryotic viruses. *FEMS Microbiol Rev* **28**:127-181.

Weinbauer MG, Brettar I, Hofle MG. (2003a). Lysogeny and virus-induced mortality of bacterioplankton in surface, deep, and anoxic marine waters. *Limnol Oceanogr* **48**:1457-1465.

Weinbauer MG, Christaki U, Nedoma A, Simek K. (2003b). Comparing the effects of resource enrichment and grazing on viral production in a meso-eutrophic reservoir. *Aquat Microb Ecol.* **31**:137-144.

Weinbauer MG, Rassoulzadegan F (2004). Are viruses driving microbial diversification and diversity? *Environ Microbiol* **6**:1-11.

Wilhelm SW, Brigden SM, Suttle CA. (2002). A dilution technique for the direct measurement of viral production: A comparison in stratified and tidally mixed coastal waters. *Microbial Ecol* **43**:168-173

Wilhelm SW, Suttle CA. (1999). Viruses and nutrient cycles in the sea - Viruses play critical roles in the structure and function of aquatic food webs. *Bioscience* **49**:781-788.

Winget DM, Wommack KE. (2008). Randomly amplified polymorphic DNA PCR as a tool for assessment of marine viral richness. *Appl Environ Microbiol* **74**:2612-2618.

Winter C, Herndl GJ, Weinbauer MG. (2004). Diel cycles in viral infection of bacterioplankton in the North Sea. *Aquat Microb Ecol* **35**:207-216.

Winter C, Moeseneder MM, Herndl GJ, Weinbauer MG. (2008). Relationship of geographic distance, depth, temperature, and viruses with prokaryotic communities in the eastern tropical Atlantic Ocean. *Microb Ecol* **56**: 383-389.

Winter C, Smit A, Herndl GJ, Weinbauer MG. (2004). Impact of virioplankton on archaeal and bacterial community richness assessed in seawater batch cultures. *Appl Environ Microbiol* **70**: 804-813.

Winter C, Smit A, Herndl GJ, Weinbauer MG. (2005). Linking prokaryotic richness with viral abundance and prokaryotic activity. *Limnol Oceanogr* **50**: 968-977.

Wommack KE, Ravel J, Hill RT, Chun JS, Colwell RR. (1999a). Population dynamics of Chesapeake bay virioplankton: Total-community analysis by pulsed-field gel electrophoresis. *Appl Environ Microbiol* **65**:231-240.

Wommack KE, Ravel J, Hill RT, Colwell RR. (1999b). Hybridization analysis of Chesapeak Bay virioplankton. *Appl. Environ Microbiol* **65**: 241-250.

Yang YH, Yao J, Hu S, Qi Y. (2000). Effects of agricultural chemicals on DNA sequence diversity of soil microbial community: A study with RAPD marker. *Microb Ecol* **39**:72-79.

Chapter 3

Links between viruses and prokaryotes throughout the water column along a North-Atlantic latitudinal transect

Daniele De Corte, Eva Sintes, Taichi Yokokawa, Thomas Reinthaler, Gerhard J. Herndl

ISME Journal in press.

Abstract

Viruses are an abundant, diverse and dynamic component of marine ecosystems and play a key role in the biogeochemical processes of the ocean by controlling prokaryotic and phytoplankton abundance and diversity. However, most of the studies on virus – prokaryotic interactions in marine environments have been done in nearshore waters. To assess potential variations in the relation between viruses and prokaryotes in different oceanographic provinces, we determined viral and prokaryotic abundance and production throughout the water column along a latitudinal transect in the North Atlantic. Depth-related trends in prokaryotic and viral abundance, and prokaryotic production were observed along the latitudinal transect, with a decrease by one order and three orders of magnitude, respectively, over the depth profile. Also, the prokaryotic and viral abundance, both declined with depth. The virus-to-prokaryote ratio, however, increased from ~19 in surface waters to ~53 in the bathy- and abyssopelagic waters. The lytic viral production also decreased significantly with depth whereas the lysogenic viral production did not vary with depth. In bathypelagic waters, pronounced differences in prokaryotic and viral abundance were found among different oceanic provinces with lower leucine incorporation rates and higher virus-to-prokaryote ratios in the North Atlantic Gyre province than in the provinces further north and south. The percentage of lysogeny increased from subpolar regions towards the more oligotrophic lower latitudes. Based on the observed trends over this latitudinal transect, we conclude that the bathypelagic waters of the different oceanic provinces of the North Atlantic exhibit remarkable differences in viral and prokaryotic parameters.

Introduction

Viruses are abundant, diverse and dynamic components in marine ecosystems (Angly et al., 2006; De Corte et al., 2010; Parada et al., 2007; Sano et al., 2004). Viral lysis is a key factor in the biogeochemical cycles as it leads to the release of intracellular material from the host cells, stimulating dissolved organic matter (DOC) cycling (Middelboe and Lyck, 2002; Middelboe et al., 2003; Middelboe and Jørgensen, 2006). Moreover, viruses control prokaryotic and phytoplankton mortality and might help maintaining microbial diversity (Bratbak et al., 1993; Breitbart et al., 2008; Thingstad and Lignell, 1997; Winter et al., 2005).

There are two main viral life strategies, the lysogenic and the lytic cycle (Weinbauer et al., 2003). The prevalence of one over the other depends on the environmental conditions. Lysogeny is considered an adaptation to oligotrophic conditions, with low host abundance and activity (Weinbauer and Suttle, 1999; Williamson et al., 2002), while the lytic cycle is dominant in highly productive regions (Weinbauer et al., 2003). Changing trophic conditions lead to changes in the prokaryotic community composition and consequently, to altered virus-host interactions (Weinbauer et al., 1993).

Several studies have examined the prokaryotic (Bacteria and Archaea) abundance and diversity along large-scale oceanographic gradients (Pommier et al., 2007; Schattenhofer et al., 2009;Varela et al., 2008a; Varela et al., 2008b). In contrast, very little information is available on global patterns of viral abundance across different oceanic regions. Also, the biogeographic distribution of viral diversity is largely unknown. Until now, only one study, using a metagenomic approach, investigated the viral diversity over different oceanic provinces (Angly et al., 2006). This study revealed a high global viral diversity with consistent differences among different latitudes (Angly et al., 2006).

Although several variables might influence the distribution of viruses on the micro- to large-scale, the availability of suitable hosts is ultimately the crucial factor controlling viral proliferation. Thus, the variability within viral communities should be highly related to changes in host metabolic abundance, activity, and diversity. All of these prokaryotic parameters, in turn, depend on abiotic and biotic variables such as nutrient availability and grazing pressure (Middelboe, 2000).

The aim of this study was to investigate the main factors controlling viral abundance, production and the distribution of different viral sub-populations, as revealed by flow cytometry, along a latitudinal transect over four North Atlantic oceanic provinces throughout the entire water column ranging from the epi- to the abyssopelagic layers. The virus – prokaryote interactions, the viral life strategies and the host specificity of viruses might be fundamentally different between different oceanographic provinces and depth layers as are the overall trophic conditions. We used the distance-based multivariate analysis for a linear model using forward selection (DISTLM forward) to identify the best set of environmental parameters explaining the variations in viral abundance, production and contribution of different viral subpopulations to the viral communities in four oceanic provinces of the North Atlantic.

Material and Methods

Study area and sampling. Water samples were obtained from 24 depth layers at 33 stations during the research cruises GEOTRACES-1 and -2 (April-July 2010) in the North Atlantic with R/V *Pelagia* (Fig. 1) in five different pelagic zones: upper epipelagic (10-75m), lower epipelagic (75-200m), mesopelagic (200-1000m), upper bathypelagic (1000-2500m), subsequently termed bathypelagic, and the layer between 2500-6000m (thus, lower bathypelagic plus abyssopelagic) indicated below by the term abyssopelagic for the sake of clarity. The samples were collected in four different oceanic provinces, based on the classification scheme of ecological regions in the ocean by Longhurst, (1998). Samples were taken in the North Atlantic Arctic (ARCT) (70°N - 55°N), the North Atlantic Drift (NADR) (55°N - 40°N), the North Atlantic Gyral (NAG) province comprising the North Atlantic Tropical and Subtropical Gyral province (40°N - 12°N), and the Western Tropical Atlantic (WTRA; 12°N - 12°S) province. Sampling was performed with a CTD (conductivity-temperature-depth; Seabird, Bellevue, WA, USA) rosette sampler equipped with 24 25-L Niskin bottles.

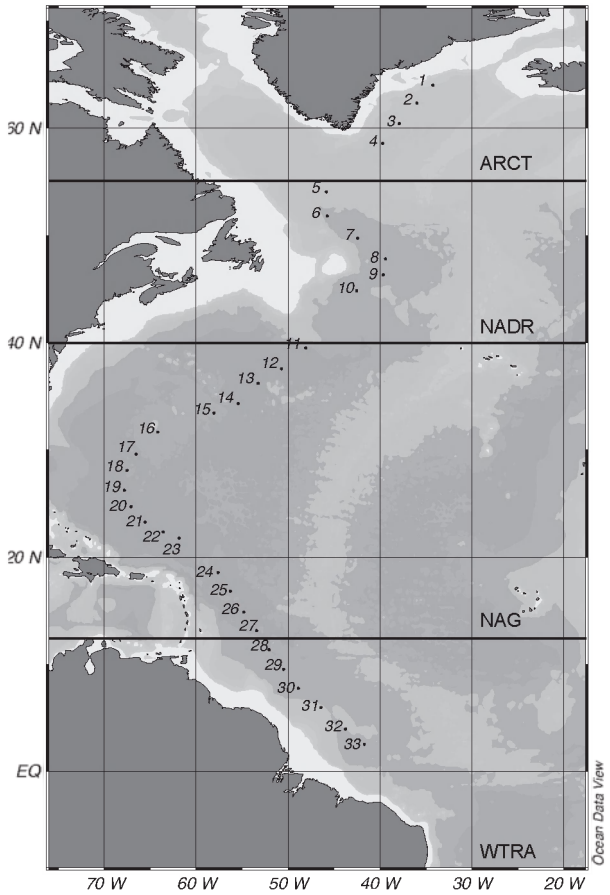

Figure 1. Cruise track and sampling stations (indicated by dots) occupied during the GEOTRACES research expeditions-1 and -2 in April-July 2010. ARCT (70°N - 55°N), NADR (55°N - 40°N), NAG (40°N - 12°N), WTRA (12°N - 12°S). Thick horizontal lines denote borders between oceanic provinces following the description given in Longhurst (1998).

Prokaryotic and viral abundance. Prokaryotic abundance was determined by flow cytometry (Brussaard, 2004; Del Giorgio et al., 1996). Two mL samples were fixed with glutaraldehyde (0.5% final concentration), shock-frozen in liquid N_2 and kept at -80ºC until analysis. To enumerate prokaryotes by flow cytometry, samples were thawed to room temperature and 0.5 mL subsamples stained with SYBR Green I (Molecular Probes, Invitrogen, Carlsbad, CA, USA) in the dark for 10 min. The prokaryotes were enumerated on a FACSAria flow cytometer (Becton Dickinson, Fraklin Lakes, NJ, USA) by their signature in a plot of green fluorescence *versus* side scatter.

Viral abundance was also measured by flow cytometry after SYBR Green I staining (Brussaard, 2004). Briefly, 2 mL samples were fixed with glutaraldehyde (0.5% final concentration), held at 4°C for 10-30 min, frozen in liquid N_2 and subsequently, stored at -80ºC until analysis. Prior to analysis, samples were thawed and 0.5 mL subsamples stained in the dark with SYBR Green I (Molecular Probes) at a final concentration of 0.5x of the manufacturer's stock solution at 80ºC for 10 min. Viruses were enumerated on a FACSAria flow cytometer (Becton Dickinson) as described above for prokaryotic abundance.

Depending on their respective signature in the cytogram of green fluorescence *vs.* side scatter, two different prokaryotic populations (high and low nucleic acid content prokaryotes) and three different viral populations (high, medium and low fluorescence viruses) were discriminated.

Leucine incorporation into heterotrophic prokaryotes as a measure of prokaryotic production. Samples to measure leucine incorporation into heterotrophic prokaryotes were collected at all the stations at selected depths. Triplicate subsamples (1.5 mL) and one trichloroacetic acid (TCA) killed blank were dispensed into screw-capped centrifuge tubes (Scientific System Inc., 2.0 mL Screw Tube), amended with 5 nmol L^{-1} (final conc.) of [^{3}H]-leucine (product #: ART 0840, American Radiolabeled Chemicals Inc., Saint Louis, MO, USA) and incubated at *in situ* temperature (± 1ºC) in the dark for 1h (samples from 0-200 m depth) or for 24 h (samples from 250 m to 6000 m) following the protocol of Smith and Azam, (1992). The incubations were terminated by adding trichloroacetic acid (TCA, final conc. 5%). Thereafter, the samples were centrifuged at 18,000 *g* for 10 min and the supernatant siphoned off. The pellet was resuspended in TCA (5%), centrifuged again for 10 min and the TCA discarded and finally, an ethanol rinse (80%, ice-cold) was applied. One mL of Ultima-GOLD (Packard) scintillation cocktail was added to the pellet after siphoning off the ethanol. The radioactivity was measured in a liquid scintillation counter (Tri-Carb 3100TR, PerkinElmer). Quenching was corrected using an external standard channel ratio. The disintegrations per minute (DPM) of the TCA-killed blank were subtracted from the average DPM of the samples, and the resulting DPM converted to leucine incorporation rates. The cell-specific leucine incorporation rate was calculated by dividing the bulk leucine incorporation rates by the prokaryotic abundance (Kirchman, 2002).

Viral production. Viral production was measured at eight stations and selected depths by the dilution approach (Wilhelm et al., 2002). Briefly, 50 mL of the prokaryotic concentrate obtained by 0.2 µm tangential-flow filtration (Vivascience, Sartorius Stedim Biotech, Aubagne Cedex, France) was added to 450 mL of virus-free filtrate produced from the same water sample using a 30

kDa molecular weight cut-off tangential-flow filtration (Vivascience). This approach resulted in a prokaryotic abundance similar to *in situ* abundance. The experiments were performed in triplicate at *in situ* temperature in the dark with and without the addition of mitomycin C (final concentration 1 μg mL^{-1}; SIGMA, St. Louis, MO, USA; Ortmann et al., 2002). Mitomycin C was added to induce the lytic cycle of lysogenic viruses. Subsamples were taken to enumerate prokaryotes and viruses at 4-6 h intervals over a time span of 72 h. Viral production (VP) was calculated as the slope of a first order regression line of viral abundance *versus* incubation time for the samples showing a single peak in viral abundance (Wilhelm et al., 2002). The lytic VP was obtained from incubations without mitomycin C added. Lysogenic VP represents the difference between the VP obtained in the mitomycin C-treated samples and the VP in the treatments without mitomycin C.

Estimation of other variables measured during the viral production experiments. *Viral-mediated mortality of prokaryotes* (VMM) was calculated by dividing the VP by the burst size. A burst size of 50 was used for the epipelagic layers (to 200 m depth) while for the deeper water (from 200 m to 6000 m depth) a burst size of 30 was used, based on the compilation of burst size in marine systems (Parada et al., 2006).

Net Prokaryotic Production (NPP) was determined from the changes in cell abundance over the sampling period using the formula:

$$\mathrm{NPP}=\left(\frac{P_1-P_0}{T_1-T_0}\right)$$

where P_1 and P_0 = prokaryotic abundance at the end and the beginning of the experiment, respectively, T_1 - T_0 = time difference in days between the end and the beginning of the experiment, i.e., the duration of the experiment.

Prokaryotic Turnover Time (PTT) was calculated using the formula:

$$PTT=\frac{1}{\left(\frac{NPP}{P_0}\right)}$$

Gross Prokaryotic Production (GPP) was estimated by adding the number of cells lysed to the net prokaryotic production (NPP) using the formula:

$$\mathrm{GPP}=\left|\frac{(P_1-P_0)+\left(\frac{V_1-V_0}{BS}\right)}{T_1-T_0}\right|$$

where P = prokaryotic abundance at different time points, V = viral abundance at different time points, T = time, BS = Burst Size

Fraction of Total Prokaryotic Abundance Lost (TPL) *by viral infection.* The percentage of TPL was calculated by dividing the VMM by the prokaryotic abundance at the beginning of the experiment.

Fraction of Prokaryotic Production Lost (PPL) *by viral infection*. The percentage of prokaryotic production lysed (% PPL) by viruses per day was calculated by dividing the NPP by the GPP.

Statistical analysis. Spearman rank correlation was performed to analyze the relations between several measured parameters. Regression analysis was used to predict the relationship between the log transformed viral and prokaryotic abundance and production *versus* temperature and depth (independent variables). Analysis of variance (ANOVA on rank) was performed to test possible differences among depth layers and, if significant differences were observed, the post-hoc Dunn's test was also performed. The distance-based multivariate analysis for a linear model using forward selection (DISTLM forward) was performed to test the relationships between viral abundance and biotic and abiotic environmental parameters (Anderson et al., 2004).

Results

Physical and chemical variables of the water column.

Temperature significantly decreased over the entire transect from the epipelagic (mean±SD: 20.2 ± 8.2°C) to the abyssopelagic layer (2.2 ± 0.2°C; ANOVA on rank, $P < 0.001$, post hoc Dunno's test, $P < 0.05$). The highest temperature in the epipelagic layers was measured in the WTRA (28.3 ± 0.7°C) followed by the NAG (24.2 ± 4.1 °C), NADR (11.8 ± 3.6ºC) and ARCT (5.7 ± 0.7ºC). The highest temperature in the lower epi- and mesopelagic waters was found in the NAG (20.9 ± 3.2ºC). The temperature in the bathy- and abyssopelagic layers did not reveal pronounced latitudinal variation, albeit in the ARCT, the temperature was slightly lower than in the other provinces (Table S1).

The salinity significantly decreased from the upper epi- to the abyssopelagic layers in all the provinces (ANOVA on rank $P < 0.001$, post hoc Dunno's test $P < 0.05$). The lowest salinity was found in the ARCT in the epi- and mesopelagic layers (Table S1). Salinity was not significantly different in the bathy- and abyssopelagic layer over the latitudinal transect (Table S1).

The Apparent Oxygen Utilization (AOU) significantly decreased in the upper epipelagic layer from the ARCT (43.49 ± 4.38 µmol O_2 kg^{-1}) to the WTRA (21.44 ± 3.61 µmol O_2 kg^{-1}; ANOVA on rank, $P < 0.001$, post hoc Dunno's test, $P < 0.05$). In contrast, AOU significantly increased with depth along the latitudinal transect from the ARCT to the WTRA (ANOVA on rank, $P < 0.001$) (Table S1). Moreover, the AOU significantly increased from the epi- to the abyssopelagic layer, from an average over all the stations of 40.07 ± 24.4 µmol O_2 kg^{-1} to 96.82± 14.1 µmol O_2 kg^{-1} (ANOVA on rank, $P < 0.001$) (Table S1).

Prokaryotic and viral abundance.

The prokaryotic abundance significantly decreased with depth from an average over all the

stations of 2.5±1.1 x 10^5 cells mL^{-1} in the epipelagic waters to 0.1±0.05 x 10^5 cells mL^{-1} in the abyssopelagic waters (ANOVA on rank, $P < 0.001$, post hoc Dunno's test, $P < 0.05$) (Table 1, Fig. 2a). Regardless of the depth horizon, highest prokaryotic abundance was found in the ARCT, while the lowest abundance was found in the NAG and WTRA (Fig. 2a). Prokaryotic abundance was negatively related to depth (linear regression $r^2 = 0.80$, $P < 0.001$), temperature (linear regression $r^2 = 0.52$, $P < 0.001$), and positively related to viral abundance (Spearman's rank correlation, $r_s = 0.90$, $P < 0.001$) and prokaryotic heterotrophic production (Spearman's rank correlation, $r_s = 0.92$, $P < 0.001$) and (Fig. 3a, b, Fig. 4a, b).

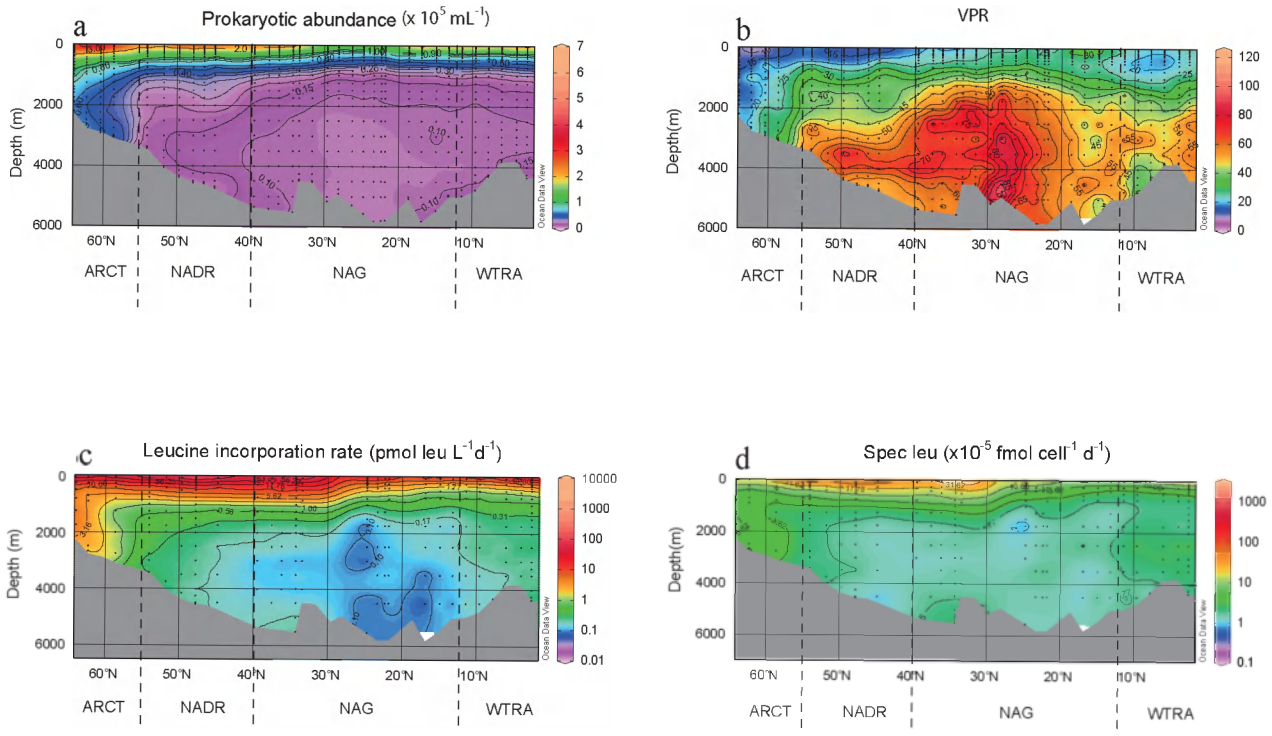

Figure 2. Biotic parameters measured along the North Atlantic latitudinal transect in the epi- meso-, bathy- and abyssopelagic layers: a) prokaryotic abundance, (b) virus to prokaryote ratio (VPR), (c) prokaryotic heterotrophic production measured via leucine incorporation and (d) cell-specific leucine incorporation rate. Broken vertical lines denote borders between oceanic provinces following the description given in Longhurst (1998). For abbreviations of the oceanic provinces see Fig. 1.

The abundance of viruses significantly decreased with depth from an average over all the stations of 4.48 ± 2.38 x 10^6 viruses mL^{-1} to 0.58 ± 0.23 x 10^6 viruses mL^{-1} in the epi- and abyssopelagic waters, respectively (Table 1) (ANOVA on rank, $P < 0.001$). The viral abundance did not change significantly between the bathy- and the abyssopelagic waters (ANOVA on rank, $P = 0.460$). Generally, viral abundance was negatively related with depth (linear regression $r^2 = 0.71$, $P < 0.001$) and temperature (linear regression $r^2 = 0.51$, $P < 0.001$), and positively correlated with prokaryotic abundance (Spearman's rank correlation, $r_s = 0.90$, $P < 0.001$) and heterotrophic production (Spearman's rank correlation, $r_s = 0.86$, $P < 0.001$) (Fig. 3a, b, Fig. 4a, b). The highest viral abundance was found in the epipelagic layers of the WTRA whereas the lowest abundance was measured in the ARCT (ANOVA on rank, $P < 0.001$, post hoc Dunno's test, $P < 0.05$). In

Table 1. Prokaryotic and viral parameters sampled in the epipelagic (10 m to 200 m depth), mesopelagic (200 m to 1000 m depth), bathypelagic (1000 m to 2500 m depth) and abyssopelagic (>2500 m depth) layers along the North Atlantic latitudinal transect during the Geotraces cruises. ARCT - North Atlantic Arctic (70°N - 55°N), NADR - North Atlantic Drift (55°N - 40°N), NAG - North Atlantic Gyral (40°N - 12°N) and WTRA - Western Tropical Atlantic (12°N - 12°S) following the classification of oceanic provinces given by Longhurst (1998).

			ARCT						NADR						NAG						WTRA					
Layer	Depth	Variables	Aver	sd	min	max	n		Aver	sd	min	max	n		Aver	sd	min	max	n		Aver	sd	min	max	n	
Upper Epipelagic	10-75 m	PA ($x10^6$ mL^{-1})	3.6	1.4	2.1	7.0	13		2.9	1.4	0.9	5.0	23		2.2	1.0	0.9	5.0	53		2.6	0.6	1.4	3.7	23	
		Viruses ($x10^6$ mL^{-1})	3.3	0.6	2.2	4.2	13		3.5	1.2	1.5	5.4	23		4.8	3.3	1.8	16.0	54		5.6	0.9	3.8	7.6	23	
		VPR	10.2	4.1	4.7	20.0	13		13.8	6.8	7.4	37.8	23		21.2	6.9	11.7	42.6	53		21.9	4.3	14.5	27.8	23	
		leu incorporation (pmol leu L^{-1} d^{-1})	142.3	41.3	105.0	187.3	3		485.0	387.6	33.9	1169.5	10		155.4	168.0	24.2	508.2	15		100.0	28.9	50.2	156.4	8	
		Cell-specific Leu ($x10^{-5}$ fmol $cell^{-1}$ d^{-1})	44.2	10.7	33.1	54.2	3		175.3	148.2	29.5	543.7	10		59.4	45.4	13.6	176.6	15		41.7	10.1	28.5	56.5	8	
		%HNA prokaryotes	59.2	4.4	52.5	66.0	13		58.4	8.6	33.0	70.4	23		53.1	8.9	34.2	79.1	53		55.6	5.5	44.5	65.5	23	
		%H-viruses	16.0	2.9	10.9	21.2	13		14.9	3.2	9.0	19.9	23		11.8	2.9	5.2	17.8	54		21.8	3.7	14.4	28.4	23	
		%M-viruses	66.3	14.1	37.2	86.5	13		66.6	6.2	51.4	74.1	23		68.8	9.9	42.2	81.7	54		66.6	4.0	60.4	73.8	23	
		%L-viruses	16.6	12.7	2.3	45.0	13		17.8	8.6	9.3	37.7	23		18.8	11.4	4.5	46.5	54		10.9	2.7	7.0	16.3	23	
Lower Epipelagic	75-200m	PA ($x10^6$ mL^{-1})	2.7	0.7	1.6	4.4	15		1.9	1.1	0.9	5.2	14		1.3	0.6	0.5	2.9	51		1.0	0.5	0.5	2.0	14	
		Viruses ($x10^6$ mL^{-1})	2.4	0.7	1.2	3.7	15		2.2	0.6	1.3	3.3	14		3.5	1.3	1.5	6.3	51		2.5	1.6	0.8	5.9	14	
		VPR	9.4	3.2	4.5	14.4	15		12.7	3.5	5.6	17.9	14		28.2	10.4	12.5	58.6	51		23.8	6.8	15.9	40.9	14	
		leu incorporation (pmol leu L^{-1} d^{-1})							59.0	23.3	42.1	92.8	4		75.8	116.9	13.8	361.4	8		14.1	9.4	7.4	20.7	2	
		Cell-specific Leu ($x10^{-5}$ fmol $cell^{-1}$ d^{-1})							46.6	40.9	17.0	107.1	4		43.1	38.0	17.6	135.5	8		12.7	5.6	8.7	16.6	2	
		%HNA prokaryotes	58.4	4.4	51.0	64.9	15		59.1	8.8	42.7	70.8	14		57.2	7.8	40.1	73.8	51		55.8	5.1	46.1	64.7	14	
		%H-viruses	13.4	3.1	5.8	18.7	15		15.0	2.9	11.4	20.3	14		12.3	3.4	2.1	19.0	51		13.0	4.5	4.4	22.8	14	
		%M-viruses	70.4	7.4	55.7	81.2	15		71.8	2.5	67.4	76.7	14		69.4	9.9	39.7	80.8	51		71.3	5.8	53.6	79.9	14	
		%L-viruses	15.7	9.4	4.0	40.5	15		12.4	3.6	8.3	21.5	14		17.7	11.3	5.8	55.8	51		15.1	8.3	6.8	39.1	14	
Mesopelagic	200-1000 m	PA ($x10^6$ mL^{-1})	0.5	0.2	0.2	1.0	28		0.2	0.1	0.1	0.7	31		0.1	0.0	0.0	0.3	88		0.1	0.0	0.1	0.2	31	
		Viruses ($x10^6$ mL^{-1})	1.0	0.4	0.5	2.0	28		0.9	0.2	0.5	1.7	31		0.6	0.2	0.3	1.8	88		0.5	0.1	0.3	0.9	31	
		VPR	21.1	8.9	10.5	42.4	28		40.0	8.7	22.2	56.8	31		53.7	20.7	24.0	146.4	88		37.7	13.6	19.9	73.9	31	
		leu incorporation (pmol leu L^{-1} d^{-1})	4.5	2.7	0.6	7.2	5		0.4	0.2	0.2	0.5	18		0.2	0.2	0.0	0.8	28		0.3	0.1	0.1	0.4	11	
		Cell-specific Leu ($x10^{-5}$ fmol $cell^{-1}$ d^{-1})	7.1	3.3	1.6	9.9	5		3.1	6.0	0.1	27.1	18		1.8	1.5	0.2	7.7	28		2.5	0.9	1.1	4.4	11	
		%HNA prokaryotes	65.0	8.3	45.5	79.6	28		52.3	5.7	43.7	69.2	31		56.8	4.9	43.6	68.8	88		55.8	3.6	52.7	68.7	31	
		%H-viruses	10.7	2.7	5.3	16.8	28		10.4	2.5	5.3	15.6	31		8.4	2.2	0.3	14.6	88		8.4	1.3	4.9	10.9	31	
		%M-viruses	76.5	6.2	59.1	87.0	28		74.3	1.9	69.8	77.2	31		67.6	9.2	32.5	79.7	88		70.5	8.0	34.4	77.1	31	
		%L-viruses	12.5	7.7	3.7	35.3	28		14.6	3.6	7.8	22.1	31		23.6	9.4	11.4	65.0	88		20.8	8.6	11.9	60.2	31	
Bathypelagic	1000-2500 m	PA ($x10^6$ mL^{-1})	1.1	0.5	0.5	2.2	29		0.7	0.3	0.1	1.5	37		0.4	0.2	0.1	0.9	102		0.4	0.1	0.2	0.6	37	
		Viruses ($x10^6$ mL^{-1})	1.6	0.5	1.2	2.9	29		1.3	0.4	0.3	2.0	37		1.1	0.5	0.5	3.2	102		0.8	0.3	0.3	1.5	37	
		VPR	16.3	6.6	8.9	36.7	29		21.6	11.0	6.5	53.6	37		27.2	8.4	13.6	66.7	102		19.5	4.4	7.9	32.4	37	
		leu incorporation (pmol leu L^{-1} d^{-1})	6.5	6.5	1.3	18.2	10		10.9	13.8	0.8	49.3	18		4.7	6.8	0.2	31.3	35		1.0	1.1	0.3	5.1	19	
		Cell-specific Leu ($x10^{-5}$ fmol $cell^{-1}$ d^{-1})	5.1	3.3	1.5	9.8	10		11.7	10.3	2.5	38.4	18		8.8	11.1	0.9	46.1	35		2.2	1.8	0.9	9.1	19	
		%HNA prokaryotes	62.2	7.6	51.9	78.9	29		55.5	7.6	40.3	69.8	37		54.2	4.1	39.8	63.0	102		56.6	3.6	50.8	65.5	37	
		%H-viruses	13.1	3.2	9.4	23.8	29		12.1	2.4	5.5	15.9	37		10.8	3.3	0.5	18.2	102		10.0	1.4	7.2	13.4	37	
		%M-viruses	76.6	5.3	65.8	84.4	29		71.7	4.7	53.7	81.8	37		68.1	8.6	40.7	79.7	102		72.0	4.7	58.2	79.9	37	
		%L-viruses	9.8	6.0	1.7	22.1	29		15.5	5.9	6.8	34.4	37		20.6	9.7	7.8	49.8	102		17.6	4.9	10.7	31.7	37	
Abyssopelagic	2500-6000 m	PA ($x10^6$ mL^{-1})	0.5	0.2	0.3	0.8	10		0.2	0.0	0.1	0.3	36		0.1	0.0	0.0	0.1	110		0.1	0.0	0.0	0.2	39	
		Viruses ($x10^6$ mL^{-1})	1.0	0.4	0.5	2.0	10		0.8	0.2	0.5	1.3	36		0.5	0.1	0.3	1.1	101		0.4	0.1	0.2	0.7	36	
		VPR	25.3	9.0	8.9	39.4	10		57.0	14.7	30.3	91.8	36		64.4	18.0	31.7	123.6	101		48.2	13.3	19.2	75.9	36	
		leu incorporation (pmol leu L^{-1} d^{-1})	2.1		1.0	3.3	2		0.2	0.1	0.1	0.5	15		0.1	0.1	0.1	0.3	35		0.2	0.1	0.1	0.4	17	
		Cell-specific Leu ($x10^{-5}$ fmol $cell^{-1}$ d^{-1})	4.4		1.1	7.7	2		1.6	0.8	0.6	3.1	15		1.5	0.6	0.6	3.2	35		2.3	1.1	0.9	4.7	17	
		%HNA prokaryotes	73.9	4.3	67.1	81.1	10		59.7	7.9	46.9	72.9	36		57.9	4.8	45.4	72.2	110		62.1	3.9	54.5	69.6	39	
		%H-viruses	13.4	3.6	8.4	22.0	10		10.7	1.9	6.8	14.7	36		8.2	2.0	2.9	13.0	101		8.4	2.0	5.3	13.0	36	
		%M-viruses	72.2	12.2	42.9	81.6	10		71.9	3.4	60.9	76.6	36		64.3	10.6	29.3	78.9	101		67.7	6.3	45.2	75.4	36	
		%L-viruses	13.7	11.3	4.0	40.3	10		16.8	4.1	11.6	28.9	36		27.2	11.1	10.6	62.5	101		23.4	7.4	11.4	48.6	36	

Abbreviation: PA, prokaryotic abundance; VPR, ratio of viral to prokaryotic abundance; leu incorporation, bulk leucine incorporation rate; cell-specific Leu, cell-specific leucine incorporation rate; %HNA prokaryotes, percentage of high nucleic acid containing prokaryotes; %H-viruses, percentage of high fluorescence viral population; %M-viruses, percentage of medium fluorescence viral population; %L-viruses, percentage of low fluorescence viral population. Average (Aver), Standard Deviation (sd), range (min-max value) and number of samples (n) are indicated for all the parameters.

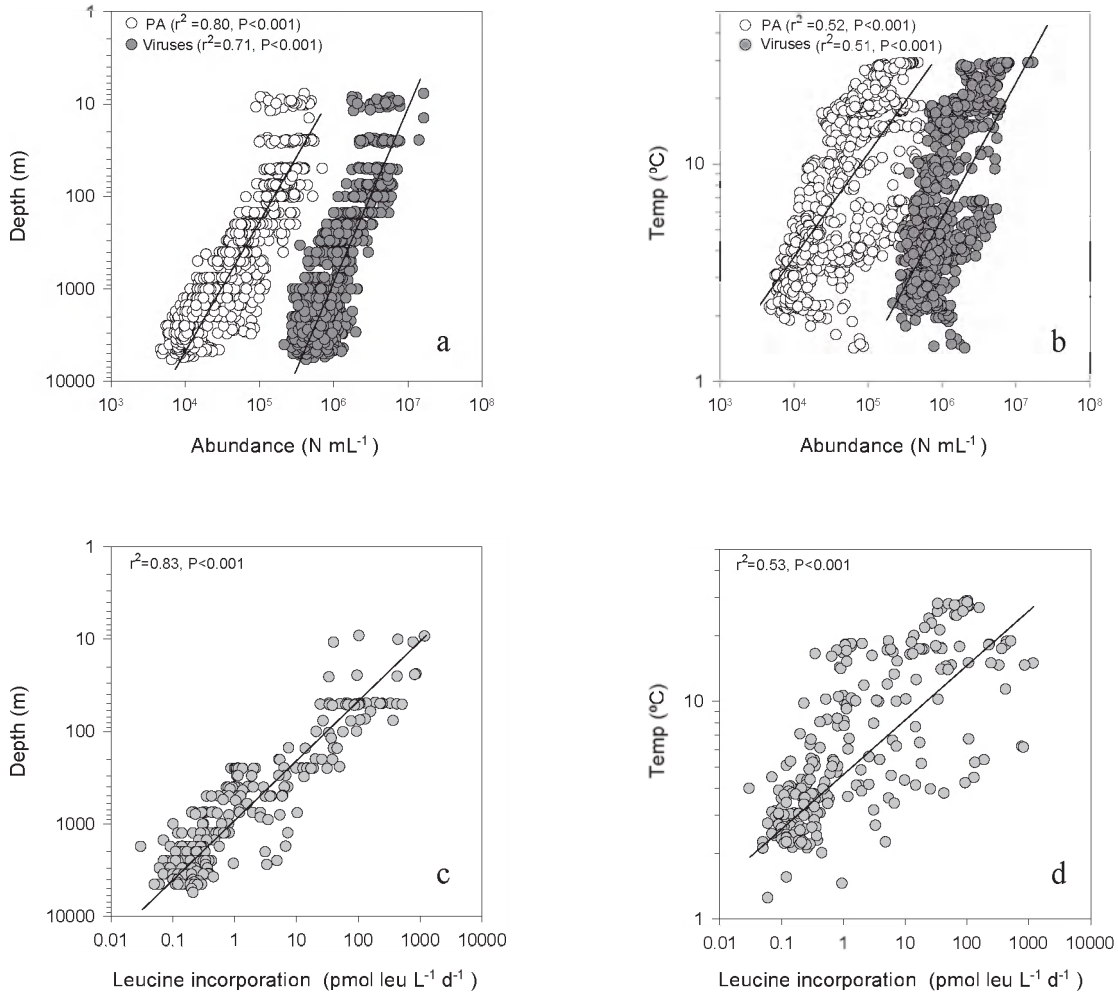

Figure 3. Relation of prokaryotic abundance (PA) and viruses versus (a) depth and (b) temperature, leucine incorporation versus (c) depth and (d) temperature.

the meso, bathy- and abyssopelagic layers, the viral abundance decreased from the ARCT to the WTRA (ANOVA on rank, $P < 0.001$).

High and low nucleic acid content prokaryotic populations were distinguished based on their signature of SYBR Green fluorescence *versus* side scatter, as determined by flow cytometry. The fraction of the prokaryotic community with high nucleic acid content did not show a significant trend neither with depth nor with latitude (Table 1).

Three different viral populations were distinguished on the basis of their fluorescence signal determined by flow cytometry. The abundance of the three viral populations decreased with depth (ANOVA on rank, $P < 0.001$). However, only the percentage of the high fluorescence viral population correlated with depth (Spearman's rank correlation coefficient $r_s = -0.531$, $P < 0.001$), ranging, on average, from 22 % in the epipelagic waters to 8 % of the total viral abundance in the abyssopelagic zone (Table 1). The medium fluorescence population comprised on average 70 % of total viral abundance without any significant trend with depth. The low fluorescence viral population showed the highest variability among the three viral populations ranging, on average,

from 10 % to 27 %, again without a specific depth-related trend (Table 1). No significant latitudinal differences over specific depth horizons were found for the three viral populations.

The virus to prokaryote ratio (VPR) significantly increased with depth from an average over all the stations of 19.2 ± 8.3 in the epipelagic layer to 59.1 ± 18.7 (ANOVA on rank, $P<0.001$) in the abyssopelagic layer (Table 1, Fig. 2b). While the VPR was positively related with depth (linear regression $r^2 = 0.50$, $P < 0.001$), it was negatively correlated with the prokaryotic abundance and production (Spearman's rank correlation coefficient, $r_s = -0.81$, $P < 0.001$ and $r_s = -0.75$, $P < 0.001$, respectively). In the bathypelagic and abyssopelagic waters of the NAG, the VPR was significantly higher than in the ARCT and WTRA provinces (ANOVA on ranks, $P < 0.001$, post hoc Dunno's test, $P < 0.05$) (Table 1, Fig. 2b).

Leucine incorporation as a proxy of prokaryotic production.

The leucine incorporation into heterotrophic prokaryotes exponentially decreased from the surface to abyssopelagic waters by three orders of magnitude from an average over the entire transect of 227.4 ± 268.1 pmol leu L^{-1} d^{-1} to 0.17 ± 0.09 pmol leu L^{-1} d^{-1} (Table 1, Fig. 2c, Fig. 3c). Significant differences in leucine incorporation were also found between the bathy- and abyssopelagic layer (ANOVA on ranks, $P < 0.001$, post hoc Dunno's test, $P < 0.05$). Leucine incorporation was also negatively related with temperature (linear regression, $r^2 = 0.53$, $P < 0.001$), and positively correlated with viral and prokaryotic abundance (Fig. 3d, Fig. 4b, c). In the bathy- and abyssopelagic waters of the NAG, leucine incorporation was significantly lower (ANOVA on ranks, $P < 0.001$, post hoc Dunno's test, $P < 0.05$) than in the bathy- and abyssopelagic waters of the ARCT and NAG regions (Table 1, Fig. 2c).

The cell-specific leucine incorporation decreased with depth from an average over all the stations of 85.2 ± 95.5 x 10^{-5} fmol $cell^{-1}$ d^{-1} to 1.6 ± 0.7 x 10^{-5} fmol $cell^{-1}$ d^{-1}. The highest cell-specific activity was found in the NADR province in the epi- and mesopelagic layers whereas in the bathypelagic zone, the highest cell-specific leucine incorporation was detected in the ARCT region (Table 1, Fig. 2d). In the bathy- and abyssopelagic waters of the NAG, cell-specific leucine incorporation rates were lower than in the ARCT province (ANOVA on ranks, $P= 0.002$, post hoc Dunno's test, $P < 0.05$) (Fig. 2d).

Viral production.

Lytic viral production decreased by one order of magnitude from 29.3 x 10^5 mL^{-1} d^{-1} in the epipelagic layers to 0.5 x 10^5 mL^{-1} d^{-1} in the bathypelagic realm (Table 2) without differences among the oceanographic provinces. While the relative contribution of the three viral populations (distinguished by flow cytometry) to the total viral production did not change with depth, their contribution changed with latitude (Table 2). The contribution of the high and medium fluorescence viral population to total lytic viral production was positively correlated with latitude and therefore, increased from the WTRA to the ARCT (Spearman rank's coefficient $r_s = 0.47$, $P = 0.049$ and $r_s = 0.60$, $P = 0.008$, respectively). In contrast, the contribution of the low fluorescence viral population to total lytic viral production was negatively correlated with latitude (Spearman rank's coefficient

r_s = -0.60, P = 0.007) hence, decreased from the WTRA to the ARCT (Table 2).

The lysogenic viral production ranged between 38.3 x 10^5 mL^{-1} d^{-1} and 0.6 x 10^5 mL^{-1} d^{-1}, contributing between 17 % and 95 % to total viral production (Table 2). Generally, the contribution of lysogeny to total viral production was negatively related to latitude (Spearman rank's coefficient r_s = -0.71, P = 0.01), however, no depth related trends were discernable.

Other prokaryotic variables derived from viral production experiments.

The percentage of total prokaryotic abundance lost due to virus-induced mortality (% TPL) ranged between 3 % and 204 % d^{-1} (Table 2) and was negatively correlated with latitude (Spearman rank's coefficient r_s = -0.55, P = 0.032). Viral lysis was responsible for removing between 0.3 % and 112 % of the total gross heterotrophic prokaryotic production (production in the absence of viral lysis), without any significant trend with depth or latitude (Table 2). In contrast to gross prokaryotic production, net prokaryotic production (production in the presence of viral lysis) was negatively related to latitude (Spearman rank's coefficient r_s = -0.88, P < 0.01; Table 2) and positively related to temperature (Spearman rank's coefficient r_s = 0.77, P = 0.001; data not shown).

The prokaryotic turnover time (PTT, Table 2) calculated from the net prokaryotic production measured during the dilution experiments was negatively correlated with temperature and positively with latitude (Spearman rank's coefficient r_s = -0.58, P = 0.02, r_s = 0.86, P < 0.01, respectively; data not shown). Also the prokaryotic turnover time based on leucine incorporation rates significantly varied with latitude in the epi- (upper and lower) and mesopelagic layers (Spearman rank's coefficient r_s = -0.45, P < 0.01; r_s = -0.59 P < 0.02; r_s = -0.46, P<0.01 respectively; data not shown)

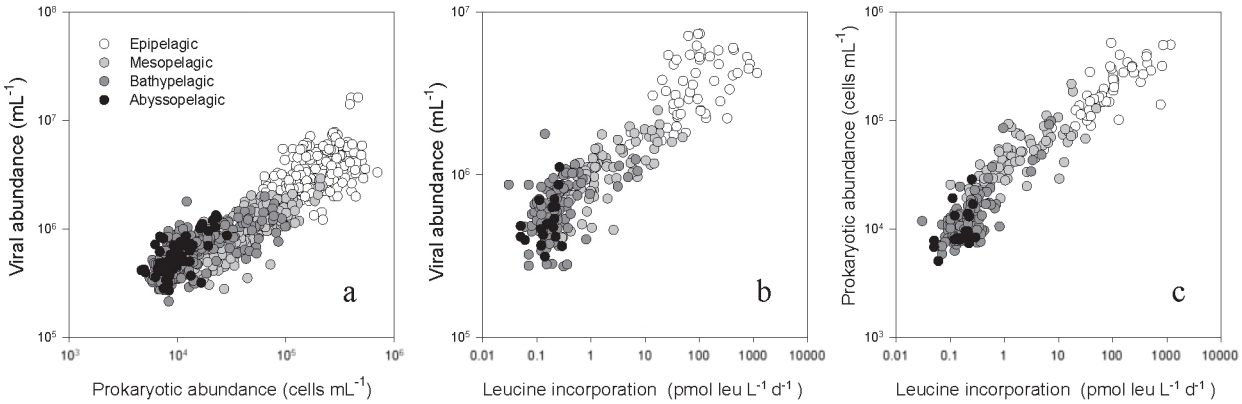

Figure 4. Relation of viral abundance versus (a) prokaryotic abundance and (b) leucine incorporation rate and (c) relation between prokaryotic abundance (PA) versus leucine incorporation rate.

Table 2. Viral parameters determined at selected stations (ST) and depths during GEOTRACES expedition. Total lytic, High, Medium, and Low fluorescence viral production (VP) and their respective percentage. Lysogenic VP versus total VP, viral turnover time (VTT), total Viral-Mediated Mortality (VMM) assuming a Burst Size (BS) of 30-50 depending on the depth (see Material and Methods), Net Prokaryotic Production (NPP), fraction of Total Prokaryotic Abundance Lost by viral infection (%TPL), percentage Prokaryotic Production Lost by viral infection (%PPL) and Prokaryotic turnover time (PTT). (ARCT-Station 4, NADR-Station 7, NAG –Stations 12-17-22-26-27 and WTRA Station 31), nd – not determined.

ST	Latitude (°N)	Depth (m)	Temp (°C)	Total Lytic VP ($x10^5$ mL^{-1} d^{-1})	VP High ($x10^5$ mL^{-1} d^{-1})	VP Medium ($x10^5$ mL^{-1} d^{-1})	VP Low ($x10^5$ mL^{-1} d^{-1})	% VP High	% VP Medium	% VP Low	Lysogenic VP ($x10^5$ mL^{-1} d^{-1})	% Lysogenic VP	VTT (d)	VMM ($x10^5$ mL^{-1} d^{-1})	% TPL d^{-1}	NPP ($x10^5$ mL^{-1} d^{-1})	%PPL	PTT (d)
4	58.60	50	7.0	18.2	4.2	13.2	0.9	23.1	72.2	4.8	nd	nd	2.3	36.5	25.8	0.47	34.2	2.98
4	58.60	600	4.0	5.1	0.9	3.5	0.6	18.3	69.6	12.1	6.9	57.7	2.4	17.0	32.6	0.06	2.5	9.12
4	58.60	1750	2.0	1.8	0.2	1.1	0.5	11.4	59.8	28.8	1.3	43.0	4.4	0.6	3.0	0.13	27.1	1.45
7	49.73	75	10.0	6.4	1.3	5.0	0.1	19.7	78.3	2.0	1.3	16.8	5.1	12.8	5.4	0.44	61.4	5.37
7	49.73	600	4.0	1.8	0.2	1.5	0.1	8.3	84.0	7.7	2.9	61.5	5.2	6.1	51.3	0.01	10.7	21.35
7	49.73	2500	2.0	0.7	0.1	0.6	0.1	10.0	79.7	10.2	4.5	86.4	11.4	2.4	nd	nd	nd	nd
12	37.55	75	15.0	25.1	1.7	15.6	7.7	6.7	62.4	30.9	nd	nd	2.2	50.1	33.3	1.19	74.3	1.27
12	37.55	750	4.0	3.1	0.2	1.5	1.4	6.1	48.4	45.5	38.3	92.5	5.3	10.3	54.8	0.32	41.8	0.60
12	37.55	4500	2.0	0.5	0.1	0.2	0.3	12.3	38.6	49.1	0.6	53.3	15.9	1.7	nd	nd	nd	nd
17	29.62	50	26.0	29.3	0.6	14.3	14.3	2.1	49.0	48.9	nd	nd	1.4	58.6	81.3	0.86	53.8	0.84
17	29.62	500	15.0	3.5	0.6	1.5	1.4	17.1	43.5	39.4	11.4	76.7	2.2	11.5	38.2	1.94	44.4	0.16
22	22.34	75	26.0	10.2	0.4	6.9	2.9	4.1	67.8	28.1	nd	nd	4.0	20.5	80.4	1.49	27.1	0.17
22	22.34	500	16.0	0.4	0.0	0.3	0.1	8.0	71.7	20.3	9.0	95.4	17.6	1.5	18.1	1.36	0.3	0.06
26	14.88	75	26.0	20.2	3.2	12.9	4.1	15.7	63.8	20.5	nd	nd	2.7	40.4	118.0	3.71	48.0	0.09
27	13.16	400	16.0	4.9	0.2	2.2	2.4	3.8	46.0	50.1	nd	nd	1.4	16.3	203.6	3.75	112.1	0.02
31	5.98	75	26.0	10.4	2.0	6.0	2.4	19.1	57.8	23.1	nd	nd	4.2	20.8	31.5	3.14	44.4	0.21
31	5.98	400	10.0	2.0	0.1	0.7	1.2	4.7	34.5	60.9	30.3	93.7	2.9	6.8	73.4	2.38	34.3	0.04
31	5.98	1750	4.0	3.5	0.2	0.5	2.8	4.6	15.0	80.4	nd	nd	1.5	11.6	nd	nd	nd	nd

and in the whole data set with temperature (Spearman rank's coefficient r_s = -0.63, P < 0.01; data not shown). Although the two estimations of the PTT showed similar trends with latitude and temperature, the PTT based on the leucine incorporation rate was at least one order of magnitude higher in the NADR and two orders of magnitude higher in the NAG and WTR provinces than the PTT estimated from the cell abundances in the dilution experiments.

The prokaryotic (calculated from the net prokaryotic production) and viral turnover times were similar in the NADR, whereas in the NAG and WTRA, the prokaryotic turnover time was one order of magnitude lower than the viral turnover time (Table 2). The viral turnover time ranged between 1 and 18 d and was significantly correlated with depth (Spearman rank's coefficient r_s = 0.48, P = 0.044).

Relationships between viral and environmental parameters.

The multivariate multiple regression analysis was used to select the best predictor variables explaining the variability of the viral abundance between the different depth layers (Table 3) and between the oceanographic provinces (Table 4).

Considering the whole data set (all depth layers and all stations), the variability of viral abundance was mainly explained by prokaryotic abundance, temperature and latitude, which together accounted for 73 % of the total variation (Table 3). The prokaryotic abundance accounted for 46 % of the variation in viral abundance, while temperature and latitude accounted for 15 % and 11 %, respectively (Table 3). The variables explaining most of the variability in viral abundance in the epipelagic zone of the whole transect were prokaryotic production, latitude and temperature explaining 56 % of the variation in viral abundance, although the contribution of latitude was low (r^2 = 0.05; P = 0.04) (Table 3). In the mesopelagic layer, the main predictor parameters for the variability in viral abundance over the latitudinal transect were prokaryotic abundance, temperature, latitude and the %HNA (cumulative r^2 = 0.62), with prokaryotic abundance and latitude explaining 52 % of the variability in viral abundance. Latitude and temperature explained 47 % and 88 % of the variations in viral abundance in the bathy- and abyssopelagic realm, respectively (Table 3).

Potential differences among the oceanic provinces in the parameters explaining the variation in viral abundance were investigated using data collected throughout the water column (Table 4). The prokaryotic abundance accounted for 69 %, 68 % and 13 % of the variation in viral abundance in the water column of the ARCT, NADR and WTRA, respectively. Temperature accounted for 12 %, 73 % and 92 % of the variation in the ARCT, NAG and WTRA, respectively (Table 4). Surprisingly, prokaryotic heterotrophic production (estimated via leucine incorporation) explained only 3 % and 1 % of the variation in viral abundance throughout the water column in the NADR and NAG and depth and the % HNA only 6 % and 2 %, respectively, in the NADR (Table 4). While the contribution of prokaryotic abundance explaining the variation in viral abundance decreased from the ARCT to the WTRA, the contribution of the temperature increased from the ARCT to the WTRA (Table 4).

The variability in lytic viral production was mainly explained by depth and viral abundance (DISTML test, cumulative r^2 = 0.82), with depth alone explaining 72 % of the variation (data not

shown).

Discussion

Latitudinal trends in prokaryotic abundance and production.

Overall, the prokaryotic abundance was higher in the ARCT than in the other provinces, particularly in the bathypelagic waters (Fig. 2a, Table 1). In this deep-water layer, prokaryotic abundance decreased from the ARCT towards the NAG and WTRA, reflecting the distribution pattern of phytoplankton productivity in these Atlantic provinces (Fig. 2a). Similarly to the prokaryotic abundance, the highest prokaryotic heterotrophic production (measured as leucine incorporation) was found in the ARCT and NADR (Table 1). Remarkably, there was a pronounced minimum in leucine incorporation detectable in the NAG below about 2000 m depth (Fig. 2c). NAG is generally characterized by low primary production in the surface waters and low export flux (Sathyendranath et al., 1995). This low supply of particulate organic matter (POM) sedimenting into the deep waters of the NAG apparently provokes the lower prokaryotic abundance and leucine incorporation in the bathy- and abyssopelagic waters in the NAG than at the same depth layers outside the NAG further north and south (Fig. 2a, c). This supports the notion that bathy- and abyssopelagic prokaryotic heterotrophic activity mainly depends on sedimenting POM supply (Baltar et al., 2009; Nagata et

Table 3. Results of the multivariate multiple regression analysis with forward selection (DISTML forward) to explain the variability in viral abundance throughout the water column (Total) and in specific depth layers (EPI – epipelagic, MESO – mesopelagic, BATHY – bathypelagic, ABYSSO – abyssopelagic). The response variable was log transformed and the resulting data was converted in Euclidian distance similarities matrix. The Pseudo-F and the p value were obtained by permutation (n=999).

Depth layer	Selected variables	Pseudo-F	p	r^2	cumulative
Total (n=256)	Prokaryotic abundance	217.2	0.001	0.46	0.46
	Temperature	103.1	0.001	0.15	0.61
	Latitude	106.2	0.001	0.11	0.73
EPI (n=53)	Prokaryotic production	27.2	0.001	0.35	0.35
	Temperature	17.1	0.001	0.15	0.50
	Latitude	4.4	0.043	0.05	0.56
MESO (n=83)	Prokaryotic abundance	50.8	0.001	0.39	0.39
	Latitude	24.5	0.001	0.13	0.52
	Temperature	11.2	0.003	0.08	0.60
	%HNA	3.6	0.049	0.02	0.62
BATHY (n=102)	Latitude	73.91	0.001	0.43	0.43
	Temperature	7.45	0.012	0.04	0.47
ABYSSO (n=18)	Latitude	71.73	0.001	0.82	0.82
	Temperature	7.47	0.019	0.06	0.88

Abbreviation, n=number of samples

al., 2000) and hence, surface water primary production.

Cell-specific leucine incorporation followed a similar trend as bulk leucine uptake with pronounced differences among the oceanic provinces particularly in the dark realm of the ocean (Fig. 2d). Cell-specific leucine incorporation exponentially decreased with depth by two orders of magnitude with lowest cell-specific activity in the NAG (Fig. 2d). A similar increase in deep-water leucine incorporation from the NAG to the WTRA as reported here for the western basin of the North Atlantic has also been shown for the eastern basin of the Atlantic (Baltar et al., 2009). Taken together, the overall prokaryotic activity in the bathy-and abyssopelagic waters appears to be related to the sedimenting particle flux, which, in turn, is related to the overall phytoplankton productivity. The cell-specific leucine incorporation rates measured in the ARCT, NAG and WTRA reported here are comparable to previously reported rates from these regions of the eastern basin of the Atlantic (De Corte et al., 2010; Reinthaler et al., 2006).

Latitudinal trends of viral abundance and production.

Generally, the viral abundance was comparable to previous studies conducted in the subtropical Atlantic and Pacific Ocean (De Corte et al., 2010; Hara et al., 1996), but it was one order of magnitude lower than the abundance determined in the eastern basin of the North Atlantic (Parada et al., 2007) using essentially the same enumeration protocol. The virus-to-prokaryote ratio (VPR) increased with depth from ~19 in the euphotic layer to ~59 in the bathy- and abyssopelagic waters (Table 1, Fig. 2b), due to the lower decrease of viral abundance with depth as compared to that of prokaryotes. A similar increase in the VPR with depth has been previously described for the eastern basin of the Atlantic (De Corte et al., 2010; Parada et al., 2007) and the Mediterranean Sea (Magagnini et al., 2007).

On a latitudinal scale, the VPR increased in all the depth layers from the ARCT towards the WTRA (Fig. 2b). Consequently, the VPR was negatively related to prokaryotic abundance (Spearman's rank correlation coefficient $r_s = -0.81$, $P < 0.001$), and leucine incorporation (Spearman's rank correlation coefficient $r_s = -0.75$, $P < 0.001$). With the current knowledge on the ecology of viruses, we cannot fully explain the relatively high abundance of viruses compared to that of prokaryotes in the deep ocean as indicated by the high VPR in the bathypelagic waters reported here and elsewhere (De Corte et al., 2010; Parada et al., 2007). A possible explanation of the high VPR ratios in the bathy- and abyssopelagic realm might be a predominant pseudolysogenic viral cycle in the deep layers (Ripp and Miller, 1997), where nutrient-limitation of infected prokaryotes exhibit low metabolic activity and consequently, increase the phage half-life (Ripp and Miller, 1997). Pseudolysogeny might eventually result in either lysogeny or lysis (Ripp and Miller, 1997). Another possible explanation for the high VPR at depth is the longer survival time of phage is (i.e., lower decay rates) in the deep waters than in the sunlit surface waters where phages remain infective for 1-2 d (Wilhelm et al., 1998). Parada et al., (2007) report a viral turnover time in the deep waters of the eastern basin of the North Atlantic of about 40 d. Studies conducted on the survival and reproduction of coliphages suggest that a successful viral reproduction strategy is not only depending on the multiplication rates of the viruses but also on the survival of the

Table 4. Results of the multivariate multiple regression analysis with forward selection (DISTML forward) to explain the variability in viral abundance in different geographic regions. The response variable was log transformed and the resulting data was converted in Euclidian distance similarities matrix. The Pseudo-F and the p value were obtained by permutation (n=999). For physical and chemical characteristics of the oceanic provinces see Table S1.

Provinces	Selected variables	Pseudo-F	p	r^2	cumulative
ARCT (n=20)	Prokaryotic abundance	40.6	0.001	0.69	0.69
	Temperature	11.5	0.003	0.12	0.82
NADR (n=61)	Prokaryotic abundance	126.8	0.001	0.68	0.68
	Depth	14.7	0.001	0.06	0.75
	Prokaryotic production	7.9	0.011	0.03	0.78
	%HNA	4.2	0.040	0.02	0.79
NAG (n=116)	Temperature	307.3	0.001	0.73	0.73
	Prokaryotic abundance	102.7	0.001	0.13	0.86
	Prokaryotic production	3.8	0.046	0.01	0.87
WTRA (n=55)	Temperature	575.84	0.001	0.92	0.92

Abbreviation, n=number of samples

virus-host system (De Paepe and Taddei, 2006). Another possible explanation for the high VPR at depth might be that the prokaryotic community in the organic carbon depleted deep-waters like the NAG province cannot afford to invest in resistance mechanisms against viral infection resulting in an increase of the frequency of infected cells in this environment. Furthermore, the lack of a relationship between viral and prokaryotic abundance in the bathy- and abyssopelagic layers (Table 3) might be caused by the allochthonous input of viruses attached to sinking particles derived from surface waters (Parada et al., 2007). Phages embedded in particles might exhibit lower decay rates and consequently longer survival rates than free-living virus (Kapuscinski and Mitchell, 1980). These fragile particles would become disrupted during conventional Niskin bottle sampling. A predominately non-random distribution of deep-water microbes including viruses might therefore also explain the high VPR. Indeed, there is genomic evidence that deep-water bacteria have more genes indicative of a particle-attached life mode than surface water bacteria (DeLong et al., 2006). This particle-attached life style is in agreement with the recent finding of remarkably stable concentration of suspended, buoyant particles throughout the water column in the ocean (Baltar et al., 2009; Bochdansky et al., 2010).

The most abundant viral population was the medium-fluorescence population (Table 2). This is in agreement with a study conducted in the subtropical Atlantic (De Corte et al., 2010), however, in contrast to coastal environments where the low-fluorescence viral population dominates (Kimmance et al., 2007; Larsen et al., 2001; Marie et al., 1999; Pan et al., 2007). Assuming that the green fluorescence of the viruses stained with SYBR-Green is related to the nucleic acid content, it suggests a higher contribution of viruses with a medium nucleic acid content in the open ocean than in coastal environments. However, only scarce information is available on the ecology of these viral subgroups, although studies indicate that the high fluorescence viral population is often associated with viruses infecting eukaryotic plankton (Brussaard et al., 2000; Brussaard, 2004). Thus, further

studies are needed to decipher the nature and source of the medium and high fluorescence nucleic acid containing viruses in the deep waters.

The lytic viral production exponentially decreased with depth (Table 2). Lytic viral production was one order of magnitude lower than in a study conducted in the same depth layers of the subtropical Atlantic Ocean (De Corte et al., 2010) and two orders of magnitude lower than in the Southern Ocean (Evans et al., 2009). The lytic viral production obtained in our study was, however, one order of magnitude higher than reported for the Mediterranean Sea (Weinbauer et al., 2003). In contrast to the lytic viral production, the lysogenic viral production did not vary with depth (Table 2). We did find, however, an increasing proportion of lysogeny to total viral production from the ARCT to the WTRA (Table 2). The increasing contribution of lysogeny to total viral production with decreasing heterotrophic production along the latitudinal transect is in agreement with the hypothesis of Weinbauer et al., (2003) of lysogeny as an adaptation to low host abundance and activity.

The bacterial turnover time obtained in the viral production assays decreased towards the WTRA while the turnover time of the lytic viral production measured in the same experiments did not vary significantly with latitude (Table 2). Thus, a discrepancy between viral and bacterial turnover times was observed in the NAG and WTRA, where the prokaryotic turnover time was one order of magnitude lower than the viral turnover time. These results support the hypothesis that oligotrophic conditions, characterized by low phytoplankton and prokaryotic production, favor the lysogenic over the lytic viral cycle (Weinbauer and Suttle, 1999; Williamson et al., 2002; Williamson and Paul, 2004).

Links between viral and environmental variables.

The relationships between viral abundance and biotic and abiotic parameters differed among the oceanic provinces and depth layers, suggesting that the controlling factors for the distribution of viruses vary (Table 3, 4).

The prokaryotic heterotrophic production (measured as leucine incorporation) was the main explanatory variable for viral abundance in the epipelagic layer over the entire latitudinal transect, suggesting a tight coupling between prokaryotes and viruses in the sunlit epipelagic waters regardless the oceanic province (Table 3). Remarkably, latitude alone explained only 5 % of the variability in viral abundance in the epipelagic layer but 43 % and 82 % in the bathy- and abyssopelagic layer, respectively (Table 3). This is counterintuitive since one would generally assume that latitudinal variability exerts more influence on surface waters with varying trophic conditions than on the bathy- and abyssopelagic realm which is generally considered more uniform over several oceanic provinces. This pattern confirms recent evidence that the deep ocean is as dynamic as surface waters (Aristegui et al., 2009).

Conclusion.

Taken together, our data show distinct patterns in prokaryotic abundance and activity along the latitudinal transect from the Arctic to the equatorial province linked to the general thermohaline

circulation pattern and water column structure. In the ocean's interior, low prokaryotic heterotrophic activity under the gyre systems coincide with high virus-prokaryote ratios. Hence, heterogeneity in the microbiota is not restricted to the euphotic zone, but it is even more pronounced in the meso- to abyssopelagic waters indicating that low epipelagic primary production, common in the gyre systems, coupled with stratification influences prokaryotic heterotrophic activity and virus-to-prokaryote ratios. A high contribution of pseudolysogeny and/or lysogeny to total viral production in the dark ocean might explain the discrepancy found between low viral and heterotrophic prokaryotic production and the comparatively high viral abundance. Our data suggest that virus-host interactions might drastically change in response to the changes in the biotic and abiotic variables throughout different oceanic provinces in the North Atlantic. This increasing virus-prokaryote ratio with depth remains enigmatic, however, and might be related to a predominately particle-attached life mode of deep-sea microbes as metagenomic analyses suggest. Whether or not fragile deep-sea particles are really responsible for the non-random distribution of microbes remains to be resolved, requiring new sampling techniques to specifically collect these particles.

Supplementary Information

Table S1. Physical and chemical characteristics in the epipelagic (from 10 to 200 m depth), mesopelagic (from 200 to 1000 m depth), bathypelagic (from 1000 to 2500 m depth) and abyssopelagic (>2500 m depth) layers along a North Atlantic latitudinal transect during the Geotraces expedition. ARCT - North Atlantic Arctic (70°N - 55°N), NADR - North Atlantic Drift (55°N - 40°N), NAG - North Atlantic Gyral (40°N - 12°N) and WTRA - Western Tropical Atlantic (12°N - 12°S) following the classification of oceanic provinces given by Longhurst (1998.) AOU – apparent oxygen utilization.

			ARCT			NADR			NAG			WTRA		
Layer	Depth range (m)		Temp °C	Salinity	AOU (µmol kg^{-1})	Temp °C	Salinity	AOU (µmol kg^{-1})	Temp °C	Salinity	AOU (µmol kg^{-1})	Temp °C	Salinity	AOU (µmol kg^{-1})
Upper Epi	10-75 m	Average	5.7	34.95	43.49	11.8	35.39	39.76	24.2	36.13	25.0	28.3	35.66	21.44
		sd	0.7	0.12	4.38	3.6	0.57	18.80	4.1	1.16	7.9	0.7	0.67	3.61
		min	4.9	34.81	35.71	4.5	34.60	13.60	17.5	32.12	14.8	26.8	34.13	13.39
		max	6.8	35.15	50.41	15.3	36.07	95.86	29.3	36.92	47.2	29.1	36.36	28.01
Lower Epi	75-200m	Average	5.4	34.99	49.84	11.1	35.45	54.41	20.9	36.73	38.2	18.4	35.93	98.51
		sd	0.9	0.11	4.10	4.0	0.54	7.53	3.2	0.26	13.5	5.3	0.54	38.14
		min	4.2	34.83	41.57	3.8	34.70	43.08	16.7	36.04	15.1	10.3	34.95	32.78
		max	6.7	35.15	56.34	14.9	36.03	69.74	27.6	37.27	81.2	26.3	36.49	146.62
Meso	200-1000 m	Average	4.5	34.94	62.48	7.8	35.16	90.63	15.0	36.06	90.9	8.6	34.85	169.26
		sd	0.8	0.07	6.50	3.7	0.38	28.32	4.1	0.62	45.7	2.3	0.25	18.74
		min	3.9	34.89	49.30	3.6	34.77	55.60	5.2	34.66	38.1	4.7	34.51	121.86
		max	6.5	35.12	77.99	14.2	35.91	144.91	21.0	37.04	185.4	14.5	35.77	199.76
Bathy	1000-2500 m	Average	3.3	34.91	73.01	3.8	34.92	75.13	4.5	35.00	99.3	4.2	34.92	115.80
		sd	0.5	0.02	4.38	0.4	0.02	4.73	1.0	0.05	20.9	0.7	0.10	30.25
		min	1.5	34.87	62.80	3.1	34.87	60.69	3.1	34.81	81.7	3.0	34.66	85.19
		max	3.9	34.96	76.68	4.8	34.98	86.43	7.8	35.21	171.8	5.2	35.01	178.92
Abysso	2500-6000 m	Average	1.9	34.90	68.63	2.4	34.91	75.57	2.4	34.90	97.1	2.4	34.90	101.24
		sd	0.5	0.01	4.09	0.4	0.01	3.97	0.3	0.03	7.4	0.4	0.04	9.10
		min	1.44	34.88	64.79	2.0	34.89	67.29	1.9	34.83	84.6	1.3	34.77	90.96
		max	2.8	34.93	77.05	3.3	34.93	82.51	3.4	34.96	117.2	3.1	34.95	137.05

Average, Standard Deviation (sd) and range (min-max value) are indicated for all the parameters.

Acknowledgements

We thank the captain and crew of R/V Pelagia for their support and splendid atmosphere on board. ES was supported by the ESF/Austrian Science Fund (FWF) grant MOCA (to GJH), TY was supported by the Dutch Science Foundation (ALW-NWO project Geotraces), DDC received a fellowship of the University of Groningen. Laboratory work was supported by a grant from ESF/FWF (MOCA project) to GJH. This work is in partial fulfillment of the requirements for a PhD degree from the University of Groningen by DDC.

References

Anderson MJ, Ford RB, Feary DA, Honeywill C. (2004). Quantitative measures of sedimentation in an estuarine system and its relationship with intertidal soft-sediment infauna. Mar Ecol-Prog Ser **272**: 33-48.

Angly FE, Felts B, Breitbart M, Salamon P, Edwards RA, Carlson C, Chan AM, Haynes M, Kelley S, Liu H, Mahaffy JM, Mueller JE, Nulton J, Olson R, Parsons R, Rayhawk S, Suttle CA, Rohwer F. (2006). The marine viromes of four oceanic regions. *PLoS Biol* **4**:2121-2131.

Aristegui J, Gasol JM, Duarte CM, Herndl GJ. (2009). Microbial oceanography of the dark ocean's pelagic realm *Limnol Oceanogr* **54**:1501-1529.

Baltar F, Aristegui J, Gasol JM, Sintes E, Herndl GJ. (2009). Evidence of prokaryotic metabolism on suspended particulate organic matter in the dark waters of the subtropical North Atlantic. *Limnol Oceanogr* **54:** 182-193.

Bochdansky AB, van Aken HM, Herndl GJ. (2010). Role of macroscopic particles in deep-sea oxygen consumption. *Proc Natl Acad Sci USA* **107:** 8287-8291.

Bratbak G, Egge JK, Heldal M. (1993). Viral mortality of the marine alga *Emiliania huxleyi* (Haptophyceae) and termination of algal blooms. *Mar Ecol-Prog Ser* **93:** 39-48.

Breitbart M, Middelboe M, Rohwer F. (2008). Marine viruses: community dynamics, diversity and impact on microbial processes. In: Kirchmam DL (ed). *Microbial Ecology of the Oceans*, Second Edition edn. John Wiley & Sons, Inc. p 443-479.

Brussaard CPD, Marie D, Bratbak G. (2000). Flow cytometric detection of viruses. *J Virol*

Methods **85:** 175-182.

Brussaard CPD. (2004). Optimization of procedures for counting viruses by flow cytometry. *Appl Environ Microbiol* **70:** 1506-1513.

De Corte D, Sintes E, Winter C, Yokokawa T, Reinthaler T, Herndl GJ. (2010). Links between viral and prokaryotic communities throughout the water column in the (sub)tropical Atlantic Ocean. *ISME J* **4**:1501-1529.

De Paepe M, Taddei F. (2006). Viruses' life History: towards a mechanistic basis of a trade-off between survival and reproduction among phages. *PLoS Biol* **4**:1248-1256.

Del Giorgio P, Bird DF, Prairie YT, Planas D. (1996). Flow cytometric determination of bacterial abundance in lake plankton with the green nucleic acid stain SYTO 13. *Limnol Oceanogr* **41:** 783-789.

DeLong EF, Preston CM, Mincer T, Rich V, Hallam SJ, Frigaard N-U, Martinez A, Sullivan MB, Edwards R, Brito BR, Chisholm SW, Karl DM. (2006). Community genomics among stratified microbial assemblages in the ocean's interior. *Science* **311:** 496 - 503.

Evans C, Pearce I, Brussaard CP. (2009). Viral-mediated lysis of microbes and carbon release in the sub-Antarctic and Polar Frontal zones of the Australian Southern Ocean. *Environ Microbiol* **11:** 2924-2934.

Hara S, Koike I, Terauchi K, Kamiya H, Tanoue E. (1996). Abundance of viruses in deep oceanic waters. *Mar Ecol-Prog Ser* **145:** 269-277.

Kapuscinski RB, Mitchell R. (1980). Processes controlling virus inactivation in coastal waters. *Water Res* **14:** 363-371.

Kimmance SA, Wilson WH, Archer SD. (2007). Modified dilution technique to estimate viral versus grazing mortality of phytoplankton: limitations associated with method sensitivity in natural waters. *Aquat Microb Ecol* **49:** 207-222.

Kirchman DL (2002). Calculating microbial growth rates from data on production and standing stocks. *Mar Ecol-Prog Ser* **233:** 303-306.

Larsen A, Castberg T, Sandaa RA, Brussaard CPD, Egge J, Heldal M, Paulino A, Thyrhaug R, van Hannen EJ, Bratbak G. (2001). Population dynamics and diversity of phytoplankton, bacteria

and viruses in a seawater enclosure. *Mar Ecol-Prog Ser* **221:** 47-57.

Longhurst AR. (1998). Ecologycal geography of the sea. Academic Press: San Diego, CA.

Magagnini M, Corinaldesi C, Monticelli LS, De Domenico E, Danovaro R. (2007). Viral abundance and distribution in mesopelagic and bathypelagic waters of the Mediterranean Sea. *Deep-Sea Res Pt.I* **54:** 1209-1220.

Marie D, Brussaard CPD, Thyrhaug R, Bratbak G, Vaulot D. (1999). Enumeration of marine viruses in culture and natural samples by flow cytometry. *Appl Environ Microbiol* **65:** 45-52.

Middelboe M. (2000). Bacterial growth rate and marine virus-host dynamics. *Microbial Ecol* **40:** 114-124.

Middelboe M, Lyck PG. (2002). Regeneration of dissolved organic matter by viral lysis in marine microbial communities. *Aquat Microb Ecol* **27:**187-194.

Middelboe M, Riemann L, Steward GF, Hansen V, Nybroe O. (2003). Virus-induced transfer of organic carbon between marine bacteria in a model community. *Aquat Microb Ecol* **32:**1-10.

Middelboe M, Jørgensen NOG. (2006). Viral lysis of bacteria: an important source of dissolved amino acids and cell wall compounds. *J Mar Biol Assn UK* ***86:605-612.***

Nagata T, Fukuda H, Fukuda R, Koike I. (2000). Bacterioplankton distribution and production in deep Pacific waters: Large-scale geographic variations and possible coupling with sinking particle fluxes. *Limnol Oceanogr* **45:** 426-435.

Ortmann AC, Lawrence JE, Suttle CA. (2002). Lysogeny and lytic viral production during a bloom of the cyanobacterium *Synechococcus* spp. *Microb Ecol* **43:** 225-231.

Pan LA, Zhang J, Zhang LH (2007). Picophytoplankton, nanophytoplankton, heterotrohpic bacteria and viruses in the Changjiang Estuary and adjacent coastal waters. *J Plankton Res* **29:** 187-197.

Parada V, Herndl GJ, Weinbauer MG. (2006). Viral burst size of heterotrophic prokaryotes in aquatic systems. *J Mar Biol Assn UK* **86:** 613-621.

Parada V, Sintes E, van Aken HM, Weinbauer MG, Herndl GJ. (2007). Viral abundance, decay, and diversity in the meso- and bathypelagic waters of the North Atlantic. *Appl Environ Microbiol*

73: 4429-4438.

Pommier T, Canback B, Riemann L, Bostrom KH, Simu K, Lundberg P, *Tunlid A, Hagstrom A.* (2007). Global patterns of diversity and community structure in marine bacterioplankton. *Mol Ecol* **16:** 867-880.

Reinthaler T, van Aken H, Veth C, Aristegui J, Robinson C, Williams PJLR, Lebaron P, Herndl GJ. (2006). Prokaryotic respiration and production in the meso- and bathypelagic realm of the eastern and western North Atlantic basin. *Limnol Oceanogr* **51:** 1262-1273.

Ripp S, Miller RV. (1997). The role of pseudolysogeny in bacteriophage-host interactions in a natural freshwater environment. *Microbiol* **143:** 2065-2070.

Sano E, Carlson S, Wegley L, Rohwer F. (2004). Movement of viruses between biomes. *Appl Environ Microbiol* **70:** 5842-5846.

Sathyendranath S, Longhurst A, Caverhill CM, Platt T. (1995). Regionally and seasonally differentiated primary production in the North Atlantic. *Deep-Sea Res Pt.I* **42:** 1773-1802.

Schattenhofer M, Fuchs BM, Amann R, Zubkov MV, Tarran GA, Pernthaler J. (2009). Latitudinal distribution of prokaryotic picoplankton populations in the Atlantic Ocean. *Environ Microbiol* **11:**2078-2093.

Smith DC, Azam F. (1992). A simple, economical method for measuring bacterial protein synthesis rates in seawater using 3H-leucine. *Mar Microb Food Webs* **6:** 107-114.

Thingstad TF, Lignell R. (1997). Theoretical models for the control of bacterial growth rate, abundance, diversity and carbon demand. *Aquat Microb Ecol* **13:** 19-27.

Varela MM, van Aken HM, Sintes E, Herndl GJ. (2008). Latitudinal trends of Crenarchaeota and Bacteria in the meso- and bathypelagic water masses of the Eastern North Atlantic. *Environ Microbiol* **10:** 110-124.

Weinbauer MG, Fuks D, Peduzzi P. (1993). Distribution of viruses and dissolved DNA along a coastal trophic gradient in the Northern Adriatic Sea. *Appl Environ Microbiol* **59:** 4074-4082.

Weinbauer MG, Suttle CA. (1999). Lysogeny and prophage induction in coastal and offshore bacterial communities. *Aquat Microb Ecol* **18:** 217-225.

Weinbauer MG, Brettar I, Hofle MG. (2003). Lysogeny and virus-induced mortality of bacterioplankton in surface, deep, and anoxic marine waters. *Limnol Oceanogr* **48:** 1457-1465.

Wilhelm SW, Weinbauer MG, Suttle CA, Jeffrey WH. (1998). The role of sunlight in the removal and repair of viruses in the sea. *Limnol Oceanogr* **43:** 586-592.

Wilhelm SW, Brigden SM, Suttle CA. (2002). A dilution technique for the direct measurement of viral production: A comparison in stratified and tidally mixed coastal waters. *Microb Ecol* **43:** 168-173.

Williamson SJ, Houchin LA, McDaniel L, Paul JH. (2002). Seasonal variation in lysogeny as depicted by prophage induction in Tampa Bay, Florida. *Appl Environ Microbiol* **68:** 4307-4314.

Williamson SJ, Paul JH. (2004). Nutrient stimulation of lytic phage production in bacterial populations of the Gulf of Mexico. *Aquat Microb Ecol* **36:** 9-17.

Winter C, Smit A, Szoeke-Denes T, Herndl GJ, Weinbauer MG. (2005). Modelling viral impact on bacterioplankton in the North Sea using artificial neural networks. *Environ Microbiol* **7:** 881-893.

Chapter 4

Spatial distribution of Bacteria and Archaea and amoA gene copy numbers throughout the water column of the Eastern Mediterranean Sea

Daniele De Corte, Taichi Yokokawa, Marta M. Varela, Hélène Agogué, Gerhard J. Herndl

Plublished in ISME Journal (2009) 3:147–158

Abstract

Until recently, ammonia oxidation, a key process in the global nitrogen cycle, was thought to be mediated exclusively by a few bacterial groups. It has been shown now, that also Crenarchaeota are capable to perform this initial nitrification step. The abundance of ammonia oxidizing Bacteria and Archaea was determined using the bacterial and archaeal ammonia monooxygenase-a subunit(amoA) gene as functional markers in a quantitative PCR approach and related to the abundance of Bacteria and Archaea in the Eastern Mediterranean Sea. Archaeal amoA copy numbers decreased from 4000–5000 copies ml^{-1} seawater from the 200–500m depth layer to 20 copies ml^{-1} at 1000m depth. β-Proteobacterial amoA genes were below the detection limit in all the samples. The archaeal amoA copy numbers were correlated with NO_2^- concentrations, suggesting that ammonia-oxidizing Archaea may play a significant role in the nitrification in the mesopelagic waters of the Eastern Mediterranean Sea. In the bathypelagic waters, however, archaeal amoA gene abundance was rather low although Crenarchaeota were abundant, indicating that Crenarchaeota might largely lack the amoA gene in these deep waters. Terminal restriction fragment length polymorphism analysis of the archaeal community revealed a distinct clustering with the mesopelagic community distinctly different from the archaeal communities of both, the surface waters and the 3000–4000m layers. Hence, the archaeal community in the Eastern Mediterranean Sea appears to be highly stratified despite the absence of major temperature density gradients between the meso- and bathypelagic waters of the Mediterranean Sea.

Introduction

In the oceanic water column, the archaeal contribution to prokaryotic abundance varies among different regions, water masses and depths (Karner et al.,2001; Herndl et al., 2005). Crenarchaeota appear to be more variable in abundance than Euryarchaeota as revealed by catalyzed reporter deposition fluorescence in situ hybridization (CARD-FISH) (Teira et al., 2006a; Varela et al., 2008). Using genomic approaches, light has been shed onto the potential role of archaeal communities in the oceanic carbon and nitrogen cycle (Hallam et al., 2006; Lam et al.,2007). It has been firmly established now that at least some Crenarchaeota are chemoauotrophs fixing CO_2 (Herndl et al., 2005; Kirchman et al., 2007) and using ammonia as an electron donor and energy source (Francis et al., 2005; Könneke et al., 2005). Crenarchaeota might be more important than Bacteria in oxidizing ammonia as a higher abundance of the archaeal gene encoding for a subunit of the enzyme ammonia monooxygenase A, amoA, was detectable than bacterial amoA gene abundance in the North Sea and the mesopelagic waters of the North Atlantic (Wuchter et al., 2006). There are only a few studies on the prokaryotic community composition of the water column of the Eastern Mediterranean Sea (Moeseneder et al.,2001a, b, 2005). One of the most peculiar features of the Eastern Mediterranean Sea is its highly oligotrophic nature, its extremely low concentration of inorganic phosphorus (Thingstad et al., 2005) and the warm deep waters (about 14 °C). The latter is a general characteristic of the bathypelagic realm of the Mediterranean. The composition of the water masses in the individual basins of the Eastern Mediterranean Sea differs remarkably (Zervakis et al., 2004). In the northern Aegean Sea, outflow of Black Sea water introduces inorganic nutrients with decreasing influence towards the south. Several deep-water basins of the Eastern Mediterranean Sea harbor fairly isolated deep-water bodies (Zervakis et al., 2004). The differences in the physical and chemical characteristics of the water bodies from north to south in the Eastern Mediterranean Sea are also reflected by considerable changes in the bacterial community composition as revealed by terminal restriction fragment length polymorphism (T-RFLP) fingerprinting (Moeseneder et al., 2001a). The aim of this study was to determine the spatial abundance of Crenarchaeota, Euryarchaeota and Bacteria and the distribution of archaeal and bacterial amoA genes throughout the water column of the Eastern Mediterranean Sea along the north to south gradient, using CARD-FISH and quantitative-PCR (Q-PCR), respectively. T-RFLP was also used to compare the archaeal community composition among the stations and depth horizons. Our results suggest that ammonia-oxidizing Archaea may play a significant role in the nitrification in the mesopelagic realm of the Eastern Mediterranean Sea, while in the bathypelagic waters, Archaea are apparently lacking the amoA gene.

Material and Methods

Study site and sampling. The cruise in the Eastern Mediterranean Sea was conducted with

the RV AEGAEO (Hellenic Center for Marine Research, Greece) occupying five stationsin May 2007 (Figure 1). The stations were located in the North Aegean (St. 1; 48° 7.0'N, 24° 32.5'E), Mid Aegean (St. 2; 37° 42.1'N, 25° 26.0'E), Western Cretan Sea (St. 3; 36° 13.2'N, 23° 18.3'E), Ionian Sea (St. 4; 36° 15.9'N, 21° 30.1'E) and South Aegean (St. 5; 35° 47.2'N, 24° 54.7'E). Water samples were obtained from the mixed surface waters (10m depth) and the meso- and bathypelagic layers (down to a maximum depth of 4350 m) with 5L-Niskin bottles mounted on a conductivity-temperature-depth rosette sampler. Dissolved oxygen concentrations were determined with a SBE oxygen sensor mounted on the conductivity-temperature-depth and nutrient concentrations (that is, phosphate, nitrate and nitrite) with a nutrient auto-analyzer (Bran & Luebbe Autoanalyzer II, Norderstedt, Germany). For later molecular analyses of the prokaryotic community, 10 l of seawater was filtered through a 0.22 µm Sterivex filter cartridge (Millipore, Millford, MA, USA) to collect

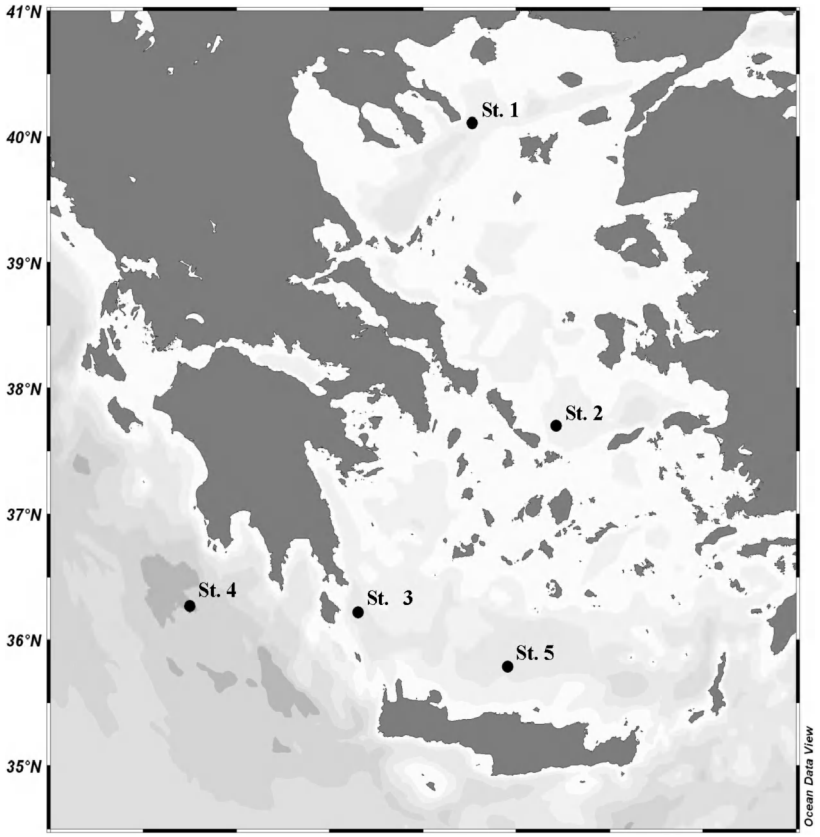

Figure 1. Sampling sites in the Eastern Mediterranean Sea occupied during the POSEIDON cruise in May 2007.

prokaryotes for molecular analyses. Thereafter, 1.8ml of lysis buffer (40mM EDTA, 50mM Tris-HCL, 0.75M sucrose) was added to the filter cartridge and the filter cartridges were stored at 80 °C.

Composition of specific phylogenetic group. The composition of Bacteria, Crenarchaeota and Euryarchaeota was determined by CARD-FISH (Teira et al., 2004). Water samples of 10 - 80 mL were collected from the Niskin bottles and preserved in paraformaldehyde (2% final concentration) at 4°C in the dark for 18 h. Thereafter, the samples were filtered onto 0.2 µm polycarbonate filters (Millipore, GTTP) supported by 0.45 µm cellulose nitrate filters (Millipore, HAWP), rinsed with

Milli-Q water, dried and stored in microfuge vials at –20°C until further processing in the laboratory.

Filters for CARD-FISH were embedded in low-gelling-point agarose and incubated either with lysozyme for the Bacteria probe mix (Eub338, Eub338II and Eub338III) or with proteinase-K for marine Euryarchaeota Group II probe Eury806 and for the marine Crenarchaeota Group I probes Cren537 (Teira et al., 2006a) and GI-554 (Massana et al., 1997) following the method described by Teira et al., (2004). Filters were cut in sections and hybridized with horseradish peroxidase (HRP)-labelled oligonucleotide probes and later incubated with tyramide-Alexa488 for signal amplification. Thereafter, the filter sections were stained with a DAPI mix [5.5 parts of Citifluor (Citifluor), 1 part of Vectashield (Vector Laboratories) and 0.5 parts of phosphate-buffered saline (PBS) with DAPI (final concentration 5 μg mL^{-1})].

Hybridized and DAPI-stained cells were detected under a Zeiss Axioplan 2 epifluorescence microscope equipped with a 100 W Hg-lamp and appropriate filter sets for Alexa488 and DAPI. More than 600 DAPI-stained cells were counted per sample. For each microscope field, two categories were determined: total DAPI-stained cells and cells stained with the specific probe.

DNA extraction. The cartridges of the Sterivex filters were cracked open and the filters and the lysis buffer transferred into 50 ml sterile centrifuge tubes. DNA extraction was performed using the Mega Kit extraction (MoBIO laboratories, Carlsbad, CA, USA) and the protocol of the manufacturer. DNA extracts were concentrated (approximately 10 times) with a Centricon device (Millipore).

Q-PCR analysis. We conducted Q-PCR targeting 16S rRNA gene fragments of Marine Crenarchaeota Group I (MCGI) and the pSL12 cluster and archaeal amoA genes for the samples collected at Sts. 1, 2 and 4 (St. 1: 100, 200 and 950 m; St. 2: 300, 400 and 750 m; St. 4: 1000,

3000 and 4350 m). β-Proteobacterial amoA genes were targeted using amoA-1F (50-GGGGTTTCTACTGGTGGT)/amoAr-new (50-CCCCTCBGSAAAVCCTTCTTC) (Hornek et al., 2006). A mix of 25% of Nitrosomonas europaea, 25% of N. eutropha, 25% of N. marina and 25% of Nitrosospira briensis was used as a standard. β-Proteobacterial amoA genes, however, were not detected at any of the stations, although the same primer set readily detected β-Proteobacterial amoA in the coastal North Sea and the open North Atlantic (Wuchter et al., 2006). All Q-PCR experiments were performed on an iCycler iQ 5 thermocycler (Bio-Rad, Philadelphia, PA, USA) equipped with iCycler iQ software (version 3.1, Bio-Rad). The amoA copy numbers in the standards and environmental samples were determined in triplicate with three different dilutions.

The reaction mixture (20 μl) contained 1 unit of Pico Maxx polymerase, 2 μl of 10 Pico Maxx PCR buffer (Stratagene, La Jolla, CA, USA), 0.25 mM of each dNTP, 8 μg of bovine serum albumin, 0.2 mM of primers, 50 000 times diluted SYBR Green I (Molecular Probes), a final concentration of 10 nM fluorescein, 3 mM $MgCl_2$ and ultra-pure sterile water (Wuchter et al., 2006). The efficiency of the quantification reaction ranged between 74.5 and 111.5% with an r^2 ranging from 0.983 to 1.000. Marine Crenarchaeota Group I (MCGI) 16S rRNA gene fragments were detected using the primer set MCGI-391f (50-AAGGTTARTCCGAGTGRTTTC) and MCGI-554r (50-TGACCACTTGAGGTGCTG) with plasmid 88exp4 as a standard and primer

annealing at 61 ºC for 40 s (Wuchter et al., 2006). The pSL12 16SrRNA gene fragments were detected using the primer set pSL 12-750F (50-GGTCCRCCAGAACGCGC) and pSL12-876R (50-GTACTCCCCAGGCGGCAA) with fosmid HF770_041/11 as a standard and primer annealing at 65 ºC for 40 s (Mincer et al.,2007). Archaeal amoA genes were detected using the specific archaeal amoA primer set arch-amoAfor (50-CTGAYTGGGCYTGGACATC) and arch-amoArev (50-TTCTTCTTTGTTGCCCAGTA) with Nitrosopumilus maritimus as a standard and primer annealing at 58.5 ºC for 40 s (Wuchter et al., 2006). The PCR efficiencies and correlation coefficients for the standard curves were as follows: for the MCGI 16S rDNA assay, 87.9–105.8% and r^2=0.991–0.999, for the pSL12-like 16S rDNA assay, 94.7–110.5% and r^2=0.949–0.999, for the archaeal amoA assay, 86.5–97% and r^2=0.983–0.999 and for the β-proteobacterial amoA assay, 77.8–88.3% and r^2=0.989–0.999.

PCR and T-RFLP. PCR conditions and chemicals were applied as described by Moeseneder et al. (2001a). One ml of the DNA extract was used as a template in a 50 µl PCR mixture. For PCR, the universal primer 1492R-JOE (Lane, 1991) and the Archaea-specific primers 21F-FAM and 958R-JOE were used (Moeseneder et al., 2001a). Samples were amplified by an initial denaturation step at 94 ºC (for 3 min), followed by 35 cycles of denaturation at 94 ºC (1 min), annealing at 55 ºC (1 min), and an extension at 72 ºC (1 min). Cycling was completed by a final extension at 72 ºC for 7 min. The PCR products were run on 1.0% agarose gel. The gel was stained with a working solution of SYBR Gold and the obtained bands were excised, purified with the Quick gel extraction kit (Genscript, Piscataway, NJ, USA), and quantified using a Nanodrop spectrophotometer. Fluorescently labeled PCR products were digested at 37 ºC overnight. Each reaction contained 30 ng of cleaned PCR product, 5U of tetrameric restriction enzyme (HhaI) and the respective buffer filled up to a final volume of 50 µl with ultra-pure water (Sigma, St Louis, MO, USA). The restriction enzyme was heat inactivated and precipitated by adding 4.5 µl LPA solution and 100 µl of 100% isopropanol. The samples were kept at room temperature for 15 min followed by centrifugation at 15 000 g for 15 min. Thereafter, the supernatant was discarded and the pellet rinsed with 100 ml 70% isopropanol and precipitated again by centrifugation (15000 g for 5 min). Subsequently, the supernatant was removed again and the sample dried in the cycler at 94 ºC for 1 min and stored at 20 ºC until further analysis. The pellet was resuspended in 2 µl of ultra-pure water and the product denatured in 7.8 µl of Hi-Di formamide at 94 ºC for 3 min. Each sample contained 0.2 µl GeneTace 1000 (ROX) marker (Applied Biosystems, Foster City, CA, USA). Fluorescently labeled fragments were separated and detected with an ABI Prism 310 capillary sequencer (Applied Biosystem) run under GeneScan mode (van der Maarel et al., 1998; Moeseneder et al., 1999). The size of the fluorescently labeled fragment was determined by comparison with the internal GeneTace 1000 (ROX) size standard. Injection was performed electrokinetically at 15 kV for 15 s (adjustable) at 60 ºC. The output from the ABI Genescan software was transferred to the Fingerprinting II (Bio-Rad) to determine the peak area and for standardization using size markers. The obtained matrix was further analyzed with Primer software (Primer-E) to determine similarities of the T-RFLP fingerprints between samples.

Table 1. Sampling station, region, depth layer, number of samples, temperature, salinity, oxygen, phosphate, nitrate and nitrite concentrations. Parameters of the top 100 m layer are given as range, all other data represent mean ± SD. Prokaryotic abundance was determined by flow cytometer.

Station	Region	Layer (m)	Number of samples	Temp. (°C)	Salinity	Prokaryotic abundance ($x10^5$ cells mL^{-1})	Dissolved Oxygen (mmol L^{-1})	PO_4 (mmol L^{-1})	NO_3 (mmol L^{-1})	NO_2 (mmol L^{-1})
1	North Aegean	< 100	2	14.3 - 16.2	36.7 - 38.4	4.3 - 2.6	129.8 - 133.6	0.043 - 0.048	0.362 - 0.680	0.052 - 0.098
		100 - 950	6	13.8 ± 0.4	39.0 ± 0.0	1.7 ± 0.6	124.2 ± 4.6	0.120 ± 0.044	3.102 ± 1.293	0.049 ± 0.007
2	Mid Aegean	< 100	2	15.5 - 16.6	39.2 - 40.0	3.9 - 4.1	109.6 - 141.9	0.021	0.074 - 0.129	0.046 - 0.048
		100 - 750	7	14.4 ± 0.3	39.0 ± 0.1	2.2 ± 1.1	132.6 ± 3.2	0.069 ± 0.020	1.757 ± 0.526	0.053 ± 0.009
3	Western Cretan	< 100	2	15.0 17.8	38.8	2.9 - 3.7	137.5	0.027	0.123 - 0.413	0.040 - 0.075
		100 - 1200	7	14.4 ± 0.1	38.9 ± 0.0	1.0 ± 0.4	130.1 ± 2.3	0.101 ± 0.040	2.556 ± 1.056	0.048 ± 0.008
4	Ionian	< 100	2	16.8 - 19.9	38.7	2.5 - 3.2	137.3 - 147.0	0.021 - 0.032	0.029 - 0.056	0.038 - 0.045
		100 - 1000	7	14.9 ± 0.8	38.8 ± 0.1	1.5 ± 1.1	129.9 ± 11.0	0.087 ± 0.065	1.755 ± 1.536	0.042 ± 0.008
		2000 - 4350	3	14.6 ± 0.8	38.8 ± 0.0	0.2 ± 0.1	123.0 ± 1.3	0.151 ± 0.003	3.571 ± 0.447	0.042 ± 0.006
5	South Aegean	< 100	2	15.6 - 20.4	36.0 - 39.0	2.8 - 5.0	117.6 - 152.3	0.027	0.071 - 0.333	0.049 - 0.083
		100 - 1350	7	14.7 ± 0.5	39.0 ± 0.1	1.5 ± 1.5	137.2 ± 4.7	0.097 ± 0.043	2.520 ± 1.258	0.074 ± 0.063

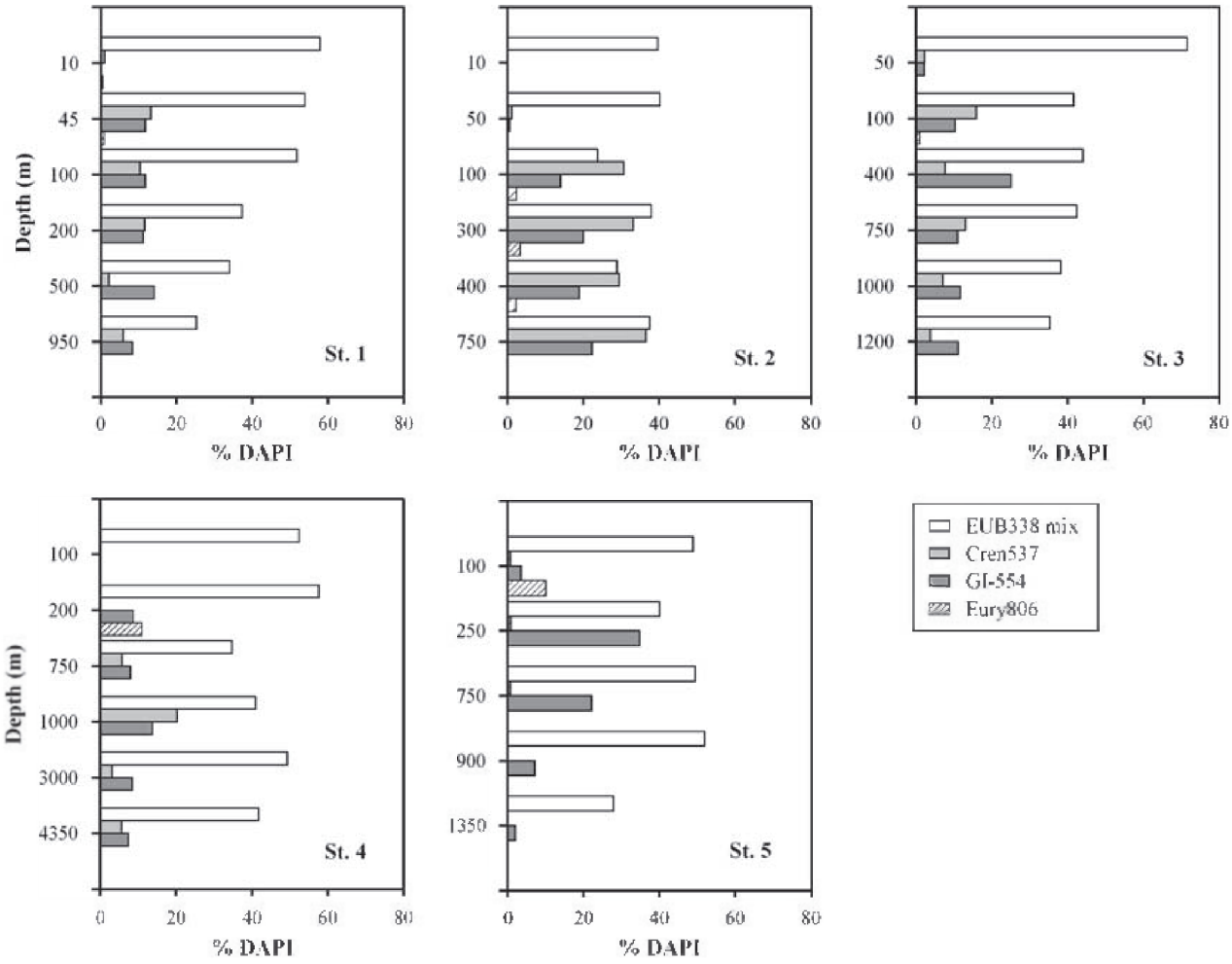

Figure 2. Contribution of Bacteria (EUB338 mix), Cren537-positive cells, GI-554-positive cells and Eury806-positive cells to total prokaryotic abundance (% of DAPI-stained cells) at the individual stations determined by CARD-FISH.

Results

There was little variability in temperature and salinity among the five stations (Table 1). Phosphate and nitrate concentrations exhibited the common depth-related trend with low concentrations in the top 100m layer and increasing with depth (Table 1). Oxygen concentrations remained rather constant with depth exhibiting no pronounced oxygen minimum layer.

Prokaryotic community composition determined by CARD-FISH.

The mean contribution of Bacteria to total prokaryotic abundance (that is, DAPI-stained cell) was 45±10% (n=29) averaged over all the stations and depth layers (Figure 2). Overall, the variability in the relative abundance of Crenarchaeota and Euryarchaeota was higher than that for Bacteria.Both, the Cren537 and the GI-554 probe, target the same crenarchaeal phylotypes with an additional 5 and 14% of phylotypes covered by the probe Cren537 and GI-554, respectively (Figure 3). The relative contribution of Cren537- and GI-554-positive cells to total prokaryotic

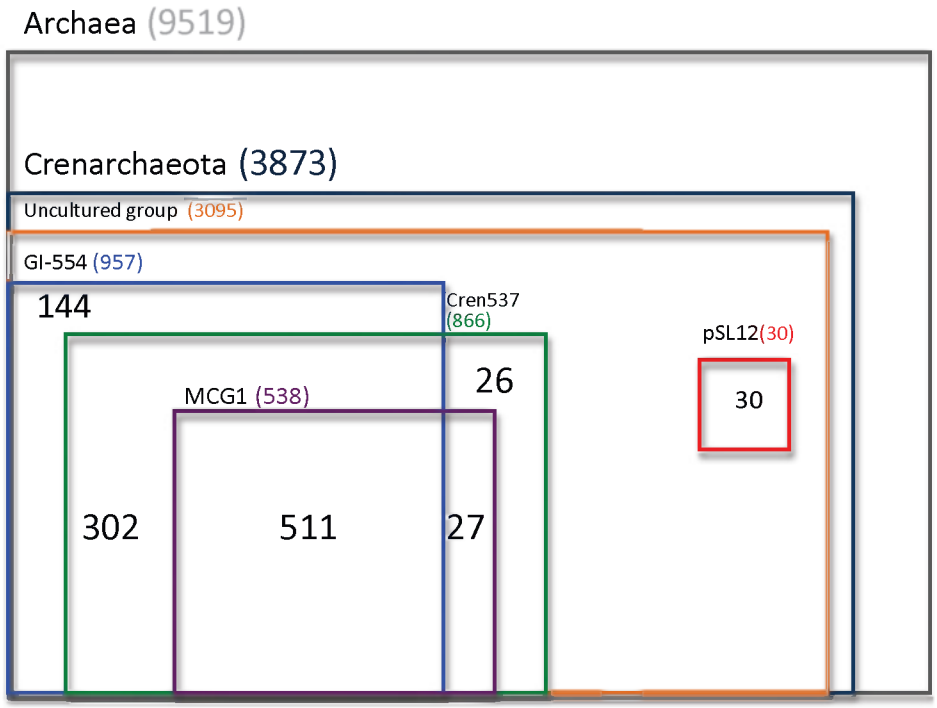

Figure 3. Scheme of the coverage of 16rRNA sequences deposited in SILVA database of the crenarchaeal FISH probes Cren537 and GI-554 and the PCR primers (give acronyms here) as of 4 April 08. Numbers in parentheses are number of phylotypes of the specific target group in the database. Numbers in the boxes represent the number of phyloytypes covered by the probe or primer.

abundance was 7±9% (average±s.d., n=29), and 12±9% (n=29), respectively (Figure 2). The ratio of GI-554- to Cren537-positive cells ranged from 0.12 to 39.70. At St. 2, the relative abundance of Cren537-positive cells was higher than of GI-554-positive cells throughout the water column, whereas GI-554-positive cells dominated at St. 5 (Figure 2). At St. 5, the maximum percentage of GI-554-positive cells was 35% at 250m decreasing with depth. Eury806-positive cells represented only a minor fraction of total prokaryotic abundance (1±3%, n=29) at all the stationsand were detected only in the top 400m of the water column (Figure 2).

Abundance of specific phylogenetic groups determined by CARD-FISH and Q-PCR.

In 14 out of 29 samples, the difference in abundance between Cren537- and GI-554-positive cells was larger than a factor of 2 (Figure 4). These differences in abundance between Crenarchaeota enumerated by the Cren537 and GI-554 probe were highest in the upper mesopelagic realm. Copy numbers of the 16S rRNA gene of the crenarchaeal MCGI and the pSL12 cluster were determined by Q-PCR from several depths at Sts. 1, 2 and 4. The average copy numbers of the 16S rRNA gene of MCGI was 10.9±11.1x10^3 copies ml^{-1} seawater (n=9), while the corresponding copy numbers of the pSL12 cluster were about three times lower (3.4±6.5x10^3 copies ml^{-1}, n=9) (Figure 4). There was a distinct difference in the spatial distribution pattern between MCGI and the pSL12 cluster. Higher copy numbers of the 16S rRNA gene of MCGI were obtained for the mesopelagic layer (200–1000 m) than for the surface and bathypelagic waters (>1000 m), while copy numbers of the

pSL12 cluster did not exhibit major fluctuations with depth (Figure 4).

Archaeal community composition based on T-RFLP fingerprinting.

The T-RFLP pattern of the archaeal community revealed in total 27 operational taxonomic units (OTUs) on the 16S rDNA level ranging from 13.2 to 1016 bp fragments (Figure 5a). Only one of the 27 OTUs (248.2 bp fragment) was present at all stations and depths and the OTUs of 580.99 and 591.29 pb were presented in almost all the samples without a clear vertical pattern. The OTU of 129.79 bp was detectable in all the samples until 1400m depth but not at greater depth. Among all the stations, St. 4 exhibited the highest and lowest number of OTUs detectable in a specific sample, 13 OTUs at 750m depth and 2 OTUs at 3000m depth (Figure 5a). The Jaccard similarity cluster analysis indicated three distinct clusters, a subsurface water, a meso- and a bathypelagic cluster (Figure 5b). Analysis of similarities (ANOSIM) revealed significant differences in archaeal community composition between the surface layer (45–100m depth) and the mesopelagic layer (200–1000m depth, $r=0.69$, significant level: 0.1) and between the mesopelagic layer and the bathypelagic layer (>1400 m, $r=0.60$, significant level: 5.5).

Depth profile of archaeal amoA copy numbers.

Copy numbers of the archaeal amoA gene were readily detectable (Figure 6a), while β-proteobacterial amoA genes were undetectable at all the stations. Copy numbers of the archaeal amoA gene were, on average, $3.9\pm1.2 \times 10^3$ copies ml^{-1} (mean±s.d., n=4) in the 200–500m layer and 1.6×10^3 copies ml^{-1} at 750m depth. Below 950m depth, archaeal amoA copy numbers never exceeded 10 copies ml^{-1} (n=4). Ratios of archaeal amoA gene copy numbers to 16S rRNA gene copy numbers (sum of MCGI and pSL12) decreased drastically with depth (Figure 6b).The ratios decreased from 0.49 at 100m to 0.12 at 400m depth. Below 750m depth, the ratios were below 0.05 (0.01±0.02, n=5). The ratios of archaeal amoA gene copy numbers to crenarchaeal abundance, determined by CARD-FISH with the probes Cren537 and GI-554 (Figure 6c), were not significantly different from those obtained using the sum of the 16S rRNA copy numbers of MCGI and pSL12 (ANOVA on ranks, $x^2=0.222$, $P=0.895$). Copy numbers of the archaeal amoA gene correlated with nitrite concentrations ($r=0.79$, $P<0.01$, n=9), while no relation was found with nitrate ($P>0.05$, n=9); unfortunately no data are available for ammonium.

Discussion

Prokaryotic community composition.

Bacteria contributed between 24 and 72% to total prokaryotic abundance at the sampling stations in the Eastern Mediterranean Sea. Although the contribution of Bacteria to total prokaryotes did not differ significantly among the stations and did not show any depth-related pattern, the bacterial contribution to total prokaryotic abundance is more variable in the Eastern Mediterranean Sea than in the North Atlantic determined by essentially the same approach as used here (Teira et al., 2006a;

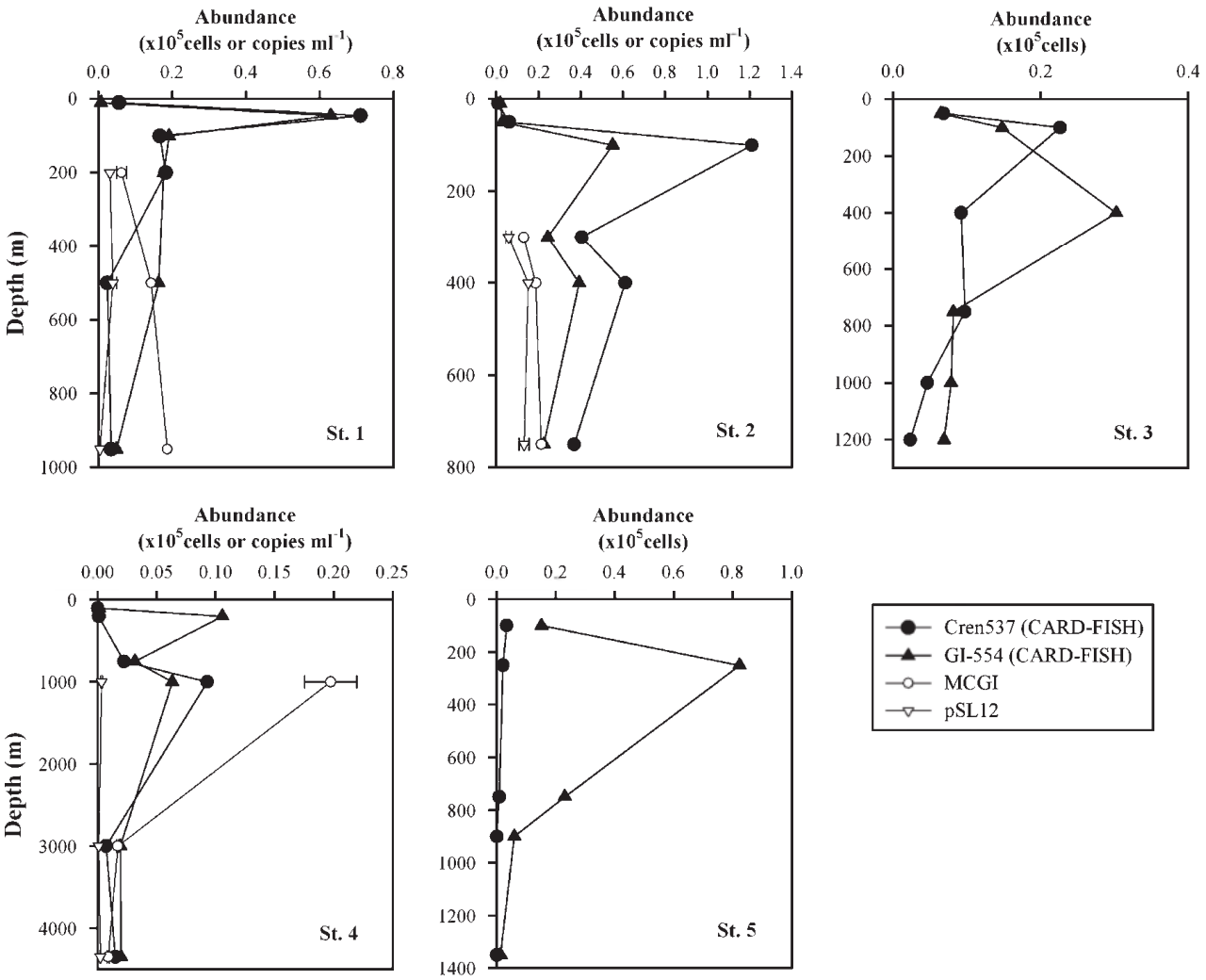

Figure 4. Depth profiles of Cren537- and GI-554-positive cells determined by CARD-FSIH (at Sts. 1 - 5), and MCGI and pSL12 gene copy numbers determined by Q-PCR (at Sts. 1, 2, and 4). For Q-PCR, the mean±SD of determination are given in the samples where we took triplicate determination, while the average of determination are given in the samples where we took duplicate determination.

Varela et al., 2008).

The mean contribution of the Euryarchaeota to total prokaryotic abundance averaged only 1.4% and they are confined to the subsurface and mesopelagic layers (Figure 2). Other studies also report only a minor contribution of Euryarchaeota to the prokaryotic community such as for the western Arctic Ocean (average: 3.5% in Table 1 of Kirchman et al., (2007)), the north-west Mediterranean coastal waters (average: 2.5% in Table 2 of Alonso-Saez et al., (2007)) and the (sub)tropical North Atlantic region (<5%, (Varela et al., 2008)). Thus, the minor contribution of Euryarchaeota to prokaryotic abundance appears to be a common feature for this group, however, higher contributions than that reported by the above studies have been found in some deep waters of the North Atlantic (Teira et al., 2006a) and by shotgun sequencing of fosmid clone libraries in the North Pacific (DeLong et al., 2006). Euryarchaeota inhabiting the surface waters have been

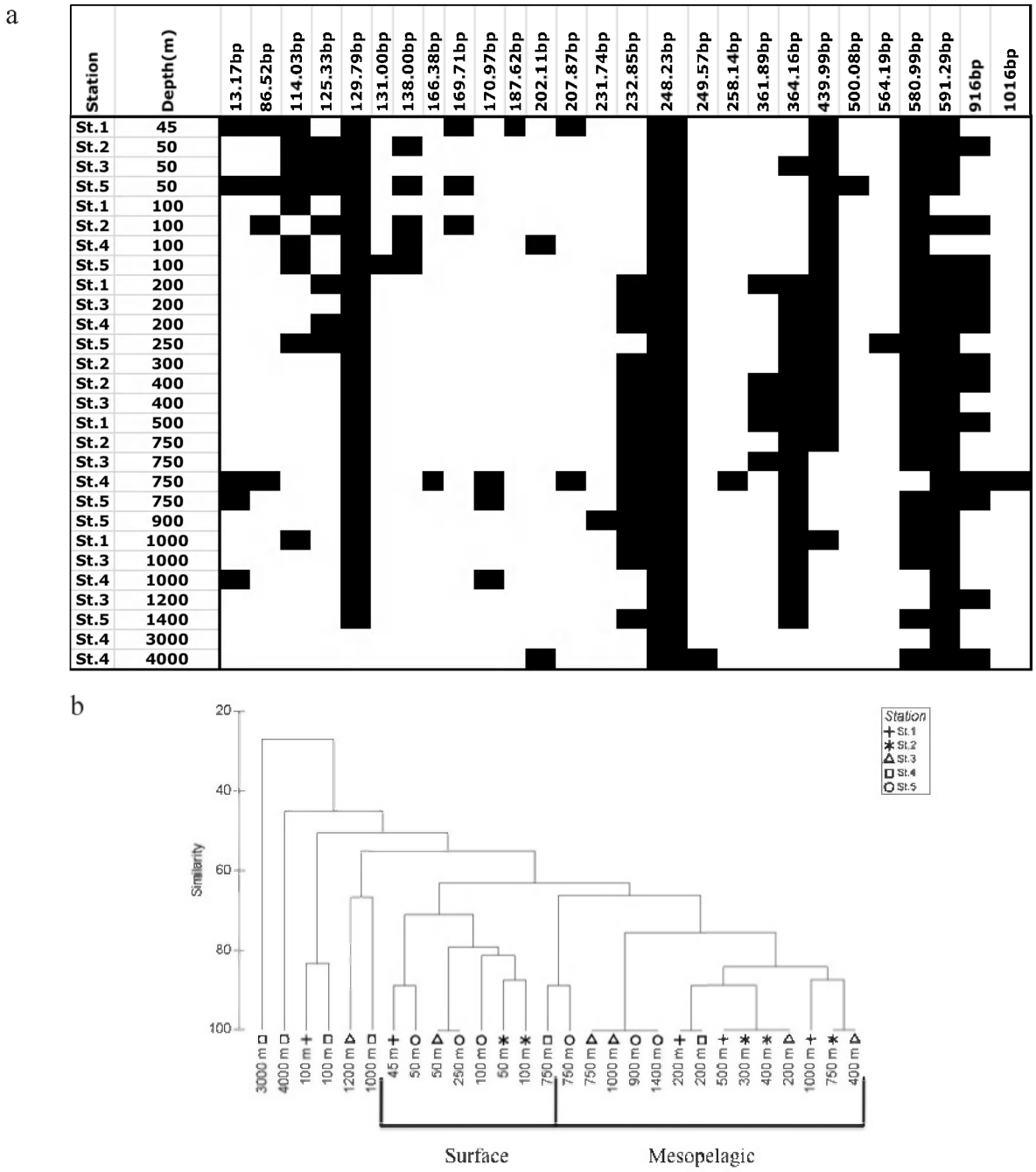

Figure 5. Archaeal community composition as revealed by T-RFLP anaylis. (A) Presence/absence distribution of all the individual archaeal OTUs detected at the individual stations and depth layers. Rows are aligned from surface to deep waters. (B) Similarity matrix for the individual samples ontained in the Eastern Mediterranean Sea.

shown to harbor the proteorhodopsin gene allowing them to use light to drive the membrane proton pump, while deep-water Euryarchaeota lacked the proteorhodopsin gene (Frigaard et al., 2006).

The relative contribution of Cren537- and GI-554-positive cells to total prokaryotic abundance was 7±9 and 12±9%, respectively (Figure 2). Cren537 covers 866 out of 3873 phylotypes of Crenarchaeota and all the MCGI present in the SILVA database as of 4 April 2008, while GI-

554 covers 957 crenarchaeal phylotypes resulting in an overlapping coverage of 813 phylotypes (Figure 3). Applying both probes separately using CARD-FISH on the same sample, we detected a variable number of Crenarchaeota. At St. 5, GI-554-positive cells dominated throughout the water column, while at St. 2, Cren537-positive cells dominated (Figure 2). These large variations in the relative abundance of Cren537 (range: 0–37%) and GI-554 (range: 0–35%) might suggest compositional differences in the crenarchaeotal community among stations. Recent studies showed that the relative abundance of marine Crenarchaeota Group I increases with depth in the North Atlantic and the Arctic Ocean (Herndl et al., 2005; Kirchman et al., 2007). However, no consistent depth-related trends in the relative abundance of both Cren537-positive and GI-554-positive cells are detectable in the Eastern Mediterranean Sea (Figure 2). The lack of a depth-related trend in the distribution of Crenarchaeota contrasts the pronounced decrease in the copy numbers of archaeal amoA genes with depth and the compositional differences in the archaeal community structure revealed by T-RFLP, discussed in more detail below.

The recovery efficiency with our CARD-FISH approach, that is, the sum of Bacteria determined by the EUB338 probe mix (average recovery efficiency: 44.7±10.0%, n =29), Euryarchaeota (detected by Eury806, 1.4±3.6%, n=19) and Crenarchaeota (detected either by Cren537 (6.8±9.5%, n=29) or GI-554 (11.7±9.1%, n =29)), ranged from 28 to 75%. Considering the almost complete coverage of all the bacterial groups with the EUB338 probe mix (Amann and Fuchs, 2008), the occasionally low recovery efficiency might be caused by a low coverage of the crenarchaeal community with the probes Cren537 and GI-554, by inefficient permeabilization of the cell membranes of certain prokaryotic cells or a variable contribution of dead or decaying cells still stainable with DAPI but lacking sufficient RNA (Del Giorgio and Gasol, 2008).

Abundance of specific phylogenetic groups determined by CARD-FISH and Q-PCR.

Both, the abundance of Cren537- and GI-554- positive cells were within the range previously reported for Crenarchaeota (using the probe Cren537) in the North Atlantic and the Arctic Ocean (Herndl et al., 2005; Kirchman et al., 2007). Commonly, the crenarchaeal abundance determined by the Cren537 probe closely matched to that obtained by the GI-554 probe (Figure 4). Remarkable differences were noticed at specific stations and depths such as at St. 3 at 400m depth, where the abundance of GI-554-positive Crenarchaeota was more than twice as high as the abundance of Cren537-positive cells. At St. 5, a pronounced peak in abundance of GI-554-positive Crenarchaeota was detected at around 200m depth, while Cren537- positive Crenarchaeota were very low in abundance throughout the water column of this station (Figure 4).

The two crenarchaeal groups, MCGI and pSL12, have recently also been detected in the mespelagic zone at St. ALOHA in the subtropical gyre of the Pacific (Mincer et al., 2007). Using Q-PCR, the abundance of MCGI was always higher than the abundance of the pSL12 cluster (Figure 4). Generally, the abundance of MCGI determined by Q-PCR should not be higher than that obtained by the Cren537 probe using CARD-FISH, because the latter targets all the known partial sequences of the MCGI (Figure 3). However, in two out of nine samples, MCGI copy numbers were higher than the crenarchaeal abundance determined by either the Cren537 or GI-

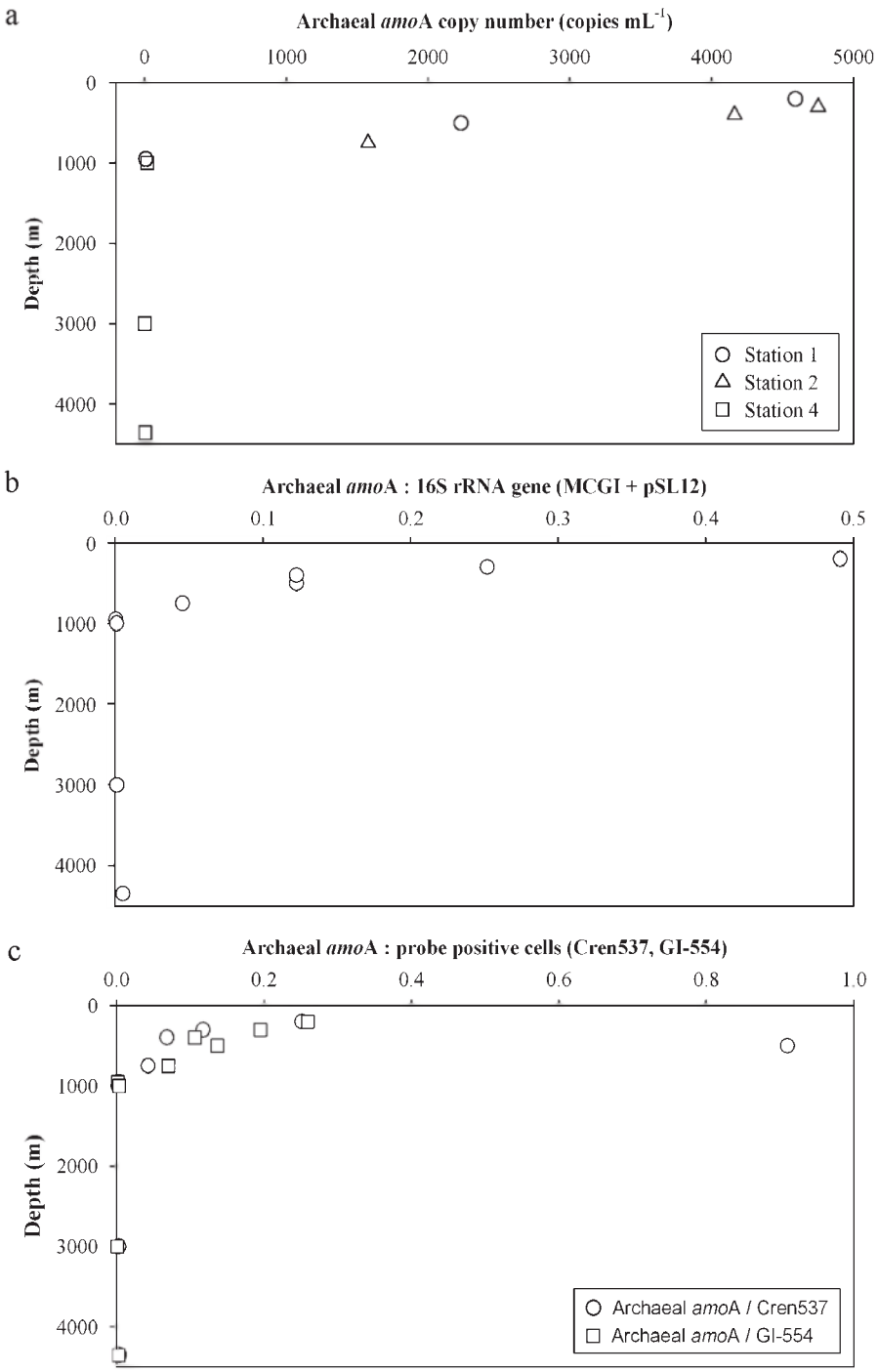

Figure 6. Depth distributions of amoA gene copy numbers at the Sts. 1, 2 and 4 (A); ratios of archaeal amoA to archaeal 16S rRNA gene (i.e., sum of MCGI and pSL12) (B); ratios of archaeal amoA to Cren537 or GI-554 (C).

554 oligonucleotide probe. This might be due to PCR bias (Becker et al., 2000) or variable DNA extraction efficiency. Besides these two major discrepancies between the Q-PCR approach and CARD- FISH, both methods were in good agreement in seven out of the nine samples analyzed.

Archaeal community composition.

Generally, the number of archaeal OTUs was almost twice as high in the top 100 m layer (8.9±2.2 OTUs) than in the layers below 1000m depth (4.8±1.9 OTUs) (Figure 5a). The lowest number of OTUs was found at St. 4 at 3000 m with only 2 OTUs, while the highest number of OTUs was found at St.4 at 750 m with 13 OTUs. Only one OTU (248.23 bp) out of a total of 27 OTUs was ubiquitously present and 3 OTUs were present in almost every sample (Figure 5a). The rest of the OTUs are responsible for the observed distinct surface water and mesopelagic clusters of archaeal communities (Figure 5b). Despite the rather homogenous water column structure in the Eastern Mediterranean Sea with only small variations in salinity and temperature with depth, the surface water archaeal community is distinctly different from that in the other water layers reflecting the depth-related distribution pattern of archaeal amoA gene copy numbers discussed below. Overall, considerable spatial heterogeneity in the archaeal community composition between the individual depth layers of the different stations is apparent.

Depth profiles of archaeal amoA gene.

Although bacterial amoA genes were not detected, archaeal amoA genes were readily detectable in the surface and mesopelagic waters (Figure 6a). A dominance of archaeal amoA over bacterial amoA genes was also found in the coastal North Sea and the mesopelagic waters of the North Atlantic (Wuchter et al., 2006), as well as in soils (Leininger et al., 2006). Our results support previous studies suggesting that marine Crenarchaeota are, at least partly, ammonia oxidizers (Francis et al., 2005; Könneke et al., 2005). Copy numbers of the archaeal amoA gene decreased with the depth and were essentially absent below 1000m depth (Figure 6a). Thus, the copy numbers of archaeal amoA decreased more rapidly with depth than the abundance of Crenarchaeota determined by CARD-FISH and of MCGI and pSL12 determined by Q-PCR (Figure 4). This becomes evident, if the ratio of archaeal amoA gene copy numbers to crenarchaeal abundance (16S rRNA copy numbers, Cren537- and GI-554-positive cells) is calculated (Figures 6b and c). While in subsurface waters the ratio of amoA gene copy numbers: (MCGI + pSL12) is about 0.5, the corresponding ratios using crenarchaeal abundance determined by probes Cren537 and GI-554 range between 0.2 and 0.3 in subsurface waters. Genomic studies on Cenarchaeum symbiosum and Nitrosopumilus maritimus revealed that both isolates contain one amoA copy per cell (Hallam et al., 2006; D Stahl, personal communication). The ratios we obtained indicate that even in the surface waters and at St. 1 at 500m depth not all of the detected Crenarchaeota harbor an amoA gene (Figures 6b and c). This ratio decreases rapidly with depth down to 1000m implying that other energy sources than ammonia might be utilized to sustain the observed crenarchaeotal abundance. It has been shown that Crenarchaeota are also capable of utilizing organic substrates (Ouverney and Fuhrman, 2000) and that crenarchaeotal heterotrophy increases with depth (Teira et al., 2006b).

For surface and mesopelagic waters, a positive relation between Crenarchaeota abundance and the concentration of ammonia was reported (Wuchter et al., 2006; Kirchman et al., 2007; Varela et al., 2008), as well as with nitrite (Teira et al., 2006a; Lam et al., 2007). In this study, nitrite concentration explains about 60% of the variation in archaeal amoA copy numbers in the water

column of the Eastern Mediterranean Sea (data not shown). This suggests that Crenarchaeota in the surface waters and in the mesopelagic realm are most likely oxidizing ammonia as an energy source (Lam et al., 2007), while in the bathypelagic waters, crenarchaeal abundance is most likely sustained by other energy sources, probably by organic compounds.

In conclusion, we have shown that in the Eastern Mediterranean Sea, crenarchaeal abundance remains fairly constant with depth and that the number of archaeal phylotypes identified by T-RFLP decreases with depth. The ratio archaeal amoA copy numbers/crenarchaeal abundance rapidly declines with depth indicating that putatively ammonia oxidizing Crenarchaeota are largely confined to the surface and mesopelagic waters, while in bathypelagic waters of the Eastern Mediterranean Sea, Crenarchaeota are likely utilizing energy sources other than ammonia, presumably organic sources as recently reported for the crenarchaeal community in the North Atlantic.

Acknowledgements

We thank Dr Aleka Gogou (HCMR) and Dr Georgina Spyres (HCMR) for all the logistic arrangements prior and during the cruise, and the captain and crew of R/V Aegaeo for their help at sea. Maaike Brink, Judith van Bleijswijk and Harry Witte helped throughout the molecular analyses. TY was supported by the Japanese Society for the Promotion of Science (JSPS) Postdoctoral Fellowship for research abroad and DDC received a fellowship of the University of Groningen. Laboratory work and molecular analyses were supported by a grant of the Earth and Life Science Division of the Dutch Science Foundation (ARCHIMEDES project, 835.20.023) to GJH. The work was carried out within the frame of the 'Networks of Excellence' MarBef and EurOceans supported by the 6th Framework Program of the European Union. This work is in partial fulfillment of the requirements for a Ph.D. degree from the University of Groningen by DDC.

References

Alonso-Saez L, Balague V, Sa EL, Sanchez O, Gonzalez JM, Pinhassi J, Massana R, Pernthaler J, Pedros-Alio C, Gasol JM. (2007). Seasonality in bacterial diversity in north-west Mediterranean coastal waters: assessment through clone libraries, fingerprinting and FISH. *FEMS Microbiol Ecol* **60**: 98–112.

Amann R, Fuchs BM. (2008). Single-cell identification in microbial communities by improved fluorescence in situ hybridization techniques. *Nature Rev Microbiol* **6**: 339–348.

Becker S, Boger P, Oehlmann R, Ernst A. (2000). PCR bias in ecological analysis: a case study for quantitative Taq nuclease assays in analyses of microbial communities. *Appl Environ Microbiol* **66:** 4945–4953.

Del Giorgio PA, Gasol JM. (2008). Physiological structure and single-cell activity in marine bacterioplankton. In: Kirchman DL (ed). Microbial Ecology of the Oceans, 2nd edn. John Wiley & Sons: New York, p 243–298.

DeLong EF, Preston CM, Mincer T, Rich V, Hallam SJ, Frigaard N-U, Martinez A, Sullivan MB, Edwards R, Brito BR, Chisholm SW, Karl DM. (2006). Community genomics among stratified microbial assemblages in the ocean's interior. *Science* **311:** 496-503.

Francis CA, Roberts KJ, Beman JM, Santoro AE, Oakley BB. (2005). Ubiquity and diversity of ammo- nia-oxidizing Archaea in water columns and sedi- ments of the ocean. *Proc Natl Acad Sci USA* **102**: 14683–14688.

Frigaard NU, Martinez A, Mincer TJ, DeLong EF. (2006). Proteorhodopsin lateral gene transfer between marine planktonic bacteria and archaea. *Nature* **439:** 847–850.

Hallam SJ, Mincer TJ, Schleper C, Preston CM, Roberts K, Richardson PM et al. (2006). Pathways of carbon assimilation and ammonia oxidation suggested by environmental genomic analyses of marine Crenarchaeota. *PLoS Biol* **4**: 520–536.

Herndl GJ, Reinthaler T, Teira E, van Aken H, Veth C, Pernthaler A et al. (2005). Contribution of Archaea to total prokaryotic production in the deep Atlantic Ocean. *Appl Environ Microbiol* **71:** 2303–2309.

Hornek R, Pommerening-Roser A, Koops HP, Farnleitner AH, Kreuzinger N, Kirschner A et al. (2006). Primers containing universal bases reduce multiple amoA gene specific DGGE band patterns when analysing the diversity of beta-ammonia oxidizers in the environment. *J Microbiol Meth* **66:** 147–155.

Karner MB, DeLong EF, Karl DM. (2001). Archaeal dominance in the mesopelagic zone of the Pacific Ocean. *Nature* **409***:* 507–510.

Kirchman DL, Elifantz H, Dittel AI, Malmstrom RR, Cottrell MT. (2007). Standing stocks and activity of archaea and bacteria in the western Arctic Ocean. *Limnol Oceanogr* **52:** 495–507.

Könneke M, Bernhard AE, de la Torre JR, Walker CB, Waterbury JB, Stahl DA. (2005). Isolation

of an autotrophic ammonia-oxidizing marine archaeon. *Nature* **437:** 543–546.

Lam P, Jensen MM, Lavik G, McGinnis DF, Muller B, Schubert CJ, Amann R, Thamdrup B, Kuypers MMM. (2007). Linking crenarchaeal and bacterial nitrification to anammox in the Black Sea. *Proc Natl Acad Sci USA* **104:** 7104–7109.

Lane DJ. (1991). 16S/23S rRNA sequencing. In: Stackebrandt E and Goodfellow M (eds). Nucleic acid techniques in bacterial systematics. John Wiley & Sons: New York, p 115–176.

Leininger S, Urich T, Schloter M, Schwark L, Qi J, Nicol GW, Prosser JI, Schuster SC, Schleper C. (2006). Archaea predominate among ammonia-oxidizing prokaryotes in soils. *Nature* **442:** 806–809.

Massana R, Murray AE, Preston CM, DeLong EF. (1997). Vertical distribution and phylogenetic characteriztion of marine planktonic Archaea in the Santa Barbara Channel. *Appl Environ Microbiol* **63:** 50–56.

Mincer TJ, Church MJ, Taylor LT, Preston C, Kar DM, DeLong EF. (2007). Quantitative distribution of presumptive archaeal and bacterial nitrifiers in Monterey Bay and the North Pacific Subtropical Gyre. *Environ Microbiol* **9:** 1162–1175.

Moeseneder MM, Arrieta JM, Herndl GJ. (2005). A comparison of DNA- and RNA-based clone libraries from the same marine bacterioplankton community. *FEMS Microbiol Ecol* **51**: 341–352.

Moeseneder MM, Arrieta JM, Muyzer G, Winter C, Herndl GJ. (1999). Optimization of terminal-restriction fragment length polymorphism analysis for complex marine bacterioplankton communities and compari- son with denaturing gradient gel electrophoresis. *Appl Environ Microbiol* **65:** 3518–3525.

Moeseneder MM, Winter C, Arrieta JM, Herndl GJ. (2001a). Terminal-restriction fragment length polymorphism (T-RFLP) screening of a marine archaeal clone library to determine the different phylotypes. *J Microbiol Meth* **44:** 159–172.

Moeseneder MM, Winter C, Herndl GJ. (2001b). Horizontal and vertical complexity of attached and free-living bacteria of the Eastern Mediterranean Sea, determined by 16S rDNA and 16S rRNA fingerprints. *Limnol Oceanogr* **46:** 95–107.

Ouverney CC, Fuhrman JA. (2000). Marine planktonic Archaea take up amino acids. *Appl Environ Microbiol* **66:** 4829–4833.

Teira E, Lebaron P, van Aken H, Herndl GJ. (2006a). Distribution and activity of Bacteria and Archaea in the deep water masses of the North Atlantic. *Limnol Oceanogr* **51:** 2131–2144.

Teira E, Reinthaler T, Pernthaler A, Pernthaler J, Herndl GJ. (2004). Combining catalyzed reporter deposition- fluorescence in situ hybridization and microauto- radiography to detect substrate utilization by bacteria and archaea in the deep ocean. *Appl Environ Microbiol* **70:** 4411–4414.

Teira E, van Aken H, Veth C, Herndl GJ. (2006b). Archaeal uptake of enantiomeric amino acids in the meso- and bathypelagic waters of the North Atlantic. *Limnol Oceanogr* **51:** 60–69.

Thingstad TF, Krom MD, Mantoura RFC, Flaten GAF, Groom S, Herut B, Kress N, Law CS, Pasternak A, Pitta P, Psarra S, Rassoulzadegan F, TanakaT, Tselepides A, Wassmann P, Woodward EMS, Riser CW, Zodiatis G, Zohary T. (2005). Nature of phosphorus limitation in the ultraoligotrophic Eastern Mediterranean. *Science* **309:** 1068–1071.

van der Maarel MJEC, Artz RRE, Haanstra R, Forney LJ. (1998). Association of marine Archaea with the digestive tracts of two marine fish species. *Appl Environ Microbiol* **64:** 2894–2898.

Varela MM, van Aken HM, Sintes E, Herndl GJ. (2008). Latitudinal trends of Crenarchaeota and Bacteria in the meso- and bathypelagic water masses of the Eastern North Atlantic. *Environ Microbiol* **10:** 110–124.

Wuchter C, Abbas B, Coolen MJL, Herfort L, van Bleijswijk J, Timmers P, Strous M, Teira E, Herndl GJ, Middelburg JJ, Schouten S, Sinninghe Damste JS. (2006). Archaeal nitrification in the ocean. *Proc Natl Acad Sci USA* **103:** 12317–12322.

Zervakis V, Georgopoulos D, Karageorgis AP, Theocharis A. (2004). On the response of the Aegean sea to climatic variability: a review. *Internat J Climatol* **24:** 1845–1858.

Chapter 5

Distinct differences in the composition of the active *versus* total bacterial community in the coastal Arctic

Daniele De Corte, Eva Sintes, Taichi Yokokawa and Gerhard J. Herndl

Submitted to Aquatic Microbial Ecology

Abstract

We collected surface- and deep-water samples (maximum depth 300 m) during the spring-summer transition in the coastal Arctic along a transect in the Kongsfjorden (Ny-Ålesund, Spitsbergen, Norway) to determine the structure of the active *vs.* total marine bacterioplankton community using different approaches. Catalyzed reporter deposition-fluorescence in situ hybridization combined with microautoradiography (MICRO-CARD-FISH) was used to determine the abundance and activity of different bacterial groups. The bacterial communities were dominated by members of Alphaproteobacteria followed by Bacteroidetes, whereas Gammaproteobacteria were present at low abundance but exhibited a high percentage of active cells taking up leucine. In contrast, groups present at higher abundance than Gammaproteobacteria, such as Bacteroidetes, exhibited a lower percentage of cells taking up leucine. The structure of the bacterial communities was also examined by establishing clone libraries of 16S rRNA genes (16S rDNA) and 16S rRNA from two different depths. Independent from the type of clone libraries analyzed (16S rDNA- or 16S rRNA-based), four major and four minor taxonomic groups were detected. The majority of the clones were related to psychrophilic or cosmopolitan phylotypes. The bacterioplankton community was mainly dominated at both, the DNA and RNA level by Alphaproteobacteria with 43 and 63% of the total clones, respectively, followed by Gammaproteobacteria. The Rhodobacteriaceae were the most abundant members of the Alphaproteobacteria in both, DNA and RNA clone libraries, followed by the SAR11 clade, which was only detectable at the 16S rDNA level. In conclusion, MICRO-CARD-FISH allowed an accurate quantification of the different bacterial group and their activity whereas the combined use of DNA and RNA clone libraries provides a detailed phylogenetic insight into the fraction of the active bacterial groups.

Introduction

During the spring to summer transition period, the coastal Arctic is characterized by increasing temperatures, large input of freshwater originating from the adjacent glaciers and melting snow and a considerable load of terrigenous particles transported via creeks into the coastal regions. Under these conditions, phytoplankton blooms and subsequently bacterial abundance and production are stimulated (Hasle and Heimdal, 1998; Owrid et al., 2000; Piwosz et al., 2009; Schoemann et al., 2005). The bacterial community in the Arctic ocean consists, like in other marine waters, of few abundant and a large number of rare phylotypes, most of them with unknown ecological functions in the biogeochemical cycling (Kirchman et al., 2010).

Over the last two decades, several molecular techniques based on 16S rDNA such as ARISA (Automated Ribosomal Intergenic Spacer Analysis), T-RFLP (Terminal Restriction Fragment Length Polymorphism), DGGE (Denaturing Gradient Gel Electrophoresis), cloning and (pyro) sequencing have been used to characterize the complexity of bacterioplankton communities (Fisher and Triplett 1999; Moeseneder et al., 1999; Muyzer and Smalla 1998; Pommier et al., 2007; Sogin et al., 2006). However, these techniques do not necessarily reflect the structure of the active microbial community (Moeseneder et al., 2005). One widely used approach to address the active bacterial community is the combination of microautoradiography and fluorescence in situ hybridization (Lee et al., 1999). This method allows the identification and quantification of specific target prokaryotic groups as well as the uptake of specific radiolabeled substrate.

The total DNA pool of a bacterial community might consist of DNA derived from living, dormant or even dead cells and extracellular DNA (Josephson et al., 1993). In contrast to DNA, RNA has a much shorter life span and can serve as an indicator of the metabolically active fraction of the community (Gentile et al., 2006; Mills et al., 2005; Moeseneder et al., 2005).

During starvation, the rRNA decreases to minimum levels in the cell (Fegatella et al., 1998). Therefore, there is a linear relation between the rRNA content and the growth rate in bacteria (Delong et al., 1989; Kemp et al., 1993; Kerkhof and Ward, 1993). The higher amount of rRNA in active than in dormant cells associated with the higher number of ribosome in active cells, provides a tool to determine the metabolically active members of the bacterial community (Poulsen et al., 1993). The detection of Bacteria on the 16S rDNA level is mainly depending on the abundance of the specific bacterial organism or group in the environment. Bacterial organisms present at low abundance and not detectable at the DNA level, but metabolically active and thus with a higher ribosome content, might be still detectable at the RNA level (Moeseneder et al., 2005). Thus, the comparison between DNA and RNA clone libraries can contribute to understand the ecological role of the low abundance phylotypes and might provide insight into community changes related to changing environmental conditions.

The rapidly changing environmental conditions in the Arctic during the spring to summer transition period from terrestrial run-off influenced nearshore to more offshore waters provide a unique framework to study the spatial changes in the bacterial community composition on the RNA

and DNA level. To address this question, the total nucleic acids (DNA and RNA) were extracted from samples collected at two different depths, the RNA was subjected to reverse transcription RT-PCR, and both DNA and cDNA from the Arctic bacterial communities were amplified and sequenced with specific bacterial primers. The composition of the DNA and RNA clone libraries, representing the total and the active bacterial community, respectively, were compared to results obtained by MICRO-CARD-FISH.

Material and methods

Study area and sampling. Water samples were taken at seven stations located in Kongsfjorden (Ny-Ålesund, Spitsbergen, Norway) following a transect from the mouth of a glacier towards open waters (Fig. S1). The samples were obtained from the surface waters (~1.5 m depth) and from a maximum depth of ~300 m during the ice melting season (June 2008). Sampling was performed from a boat with a CTD rosette sampler holding three 10-L Niskin bottles and sensors for conductivity, temperature and depth.

MICRO-CARD-FISH. The MICRO-CARD-FISH was analyzed in the whole transect at two depths between the 26 and 27 of June 2008. Four ml water samples were spiked with [^{3}H]-leucine (final concentration 20 nM), incubated at in situ temperature for 4 h and subsequently, fixed with formaldehyde (2 % final concentration) and stored at 4ºC for 24 h. The samples were subsequently filtered onto 0.2 μm white polycarbonate filters (Millipore) using a 0.45 μm cellulose nitrate supporting filter (Millipore). Processing of the filters followed established protocols (Pernthaler et al., 2002a; Pernthaler et al., 2002b; Teira et al., 2004). Briefly, after lysozyme permeabilization for Bacteria and proteinase-K for Archaea (10 mg mL^{-1}, 37°C for 1h), the filters were cut into sections for hybridization with the following oligonucleotide probes: a mix of Eub338-I (Amann et al., 1990), Eub338-II, and Eub338-III (Daims et al., 1999) to target Bacteria, Non338 (Amann et al., 1995), ALF968 (Neef 1997) for Alphaproteobacteria, GAM42a for Gammaproteobacteria (Manz et al., 1992), CF319a for Bacteroidetes (Manz et al., 1996), a mix of SAR11-152R, SAR11-441R, SAR11-542R and SAR11-732R targeting the SAR11 cluster (Morris et al., 2002), and ROS537 (Eilers et al., 2001) targeting the Roseobacter-Sulfitobacter-Silicibacter clade. A mix of Cren537 and Cren554 was used to target marine Crenarchaeota Group I (MCGI) while Eury806 was used to target Euryarchaeota Group II (De Corte et al., 2009). The horseradish peroxidase-labeled probes were added at a final concentration of 2.5 ng μL^{-1}, and hybridization was performed at 35°C for 12 to 15 h. After the washing steps, amplification was carried out by adding H_2O_2 and tyramide-Alexa488 and incubating the filters at 37°C for 30 min (Pernthaler et al., 2002a).

The microautoradiography was performed following the protocol of (Alonso and Pernthaler, 2005). The probe-hybridized filters were glued onto glass slides and embedded in photographic emulsion (KODAK NTB-2) containing 0.1% agarose, and stored in the dark at 4°C for 48 h.

The slides were subsequently developed and fixed using the specifications of the manufacturer. Thereafter, the slides were dried in a desiccator overnight and stained with a DAPI mixture (5.5 parts Citifluor, 1 part Vectashield, and 0.5 part phosphate-buffered saline with DAPI at a final concentration of 1 μg mL^{-1}), and the bacterial cells counted under a Zeiss microscope at 1250x magnification.

Nucleic acids extraction and complementary DNA (cDNA) synthesis. Fifteen L of seawater were collected at St. 5 at two depths on the 26 of June 2008 (~1.5 and 270 m) and filtered onto 0.2 μm polycarbonate filters (142 mm diameter, Whatman Nuclepore). Subsequently, 5 mL of 2-mercaptoethanol was added to the filters and stored at -80°C until further processing. The total nucleic acids (DNA and RNA) were extracted from the filters using the phenol extraction protocol (Weinbauer et al., 2002). One fraction was kept at -80ºC for subsequent DNA analysis, while the other fraction was used to extract RNA. The RNA was isolated from the total nucleic acids by DNAase digestion (Deoxyribonuclease I, amplification grade, Invitrogen) at 37°C for 30 min. The RNA concentration was determined using a NanoDrop ND-1000 spectrophotometer (NanoDrop Technologies). The efficiency of the DNA removal was tested by PCR reactions using bacterial primers. Superscript III First-Strand Synthesis supermix (Invitrogen) was used to produce cDNA from the RNA extract following the protocol of the manufacturer. The RNA and the cDNA were stored at -80ºC until further processing.

Cloning and sequencing. The bacterial 16S rDNA gene and 16S rRNA were amplified using the bacterial primer 27F (5'-AGA GTT TGA TCC TGG CTC AG-3') and the universal primer 1492R (5'-GGT TAC CTT GTT ACG ACT T-3') (Lane, 1991). One μL of extracted nucleic acids (DNA or cDNA) was used as a template in a PCR mixture consisting of 0.3 μL of each primer, 5 μL of dNTPs, 0.3 μL of Taq polymerase Biotherm (Genecraft) and the corresponding buffer, made up to 50 μL with UV-treated ultra-pure water (Sigma). Samples were amplified by an initial denaturation step at 94ºC (for 3 min), followed by 35 cycles of denaturation at 94ºC (for 1 min), annealing at 55ºC (for 1 min), and an extension at 72ºC (for 1 min). Cycling was completed by a final extension at 72ºC for 7 min. The quality of the PCR products was checked on 1.0 % agarose gel. The PCR products were purified with QuickClean 5M PCR purification Kit (Genscript) and cloned with the TOPO-TA cloning kit (Invitrogen) according to the manufacturer's instructions. Sequencing was performed at MACROGEN Inc. (Korea) using the 27F primer.

Sequence information obtained in this study was deposited in GenBank under the following accession numbers: JN409997-JN410218.

Phylogenetic analysis. The obtained sequences were compiled using Ribosomal Database Project (RDP) online software (http://rdp.cme.msu.edu/), and aligned together with environmental bacterial sequences obtained from the NCBI database. Chimera formation were checked by Pintail software (Ashelford et al., 2005).

The phylogenetic tree was built using Neighbour-Joining method and Jukes-Cantor distance matrix in Mega-4 software and drawn using iTOL (Interactive Tree Of Life) (Letunic and Bork, 2007). The phylogenetic affiliation of the bacterial 16S rDNA and 16S rRNA sequences was

determined by Naïve Bayesian Classifier implemented in RDP (Wang et al., 2007).

Rarefaction analysis was performed using DOTUR (Schloss and Handelsman, 2005). Operational taxonomic units were defined as a group of sequences differing by less than 2 %. The phylogenetic composition of microbial communities (based on the 16S rDNA and 16S rRNA) was compared using Unifrac (Lozupone and Knight, 2005).

Results

Composition and activity of the coastal Arctic prokaryotic community.

Along the transect (Fig. S1), the prokaryotic community was dominated by Bacteria (86% of DAPI-stained cells). Euryarchaeota and Crenarchaeota were found only in low abundance, contributing, on average, 1 % and 0.6 % to the DAPI-stained cells, respectively (data not shown). Alphaproteobacteria were the most abundant group accounting, on average, for 34±19 % at the surface and 36±13 % in the deeper layers to the total bacterial abundance (Fig. 1). Bacteroidetes also accounted for a large fraction of the bacterial community (on average 28±23 % of bacterial abundance), with a higher contribution in surface than in deep waters at 6 out of the 8 stations (Fig. 1). The abundance of Gammaproteobacteria ranged between 2 and 26 % of total bacterial abundance, with no clear trend in its spatial distribution along the transect (Fig. 1).

Within the Alphaproteobacteria, we determined the abundance of two specific groups: SAR11 and Roseobacter. These two groups contributed to a low percentage of the Bacteria, and particularly Roseobacter was under the detection limit at the majority of the stations (data not shown). The SAR11 clade was present at low abundance at the stations located close to the glacier and increased in its contribution to bacterial abundance to up to 36 % at the mouth of the fjord (Fig. 1).

The leucine uptake of the different bacterial groups was investigated by MICRO-CARD-FISH. Members of the Alpha- and Gammaproteobacteria exhibited a high percentage of cells taking up

Table 1. Total number of OTUs, Margalef's species richness (SR), Shannon index (H') of diversity and Pielou's species evenness (J') obtained from 16S rDNA and 16S rRNA clone libraries.

Samples	Total OTUs	SR	H'	J'
Total 16S rDNA	102	17.25	3.59	0.78
Total 16S rRNA	62	10.32	2.69	0.65
16S rDNA surface	64	12.07	3.34	0.80
16S rRNA surface	20	3.647	1.20	0.40
16S rDNA deep	61	11.78	3.09	0.75
16S rRNA deep	48	9.013	3.25	0.84

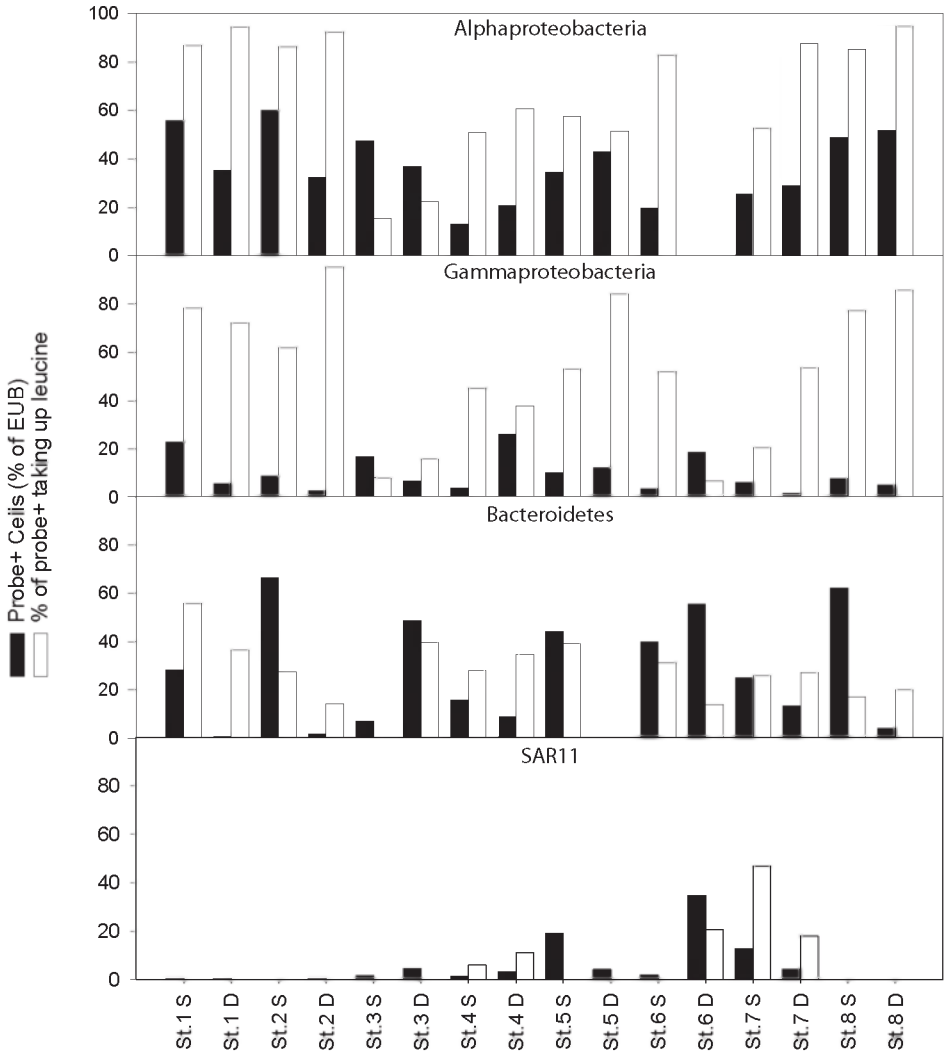

Figure 1. Percentage of specific bacterial groups (Alpha-, Gammaproteobacteria, Bacteroidetes and SAR11) detected by CARD-FISH at the stations along the transect in Kongsfjorden, Spitsbergen as percentage of the total bacterial abundance (cells hybridized with the probe mix Eub338-I to Eub338-III), and the percentage of cells of the specific groups taking up [3H]-leucine. S indicates surface water sample, D indicates deep-water sample.

leucine averaging 68±26 % and 51±29 % of probe+ cells, respectively (Fig. 1). The percentage of Alpha- and Gammaproteobacteria taking up leucine was not significantly different between surface and deep waters (Mann-Whitney T-test, p=0.23 and p=0.64, respectively) (Fig. 1). The percentage of Bacteroidetes taking up leucine was low (25±13 %) (Fig. 1). Also SAR11 was characterized by a low percentage of cells taking up leucine (11±17 %). However, the fraction of SAR11 taking up leucine tended to increase towards the mouth of the fjord (Fig. 1).

Comparison between 16S rDNA and 16S rRNA clone libraries

Rarefaction analyses revealed that the sequencing effort was sufficient to sample most of the members of the bacterial community given the limitations of this approach as compared to new generation sequencing (Fig. 2). The Chao richness index estimated 14 and 18 OTUs on the 16S rRNA level and 33 and 31 OTUs on the 16S rDNA level for surface- and deep-waters, respectively (Fig.

2). Similar results were obtained with the ACE richness index (data not shown). The phylogenetic composition of the 16S rDNA and 16S rRNA clone libraries was significantly different between the two different depths as revealed by the Unifrac significance test ($p < 0.01$).

On the 16S rDNA level, a total of 102 OTUs (Operational taxonomic units were determined by the decrease redundancy software; www.expasy.org) and 62 OTUs in the 16S rRNA clone library. The number of 16S rDNA OTUs was higher than that of the 16S rRNA OTUs in both the surface- and deep-waters (Table 1). The Shannon index of diversity (H') was higher for the 16S rDNA than for the 16S rRNA in the surface waters while in the deep waters, the diversity indexes of 16S rRNA and 16S rDNA were similar (Table 1). The Pielou's evenness (J') index showed the same trend as the Shannon index, whereas Margalef's species richness (SR) was higher for 16S rDNA than for the 16S rRNA clone libraries at both depths.

Distribution of OTU abundance in the 16S rRNA and 16S rDNA clone libraries

The clone library of the surface water bacterioplankton community using the 16S rRNA was dominated by one OTU that represented alone 74 % of the clone library (Fig. S2); 8 OTUs constituted 92 % of the total bacterial 16S rRNA clone library, while singletons (i.e., occurring only once) amounted to 7 % of the bacterial 16S rRNA clone library. In the clone library of the surface water bacterial community using the 16S rDNA, 5 OTUs represented 50 % of the clone library and the singletons constituted 23 % of the clone library (Fig. S2).

In the clone library of the deep-water bacterioplankton using the 16S rRNA, 8 OTUs represented

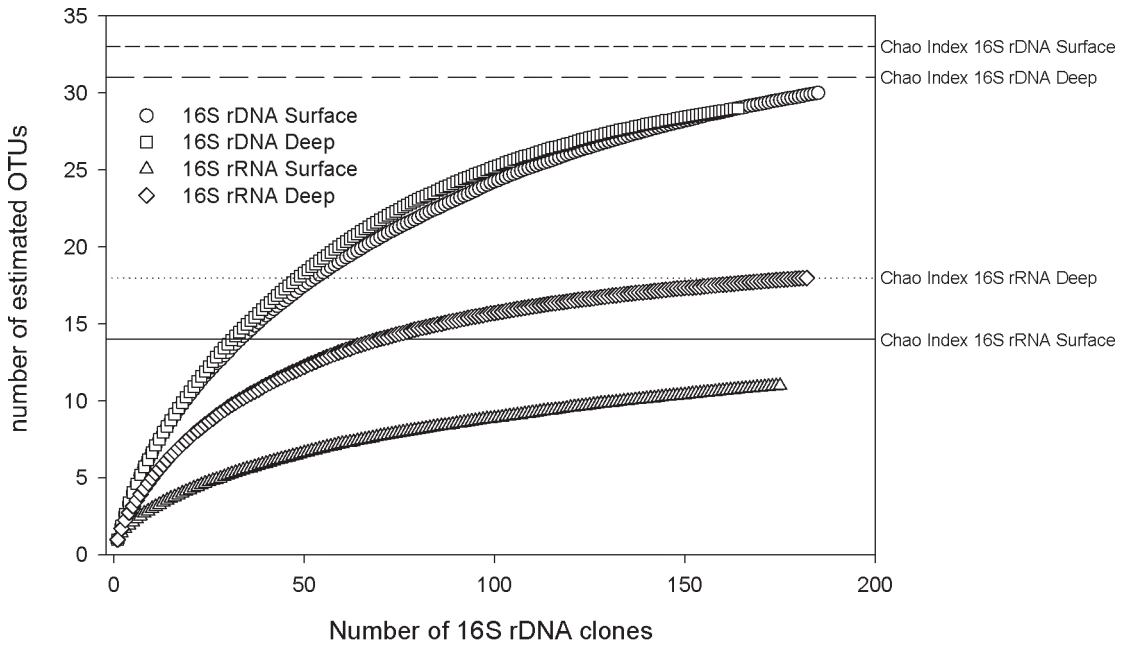

Figure 2. Rarefaction analysis of the clone libraries from the bacterial communities obtained from surface- and deep-waters at the 16S rDNA and 16S rRNA level. The Chao index for the OTUs sharing ≥98 % similarity is indicated for the respective categories by horizontal lines.

50 % of this clone library while the singletons accounted for 13 % of the total 16S rRNA (Fig. S2). In the 16S rDNA based clone library from deep-water bacteria, 3 OTUs represented ≈ 50 % and the singletons 23 % of the clone library (Fig. S2). Generally, the contribution of singletons was higher in the rDNA than in the rRNA clone libraries.

Phylogenetic affiliation of 16S rRNA and 16S rDNA clones.

The phylogenetic analysis of the 716 clones obtained in total revealed four major and four minor groups (Fig. 3). Significant phylogenetic differences (Unifrac significance test, $p < 0.01$) were found between the rDNA- and rRNA-based clone libraries in both, surface and deep-water communities (Fig. 3, Fig. S3).

The rDNA clone library from surface water bacterioplankton was dominated by members of the Alphaproteobacteria and Bacteroidetes with 47 % and 32 % of the total number of clones, respectively, followed by Gammaproteobacteria (12 %) and Betaproteobacteria (0.5 %) (Fig. 3a). The Alphaproteobacteria class, in terms of abundance of clones, consisted mainly of the family Rhodobacteracea (37 % of the total number of clones) closely related to Sulfitobacter, and of SAR11 (9 %) closely related to Pelagibacter (Fig. 3e, Table 2). The members of the Bacteroidetes class were mainly affiliated to Flavobacteriales (16 % of the total number of clones), closely related to the genera Polaribacter (Table 2). Oceanospirillaceae was the most abundant family of the Gammaproteobacteria, amounting to 3 % of the total rDNA clones (Table 2).

The rRNA clone library of surface water bacteria was largely dominated by Alphaproteobacteria (92 % of the total clones) followed by Gammaproteobacteria (7%) (Fig. 3b). The alphaproteobacterial family Rhodobacteracea, closely related to the genus Sulfitobacter, contributed 90 % to the total number of clones (Fig. 3f, Table 2).

The 16S rDNA clones from the deep-water bacterial community were dominated by Gamma- and Alphaproteobacteria with 42 % and 40 % of the total number of clones, respectively, followed by Bacteroidetes (13 %), Betaproteobacteria (2 %) and Epsilonproteobacteria (1%) (Fig. 3c).

Table 2. Phylogenetic affiliation at several phylogenetic levels and the contribution of the individual families to the total number of clones obtained from 16S rDNA and 16S rRNA clone libraries in the coastal Arctic.

	Phylum	Class	Order	Family	% of total clones	
					16S rDNA	16S rRNA
Surface	Proteobacteria	Alphaproteobacteria	Rhodobacterales	Rhodobacteraceae	36.8	90.2
	Proteobacteria	Alphaproteobacteria	Rickettsiales	SAR11	9.2	n.d.
	Proteobacteria	Gammaproteobacteria	Oceanospirillales	Oceanospirillaceae	3.2	0.5
	Bacteroidetes	Flavobacteria	Flavobacteria	Flavobacteriales	16.2	n.d.
Deep	Proteobacteria	Alphaproteobacteria	Rhodobacterales	Rhodobacteraceae	3.7	18.5
	Proteobacteria	Alphaproteobacteria	Rickettsiales	SAR11	36.0	0.5
	Proteobacteria	Alphaproteobacteria	Rhodobacterales	Rhodospirillaceae	n.d.	6.5
	Proteobacteria	Gammaproteobacteria	Oceanospirillales	Oceanospirillaceae	18.9	19.0
	Proteobacteria	Gammaproteobacteria	Alteromonadales	Alteromonadaceae	2.4	7.6
	Bacteroidetes	Flavobacteria	Flavobacteria	Flavobacteriales	4.9	0.5

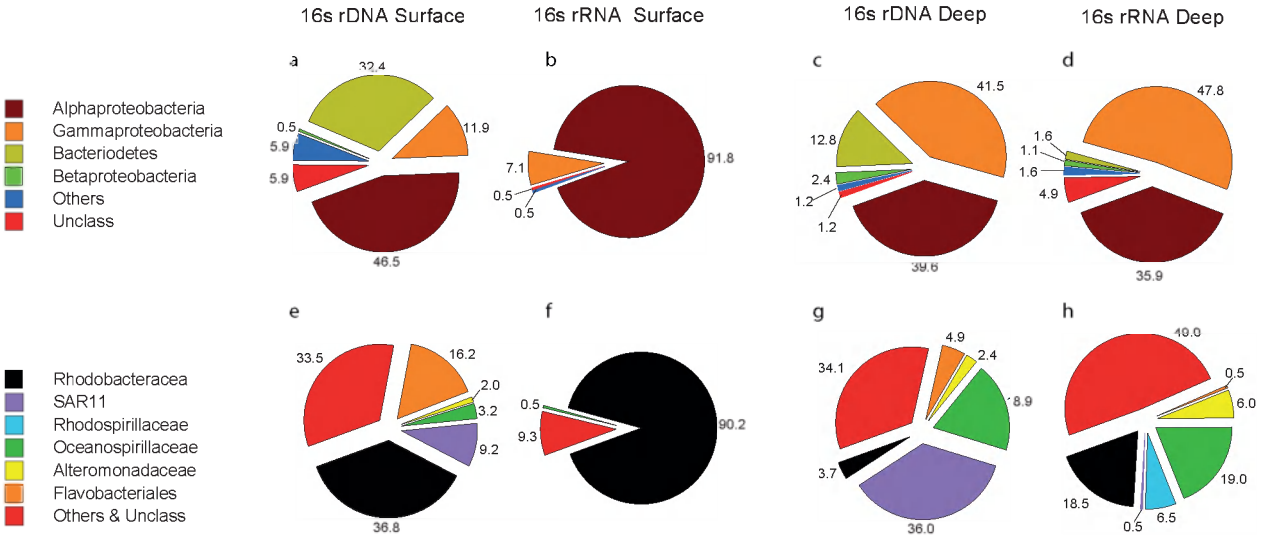

Figure 3. Relative contribution of (a – d) the most abundant phylogenetic classes and (e – h) families to the total number of OTUs obtained by 16S rDNA and 16S rRNA clone libraries in the surface and deep layer.

Oceanospirillaceae (19 % of the total number of clones) and Alteromonadaceae (2 %) were the main families of Gammaproteobacteria while the Alphaproteobacteria consisted mainly of the SAR11 clade (36 % of the total number of clones) closely related to the genus Pelagibacter, and Rhodobacteraceae (4 %) (Fig. 3g). Also the 16S rRNA clone library from the deep-waters was dominated by Gammaproteobacteria (48 %) and Alphaproteobacteria (36 %), followed by the Bacteroidetes (2 %), Betaproteobacteria (1 %) and Epsilonproteobacteria (1 %) (Fig. 3d). The Oceanospirillaceae was again the dominant family of the Gammaproteobacteria with 19 % of the total number of clones followed by the Alteromonadaceae (6 %), while the Alphaproteobacteria were dominated by Rhodobacteraceae accounting for 19 % of the total number of clones followed by Rhodospirillaceaea (7 %) and SAR11 (0.5 %) (Fig. 3h, Table 2).

Contribution of different phylogenetic groups to the active and total communities.

The contribution of Alphaproteobacteria to the total number of Bacteria taking up leucine as determined by MICRO-CARD-FISH was higher than their contribution to the total bacterial abundance (Fig. 4a) while the percentage of Gammaproteobacteria taking up leucine was largely proportional to their contribution to the total bacterial abundance (Fig. 4a). In contrast to Alphaproteobacteria, Bacteroidetes and SAR11 contributed disproportionally less to the bacterial community taking up leucine than to total bacterial abundance (Fig. 4a).

In the surface waters, Alphaproteobacteria and especially the members of the Rhodobacteraceae contributed relatively more to the 16 rRNA clone library than to the 16 rDNA library (Fig. 4b). The contribution of Gammaproteobacteria to the 16S rRNA library was proportional to their contribution to the 16S rDNA library in the surface waters (Fig. 4b). In the deep waters, Alpha- and Gammaproteobacteria contributed proportionally to both the 16S rRNA and 16S rDNA library (Fig. 4b). Bacteroidetes and SAR 11 contributed substantially less to the 16S rRNA than to the

16S rDNA clone library in both, surface and deep waters (Fig. 4b). Overall, the contribution to the 16S rRNA clone library was higher for members of the Rhodobacteraceae, closely related to Sulfitobacter, than for other bacterial groups at both surface and deep waters (Fig. 4b).

Discussion

During the transition period between spring and summer, the physico-chemical characteristics of the water column drastically change, leading to associated alterations of biological parameters in the coastal Arctic Ocean. Two main factors drive these changes in the environmental characteristics of the water column, time and depth, both resulting mainly in temperature changes (De Corte et al., 2011). The terrestrial run-off entering the study site during this period of the year causes major gradients in salinity and transparency along the transect from nearshore to offshore (Hop et al., 2002). These changing conditions along the transect makes it particularly suitable to investigate the changes in the phylogenetic composition of the total and the active communities. A comparative approach was taken in this study using MICRO-CARD-FISH and 16S rDNA and 16S rRNA clone libraries to resolve the dynamics in the active *versus* total bacterial community along the transect.

Bacterial community composition and activity assessed by MICRO-CARD-FISH.

The prokaryotic community was dominated by Bacteria contributing up to 86 % to the total DAPI-stained cells, while Archaea accounted, on average, only for 1 % of the total picoplankton abundance with no clear trends in their spatial distribution (data not shown). The low contribution of archaeal cells in Kongsfjorden during the spring to summer transition period is in accordance with previous reports on the decrease of the contribution of Archaea to the prokaryotic community from the winter towards the summer season in Arctic and Antarctic waters (Alonso-Saez et al., 2008; Church et al., 2003). The bacterial community was dominated by members of the Alphaproteobacteria, however, the abundance of the SAR11 (Fig. 1) and Roseobacter (under the detection limit in most of the samples) was lower than in previous studies from the Arctic and other oceanic regions using FISH (Alonso-Saez et al., 2008; Morris et al., 2002). A higher percentage of Alpha- and Gammaproteobacteria was taking up leucine than Bacteroidetes (Fig. 1). The contribution of Alphaproteobacteria to the total number of Bacteria taking up leucine was higher than that of Gammaproteobacteria, due to its higher contribution to the bacterial abundance (Fig. 4a) in agreement with earlier studies conducted in other marine environments (Cottrell and Kirchman, 2003; Longnecker et al., 2006; Zhang et al., 2006). The number of Bacteroidetes taking up leucine was significantly lower than that of Alpha- and Gammaproteobacteria as reported in other studies as well (Alonso-Saez et al., 2008; Cottrell and Kirchman, 2003; Longnecker et al., 2006). It is well documented that members of the Bacteroidetes preferentially utilize high molecular weight dissolved organic matter (Cottrell and Kirchman, 2000). However, the fraction of *Polaribacter*, a member of the Bacteroidetes clade, taking up leucine is proportional to its contribution to overall bacterial abundance during the Arctic summer (Malmstrom et al., 2007).

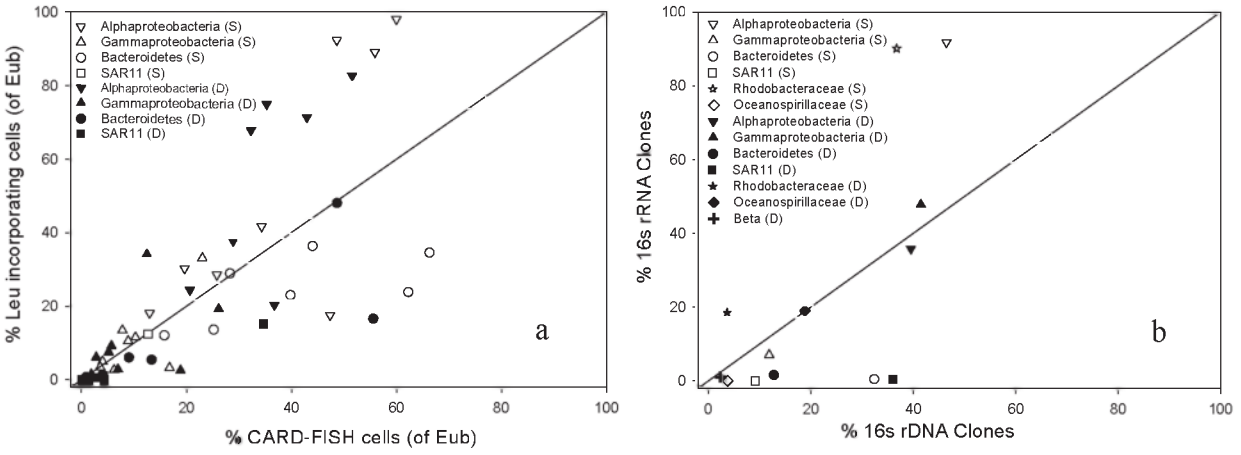

Figure 4. Relative contribution of specific bacterial groups to the bulk bacterial abundance determined by CARD-FISH vs. the percentage of cells of the respective bacterial group taking up leucine assessed by MICRO-CARD-FISH (a) and by 16S rDNA vs.16S rRNA clone libraries (b).

Bacterial community composition and activity assessed by clone libraries.

Clear differences between the composition of the 16S rDNA and 16S rRNA bacterial clone libraries were found, in agreement with previous studies (Gentile et al., 2006; Moeseneder et al., 2005). These differences in the composition of the 16S rDNA and 16S rRNA clone libraries have been interpreted to result from differences between the active, detected by 16S rRNA analysis, and the total community, revealed by 16S rDNA libraries (Moeseneder et al., 2005). The 16S rDNA clone libraries exhibited a higher diversity than the 16S rRNA clone libraries originating from the same samples (Table 1) indicating that only a fraction of the bacterial community is active.

The majority of the 16S rDNA and 16S rRNA clones obtained in the coastal Arctic waters were related to psychrophilic or ubiquitous phylotypes, previously found in Arctic and Antarctic marine environments (Bano and Hollibaugh, 2002; Brinkmeyer et al., 2003; Malmstrom et al., 2007; Pommier et al., 2007; Zaballos et al., 2006).

The bacterial community composition, as revealed by the 16S rDNA clone libraries, was dominated by Alphaproteobacteria, specifically by SAR11 and Rhodobacteraceae (Table 2), similar to previous studies on the Arctic region and sea-ice using CARD-FISH and clone libraries (Alonso-Saez et al., 2008; Hollibaugh et al., 2002; Zaballos et al., 2006). SAR11 often dominates marine bacterial communities (Morris et al., 2002). In the coastal Arctic, the contribution of SAR11 to the 16S rDNA clone libraries was 9 % and 36 % to the surface and the deep bacterial communities, respectively (Table 2). Their contribution to the 16S rRNA clone libraries, however, was negligible (Table 2) corresponding to their low contribution to the bacterial community obtained by CARD-FISH (see above). This indicates that SAR11, albeit present, is not particularly active in the coastal Arctic around Spitsbergen at the spring-summer transition (Fig. 3, Fig. 4b). Our results are in agreement with previous studies describing SAR11 as highly abundant albeit with low metabolic activity (Alonso-Saez et al., 2008; Morris et al., 2002; Rappe et al., 2002). SAR11 is abundant in both coastal and open waters (Malmstrom et al., 2004), but they were described to be relatively

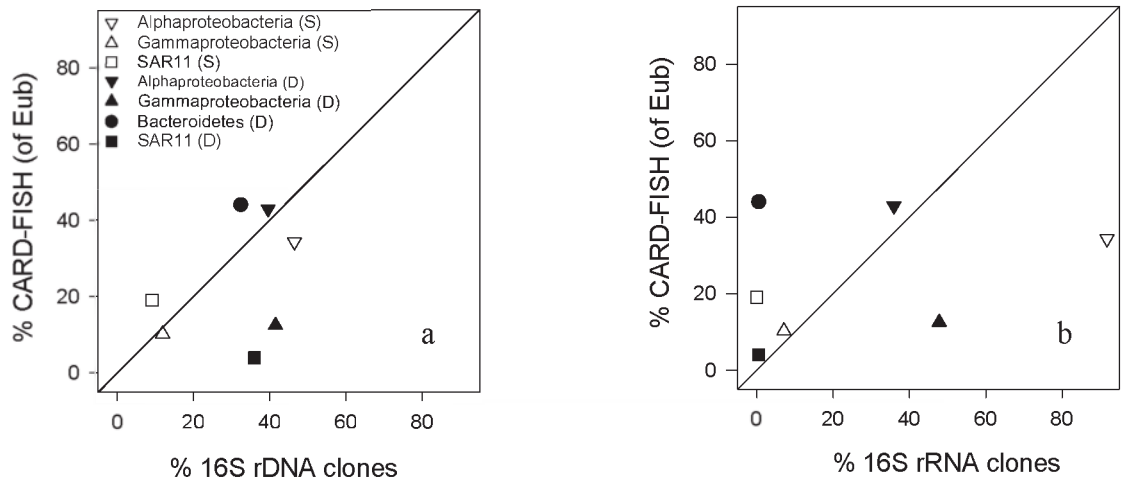

Figure 5. Relative contribution of specific bacterial groups to the bacterial community assessed by the 16S rDNA clone libraries vs. CARD-FISH (a), and by 16S rRNA clone libraries vs. CARD-FISH (b).

more active in the open ocean (Malmstrom et al., 2004) suggesting that SAR11 is well adapted to the oligotrophic conditions of the open ocean. In support of this, in the present study we found a higher contribution of SAR11 to bacterial abundance and a higher fraction of SAR11 taking up leucine towards the entrance of the fjord, i.e., towards the open Arctic (Fig. 1).

Rhodobacteraceae was the most abundant family in both the 16S rDNA and 16S rRNA clone library of the surface waters (Table 2) as found also in other studies on Arctic and temperate coastal waters (Buchan et al., 2005). Their high contribution to the 16S rRNA clone library in surface waters (Table 2) indicates that Rhodobacteraceae are highly active members of the bacterial community related to the presence of phytoplankton blooms during spring-summer transition period in the Arctic (Gonzalez et al., 2000, Suzuki et al., 2001).

In contrast to the Alphaproteobacteria with the Rhodobacteraceae, the contribution of the Bacteroidetes to the 16S rRNA clone library and hence, active community was very low (Table 2) in contrast to a previous study in the Arctic Ocean (Malmstrom et al., 2007). The reported preference of members of the Bacteroidetes for high molecular weight DOM (Elifantz et al., 2005), which is more likely released during the senescent stage of phytoplankton blooms, might indicate that the substrate conditions were not favorable for most members of the Bacteroidetes during the sampling period. Gammaproteobacteria contributed a similar or higher fraction to the total bacterial abundance than previously reported for the Arctic (Bano and Hollibaugh, 2002; Zaballos et al., 2006).

MICRO-CARD-FISH versus 16S rDNA and 16S rRNA clone libraries to assess prokaryotic community composition and the fraction of active bacteria.

Some differences were found between the contribution of specific bacterial groups to the total community assessed by MICRO-CARD-FISH and clone libraries (Fig. 5). The low contribution of the two Alphaproteobacteria subgroups (Roseobacter and SAR11) to the bulk bacterial

community determined with MICRO-CARD-FISH was not paralleled in the clone libraries, where Rhodobacteraceae and SAR11 accounted for a high contribution (21 and 22 % of the total DNA sequences) to the total Alphaproteobacteria (Fig. 3e, f, g, h). To evaluate the discrepancy between MICRO-CARD-FISH and clone libraries, SAR11 and Roseobacter probes were matched against the 16S rDNA clone sequences. The Roseobacter probe used in this study covered 36 % of the identified clones from the Rhodobacteraceae group and only 8 % of the total DNA clones. Thus, more than 64 % of the Roseobacter group is not covered by the Ros537 probe. Bacteria from the Roseobacter RCA clade recently discovered by (Selje et al., 2004)) preferentially live in temperate and polar regions, supporting the emerging view that the global distribution of marine bacterioplankton is related to the environmental and biogeochemical properties of the water masses. Thus, arctic assemblages are distinct from other oceanic communities and contain autochthonous phylogenetic groups adapted to live under polar conditions (Malmstrom et al., 2007). This distinct phylogenetic composition of the Arctic assemblages might explain the low affinity found for the Ros537 probe against the Arctic Rhodobacteraceae clones. This low affinity results in a low number of Roseobacter cells detected by CARD-FISH in Kongsfjorden.

In contrast, the mix of SAR11 oligonucleotide probes covered > 98 % of the Rickettsiales group and 21 % of the total DNA clones. Thus, the discrepancy between the two methods cannot be explained by the low affinity of the oligonucleotide probe to the target group. Despite this discrepancy for the SAR11 and Roseobacter subgroups, the contribution in abundance of the main bacterial groups *versus* their contribution in activity was in general comparable (Fig. 4a, b).

The relative contribution of the bacterial groups obtained by CARD-FISH and by the 16S rDNA clone libraries agreed well except for SAR11 and Gammaproteobacteria of the deep waters (Fig. 5a). In contrast, the contribution of the different groups determined by CARD-FISH *versus* the 16S rRNA clone libraries differed for most of the groups except for Alphaproteobacteria from the deep and Gammaproteobacteria from the surface (Fig. 5b). This discrepancy might be explained by the variability of the cell's RNA content directly depending on the physiological state of the cell. Thus, low abundant groups not detected by CARD-FISH but metabolically active may still be detectable at the 16S rRNA level.

In conclusion, our results suggest that the combined use of 16S rDNA -16S rRNA clone libraries and MICRO-CARD-FISH allows obtaining a refined view on the composition of the microbial community and its potentially active fraction. This approach might be used to better explain the ecological role of the low abundant groups and their function in the biogeochemical cycle. In the light of our results, the approach of cloning both the 16S rDNA and 16S rRNA and subsequent sequencing provides in-depth information on the phylogenetic affiliations of the bacterial community and its active fraction, while the MICRO-CARD-FISH allows for more accurate quantification of the members of a specific target group and their activity. The integrated use of these two approaches proves to be a powerful tool to improve our knowledge on the bacterial community dynamics during environmental changes.

Supplementary Information

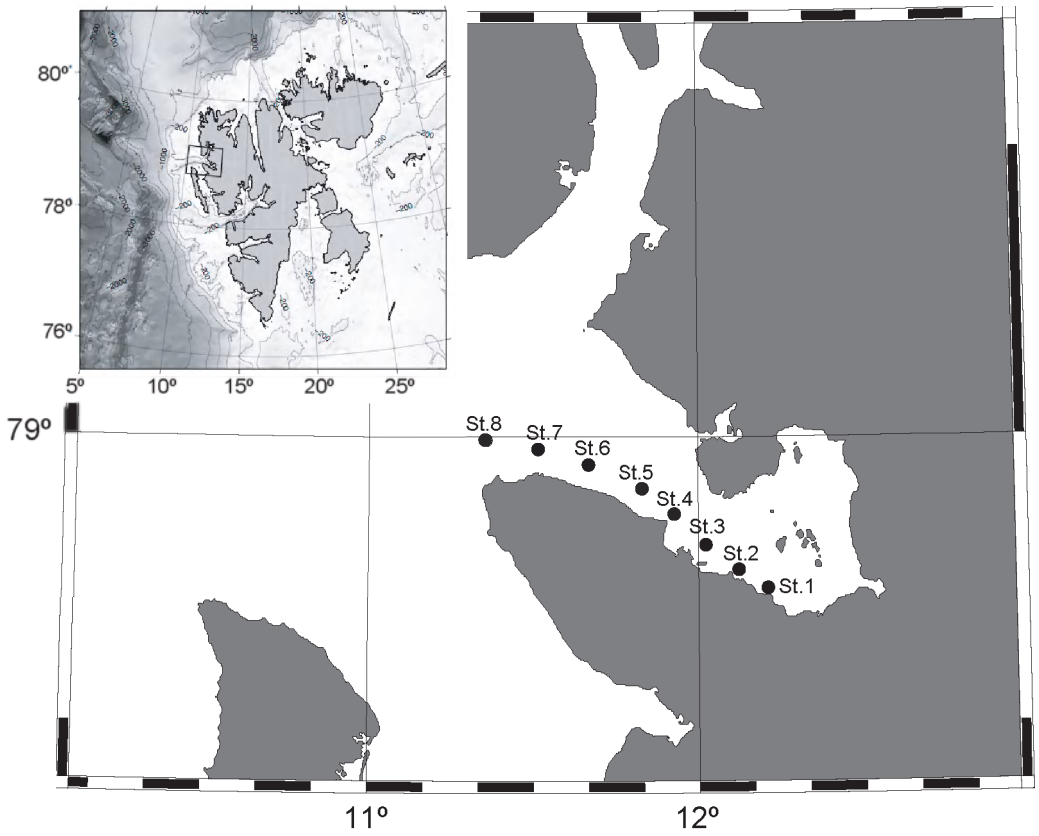

Figure S1. Map of the sampling sites with St.1-8 at the Kongsfjorden, Ny-Alesund (Spitsbergen).

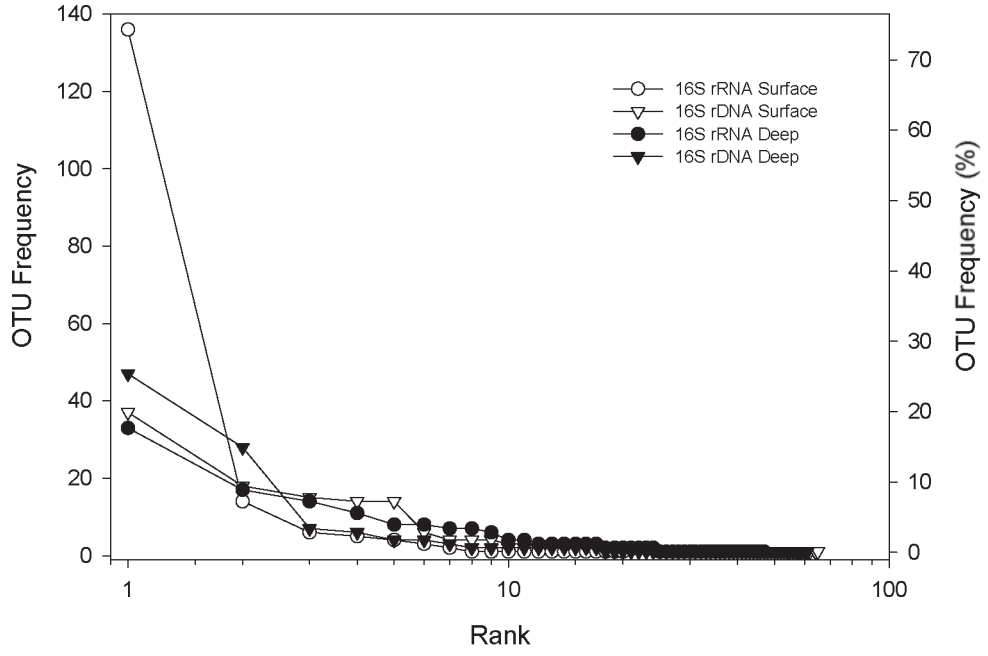

Figure S2. Rank-frequency distribution of OTUs sharing ≥98% similarity obtained from 16S rDNA and 16S rRNA clone libraries obtained from surface- and deep-waters.

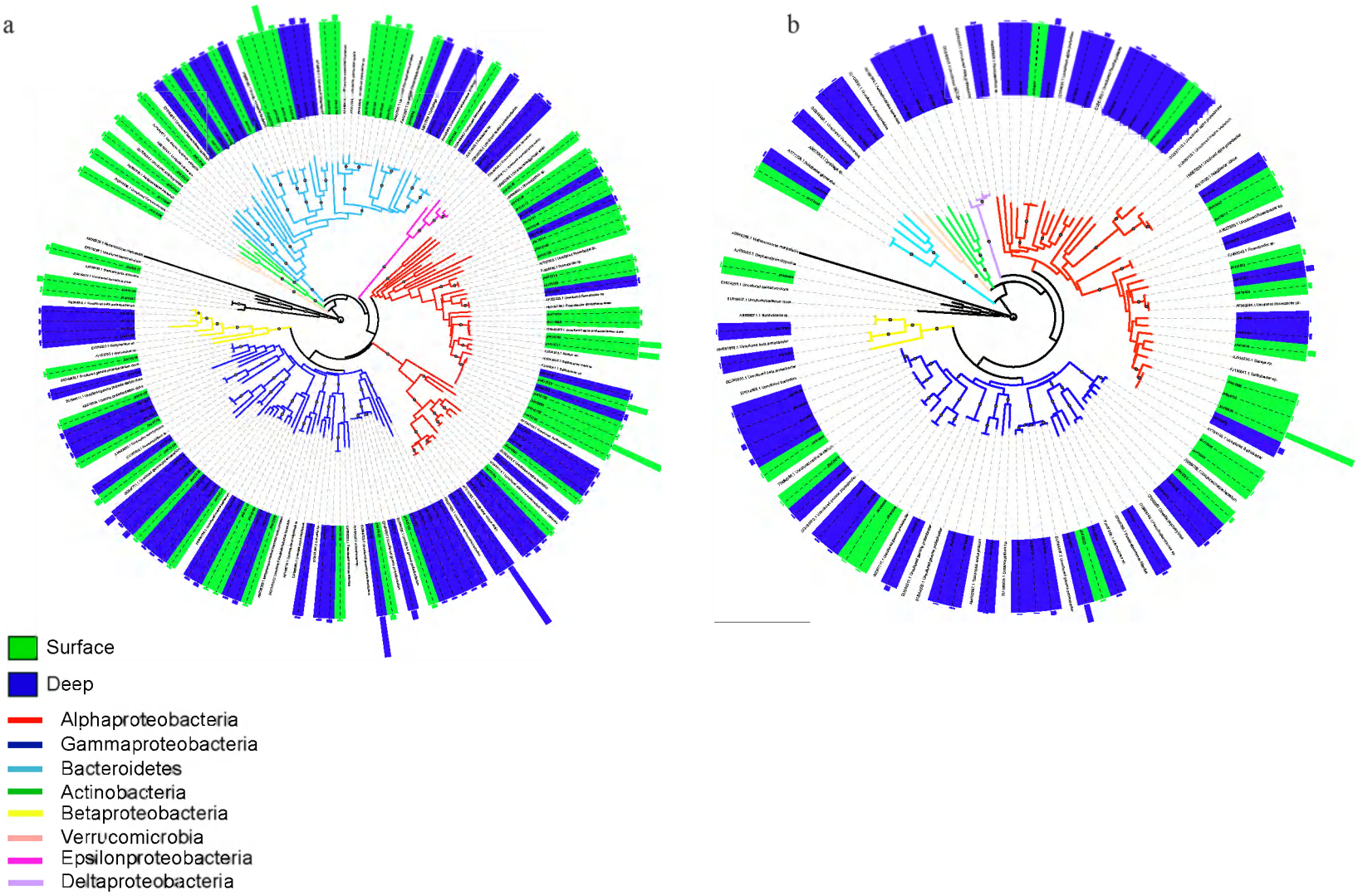

Figure S3. Phylogentic tree based on 16S rDNA (a) and 16S rRNA sequences (b) obtained from the surface- (green bars) and deep-waters (blue bars). The NCBI database sequences are in black. One representative of OTUs ≥ 98% similarity is shown. The bars in the two panels are scaled to the maximum number of OTUs for DNA (a, 47) and RNA (b, 136) sequences. Bootstrap values (>50%) are indicated by the grey circles at branch point. Branch color indicates class association, label color indicates depth.

Acknowledgments

We thank A. K. Olstad, captain of the Teisten, and the lab manager E. Austerheim from Kings Bay AS, for their support and generating a splendid atmosphere. T.Y. was supported by the Japanese Society for the Promotion of Science (JSPS) Postdoctoral Fellowship for research abroad, E.S. was supported by the Earth and Life Science Division of the Dutch Science Foundation (ALW-NWO) in the frame of the PACCA project to G.J.H. D.D.C. received a fellowship of the Univ. of Groningen. Lab work was supported by the ALW-International Polar Year project PACCA (851.40.032).

References

Alonso-Saez L, Sanchez O, Gasol JM, Balague V, Pedros-Alio C. (2008). Winter-to-summer changes in the composition and single-cell activity of near-surface Arctic prokaryotes. *Environ Microbiol* **10:** 2444-2454.

Amann RI, Binder BJ, Olson RJ, Chisholm SW, Devereux R, Stahl DA. (1990). Combination of 16s Ribosomal-RNA-targeted oligonucleotide probes with flow-cytometry for analyzing mixed microbial-populations. *Appl Environ Microbiol* **56:** 1919-1925.

Amann RI, Ludwig W, Schleifer KH. (1995). Phylogenetic identification and in-situ detection of individual microbial-cells without cultivation. *Microbiol Rev* **59:** 143-169.

Ashelford KE, Chuzhanova NA, Fry JC, Jones AJ, Weightman AJ. (2005). At least 1 in 20 16S rRNA sequence records currently held in public repositories is estimated to contain substantial anomalies. *Appl Environ Microbiol* **71:** 7724-7736.

Bano N, Hollibaugh JT. (2002). Phylogenetic composition of bacterioplankton assemblages from the Arctic Ocean. *Appl Environ Microbiol* **68:** 505-518.

Brinkmeyer R, Knittel K, Jurgens J, Weyland H, Amann R, Helmke E. (2003). Diversity and structure of bacterial communities in arctic versus antarctic pack ice. *Appl Environ Microbiol* **69:** 6610-6619.

Buchan A, Gonzalez JM, Moran MA. (2005). Overview of the marine Roseobacter lineage. *Appl Environ Microbiol* **71:** 5665-5677.

Church MJ, DeLong EF, Ducklow HW, Karner MB, Preston CM, Karl DM. (2003). Abundance and distribution of planktonic Archaea and Bacteria in the waters west of the Antarctic Peninsula.

Limnol Oceanogr **48:** 1893-1902.

Cottrell MT, Kirchman DL. (2000). Natural assemblages of marine proteobacteria and members of the Cytophaga-Flavobacter cluster consuming low- and high-molecular-weight dissolved organic matter. *Appl Environ Microbiol* **66:** 1692-1697.

Cottrell MT, Kirchman DL. (2003). Contribution of major bacterial groups to bacterial biomass production (thymidine and leucine incorporation) in the Delaware estuary. *Limnol Oceanogr* **48:** 168-178.

Daims H, Bruhl A, Amann R, Schleifer KH, Wagner M. (1999). The domain-specific probe EUB338 is insufficient for the detection of all Bacteria: development and evaluation of a more comprehensive probe set. *Syst Appl Microbiol* **22:** 434-444.

De Corte D, Yokokawa T, Varela MM, Agogue H, Herndl GJ. (2009). Spatial distribution of Bacteria and Archaea and amoA gene copy numbers throughout the water column of the Eastern Mediterranean Sea. *ISME J* **3:** 147-158.

De Corte D, Sintes E, Yokokawa T, Herndl GJ. (2011). Changes in viral and bacterial communities during the ice-melting season in the coastal Arctic (Kongsfjorden, Ny-Ålesund). *Environ Microbiol* **13:** 1827-1841.

Delong EF, Wickham GS, Pace NR. (1989). Phylogenetic stains - ribosomal RNA-based probes for the identification of single cells. *Science* **243:** 1360-1363.

Eilers H, Pernthaler J, Peplies J, Glockner FO, Gerdts G, Amann R. (2001). Isolation of novel pelagic bacteria from the German bight and their seasonal contributions to surface picoplankton. *Appl Environ Microbiol* **67:** 5134-5142.

Elifantz H, Malmstrom RR, Cottrell MT, Kirchman DL. (2005). Assimilation of polysaccharides and glucose by major bacterial groups in the Delaware Estuary. *Appl Environ Microbiol* **71:** 7799-7805.

Fegatella F, Lim J, Kjelleberg S, Cavicchioli R. (1998). Implications of rRNA operon copy number and ribosome content in the marine oligotrophic ultramicrobacterium Sphingomonas sp. strain RB2256. *Appl Environ Microbiol* **64:** 4433-4438.

Fisher MM, Triplett EW. (1999). Automated approach for ribosomal intergenic spacer analysis of microbial diversity and its application to freshwater bacterial communities. *Appl Environ*

Microbiol **65:** 4630-4636.

Gentile G, Giuliano L, D'Auria G, Smedile F, Azzaro M, De Domenico M, Yakimov MM. (2006). Study of bacterial communities in Antarctic coastal waters by a combination of 16S rRNA and 16S rDNA sequencing. *Environ Microbiol* **8:** 2150-2161.

Gonzalez JM, Simo R, Massana R, Covert JS, Casamayor EO, Pedros-Alio C, Moran MA. (2000). Bacterial community structure associated with a dimethylsulfoniopropionate-producing North Atlantic algal bloom. *Appl Environ Microbiol* **66:** 4237-4246.

Hasle GR, Heimdal BR. (1998). The net phytoplankton in Kongsfjorden, Svalbard, July 1988, with general remarks on species composition of arctic phytoplankton. *Polar Res* **17:** 31-52.

Hollibaugh JT, Bano N, Ducklow HW. (2002). Widespread distribution in polar oceans of a 16S rRNA gene sequence with affinity to Nitrosospira-like ammonia-oxidizing bacteria. *Appl Environ Microbiol* **68:** 1478-1484.

Hop H, Pearson T, Hegseth EN, Kovacs KM, Wiencke C, Kwasniewski S, Eiane K, Mehlum F, Gulliksen B, Wlodarska-Kowalezuk M, Lydersen C, Weslawski J M, Cochrane S, Gabrielsen GW, Leakey RJG, Lonne OJ, Zajaczkowski M, Falk-Petersen S, Kendall M, Wangberg SA, Bischof K, Voronkov AY, Kovaltchouk NA, Wiktor J, Poltermann M, di Prisco G, Papucci C, Gerland S. (2002). The marine ecosystem of Kongsfjorden, Svalbard. Polar Res **21**: 167-208.

Josephson KL, Gerba CP, Pepper IL. (1993). Polymerase chain-reaction detection of nonviable bacterial pathogens. *Appl Environ Microbiol* **59:** 3513-3515.

Kemp PF, Lee S, Laroche J. (1993). Estimating the growth-rate of slowly growing marine-bacteria from Rna-Content. *Appl Environ Microbiol* **59:** 2594-2601.

Kerkhof L, Ward BB. (1993). Comparison of nucleic-acid hybridization and fluorometry for measurement of the relationship between RNA/DNA Ratio and growth-rate in a marine bacterium. *Appl Environ Microbiol* **59:** 1303-1309.

Kirchman DL, Cottrell MT, Lovejoy C. (2010). The structure of bacterial communities in the western Arctic Ocean as revealed by pyrosequencing of 16S rRNA genes. *Environ Microbiol* **12:** 1132-1143.

Lane DJ. (1991). 16S/23S rRNA sequencing. In: Stackebrandt E, Goodfellow M (eds). *Nucleic acid techniques in bacterial systematics.* Wiley and Sons Ltd.: Chichester, United Kingdom. p 115-

175.

Lee N, Nielsen PH, Andreasen KH, Juretschko S, Nielsen JL, Schleifer KH, Wagner M. (1999). Combination of fluorescent in situ hybridization and microautoradiography - a new tool for structure-function analyses in microbial ecology. *Appl Environ Microbiol* **65:** 1289-1297.

Letunic I, Bork P. (2007). Interactive Tree Of Life (iTOL): an online tool for phylogenetic tree display and annotation. *Bioinformatics* **23:** 127-128.

Longnecker K, Homen DS, Sherr EB, Sherr BF. (2006). Similar community structure of biosynthetically active prokaryotes across a range of ecosystem trophic states. *Aquat Microb Ecol* **42:** 265-276.

Lozupone C, Knight R. (2005). UniFrac: a new phylogenetic method for comparing microbial communities. *Appl Environ Microbiol* **71:** 8228-8235.

Malmstrom RR, Kiene RP, Cottrell MT, Kirchman DL. (2004). Contribution of SAR11 bacteria to dissolved dimethylsulfoniopropionate and amino acid uptake in the North Atlantic ocean. *Appl Environ Microbiol* **70:** 4129-4135.

Malmstrom RR, Straza TRA, Cottrell MT, Kirchman DL. (2007). Diversity, abundance, and biomass production of bacterial groups in the western Arctic Ocean. *Aquat Microb Ecol* **47:** 45-55

Manz W, Amann R, Ludwig W, Wagner M, and Schleifer H. (1992). Phylogenetic oligodeoxynucleotide probes for the major subclasses of Proteobacteria: problems and solutions. *Appl Microbiol* **15:**593-600.

Manz W, Amann R, Ludwig W, Vancanneyt M, Schleifer KH. (1996). Application of a suite of 16S rRNA-specific oligonucleotide probes designed to investigate bacteria of the phylum cytophaga-flavobacter-bacteroides in the natural environment. *Microbiology* **142:** 1097-1106.

Mills HJ, Martinez RJ, Story S, Sobecky PA. (2005). Characterization of microbial community structure in Gulf of Mexico gas hydrates: Comparative analysis of DNA- and RNA-derived clone libraries. *Appl Environ Microbiol* **71:** 3235-3247.

Moeseneder MM, Arrieta JM, Muyzer G, Winter C, Herndl GJ. (1999). Optimization of terminal-restriction fragment length polymorphism analysis for complex marine bacterioplankton communities and comparison with denaturing gradient gel electrophoresis. *Appl Environ Microbiol* **65:** 3518-3525.

Moeseneder MM, Arrieta JM, Herndl GJ. (2005). A comparison of DNA- and RNA-based clone libraries from the same marine bacterioplankton community. *Fems Microbiol Ecol* **51:** 341-352.

Morris RM, Rappe MS, Connon SA, Vergin KL, Siebold WA, Carlson CA. Giovannoni SJ. (2002). SAR11 clade dominates ocean surface bacterioplankton communities. Nature **420**: 806-810.

Muyzer G, Smalla K. (1998). Application of denaturing gradient gel electrophoresis (DGGE) and temperature gradient gel electrophoresis (TGGE) in microbial ecology. *Anton Leeuw Int J G* **73:** 127-141.

Neef A. (1997). Anwendung der in situ-Einzelzell- Identifizierung von Bakterien zur Populationsanlayse in komplexen mikrobiellen biozönosen. PhD Thesis. Technische Universität München. Munich, Germany.

Owrid G, Socal G, Civitarese G, Luchetta A, Wiktor J, Nothig EM, Andreassen I, Schauer U, Strass V. (2000). Spatial variability of phytoplankton, nutrients and new production estimates in the waters around Svalbard. *Polar Res* **19**: 155-171.

Pernthaler A, Pernthaler J, Amann R. (2002a). Fluorescence in situ hybridization and catalyzed reporter deposition for the identification of marine bacteria. *Appl Environ Microbiol* **68:** 3094-3101.

Pernthaler A, Preston CM, Pernthaler J, DeLong EF, Amann R. (2002b). Comparison of fluorescently labeled oligonucleotide and polynucleotide probes for the detection of pelagic marine bacteria and archaea. *Appl Environ Microbiol* **68:** 661-667.

Piwosz K, Walkusz W, Hapter R, Wieczorek P, Hop H, Wiktor J. (2009). Comparison of productivity and phytoplankton in a warm (Kongsfjorden) and a cold (Hornsund) Spitsbergen fjord in mid-summer 2002. *Polar Biol* **32:** 549-559.

Pommier T, Canback B, Riemann L, Bostrom KH, Simu K, Lundberg P, Tunlid A, Hagstrom A. (2007). Global patterns of diversity and community structure in marine bacterioplankton. *Mol Ecol* **16:** 867-880.

Poulsen LK, Ballard G, Stahl DA. (1993). Use of Ribosomal-Rna Fluorescence Insitu Hybridization for Measuring the Activity of Single Cells in Young and Established Biofilms. *Appl Environ Microbiol* **59:** 1354-1360.

Rappe MS, Connon SA, Vergin KL, Giovannoni SJ. (2002). Cultivation of the ubiquitous SAR11 marine bacterioplankton clade. *Nature* **418:** 630-633.

Schloss PD, Handelsman J. (2005). Introducing DOTUR, a computer program for defining operational taxonomic units and estimating species richness. *Appl Environ Microbiol* **71:** 1501-1506.

Schoemann V, Becquevort S, Stefels J, Rousseau W, Lancelot C. (2005). Phaeocystis blooms in the global ocean and their controlling mechanisms: a review. *J Sea Res* **53:** 43-66.

Selje N, Simon M, Brinkhoff T. (2004). A newly discovered Roseobacter cluster in temperate and polar oceans. *Nature* **427:** 445-448.

Sogin ML, Morrison HG, Huber JA, Mark Welch D, Huse SM, Neal PR. Arrieta JM, Herndl GJ. (2006). Microbial diversity in the deep sea and the underexplored "rare biosphere". *P Natl Acad Sci USA* **103:** 12115-12120.

Suzuki MT, Preston CM, Chavez FP, DeLong EF. (2001). Quantitative mapping of bacterioplankton populations in seawater: field tests across an upwelling plume in Monterey Bay. *Aquat Microb Ecol* **24:** 117-127.

Teira E, Reinthaler T, Pernthaler A, Pernthaler J, Herndl GJ. (2004). Combining catalyzed reporter deposition-fluorescence in situ hybridization and microautoradiography to detect substrate utilization by bacteria and Archaea in the deep ocean. *Appl Environ Microbiol* **70:** 4411-4414.

Wang Q, Garrity GM, Tiedje JM, Cole JR. (2007). Naive Bayesian classifier for rapid assignment of rRNA sequences into the new bacterial taxonomy. *Appl Environ Microbiol* **73:** 5261-5267.

Weinbauer MG, Fritz I, Wenderoth DF, Hofle MG. (2002). Simultaneous extraction from bacterioplankton of total RNA and DNA suitable for quantitative structure and function analyses. *Appl Environ Microbiol* **68:** 1082-1087.

Zaballos M, Lopez-Lopez A, Ovreas L, Bartual SG, D'Auria G, Alba JC, Legault B, Pushker R., Daae FL, Rodriguez-Valera F. (2006). Comparison of prokaryotic diversity at offshore oceanic locations reveals a different microbiota in the Mediterranean Sea. *Fems Microbiol Ecol* **56:** 389-405.

Zhang Y, Jiao NZ, Cottrell MT, Kirchman DL. (2006). Contribution of major bacterial groups to bacterial biomass production along a salinity gradient in the South China Sea. *Aquat Microb Ecol* **43:** 233-241.

Summary

A high variability in the prokaryotic and viral abundance and production was found in the bathy- and abyssopelagic zones, indicating that the heterogeneity in the microbiota in the meso- and abyssopelagic waters is as pronounced as in the epipelagic layer. Thus, overall the results presented in this PhD thesis suggest that the dark ocean is more dynamic than commonly assumed.

The two studies carried out in the North Atlantic Ocean showed that prokaryotic and viral abundance are in general highly correlated, although the virus to prokaryote ratio (VPR) significantly changed with depth and with latitude. Generally the viral abundance was one to two orders of magnitude higher than the prokaryotic abundance and VPR increased with depth due to the viruses decreased less pronouncedly with depth than prokaryotes. The VPR was negatively related with prokaryotic abundance and heterotrophic production. The discrepancies between low viral and heterotrophic prokaryotic production and the relatively high viral abundance might be explained by an increasing contribution of lysogenic and/or pseudolysogenic to total viral production in the deep waters. Also, the low temperature in the abyssopelagic realm might provoke a longer persistence of infective viruses (lower decay rates) than in epipelagic waters exposed to high temperature and ultraviolet radiation. Another possible explanation for the increasing VPR with depth might be that in the oligotrophic environments such as the deep sea, prokaryotes might not be able to invest sufficient energy to generate resistance mechanisms against viral infection, thus resulting in an increase of the frequency of infected cells in this environment. Moreover, the lack of a relationship between prokaryotes and viral parameters in the dark ocean (tested with DISTML statistical test) might indicate the occurrence of allochthonous input of viral particles from adjacent water masses. Thus, a predominately particle-attached life strategy of the virus-host systems in the deep ocean, as indirect evidence suggests, is in agreement with recent conclusions based on metagenomics of deep-sea prokaryotes. The suggested particle-attached life style (DeLong et al 2006) is also consistent with our finding that provinces characterized by low phytoplankton production and low particulate organic matter (POM) export flux exhibit a correspondingly lower prokaryotic abundance and heterotrophic production in the bathy- and abyssopelagic layers than more mesotrophic oceanic provinces with a high phytoplankton production. The latter supports the notion that heterotrophic prokaryotic production in the dark ocean is mainly depending on sedimenting POM derived from surface water primary production.

Studies on the community composition of different microbial components, assessed by well-established methods, allowed us to show that the bacterial, archaeal and viral communities were well stratified in the Subtropical Atlantic Ocean. The three depth-related prokaryotic communities showed at least two distinct clusters associated to depth (epi-mesopelagic and bathy-abyssopelagic). The bacterial and viral richness exhibited a contrasting pattern with depth, the bacterial OTUs abundance increased below 3000 m depth whereas the viral OTUs decreased. This discrepancy between prokaryotic and viral abundance might indicate a wider host range of viruses in these deep waters than in the near-surface layers.

Overall our data clearly show that the parameters controlling the viral abundance in the North Atlantic Ocean vary significantly with depth and latitude, suggesting that viral-host interactions change in response to the changes in the biotic and abiotic variables

To further explore the relationships between viruses and their host in marine ecosystems, a study was conducted in the coastal Arctic during the ice-melting season, when dramatic changes in environmental conditions occur. The prokaryotic and viral community were strongly affected by the changes in the environmental conditions. Two factors drove the changes in the environmental parameters and consequently, the prokaryotic and viral variables, time and depth, both in lieu caused mainly by temperature changes. Under these dynamic environmental conditions, the two communities appeared to be weakly linked, although the prokaryotic abundance and heterotrophic production increased over the sampling time while the viral abundance did not significantly change.

Thus, the VPR decreased significantly over the sampling period in the surface waters. In contrast, the prokaryote and viral community revealed by ARISA and RAPD-PCR, respectively, were well-stratified and the number of OTUs co-varied with depth, suggesting that the dynamic environmental conditions influence the expression of the main components of the different components of the microbial food web. The discrepancies found between viral and prokaryotic communities might be explained by the differential effect of the UV, and/or the high particle load from terrigenous origin on the prokaryotic and viral production.

The prokaryotic communities from the Arctic were explored more comprehensively by the combined use of 16S rDNA -16S rRNA clone libraries and microautoradiography catalyzed reporter deposition fluorescence in situ hybridization MICRO-CARD-FISH approaches. The results showed clear differences between the bulk bacterial community and its active fraction. The bacterial communities were dominated by members of Alphaproteobacteria followed by Bacteroidetes, whereas Gammaproteobacteria were present at low abundance but exhibited a high percentage of active cells taking up leucine. In contrast, groups present at higher abundance than Gammaproteobacteria, such as Bacteroidetes, exhibited a lower percentage of active cells. The bacterial community of the Arctic coastal waters was in general composed by psychrophilic or cosmopolitan phylotypes as revealed by clone libraries.

The archaeal cell abundance was very low at the spring-summer transition phase (~1% total DAPI count), probably due to the lack of adaptation of the Archaea to the fast-changing environmental conditions occurring during the ice-melting season (r-selection). Nevertheless, several studies have shown that the archaeal community increases its contribution to the prokaryotic community in winter, under more stable climatic conditions (k-selection). The integrated use of the two techniques (16S rRNA, 16S cDNA) proved to be a powerful tool improving our knowledge on the prokaryotic community succession during environmental changes such as algal proliferation, when few metabolically active prokaryotes dominate. Our data clearly show that the bulk prokaryotic community does not completely reflect the structure of the active fraction of the community.

An in-depth study on the metabolic activity of prokaryotic communities was conducted in the Eastern Mediterranean Sea. The archaeal community appeared to be highly stratified as revealed by

terminal-restriction fragment length polymorphism (T-RFLP) analysis despite the absence of major temperature and density gradients between the meso- and bathypelagic waters in the Mediterranean Sea. Three main distinct clusters were detected, one grouped the archaeal communities from surface waters, one grouped mesopelagic communities and the third one grouped around archaeal communities from 3000-4000 m depth. Although the crenarchaeal abundance did not vary with depth, the abundance of archaeal OTUs significantly decreased with depth. The archaeal amoA gene abundance exponentially decreased with depth, whereas the β-Proteobacteria amoA were below the detection limit. The ratio archaeal *amo*A copy number *vs*. crenarchaeal abundance declines with depth indicating that ammonia-oxidizing Crenarchaeota are largely confined to the surface and mesopelagic waters, while in deep waters of the Eastern Mediterranean Sea, Crenarchaeota are likely utilizing energy sources other than ammonia.

References

DeLong EF, Preston CM, Mincer T, Rich V, Hallam SJ, Frigaard N-U, Martinez A, Sullivan MB, Edwards R, Brito BR, Chisholm SW, Karl DM. (2006). Community genomics among stratified microbial assemblages in the ocean's interior. *Science* **311**:496-503.

Samenvatting

In de bathypelagische zone (1000-4000m diep) en abyssopelagische zone (dieper dan 4000m) werd een hoge variabiliteit gemeten in de hoeveelheid en de productie van prokaryoten en virussen. Dit suggereert dat de microbiële gemeenschap in de diepe waterlagen even heterogeen is als in de ondiepe epipelagische waterlaag (0-200m diep).

Uit twee studies in de Atlantische Oceaan bleek dat de hoeveelheden prokaryoten en virussen niet altijd sterk gecorreleerd waren omdat dat de verhouding van virussen en prokaryoten (VPR) significant veranderde met diepte en breedtegraad. Het aantal virusdeeltjes was doorgaans 10-100x zo groot als het aantal prokaryoten en de VPR ratio nam toe in de diepte omdat het aantal prokaryoten sterker afnam dan het aantal virussen. De VPR ratio was negatief gecorreleerd met het aantal prokaryoten en de heterotrofe productie.

De lage productie van virussen en prokaryoten bij aanwezigheid van grote aantallen virusdeeltjes in de diepe waterlagen kan worden verklaard door een groter aandeel lysogene en/of pseudolysogene virussen. Ook is het mogelijk dat infectieve virussen zich langer kunnen handhaven (door een lagere afbraaksnelheid) bij de lage temperaturen in de diepzee. Een andere mogelijke verklaring voor de toename van de VPR ratio in de diepte is dat in een voedingsarme omgeving, zoals in de diepzee, prokaryoten niet voldoende energie beschikbaar hebben voor het afweren van virusinfecties waardoor het aantal geïnfecteerde cellen in de diepzee hoger is dan in oppervlaktewateren. Ook kan het ontbreken van een correlatie tussen prokaryoten en virussen in de diepzee (getest met DISTML) wijzen op de import van virusdeeltjes vanuit aangrenzende watermassa's. Indirect bewijs op basis van een recente metagenoom analyse van diepzee prokaryoten suggereert dat virus-gastheersystemen in de diepzee hoofdzakelijk zijn geassocieerd met deeltjes (De Long et al. 2006). Een deeltjesgeassocieerde leefwijze is ook in overeenstemming met onze waarneming dat watermassa's met lage fytoplanktonproductie en een lage exportflux van particulair organisch materiaal (POM) een corresponderende lage hoeveelheid prokaryoten en een lage heterotrofe activiteit vertonen. Bovengenoemde waarneming onderschrijft het idee dat heterotrofe activiteit door prokaryoten in de diepzee vooral afhangt van sedimenterend POM afkomstig van primaire productie uit de oppervlakte wateren.

Studies van de levensgemeenschap van verschillende groepen micro-organismen, uitgevoerd met beproefde methodieken, maakten het ons mogelijk om aan te tonen dat zowel de bacteriën als de archaea en de virussen gestratificeerd voorkomen in de subtropische Atlantische Oceaan. Hun levensgemeenschappen vertoonden tenminste twee aparte clusters die geassocieerd waren met bepaalde dieptezones (epi-en mesopelagiaal en bathypelagiaal). De bacterie- en virusdiversiteit vertoonden contrasterende patronen met diepte. Bij dieptes groter dan 3000m nam het aantal bacterie OTUs (operationele taxonomische units) toe, terwijl het aantal virus OTUs afnam. Dit wijst er mogelijk op dat virussen in de diepzee een grotere gastheerrange hebben dan virussen in de oppervlaktewateren.

Al met al, laat onze data duidelijk zien dat de factoren die de hoeveelheid virusdeeltjes controleren aanzienlijk veranderen met diepte en breedtegraad in de Noord Atlantische Oceaan.

Een vervolgonderzoek naar de relatie tussen virussen en hun gastheer in mariene ecosystemen werd uitgevoerd in Arctisch kustwater tijdens de dooiperiode. De gemeenschappen van prokaryoten en virussen werden sterk beïnvloed door veranderingen in omgevingsfactoren, met name temperatuur en indirect monsterdiepte en tijdstip omdat deze factoren ook gepaard gaan met temperatuursverschillen. In sterk dynamische omstandigheden waren de bacterie- en virusgemeenschappen slechts zwak gekoppeld.

In het oppervlaktewater nam de hoeveelheid prokaryoten en de heterotrofe activiteit toe gedurende de tijdserie terwijl de hoeveelheid virusdeeltjes nauwelijks veranderde. Dus, de virus-prokaryoot ratio (VPR) daalde significant gedurende de tijdserie. De verschillen tussen de hoeveelheid virussen en de hoeveelheid prokaryoten kunnen worden verklaard door verschillende gevoeligheden voor UV-straling, en ook door verschillende gevolgen van de input van landmateriaal op de productie van prokaryoten en virussen.

De Arctische levensgemeenschap van prokaryoten werd nader onderzocht d.m.v. sequensen van 16S ribosomaal RNA gen kloonbibliotheken en micro-autoradiografie gekoppeld aan in-situ hybridisatietechnieken. Resultaten toonden een duidelijk verschil tussen de totale bacteriegemeenschap en de actieve fractie. De bacteriegemeenschappen werden gedomineerd door alfaproteobacteriën en bacteroidetes, terwijl gammaproteobacteriën weinig voorkwamen maar toch het grootste percentage van de actieve populatie vormden. In het algemeen waren de gevonden bacteriën psychrofielen of kosmopolieten.

De hoeveelheid archaeale cellen was laag tijdens de overgang van lente naar zomer. Echter, meerdere studies hebben aangetoond dat de archaeagemeenschap groeit in de winter wanneer de omgevingsfactoren stabieler zijn (k-selectie). De analyse van zowel 16S ribosomaal DNA als RNA bleek een goed middel voor het verwerven van kennis over de successie van prokaryoten tijdens veranderingen in de omgevingsfactoren zoals algengroei, wanneer een klein aantal soorten de actieve fractie prokaryoten domineert. Onze gegevens laten duidelijk zien dat de totale prokaryotengemeenschap niet geheel de structuur van de actieve fractie weergeeft.

Een gedegen studie van de metabolische activiteit van prokaryoten werd uitgevoerd in de Middellandse Zee. Ondanks de afwezigheid van temperatuur- en dichtheidsgradiënten over de meso- en bathypelagische wateren in de Middellandse Zee bleek uit TRFLP (terminaal restrictiefragmentlengte analyse) dat de archaeagemeenschap sterk gestratificeerd is. Drie verschillende clusters werden gevonden: Een cluster met archaea uit oppervlaktewateren; een met mesopelagische archaea en een derde groep met archaea van 3000-4000m diepte. Hoewel de hoeveelheid crenarchaea niet veranderde met de diepte, nam het aantal archaea OTUs wel af met de diepte. De hoeveelheid archaea amoA genen nam exponentieel af met de diepte, terwijl bacterieel amoA overal onder de detectielimiet bleef. De verhouding tussen de hoeveelheid archaea amoA genen versus crenarchaea ribosomaal RNA genen nam af met de diepte. Dit wijst erop dat ammonia oxiderende crenarchaea vooral voorkomen in de oppervlakte en mesopelagische waterlagen,

terwijl crenarchaea in de diepere waterlagen van de Middellandse Zee waarschijnlijk alternatieve energiebronnen gebruiken voor ammonia.

Referenties

DeLong EF, Preston CM, Mincer T, Rich V, Hallam SJ, Frigaard N-U *et al* (2006). Community Genomics Among Stratified Microbial Assemblages in the Ocean's Interior. *Science* **311:** 496 - 503.

Acknowledgments

The last few years have been quite intense but I was lucky enough to have friends and colleagues that helped me through all the good and bad moments.

During this time I had the opportunity to work and live in two different countries, thus I would like to thank the people of the Royal Netherlands Institute for Sea Research (The Netherlands) and of the Marine Biology Department of the University of Vienna (Austria) for their hospitality and support during the last four years.

First of all I would like to show my gratitude to Gerhard Herndl for giving the opportunity to do my Phd thesis in his working group (even if I am not the Italian girl that he would have liked to have as PhD student). He was always able to motivate me with his enthusiasm giving me the freedom to learn from my mistakes. Also I would like to thank my PhD promotor Hein de Baar.

Special thanks to Eva Sintes and Taichi Yokokawa that advised me, helped me during the past years, this dissertation could not have been written without them.

I am truly indebted and thankful to the people of the NIOZ especially those of the molecular biology lab, where I have done most of my practical work. Many thanks to all the people working in the lab, in particular to Harry Witte and Judith van Bleijswijk, that always helped me when something was going wrong.

Many thanks to the *R/V* Pelagia's cruise leaders especially Micha and Loes, crew and to the captains John and Berth for their unconditional support, especially when the weather was getting too rough and everything was flying away. Unforgettable were the swims that we took in the middle of the Atlantic Ocean.

During this long journey I met so many people and most of them became friends of mine. I would like to thank (in alphabetic order) Adam, Alejandra, Alex, Beate, Catalina, Caterina, Charles, Christian, Claudia, Eva, Fede, Harald, Ishraga, Itziar, Jana, Julie, Joaquim, John, Kerstin, Kristin, Lucia, Nicole, Pedro, Rita, Roberta, Santiago, Silvia, Simone, Sofia, Taichi, Theodora, Thomas, Uli.

Beside I would like to thank my parents that supported me through all my life.

Last, but certainly not least I am truly indebted and thankful to Silvio that during the harder moments of the past years was always able to cheer me up with some of his funny jokes. Thanks to him during these moments I was always thinking that spending some time abroad was not such a bad idea.